





Interactions between plant roots and the structure of compacted soils

Jasmine E. Burr-Hersey

BSc (Hons), MSc (Hons)

Thesis submitted to the University of Nottingham for the degree of Doctor of Philosophy

July 2019

Acknowledgments

I would like to express particular appreciation and thanks to my supervisors Prof Karl Ritz, Prof Sacha Mooney and Dr Glyn Bengough for their invaluable guidance and support which has been critical in helping me shape my work over the course of this project.

Many thanks to all members of the Hounsfield Facility group, past and present, all of which it has been an absolute pleasure to work with so closely over the last few years. With special thanks to Dr Craig Sturrock, Dr Sebastian Blunk, Dr Aurelie Bacq-Labreuil and Dr Stefan Mairhofer. I would like to extend particular gratitude to Dr Brian Atkinson whose support was of paramount importance in so many areas of this work.

A special thank you to the STARS CDT community in particular Prof Phil Haygarth and Olivia Lawreson, for inspiring me to do more, and to be more. The opportunities which being part of the consortium opened up to me have been truly unique, have shaped my PhD experience and made this journey both interesting, engaging, challenging and rewarding.

I have consulted with a number of experts from many fields and would like to acknolwedge the contribution their advice has made to shaping the development of my project: Paul Brown, Paul Hatcher, Bob Froud-Williams, Henery Ford, Helen Peat and Steve Morton. Thank you!

I also extend thanks to my collegues at Defra, particularly my supervisors Dr Willem Roelofs and Lisa Smith who facilitated an excellent professional placement experience within the Plant Health Department.

This work was funded through the Soils Training and Research Studentships, a BBRSC:NERC Doctoral Training Programme. I would like to extend thanks to the British Society of Soil Science, the International Union of Soil Science and the Nottingham Gradute school, all of which provided funding for me to attend international conferences as part of my PhD.

Finally I would like to acknowledge the support of my family and friends over the last few years. With particular thanks to my siblings, parents and partner Dr Christopher Till, all who have helped me enormously in their own ways.

Abstract

Compaction is a form of soil physical degradation. It occurs through both human-induced and natural mechanisms such as the passage of heavy farm machinery in agricultural settings as well as the impact of animal trampling and glaciation in natural ecosystems. It results in the rearrangement of soil particles, resulting in an increase in bulk density and subsequent loss of porosity and pore connectivity. These changes in the soil matrix make it difficult for plant roots to penetrate deep into the soil profile as the connected macropore network which provides the path of least resistance has been destroyed. Currently, there are limited ways to remediate the impact of soil compaction, mechanical methods that exist only provide temporary relief and often exacerbate the problem at depth. The use of plant roots as a 'biotillage' tool could offer a natural means to help remediate soils subject to compaction. The objective of this study was to visualise and quantify the root architectures of selected cover crop and wild plant species grown in a variety of compacted soil conditions. To do this three-dimensional visualisations of the root architecture were generated via X-ray Computed Tomography, using a number of different automated and semi-automated root-segmentation techniques. The impact of plant root growth on soil structure was then analysed at both rhizosphere and soil column scales, over timescales of several weeks. In high soil compaction treatments changes in pore space were localised to the rhizosphere zone up to 420 µm distance from the root surface. Across the species investigated the porosity was always greatest closest to the root surface and decreased with distance form

the roots surface. This trend was also observed when plants were grown in different soil textures. Soil texture was observed to significantly affect plant growth, with notably less root and shoot development by plants grown in the clay soils in comparison to the clay loam and sand treatments. The generation of root mass was species-dependent and linked to the penetration resistance of the soil. These parameters subsequently affected average root diameters of the plants, which had a direct effect on pore space creation in the rhizosphere. Roots with different morphological traits were observed to respond contrastingly to a compacted soil layer, with taprooted species undergoing greatest architectural change in comparison to fibrous root systems. The work indicates that changes to soil structure via the growth of plant roots occurs primarily in root:soil contact zone, and is a temporally dynamic process. Tap-rooted plants appear to be particularly effective in terms of being able to grow in highly compacted soils. These findings have implications for the potential remediation of compacted soils, as they indicate that plants demonstrate an inherent ability to instigate soil structural genesis, but this differs between species.

Contents

Acknowledgments ii
Abstract iii
List of figures ix
List of tables xiii
Chapter 1: Introduction and Literature Review 15
1.1 Introduction 15
1.1.1 Rationale 15
1.2 Literature review 16
1.2.1 The importance of soil 16
1.2.2 Soil texture & structure 17
1.2.3 'Healthy' soil 18
1.2.4 Degraded and compromised soils 19
1.3 Soil compaction 20
1.3.1 Soil compaction and its impact 20
1.3.2 Causes of soil compaction 21
1.3.3 Effects of soil compaction 22
1.3.4 Compaction effects on soil moisture and aeration 23
1.3.5 Compaction effects on root and shoot biomass 25
1.3.6 Remediation of compacted soils 26
1.4 Plant roots 27
1.4.1 Root development 27
1.4.2 Root elongation and radial expansion 31
1.4.3 Root growth into pores 33
1.4.4 Root response to soil compaction and mechanical impedance 35
1.4.5 The rhizosphere 36
1.5 X-ray Computed Tomography 38
1.5.1 Soil and pore space imaging 38
1.5.2 Root imaging 40
1.6 Research aims and objectives 41
1.7 Thesis structure 43
Chapter 2: Generic methods 44
2.1 Soil 44
2.1.1 Soil preparation 44
2.1.2 Soil compaction 45
2.1.3 Soil moisture 48
2.1.4 Soil strength (penetrometer resistance) 51
2.1.5 Soil texture (quantitative analysis by hydrometer) 52

2.1.6 Aggregate size distribution 52
2.2 Plants 53
2.2.1 Pre germination for non-crop species 53
2.2.2 Germination 53
2.2.3 Growth conditions 54
2.2.4 Plant harvesting & biomass storage 55
2.2.5 Biomass root and shoot analysis 55
2.2.6 Quantifying mycorrhizal roots 56
Chapter 3: Investigating cover crop species root architecture responses to soil compaction 57
3.1 Consultation with Frontier Agriculture 58
3.2 Preliminary trials 58
3.2.1 Experimental material and methods for 2D investigation 59
3.2.2 Results 59
3.2.3 Experimental material and methods for 3D investigation 66
3.3 Summary of preliminary investigations 69
3.4 Authors accepted manuscript 70
3.4.1 Abstract 72
3.4.2 Key words 73
3.4.3 Introduction 73
3.4.4 Materials and methods 77
3.4.5 Results 82
3.4.6 Discussion 93
3.4.7 Conclusion 99
3.4.8 Supporting information 100
3.4.9 Acknowledgements 100
3.4.10 References 101
Chapter 4: Investigating the potential for wild plant roots to modify compacted soil structure in the rhizosphere 106
4.1 Identification of plant species 107
4.1.1 Literature search 107
4.1.2 Database consultation 108
4.1.3 Field observations 109
4.1.4 Liaison with experts 110
4.1.5 Identification of candidate species 110
4.2 Screening 111
4.2.1 Germination 111
4.2.2 Screening trial 112
4.2.3 Database creation (from physical biomass quantification) 117

4.2.4 Final species selection 118
4.3 Computer based method development 120
4.3.1 Root segmentation methodologies 120
4.3.2 Root analysis 126
4.3.3 Soil porosity analysis 129
4.3.4 Rhizosphere porosity analysis 136
4.4 Summary of computer based method development 138
4.5 Authors manuscript 139
4.5.1 Abstract 141
4.5.2 Key words 142
4.5.3 Introduction 142
4.5.4 Materials and methods 145
4.5.5 Statistical analysis 150
4.5.6 Results 152
4.5.7 Discussion 159
4.5.8 Conclusions 164
4.5.9 Acknowledgments 165
4.5.10 Supplementary information 165
4.6 Mycorrhizae association 166
4.7 Further analysis 166
4.7.1 Principal component analysis 167
4.7.2 Final species selection 167
4.8 Chapter summary 169
Chapter 5: Assessing the impact of soil texture on *Cirsium vulgare* root architectural development and soil porosity formation in the rhizosphere 171
5.1 Soil classification 172
5.1.1 Soil texture 172
5.1.2 Soil core preparation 173
5.1.3 Soil penetration resistance 175
5.1.4 Growth conditions 175
5.2 Primary imaging processing 176
5.2.1 Reconstructing X-ray data 176
5.2.2 Greyscale equalisation 176
5.3 Root segmentation methodologies 182
5.3.1 Results of segmentation trial 183
5.4 X-ray CT analysis methods 187
5.4.1 Root analysis VG Studio 187
5.4.2 Poly angle measurement tool (PAM) 189

5.4.4 Rhizosphere porosity analysis 189
5.5 Biomass and 2D characteristics analysis..... 192
5.5.1 Shoots..... 192
5.5.2 Roots..... 193
5.6 Physical soil characteristics 195
5.6.1 Aggregate size distribution 195
5.7 Authors manuscript..... 196
5.7.1 Abstract..... 198
5.7.2 Introduction 199
5.7.3 Materials and methods..... 202
5.7.4 Destructive harvest 204
5.7.5 3D Image processing segmentation and analysis 206
5.7.6 Results 209
5.7.7 Discussion..... 220
5.7.8 Conclusion 223
5.7.9 Acknowledgments 224
Chapter 6: General discussion 225
6.1 Introduction..... 225
6.2 Application of novel image analysis techniques 225
6.3 Response of root system architecture to soil bulk density 227
6.4 Response of root system architecture to soil texture..... 233
6.5 Generation of soil porosity via plant root development 236
6.6 Implications in the field 239
6.7 Limitations to the study 239
6.7.1 System size..... 240
6.7.2 Length of experiments 240
6.7.3 Scan resolution 241
6.7 Conclusions..... 242
6.6.1 Overarching conclusion 244
6.7 Further work 244
References 249
Appendix Chapter 2..... 265
Appendix Chapter 3..... 270
Appendix Chapter 4..... 281
Appendix Chapter 5..... 294

List of figures

Figure 1.1: Causes of soil compaction and the effects on soil physical properties **24**

Figure 1.2: Root cap structure and development **29**

Figure 1.3: Steps in the root expansion model **33**

Figure 2.1: Diagram of soil core compaction equipment **48**

Figure 2.2: Diagram of soil tension table set up **50**

Figure 2.3: Diagram of Instron universal testing machine equipment **51**

Figure 3.1: WinRHIZO scan images of tillage radish **61**

Figure 3.2: WinRHIZO scan images of vetch **62**

Figure 3.3: WinRHIZO scan images of black oat **63**

Figure 3.4: Average root length and diameter of cover crop species day 20 and 58 ..... **64**

Figure 3.5: Average root length found within specified diameter classes **66**

Figure 3.6: X-Ray CT visualisations of cover crop plants grown for 20 days scanned at 60 µm **68**

Figure 3.7: Representative 3D renderings of root systems grown in repacked soil columns **83**

Figure 3.8: Location maps of roots in 2D cross-section representative slices of segmented root systems **84**

Figure 3.9: Average surface area of root (cm^2) and root volume as % of full soil column **86**

Figure 3.10: Visual representation of convex hull volumes for representative root systems **87**

Figure 3.11: Average root systems convex hull (cm^3) and solidity value of full soil column **88**

Figure 3.12: Average surface area (cm^2), volume of root (%), number of laterals and lateral angle (°) of tillage radish root systems **89**

Figure 3.13: Average surface area (cm^2), volume of root (%), number of laterals and lateral angle (°) of vetch root systems **91**

Figure 3.14: Average surface area (cm^2), volume of root (%) of black oat root systems **91**

Figure 3.15: Soil porosity of uncompacted and compacted layers with tillage radish, vetch and black oat roots systems growing at three time points **92**

Figure 4.1: Biomass and WinRHIZO characteristic graphs for *R. sativus*, *Plantago*, *Taraxacum*, *Sonchus* and *Cirsium* **115**

Figure 4.2: *Cirsium* and *Plantago* plants at 28 days growth visualised using WinRHIZO, VG studio Max and RooTrak **122**

Figure 4.3: *Taraxacum* and *R. sativus* plants at 28 days growth visualised using WinRHIZO, VG studio Max and RooTrak **123**

Figure 4.4: Example of root death visualised with X-ray CT **125**

Figure 4.5: Cirsium root segmentations depicting root growth **127**

Figure 4.6: Example of root system processing using RooTh **129**

Figure 4.7: *Cirsium* replicate 3 indicating soil pore formation in vicinity of root growth from Day 0, 14 and 28 ..... **130**

Figure 4.8: Representative 3D renderings of the top 3.5 cm^3 column pore space determined from thresholding **134**

Figure 4.9: QuantIm graphs depicting number of pores, percentage of pore volume of the total pore volume and Euler number **135**

Figure 4.10: Example rhizosphere zone creation from original plant root ROI **137**

Figure 4.11: Delineation of rhizosphere zones, and example of 2D & 3D pore space identification and visualisation **151**

Figure 4.12: Representative 3D renderings of root systems grown in repacked soil columns with bulk density 1.8 g cm^{-3} **153**

Figure 4.13: Average surface area of roots (cm^2) and root volume (cm^3) of plant species derived from X-Ray Computed Tomography segmentation **154**

Figure 4.14: Example renderings of 3D segmented pore space incremental rhizosphere zones with distance from the root surface **158**

Figure 4.15: Porosity of incremental rhizosphere zones over time with distance from root surface **159**

Figure 4.16: Images of plant root hairs and mycorrhizae **166**

Figure 4.17: Principle component plots (PC) based on plant root and shoot characteristics with relation to soil and rhizosphere porosity measurements..... **168**

Figure 4.18: Straight ordination between root volume (cm^3) and rhizosphere porosity (%) for the 0-70 µm incremental zone **169**

Figure 5.1: Saturated moisture contents of soil cores and relative soil moisture contents of cores **174**

Figure 5.2: Average minimum and maximum greyscale values recorded over a 42 day period **179**

Figure 5.3: Example greyscale imagery of clay, clay loam and sandy loam soil **181**

Figure 5.4: Imagery detailing Root1 image import into VG Studio Max **184**

Figure 5.5: Root imagery of three different segmentation methodologies for *Cirsium* plants grown for 14 days in three contrasting soil types **186**

Figure 5.6: Root imagery of three different segmentation methodologies for *Cirsium* plants grown for 28 days in clay soil **187**

Figure 5.7: Example Root1 segmentation of Spear thistle roots grown in sandy loam soil for 14 days and root classification **188**

Figure 5.8: Example visualisation of *Cirsium* taproot convex hull's (mm^3) **190**

Figure 5.9: Example Root1 segmentation of Spear thistle roots grown in sandy loam soil for 14 days and root/ rhizosphere porosity classification ... **191**

Figure 5.10: Example pore thickness binary input and BoneJ output **192**

Figure 5.11: Images of *Cirsium* plant shoots subject to X-ray CT at 14, 28 and 42 days growth **193**

Figure 5.12: WinRHIZO 2D scans of *Cirsium* grown to 42 days in clay, sandy loam and clay loam soil **194**

Figure 5.13: Example greyscale image slice of each soil type at Day 0 ..... **204**

Figure 5.14: Example Root1 segmentation of *Cirsium vulgare* roots grown in sandy loam soil for 14 days and root/rhizosphere porosity classification **209**

Figure 5.15: Example 2D WinRHIZO scans of *Cirsium vulgare* root systems grown for 42 days **210**

Figure 5.16: Photographs of plant shoot material, graphs of shoot fresh and dry weight (g) and shoot surface area (cm^2) **211**

Figure 5.17: Aggregate size distribution of soil cores at Day 0 and 42 ..... **213**

Figure 5.18: Example 3D visualisations of *Cirsium vulgare* root systems .. **215**

Figure 5.19: 3D root system characteristic of *Cirsium vulgare* plants grown for 14, 28 and 42 days **217**

Figure 5.20: Average taproot length (cm) and Average taproot convex hull (cm^3) of Cirsium plants **218**

Figure 5.21: Porosity of incremental taproot rhizosphere zones of *Cirsium vulgare* plants over time (Days 14, 28 and 42) **219**

Appendix

A.2.1: Schematic of mycorrhiza identification using petri dish method **268**

A.3.1: 2D images of cover crop plants grown for 20 days scanned using WinRHIZO **272**

A.3.2: 2D images of cover crop plants grown for 58 days scanned using WinRHIZO **273**

A.3.3: X-ray CT visualisations of cover crop plants grown for 20 days scanned at 60 µm **274**

A.3.4: X-ray CT visualisations of cover crop plants grown for 58 days scanned at 60 µm **275**

A.3.5: Photograph of Tillage radish plants (*Raphanus sativus*), grown in 1.5 g cm^{-3} bulk density soil **280**

A.4.1: Ecoflora liaison emails **281**

A.4.2: Weed experts liaison emails **282**

A.4.3: Herbiseed liaison emails **285**

A.4.7: 2D images of novel species grown for 28 days scanned using WinRHIZO **289**

A.4.8: X-ray CT visualisations of *Plantago* plants grown for 14 and 28 days **290**

A.4.9: X-ray CT visualisations of *Cirsium* plants grown for 14 and 28 days **291**

A.4.10: X-ray CT visualisations of *Taraxacum* plants grown for 14 and 28 days **291**

A.4.11: X-ray CT visualisations of rhizosphere porosity for *Cirsium* plants grown for 14 and 28 days **292**

A.4.12: X-ray CT visualisations of rhizosphere porosity for *Plantago* plants grown for 14 and 28 days **292**

A.4.13: X-ray CT visualisations of rhizosphere porosity for *Taraxacum* plants grown for 14 and 28 days **293**

A.4.14**:** Example or Root Mask for *Cirsium* at Day 14 overlaying greyscale soil imagery for soil porosity calculation..... **293**

A.5.1: *Cirsium* plant shoots grown in sandy loam, clay loam and clay soil for 14 days **294**

A.5.2: *Cirsium* plant shoots grown in sandy loam, clay loam and clay soil for 28 days **295**

A.5.3: *Cirsium* plant shoots grown in sandy loam, clay loam and clay soil for 42 days **296**

A.5.4: 2D WinRHIZO scans of *Cirsium* plant roots grown in clay loam soil for 42 days **297**

A.5.5: 2D WinRHIZO scans of *Cirsium* plant roots grown in sandy loam soil for 42 days **298**

A.5.6: 2D WinRHIZO scans of *Cirsium* plant roots grown in clay soil for 42 days **299**

A.5.7: 3D visualisations of *Cirsium* plants grown for 14 days **300**

A.5.8: 3D visualisations of *Cirsium* plants grown for 28 days **301**

A.5.9: 3D visualisations of *Cirsium* plants grown for 42 days **302**

A.5.10: Percentage distribution of root mass between taproot and lateral roots of *Cirsium* plants grown for 14, 28 and 42 days **303**

A.5.11: Root1 macro code **305**

List of tables

Table 1.1: Typical bulk density and porosity values for agricultural soils **21**

Table 2.1: Indicates soil type, collection co-ordinates and date of collection **44**

Table 2.2: Indicates the calculation inputs for determining column volume and soil mass measurements for bulk density in dry compaction experiments ... **46**

Table 2.3: Indicates the calculation inputs for determining column volume and soil mass measurements for bulk density in wet compaction experiments .. **47**

Table 3.1: List of cover crop species identified from field consultation **58**

Table 4.1: List of plant species, how seed were procured and how species were initially identified for inclusion in the study **111**

Table 4.2: Details the results of the three way ANOVA conducted on biomass characteristics **114**

Table 4.3: Average biomass and WinRHIZO database from screening trial **119**

Table 4.4: Indicates time taken to segment root systems at 28 days old **123**

Table 4.5: Details dry biomass weights (g) and 2D WinRHIZO parameters average diameter (mm) and total root length (cm) for control and X-ray exposed plants **155**

Table 5.1: Percentages of clay, silt and sand determined by soil textural analysis **172**

Table 5.2: Equalised greyscale input 32 bit and output 16 bit values for each soil type at each scan time point **180**

Table 5.3: Root segmentation times of *Cirsium* plants from different soil textures **185**

Table 5.4: Results of root segmentation method grading **187**

Appendix

T.2.1: Outlines the amount of water needed to obtain to pack soil cores to specific moisture contents **269**

T.3.1: Table detailing the p values of individual ANOVA's calculating the significance of plant root diameters between plants being grown in 1.2 gm cm^{-3} or 1.4 g cm^{-3} soil **270**

T.3.2: Supplimentary data for published manuscript, indicates representative soil porosity of low and high phases within soil columns across the study period **276**

T.3.3: Supplimentary data for published manuscript, indicates representative whole root system characteristics within a column **278**

T.3.4: Supplimentary data for published manuscript, indicates representative root system characteristics confined to different bulk density layers within a column **279**

T.4.1: Ecoflora output database generated from online database resource **284**

T.4.2: Plant germination database detailing germination conditions and success rate (part 1) **285**

T.4.2: Plant germination database detailing germination conditions and success rate (part 2) **286**

Chapter 1: Introduction and Literature Review

1.1 Introduction

1.1.1 Rationale

Good soil structure is paramount in facilitating plant growth. In soils that have been physically degraded such as those subject to compaction, the structure of the pore network can be compromised. The associated increase in bulk density results in a decrease in total porosity, reduction in pore connectivity, changes to pore shape and reductions in pore size. These changes to the physical pore network subsequently have a detrimental effect on plant root growth, with greater penetrative forces being required for roots to extend through the compacted soil profile. However, growing plant roots have the ability to alter the environment in their immediate vicinity and therefore have the potential to ameliorate soil that is in a compromised physical condition. Changes in soil porosity in the rhizosphere zone that occur as a result of root growth indicate the potential they have to be used as a natural means to help alleviate soil compaction via the generation and modification of pore space.

This research aims to further the understanding of root-soil interactions by investigating how soil physical degradation in the form of compaction, and resultant soil architecture, affects the ability of plant roots to develop and grow in these sub-optimal conditions. By employing X-ray Computed Tomography to image plant roots and soil porosity *in situ,* assessments of plant species' suitability in remediating soil structure is then considered.

1.2 Literature review

1.2.1 The importance of soil

Soil supports an intricate system of plants and microbes in a heterogeneous porous medium with a variety of constantly-changing chemical and physical conditions (Enriqueta Arias et al. 2005). Organisms that reside in soils contribute to a range of ecosystem services, which are vital for the continued sustainable function of both managed and natural ecosystems (Barrios, 2007). In addition to supporting biological communities, appropriate soil structure and its maintenance can help to reduce the risk of soil erosion, regulate water quality/supply and help to ensure continuous agricultural production (Haygarth and Ritz, 2009; Power, 2010). Therefore maintaining adequate soil quality is important both within agricultural systems and the wider environment (Kibblewhite et al. 2008) as soil profiles play a key role in supporting below ground habitats which support these complex biological communities (Barrios, 2007). By far the greatest species diversity in agricultural systems is found within the soil profile (Brussard et al. 2007). However, soil remains an undervalued and underappreciated resource globally. It has been identified within the European Commission's Thematic Strategy for Soil Protection (2002) that erosion, organic matter decline, compaction, landslides, contamination and soil sealing are some of the most pressing threats to soil quality.

1.2.2 Soil texture & structure

The texture of a soil is conventionally defined by the proportion of sand, silt and clay particles (Gregory and Nortcliff, 2013). Soil structure refers to the arrangement of these particles as well as soil organic matter (SOM) into aggregates of different sizes (Barrios, 2007). Soils with a higher proportion of clay particles are likely to have stronger aggregates which are larger and more difficult to break, in comparison to aggregates in sandy soils which will be more easily broken (White, 2006). The quantity, size and stability of soil aggregates is dependent on a number of factors including organic matter, soil microorganisms and fauna and disruption dynamics such as bioturbation and cultivation (Tisdall and Oades, 1982). Soils are comprised of aggregates of different sizes, microaggregates (< 250um diameter) are bound in macroaggregates (>250 um) (Edwards and Bremner, 1967). Aggregates are stabilised by organic binding agents and are bound together by roots and fungal hyphae and plant and microbial polysaccharides (White, 2006). The structure of soil aggregates has a direct effect on the composition of macropores, mesopores and micropores within the soil profile, which in turn affect the extent of root growth (Passioura, 2002). This is because larger aggregates contain larger pores than smaller aggregates, with larger pores more likely to form areas of weakness, this results in reduced strength of the macroaggregate in comparison to a micro-aggregates (Dexter, 1988).

The structure of a soil can change naturally due to wetting and drying cycles as well as freeze thaw cycles, notably clay soils are more likely to be affected

by these conditions resulting in increased aggregation. Conversely, sandy and silty soils have less well defined structures and are more likely to be affected by these conditions, resulting in slumping, particularly if they have been subject to excessive cultivation and have been weakened (Batey and McKenzie, 2006). The structural stability of a soil can be defined as the resistance of the soil structure to external factors such as water (Evans et al. 1996). For example a poorly drained soil when waterlogged is at an increased risk of compaction; conversely compaction increases the bulk density and decrease porosity (Diaz-Zorita et al. 2002) resulting in increased risks of waterlogging, leading to a cycle of degradation (Evans et al. 1996).

1.2.3 'Healthy' soil

The health of a soil, which is essentially the extent to which it is fit for intended purpose, is arguably dependent on the provision and maintenance of four major functions, *viz*. carbon transformations, nutrient cycling, soil structural maintenance and the regulation of pests and diseases (Kibblewhite et al. 2008). It can be defined as the capacity for a soil to function to provide a range of ecosystem services that are dependant on the soils localised environment (Ferris and Tuomisto, 2015). For example, in an agricultural setting a healthy soil is one that reaches a level of fertility which is capable of supporting the production of food and fibre to a quality level sufficient to meet human requirements (Kibblewhite et al. 2008). Comparatively soil health in unmanaged natural systems can be determined by its ability to

support native plant growth. It can be measured by assessing biological, chemical and physical characteristics such as; bulk density, aggregate stability, cation exchange capacity (CEC), pH level, water holding capacity, water infiltration rate and macro/micronutrient analysis (Enriqueta Arias et al. 2005). Describing soil as having health treats soil as a living biological entity that subsequently affects plant health. Therefore through the growth of plants, soil health is also connected with the health of animals, humans, and ecosystems within its domain (Lal, 2016).

1.2.4 Degraded and compromised soils

The negative effects of land use on soil can be summarised as soil degradation. Soil degradation describes the deterioration of the productivity and further environmental services of a soil as a direct result of human activity (Kuhn, 2014). A degraded soil includes any soil by which the destruction of the topsoil has occurred by wind and water erosion, it can also be determined by the losses to the soil through lack of nutrients, structural damage or introduction of pollutants (Morgan, 2005). Another type of physical soil degradation is soil compaction. Soil compaction enhances harmful physical, chemical and biological processes which, in the context of inappropriate soil management then lead to further degradation (Soane and Ouwerkerk, 1995).

1.3 Soil compaction

1.3.1 Soil compaction and its impact

Soil compaction is a globally-pervasive problem (Chen et al. 2014, Gregory et al. 2007), with an estimated 33 million hectares of land being directly affected in Europe alone (Batey, 2009). In England, soil compaction has been identified by Defra (2007) as one of three key threats to the agricultural and the environmental productivity of soils, along with soil organic matter (SOM) decline and soil erosion (Hamza and Anderson, 2005). Soil compaction is classed as a form of physical degradation (Van den Akker and Soane, 2005). The phenomenon is defined as '*the process by which soil grains are rearranged to decrease pore space by bringing them into closer contact with one another, thereby increasing the bulk density*' (Hamza and Anderson, 2005). This increase in density results in a subsequent reduction in the volume of air (Table 1.1) but not necessarily a significant change in the volume of water within the soil (Knappett and Craig, 2012). As a result, soil strength is increased and the structure is partly destroyed resulting from induced changes in the soil fabric (Van den Akker and Soane, 2005). For this reason the dry soil bulk density is the most frequently used parameter to characterise the state of soil compactness (Hamza and Anderson, 2005).

Table 1.1: Typical bulk density and porosity values for agricultural soils, these values are highly dependent on soil texture (after Soffe, 2003).

Bulk Density (g cm^{-3})	Porosity (%)	Description
0.5-0.8	>70	Loose, uncompacted topsoils,
~1.0	60-65	Well structured soil
~1.5	45	Compacted, root penetration difficult
~2.0	25	Dense, no root growth

1.3.2 Causes of soil compaction

The compaction of soil can occur under both under natural conditions such as rain impact, natural packing, drying, bonding and cementation as well as those subjected by human and animal activity (Soane et al. 1981; Batey and McKenzie, 2006). It is a phenomenon associated primarily with agricultural settings but it can also be prominent within areas undergoing land restoration, timber harvesting, amenity land use, underground pipeline instillation, wildlife pathways and the remodelling of landscapes (Batey, 2009; Passioura 2002). Typically within an agricultural environment, compaction most commonly occurs via the compressive force derived from the passage of wheels, tracks or rollers, tillage machinery and the trampling/ passage of draft or grazing animals (Soane et al. 1981; Ball et al. 1997; Van den Akker and Soane, 2005; Batey, 2009) or as a result of short crop rotations, intensive grazing and inappropriate soil management practices (Hamza and Anderson, 2005; Chen et al. 2014). Although less common, soil compaction can also occur naturally, for example via the hard dense layers formed during periglacial phenomena (Batey, 2009; Grzesiak et al. 2013).

1.3.3 Effects of soil compaction

Compaction anywhere in a soil matrix can compromise effective functioning of the system, but once it extends to the subsoil it becomes increasingly hard to alleviate (Spoor et al. 2003). The ability of a subsoil to support given loads without suffering compaction damage is dependent upon the soil type and the arrangement of particles and aggregates (Spoor, 2006). Subsoil compaction has been acknowledged by the European Union as a serious form of soil degradation due to its persistence once established and a lack of effective remedial methods to counteract it once manifested (Hazma and Anderson, 2005). In the majority of soils which have been subject to arable cropping systems there is frequently a strong soil layer located just below the cultivation depth often referred to as the 'pan' layer, which often absorbs compaction stresses and subsequently prevents the subsoil from becoming compacted (Spoor et al. 2003). In the field compaction on the upper surface can be detected by features such as areas of waterlogging on the surface, an increase in soil strength, a reduction in porosity, changes in soil structure, soil colour and the altered distribution of roots within the soil profile (Batey and McKenzie, 2006; Batey, 2009). Compaction results in the alteration of soil properties including the mean size of pores in the soil matrix (Tracy et al. 2011), a loss of these structural macropore networks results in poor aeration, nutrient depletion and reduced permeability of water and roots into the soil (Ball et al. 1997; Batey, 2009). In most cases an increase in compaction leads to an increase in soil strength (Gregory et al. 2007), a dynamic

parameter which is directly affected by soil structure, texture and relative water content (Chen et al. 2014). The compaction process of the soil reduces biotic activity and changes the soil from an aerobic to anaerobic state (Whalley et al. 1995). The presence of roots, earthworms and other fauna are subsequently decreased and this results in damaging effects on soil physical properties (Gregory et al. 2007; Figure 1.1).

1.3.4 Compaction effects on soil moisture and aeration

Soil water content is the most important factor influencing soil compaction processes (Hamza and Anderson, 2005). At all compaction levels, the penetration resistance increases with decreasing soil water potential (Lipiec and Hatano, 2003), and increasing soil moisture content causes a reduction in the load a soil is able to support before deformation (Hamza and Anderson, 2005). As a soil dries, water availability declines and mechanical impedance increases, which has a subsequent negative effect reducing root elongation rates (Schmidt et al. 2013). In wet compacted soil the elongation rate of individual roots may be limited by oxygen deficiency and mechanical impedance (Valentine et al. 2012), comparatively in compacted dry soil, root elongation may be limited by a water deficit and mechanical impedance (Bengough et al. 2011). Soil aeration is a dynamic parameter which is largely influenced by soil structure, texture and water content (Chen et al. 2014). Compaction affects the extent to which soil is permeable to air, which controls gas transport processes through the soil profile (Batey,

2009). Compaction forces alter geometric characteristics of pores such as pore size, total porosity, pore continuity, pore size distribution and shape (Chen et al. 2014). In sandy or granular soils, the level of air permeability is highly correlated to the level of macropores, compared to clay soils where pore continuity plays a key role in air dispersion throughout a soil profile (Stokes et al. 2009).

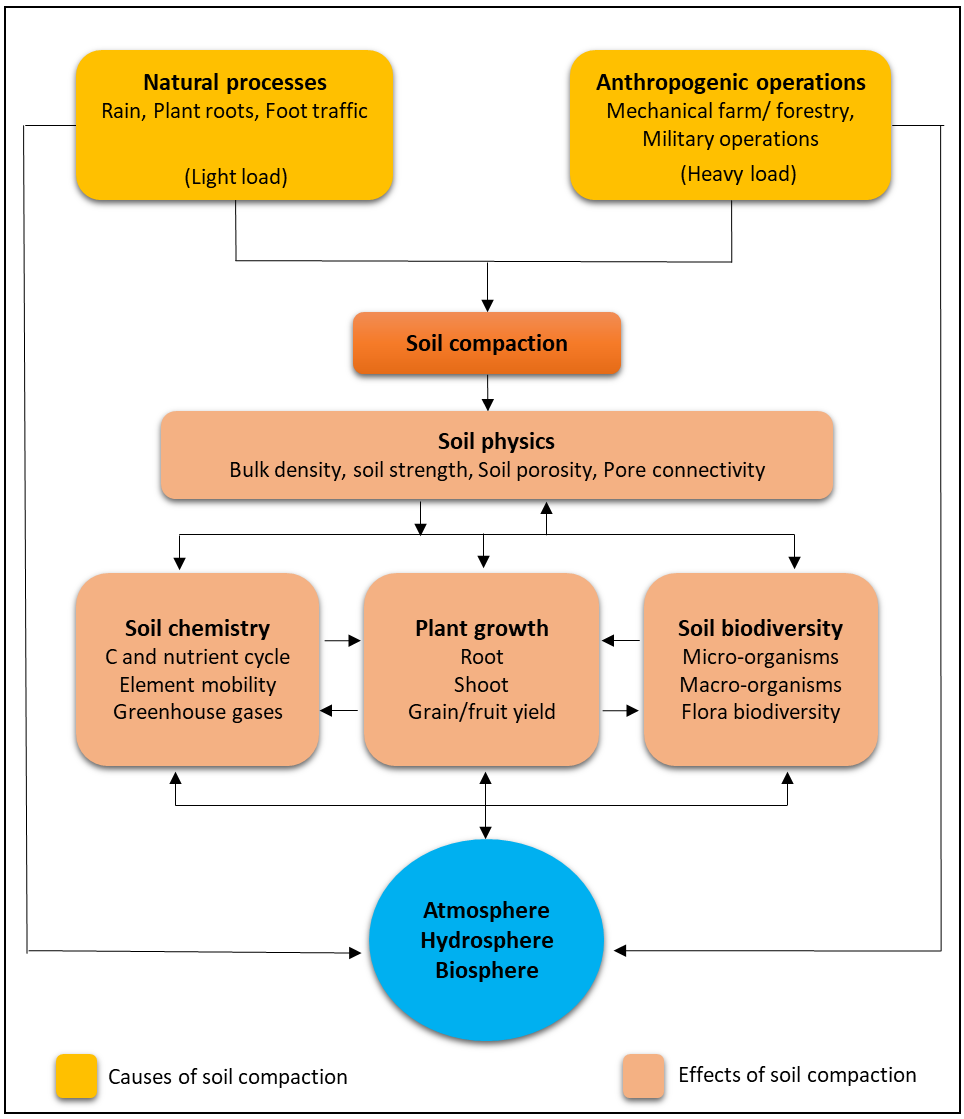


Figure 1.1: Causes of soil compaction and the effects on soil physical properties with ultimate direct effects on soil chemistry, plant growth and soil biodiversity. Figure adapted from Nawaz (2012).

1.3.5 Compaction effects on root and shoot biomass

The restrictive effects of soil compaction can be physically constraining to overall plant growth and yield underpinned by the poor development of root systems (Barzegar et al. 2006; Grzesiak et al. 2013). It has been suggested that root impedance in soils is texture-dependent but generally occurs between 1.55 - 1.85 g cm^{-3} (Bowen, 1981). Compaction restricts plant root growth by increasing mechanical resistance or decreasing the supply of oxygen which thereby impedes root development (Chen et al. 2014). The impact of soil compaction extends beyond affecting root growth characteristics, by affecting both shoot morphology and general plant physiology and growth (Passioura 2002; Tubeileh et al. 2003). A number of studies, including one that assessed 22 crop species (Materechera et al. 1991) suggest that dicot roots are better able to penetrate compacted subsoil in the field than monocot roots, and species with thicker roots tend to exhibit great penetration of the subsoil, however they are subject to greater morphological changes in root architecture due to compaction pressures (Chen and Weil, 2009; Materechera et al. 1991). Other changes such as reductions in mineral nitrogen may take place due to poor ventilation of compacted soils reducing the rate of organic matter mineralisation, this subsequently reduces nitrification (Motavalli et al. 2003). This can be observed in physical changes to crops such as pale leaf colours and distribution of roots in the soil profile (Batey and McKenzie, 2006). The secondary effects of soil compaction include yield reduction in crop species, this reduced plant growth can lead to low inputs of organic

matter into the soil, reduced nutrient cycling and reduced activity of micro-organisms (Rosolem et al. 2002).

1.3.6 Remediation of compacted soils

Once a soil has been degraded by compaction it can take a considerable amount of money, time and energy to alleviate (Spoor, 2006), since conventional remediation techniques such as deep tillage are expensive and energy intensive, and in any case often only provide transient remediation (Williams and Weil, 2004). Secondary problems may also occur from mechanical remediation including cloddiness of the soil, disruption of natural root and water pathways, the absence of subsurface drainage, increased waterlogging and the recompaction of the remediated area (Spoor et al. 2003). As soil compaction occurs via the decreases in soil porosity (or increases soil bulk density), increasing a soil's porosity (or decreasing bulk density) is a logical way of reducing soil compaction.

Plant species that have the ability to penetrate soils of a high strength are usually observed to possess a deep tap-root system, such as forage radish (*Raphanus sativus*), rapeseed (*Brassica rapa*), pea (*Pisum sativum*) and lupin (*Lupinus spp*.) (Clark and Barraclough, 1999; Hamza and Anderson, 2005; Chen and Weil, 2009). Deep-rooted cover crops may help to alleviate effects of subsoil compaction and increase infiltration rates when incorporated into a cover crop rotation especially on no till systems (Williams and Weil, 2004). An experiment by Colombi et al (2017) illustrated this phenomenon when they

assessed the root growth patterns of soybean (Glycine max L.), wheat (Triticum aestivum L.) and maize (Zea mays L.) towards artificial macropore systems using X-ray CT. The specific effect of the root system on soil structure depends on the plant species grown, their root architecture and the initial composition of the soils structure (Hamza and Anderson, 2005). Biopore creation as a result of root growth may provide a path of least resistance through the soil profile and be utilised by subsequent crop species (Williams and Weil, 2004). Plant roots also help to stabilise soil structure and once they start to decay they contribute a source of organic matter helping to increase the soil's resilience to degradation (Ziyaee and Roshani, 2012). Improved land management techniques that incorporate cover crops into agricultural systems will help to ensure the sustained remediation of soil physical conditions via plant root growth and death (Storr et al. 2019).

1.4 Plant roots

1.4.1 Root development

The first root which emerges from a seed (the radicle) grows downwards gravitropically, and typically in dicotyledonous species the radicle becomes the taproot (Stokes et al. 2009). The rooting depth of the radicle is particularly important as it provide the initial anchorage of the plant within the soil (Stokes et al. 2009). Additionally lateral roots develop often in the upper soil horizons which can form a mesh that stabilises the soil (Schmidt et al. 2013). The topology of a developing root system largely determines how

roots occupy a given area of soil, with the development of thick roots generally determining the arrangement of associated thin roots, with this relationship having an effect on the reinforcement of the soil profile (Stokes et al. 2009).

1.4.1a The root cap and its function

The root cap provides protection against mechanical damage to the root apical meristem via the protection of the stem cell zone (Arnuad et al. 2010) (Figure 1.2) and increases the penetration strength of a root when growing into compact soils (Hahn et al. 2008). As well as protecting against mechanical damage to the root tip and aiding physical penetration, the root cap is the first point of contact between growing roots and the immediate soil environment (Tracy et al. 2011). Here the root cap plays a role in the identification of environmental sensing pathways (Arnaud et al. 2010), processing both external and internal stimuli resulting in altered root growth and development (Hahn et al. 2008). When roots are advancing in a soil, if continuous pores of sufficiently large diameter do not already exist the root tip must exert a force to deform the soil to allow its passage (Bengough and Mullins, 1990). The root tip has been observed to increase in diameter in roots that are impeded (Clark et al. 2003). Other factors determining the movement of a root tip though the soil include hydrostatic pressure forces, and if these are not sufficient to overcome soil impedance then the elongation of the particular root tip will stop (Hamza and Anderson, 2005).

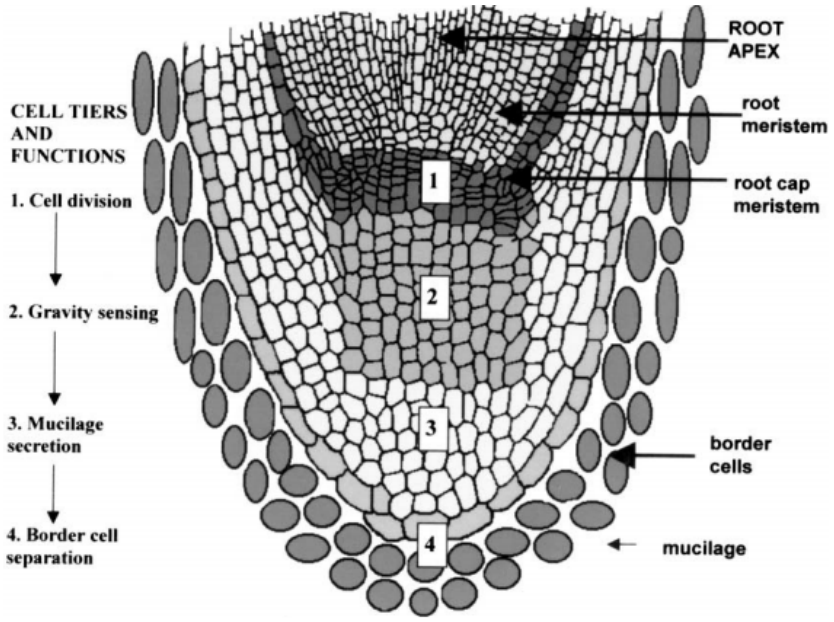


Figure 1.2: Root cap structure and development (Barlow, 1975). Note root meristem protected by the root cap.

1.4.1b Root hairs

The presence of root hairs greatly affects the surface-volume ratio of a root and they have been linked to good root penetration levels in hard soils by providing anchorage, acting as a bracing structure to the growing root tip (Bailey et al. 2002; Chimungu et al. 2015). For example Haling et al. (2013) found that plant genotypes with root hairs had an advantage for root penetration into high-strength layers in comparison to hairless root genotypes. Additionally root hairs aid the acquisition of resources such a nutrient uptake (Lamont, 2003) across air-filled pores within the soil (Bengough, 2011).

1.4.1c Lateral root development

Lateral roots originate from the primary root with their direction of growth being a genetically defined and environmentally regulated process (Negi et al. 2008). The initiation of lateral root development starts with the asymmetric cell division of founder cells, requiring new primordia to break through the overlying tissues before the root is able to emerge into the soil (Peret et al. 2009). Hydrostatic pressure (turgor) within the elongating region of the root provides the force necessary to push the root cap and meristematic region through the resisting soil (Hamza and Anderson, 2005). It has been observed that an accumulation of ethylene around the meristematic tissue can cause a dramatic increase in the formation of both lateral roots and root hairs as ethylene gas accumulates under soil conditions where diffusion of oxygen is low and biological respiration is high (Taylor and Brar, 1991).

Ultimately, the lateral root elongates and undergoes further reiterative branching resulting in a complex root architecture that allows optimum nutrient uptake and creates the underground support network that is essential for anchoring the plant (Negi et al. 2008).

1.4.1d Root exudates

Increasing evidence indicates that plants can shape the soil microbiome through the secretion of root exudates (Chaparro et al. 2012; Hu et al. 2018; Olanrewaju et al. 2019). The release of root exudates can alter the structural and hydraulic properties of a soil in a similar way to repeated wet drying

cycles, it may also contribute to the aggregation of soil particles in dry soil in which the viscosity of exudates often increases (Tracy et al. 2011). Additionally exudates may stabilise soil structure in the rhizosphere by increasing the strength of the bonds between particles increasing soil macro-aggregation (Baumert et al. 2018). Exudates are also important in maintaining root:soil contact in drying soils because the surface tension of the exudate decreases as the soil dries, increasing its ability to wet surrounding soil particles (Tracy et al. 2011). Other studies suggest that the rhizosphere may be wetter than bulk soil despite relatively high water extraction rates due to the formation of a 'coherent sheath of soil permeated by mucilage and root hairs' known as the rhizosheath (Walker et al. 2003; Tracy et al. 2011). The rhizosheath subsequently aids nutrient acquisition by the plant due to localised increased levels of water content in the sheath (McCully, 1999). This acquisition can be hindered if the matric potential of the soil drops below -5kPa, where lower conductivity of the soil can result in reduced transpiration rate of plants resulting in root shrinkage, reduced root: soil contact and therefore decreasing nutrient and water acquisition (Carminati et al. 2013).

1.4.2 Root elongation and radial expansion

Root elongation decreases in compacted soils as a result of reduced rates of cell division in the meristem and a decrease in individual cell length (Bengough and Mullins, 1990). The impedance to the roots may also result in changes in root diameter and patterns of lateral root branching. Root

elongation depends on the ability of the root to produce a growth pressure large enough to deform the soil (Jin et al. 2013). As a result, when roots encounter compacted soil, their initial response is an increase in radial expansion, resulting in shorter, thicker roots with an increased root hair density (Tracy et al. 2011). This resistance of the root to compressive forces is known to increase with the thickness of the epidermal layer and observations show that cells in the outer cortical region tend to have thick cell walls and be closely packed, which may make the root stronger and more resistant to deformation (Bengough and Mullins, 1990; Atwell, 1993; Chimungu et al. 2015). The phenomenon of root thickening in response to strong soil has been interpreted as an important root trait to enable the reduction of axial stress at the tips of roots elongating through strong soil (Hettiaratchi, 1990). Roots are able to penetrate soil through alternating radial and axial expansions (Benough and Mullins, 1990; Figure 1.3). This fluctuation in diameter helps to destabilise the soil and as a result helps to produce a level of remediation to compacted soil (Hamza and Anderson, 2005) via the radial expansion of the region behind the root tip weakening the soil in the root cap zone (Hettiaratchi, 1990).

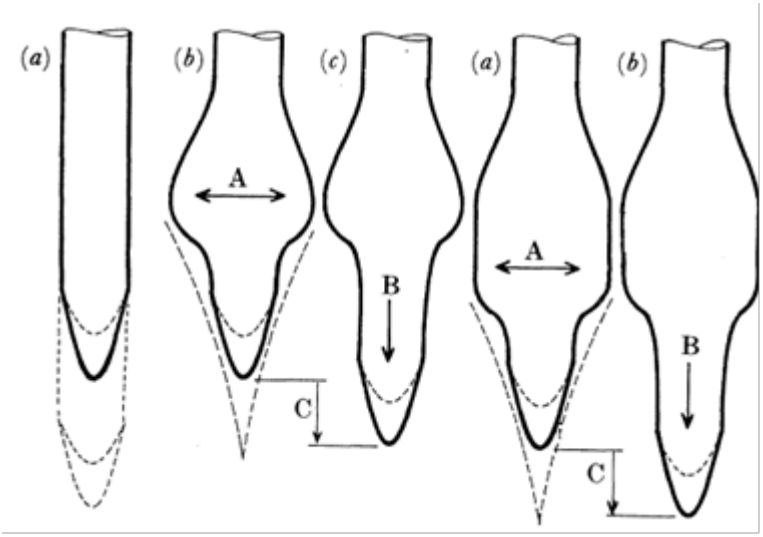


Figure 1.3: Steps in the root expansion model. (a) Initial axial extension in root cap zone, (b) Radial expansion of region behind root tip, (c) Axial extension resumed; A, radial growth, B, axial growth, C root extension increment. Diagram taken from (Hettiaratchi, 1990).

1.4.3 Root growth into pores

The size of a pore in which a root is growing can directly limit the rate of root growth (Passioura, 2002). Roots grow preferentially towards zones of low mechanical impedance such as biopores, because soil failure ahead of the growing root will tend to lead the root towards new zones of weakness such as other cracks of biopores (Cresswell and Kirkegaard, 1995). When facing a constraint imposed by a rigid pore, a root must adapt its shape and size in order to fit with the pore dimensions (Kolb and Hartmann, 2012). Therefore the larger the pore is, the less the root has to adapt to penetrate it. Roots can penetrate soil with very small pores by deforming soil to make a new root channel, elongate along an existing pore or crack, or negotiate a crack at an angle of incidence before penetrating the soil (Jin et al. 2013). To elongate through existing channels which are smaller than the root diameter, roots

must exert a growth pressure to deform the soil ahead and around the root (Clark and Barraclough, 1999). The growth pressure (kPa) that the roots exert on the soil is equal in magnitude to the soil pressure that opposes root elongation and it may differ in the radial and axial directions (Kolb and Hartmann, 2012). The maximum axial pressure that a root can exert is between 0.9-1.3 MPa (Bengough and Mullins, 1990). The presence of fine roots, which are of greatest similarity to the size of soil pores, is therefore also advantageous as they can elongate into a textured pore space and are less likely to be affected by an increase in soil strength (Jin et al. 2013). The production of mucilage (Clark et al. 2003) helps to contribute to low soil-root friction, which is considered a trait conferring better penetration of strong soils, it may also increase the axial pressure on the root tip and in so doing reduce the rate of cell division and or expansion (Jin et al. 2013).

Passioura (2002) identified that plant roots will preferentially grow into large continuous biopores which have been previously made and maintained by roots or soil fauna. Root channels help to increase the total soil porosity as well as advantageously affecting pore size and continuity often restructuring soil particle arrangements as they grow, as well as playing an important role in root anchorage efficiency (Stokes et al. 2009; Chen et al. 2014; Ehrmann and Ritz, 2014).

1.4.4 Root response to soil compaction and mechanical impedance

Mechanical impedance is experienced to a varying degree by virtually all roots growing through soil and is one of the most important factor in determining root elongation, with a number of studies suggesting that as the level of mechanical impedance increases, the rate of root elongation and proliferation decreases (Bengough and Mullins, 1990). The depth of root proliferation in a soil profile is limited by both abiotic factors such as temperature, aeration and physical factors such as high levels of mechanical impedance (Lynch and Wojciechowski, 2015). Impedance causes physical limitations to root growth with a typical soil penetrometer resistance of 2.0 MPa being described as the threshold for root elongation (Chimungu et al. 2015). High levels of mechanical impedance are associated with strong compacted soils of high bulk density or low water content (Lynch and Wojciechowski, 2015).

Plants possess an impressive ability to adapt their root development to maximize both reproductive success and survival in suboptimal environments (Negi et al. 2008). The pattern of a root system is one of the most important criteria in assessing the significance of soil compaction. Typically within compacted layers, roots will attempt to grow through conducive soil between sections of compacted soil (Batey and McKenzie, 2006). When plant roots encounter compacted layers they react in a number of ways including slower downward growth and reduction in overall root frequency (Batey and McKenzie, 2006). Throughout their development plants require a sufficient level of soil mechanical strength to be delivered by

the soil to provide adequate anchorage (Bengough and Mullins, 1990). The maximum soil strength which roots can overcome is determined by the maximum turgor generated within the root elongation zone and both the shape and frictional characteristics of the root tip (Bengough and Mullins, 1990). As soil strength increases the levels of mechanical impedance to plant root growth also increases (Chimungu et al. 2015). As a result roots which are able to grow into compacted layers are observed to have a greater thickness and often distorted appearance (Batey and McKenzie, 2006).

1.4.5 The rhizosphere

Soil is a dynamic environment and presents changes in physical and biological characteristics with depth through a profile over small spatial and wide temporal scales. Subsequently each plant root has a unique rhizosphere environment, its ability to survive depends on the capability of the root system to react to changes in this local environment and respond accordingly (Walker et al. 2003). The zone of soil in immediate proximity to the root surface is known as the rhizosphere (Hiltner, 1904). The soil and rhizosphere environment has significant influence on the overall development of a root system's size and shape (Downie et al. 2014), with the rhizosheath and rhizosphere representing some of the most dynamic zones (Rabbi et al. 2018). In compacted soils it has been observed that plant root exudates can improve mechanical conditions for root penetration (Oleghe et al. 2017). Conversely roots have been observed to influence processes of soil aggregation and can

result in the compression of soil structure in the rhizosphere due to root expansion (York et al. 2016). The arrangements of roots directly determines the volume of soil altered by the roots presence with respect to specific processes (Schluter et al. 2018), such as the release of root exudates (a process which has been well studied) that create an environment that includes, fatty acids, proteins, amino acids and sugars (Chaparro et al. 2012). The dynamic nature of the rhizosphere provides both biophysical and chemical gradients with distance from the root surface (Kuzyakov and Razavi, 2019). These gradients impact on a number of physical factors such as water and nutrient uptake, gas exchange and particle rearrangement (Helliwell et al. 2019). The latter results in physical structural alteration of the soil network. Due to the fragile nature of soil, understanding the role of root growth on the structure of the rhizosphere is challenging. A variety of techniques have been developed to try to facilitate the study of the rhizosphere including; thin sections, rhizoboxes as reviewed by York et al, (2016). Transparent media has been used to enable *in situ* 3D imaging of living plants and root-associated microorganisms (Downie et al. 2012), X-ray CT has been used to study both root- soil contact (Schmidt et al. 2012) and rhizosphere porosity (Heilliwell et al. 2017; 2019) over time, generating data about structural changes without the need for destructive sampling.

1.5 X-ray Computed Tomography

The ability to non-destructively observe and measure plant root traits and soil structure *in situ* represents an important goal for many plant and soil scientists (Hodge, 2004). Research using non-destructive methods persistently emerges (Gregory, 2009), with high throughput, plant root phenotyping becoming increasingly more common and accessible (Atkinson et al. 2019). As a result, significant advances are being made in the way raw X-ray CT greyscale data is processed. Three specific types of image segmentation techniques are pertinent to studying root:soil interactions, specifically soil and pore space imaging, plant root imaging and rhizosphere imaging.

1.5.1 Soil and pore space imaging

X-ray CT allows the observation of 3D structure of soil macro and micro porosity, information about the pore geometry of soil is important when considering the implications for plant root growth and transfer of air, water and nutrients through soil profiles (Pierret, 2002). Boundaries between different soil constituents such as air, organic matter, minerals and the soil solid phase can be difficult to classify accurately (Houston, 2013). Global thresholding approaches to convert greyscale imagery into binary imagery originating from Otsu, (1979) are often employed, however these do not take into account the heterogeneity of the soil system across its profile.
One method for determining porosity, pore size distribution and pore connectivity is to use a bin bi-level approach (Vogel et al. 2010) in the open

access software Quantim (http://www.quantim.ufz.de/) which quantifies the parameters in 3D. This process allows each image to have an individual threshold value. This method has previously been used to assess the impact of different management practices on soil structure (Bacq-Labreuil et al. 2018) and accounts for the spatial heterogeneity observed within a soil core.

X-ray CT has been used increasingly as a tool to investigate the undisturbed rhizosphere with a focus on root-soil contact (Schmidt et al. 2012) and soil pore formation (Helliwell et al. 2017; Koebernick et al. 2018;; Rabbi et al. 2018; Schluter et al. 2018; Helliwell et al. 2019). Roots have been observed to alter soil structure as they grow, with some studies noting deformation at the root tip and a reduction in pore space in the zone immediately adjacent to the root (Aravena et al. 2011). This has been attributed to the soil being compressed as the growing root expands, subsequently increasing root-soil contact. Other studies have depicted increased in porosity from the presence of plant roots over short time scales in different soil textures (e.g. Feeney et al. 2006; Helliwell et al. 2017). The ability to assess soil structural changes at microscale resolutions with proximity to plant roots enables links to be made between plant phenotypic traits and their subsequent ability to modify their environment. Due to the uncertainties around the impact structural changes have over time has at the rhizosphere scale, the generation of soil structure by plant roots at a pore scale warrants further investigation.

1.5.2 Root imaging

In situ measurements of root architecture and its evolution over time, without the need for physical removal of roots provides an enormous contribution to many areas of fundamental and applied plant science (Maenhout et al. 2019). Increasingly the imaging of plant roots over time is being incorporated into experimental design allowing the quantification of the dynamics of plant root development (Tracy et al. 2012). Numerous methods have been developed that employ different segmentation techniques. These range from manual segmentation methods (Ahmed et al. 2016) which rely on region growing using an adaptive threshold (Gregory, 2003), through to semi-automated such as RooTrak (Mairhofer et al. 2012). The latter employ a tracking-based strategy which follows the root cross-sections through a sequence of images, with the initial digital processing seed-point being identified manually by the user. Finally automated methods such as RooT1 (Flavel et al. 2017) which uses the ImageJ platform to segment root material based on user selected greyscale ranges imported into a macro. The application of techniques depends on multiple factors such as the resolution of the dataset, the soil type, moisture content and plant species grown.

1.6 Research aims and objectives

The overall aim of this research was to investigate the interdependent relationships between root system architecture and soil structural development in compacted soils, specifically in relation to the capability of plant roots to generate pore space at micro-scales. The work utilised X-ray Computed Tomography to non-invasively image plant root development over time in soils of different textures and bulk densities.

Overarching hypothesis:

'Plant species able to penetrate severely-compacted soils exhibit root system architectural traits that enable them to do so, and facilitate soil structural genesis.'

Sub-aims with associated individual hypotheses:

1. To assess the variation in the ability of cover crop and wild plant species to generate root mass in extremely compacted soils.
   Hypothesis: *Plant species with taproots will be able to generate greater root mass in compacted soil conditions.*

2. To identify what impact compacted soil layers have on plant root architecture development.
   Hypothesis: *Compacted soil layers will modify the architecture of plant root systems, with variation in such responses between species with contrasting inherent root system types.*

3. To quantify the ability of plant roots to generate porosity at both soil core and rhizosphere scale

   Hypothesis: *Pore space created via the action of plant roots is greater in the rhizosphere than bulk soil.*

4. To assess changes in rhizosphere structural development over time.

   Hypothesis: *Temporal changes will occur in the pore structure of the rhizosphere as a result of plant root development*

1.7 Thesis structure

Chapter 1 has provided an overview of the subject area covered in this thesis and introduced the rationale behind the research conducted and outlined the aims and objectives. **Chapter 2** provides an overview of the generic methods used to prepare materials, collect data and analyse outputs. **Chapter 3** assesses the effect of soil compaction on cover crop root architecture. This work has been published in PLOS ONE (Burr-Hersey et al. 2017) and hence the second half of this chapter is structured in guidance with the journal format. **Chapter 4** assesses the impact of soil compaction on novel plant root architecture and subsequent pore space creation at both rhizosphere and system scales**.** This work has been submitted to the Journal of Experimental Botany and is currently under review, hence the second half of the chapter is structured in accordance with the journal format. **Chapter 5** assesses the impact of soil texture on the root system architecture of *Cirsium vulgare* and associated pore space creation in the rhizosphere. This work has been prepared as a manuscript for submission to the Journal Plant and Soil, hence the second half of this chapter is structured in accordance with the journal format. **Chapter 6** provides a general discussion of the key findings reported in each chapter and highlights the major conclusions and areas of further work from the research conducted.

Chapter 2: Generic methods

An overview of the practical methods used to determine a range of experimental parameters presented in this chapter.

2.1 Soil

2.1.1 Soil preparation

2.1.1a Collection

Soil was collected from the University of Nottingham Sutton Bonington Campus Farms. Over the course of the study three different soil types were obtained from three different locations (Table 2.1). Soil samples were collected from at least 2 m into the field from the field margin. At each sample site soil was collected from 5-30 cm depth. On each collection date approximately 50 kg of each soil type was obtained.

Table 2.1: Indicates soil type, collection co-ordinates, soil textural properties, and date of collection and corresponding chapter number.

Soil type	Grid co-ordinates	Chapter No.	% Clay	% Silt	% Sand	Date
Sandy loam	52°50'07"N, 1°15'04.0"W	1	9.52	26.12	64.35	18.01.2016
Sandy loam	52°50'07"N, 1°15'04.0"W	2	9.52	26.12	64.35	29.08.2016
Sandy loam	52°50'07"N, 1°15'04.0"W	3	9.52	26.12	64.35	13.09.2017
Clay	52°85'44"N, 1°12'59.9"W	3	43.32	28.45	28.23	13.09.2017
Clay loam	52°85'77"N, 1°12'69.3"W	3	31.62	30.52	37.86	13.09.2017

2.1.1b Preparation and storage

Soil was spread to air dry at 16°C for between 3-5 days before sieving. A sample of each soil type was then oven dried at 105 °C for 48 h to determine the moisture content of the stored soils. All soil was sieved to <2 mm, for the clay and clay loam soil types it was necessary in some instances to break apart large soil aggregates using a hammer prior to sieving. Sieved soil was stored in labelled black bin bags in a cold store at 5°C for up to 6 months.

2.1.2 Soil compaction

2.1.2a Dry compaction technique

For the dry soil compaction technique used in Chapter 3 PVC columns (17 cm height and 7.56 cm diameter) were used. Each column was fitted with a fine mesh base secured with double-sided tape to ensure maximum soil retention within the core throughout the course of the study. Two bulk densities were established, *viz.* 1.2 and 1.4 g cm^{-3} for 0-6 and 6-16 cm depths respectively. This was achieved by compacting the appropriate mass of oven dry soil with respect to volume, i.e. 318 and 619 g respectively (Table 2.2).

Table 2.2: Input parameters for determining column volume and oven dry soil mass measurements for bulk density in dry compaction experiments.

Volume calculations			
	Radius (cm)	Height (cm)	Volume (cm^3)
Full core	3.75	16.00	706
Top 6 cm	3.75	6.00	265
Bottom 10 cm	3.75	10.00	441
Bulk density calculations			
	Bulk density ($g\ cm^{-3}$)	Volume (cm^3)	Mass (g)
Top 6 cm	1.2	265.07	318.08
Bottom 10 cm	1.4	441.79	618.50

To compact the bottom 10 cm of the core the soil was added in approximately 3 x 200g sections. Each aliquot was compacted using a 1 kg mass attached to a 75mm metal compaction disc that fitted inside the core (Figure 2.1). The mass was dropped from a height of 10 cm repeatedly for 10 impacts. After 10 impacts, the next 200 g of soil was added and the process repeated until the metric line was just visible. The layer was then scarified using a toothpick to ensure homogenous packing between the two layers (Lewis and Sjostrom 2010). The top section of 6 cm was packed using the same methodology however the soil was only subject to 5 impacts from the mass at 10 cm drop height. The soil for this layer was addeded in two approximate 150 g sections. Once packed columns were stored in a cold store for 24 h before saturation.

2.1.2b Wet compaction technique

For the wet soil compaction technique used in Chapter 4 & 5 PVC columns were used with specific measurements of 10 cm height and 5.10 cm diameter. Each column was fitted with a fine mesh base secured with double sided tape to ensure maximum soil retention within the core. Cores were packed at a single bulk density, *viz.* 1.4 g cm^{-3}, 1.6 g cm^{-3} and 1.8 g cm^{-3}. The calculations for determining volume and bulk density remain the same. Table 2.3 indicates the packing requirements. These cores were packed using the same methodology used in the dry compaction technique, apart from the soil was pre mixed with defined water contents and the soil was added to the core in 50 g aliquots.

Table 2.3: Indicates the calculation inputs for determining column volume and soil mass measurements for bulk density in wet compaction experiments.

Volume calculations			
	Radius (cm)	Height (cm)	Volume (cm^3)
Full core	2.55	7.00	142.92
Bulk density calculations			
	Density (g cm^{-3})	Volume (cm^3)	Mass (g)
1.4	1.4	142.92	200.08
1.6	1.6	142.92	228.67
1.8	1.8	142.92	257.25

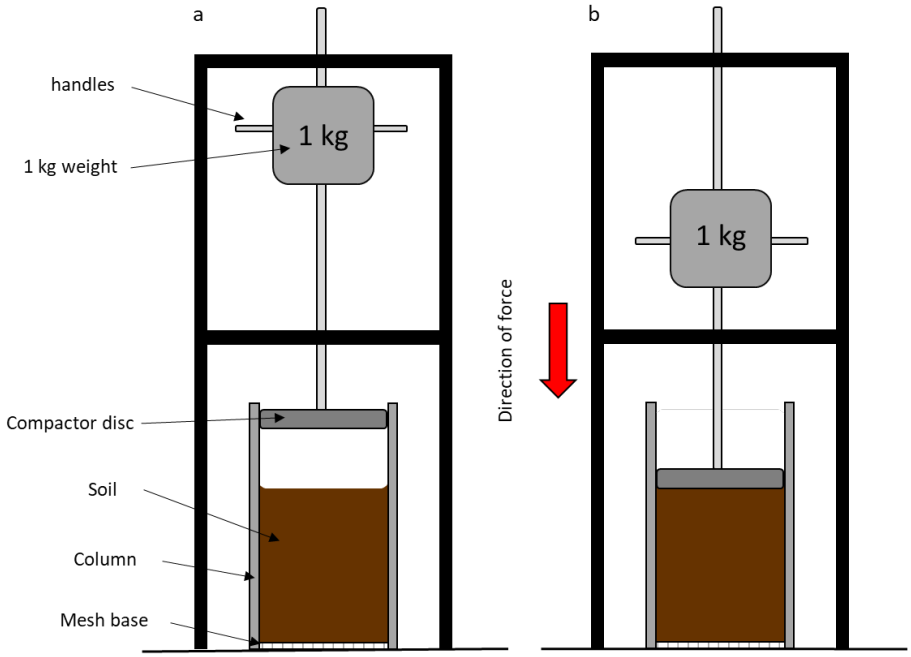


Figure 2.1: Schematic diagram of soil core compaction equipment. A) compactor idle B) compacter in use.

2.1.3 Soil moisture

2.1.3a Field capacity

The water-holding field capacity of all soil types was determined for the different levels of soil compaction. Where the wet compaction technique was used the amount of water added to the soil was noted and taken into consideration when calculating results. Each core was packed and weighed, this was recorded as 'start core weight'. Each core was then placed in a bucket which was filled with water to 0.5 cm below the top of each core. Cores were left for 24 h to saturate, evident by water pooling on the cores surface. Once saturated cores were re-weighed, recorded as 'saturation weight'. Cores were left to gravimetrically drain for 48 h and re-weighed, recorded as 'drained weight'.

To calculate the water holding capacity of the soils the following equation was used:

$$SW = (SCW - DW) \quad (1)$$

where: SW= saturation weight (g); SCW= start core weight (g); DW= drained weight (g)

2.1.3b Soil equilibration and water release characteristics

Soil water content was measured as a function of soil suction or matric potential of the different soil types using a tension table (Figure 2.2). Sand used in the tension table was HIQ5 Silica Sand (Hoben International Ldt, Brassington England) overlaying Garside 80EW sand (Aggregate Industries, Derby England). Soil cores were prepared using the wet compaction technique and compacted to 1.2 g cm^{-3} and 1.8 g cm^{-3}. Five replicates of sandy loam, clay loam and clay soil cores (x2 densities) were established (total n=30). Once compacted, cores were left to saturate for 3 days until there was evidence of water pooling on the top of the cores[1]. Once saturated the cores were weighed. To start the experiment the water container was placed at a height of 0 cm (equivalent to 0 kPA), and left to equilibrate for 48 h. Cores were then placed on top of the sand layer and hydraulic contact was formed by gently pressing the cores down. Once placed on the table core were left for 5 h, removed weighed to assess mass of water loss at 0 kPA, then replaced and re-

[1] This saturation process was longer than when calculating field capacity due to the larger density and finer texture of the soil cores.

weighed after 24 h. Mass was further recorded after 5 and 24 h at 3, 5, 7 kPa. Whilst being weighed, cores were place on Petri dishes to retain any water lost from the samples when removing them from the table. Gravimetric water content was calculated at each matric potential.

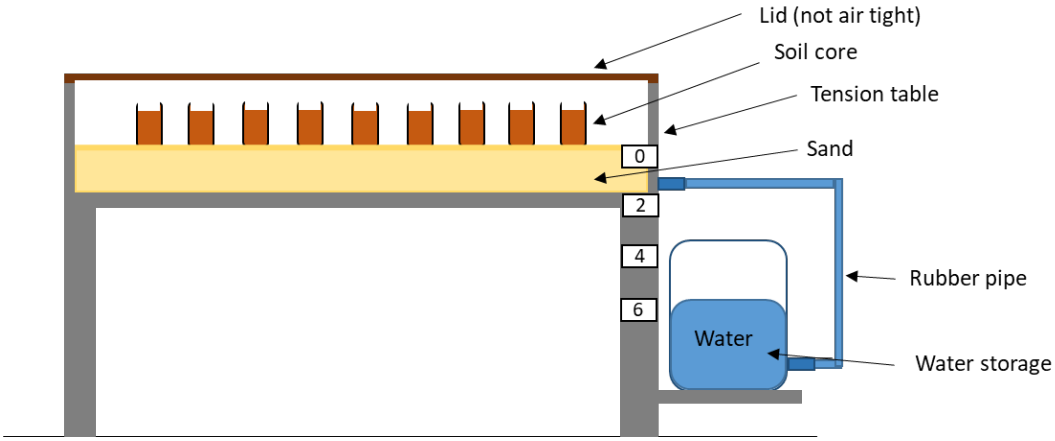


Figure 2.2: Schematic diagram of soil tension table set up.

2.1.3c Determining suitable compaction density as a function of soil water content

A number of different soil moisture contents were compared at bulk densities of 1.6 g cm^{-3} and 1.8 g cm^{-3}. The soil was pre-mixed to the specific moisture contents based on Table T.2.1 (Appendix 2). Cores were packed using the wet compaction technique. At 20-22 g . 100 g^{-1} water content soil was unable to be compacted due to excess water pooling on the soil surface. At water contents between 18-20 g . 100 g^{-1} the compression disc tended to bounce back of the soil making it hard to compress the soil evenly. At 16 g . 100 g^{-1} the soil core could be consistently packed and provided a homogenous soil core.

2.1.4 Soil strength (penetrometer resistance)

Soil penetrometer resistance was measured for both soil compaction techniques at different bulk densities, using a modification of the penetrometer resistance method outlined by Gao et al. (2012). A small cone penetrometer with a cone-base diameter of 1 mm and 30° cone angle/ 0.8 mm diameter relieved shaft was driven into the soil at a rate of 4 mm min^{-1} using an Instron Universal Testing System Frame 5969 (Illinois Tool Works Inc.). The penetrometer was pushed 15 mm into the soil and recordings were averaged over each 1 mm depth intervals. Three replicate readings were taken per core. The force required to push the cone into the soil was measured using an electronic balance and recorded onto a computer (Figure 2.3).

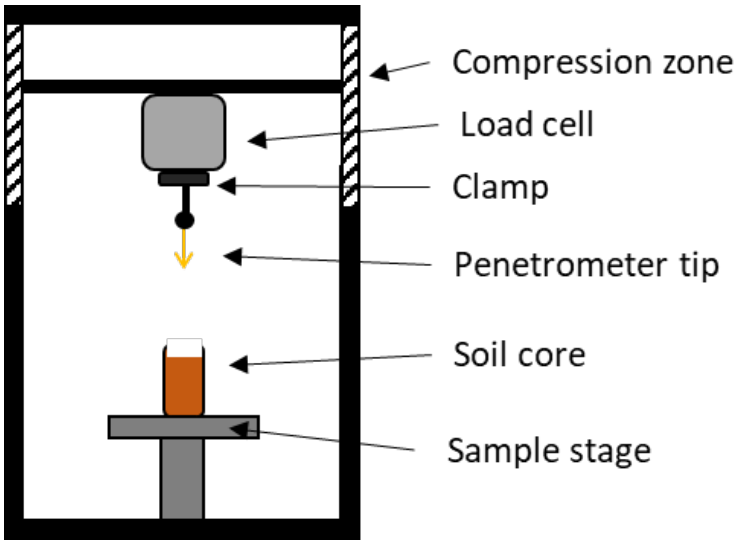


Figure 2.3: Schematic diagram of Instron universal testing machine equipment.

2.1.5 Soil texture (quantitative analysis by hydrometer)

Soil texture was determined by the hydrometer method, the standard operating procedure for which is given in Appendix 2, A.2.1. The percentage of sand, silt and clay in each of the samples was used to determine the soil texture using the soil texture triangle as defined by the Soil Survey of England and Wales (Hodgson, 1997).

2.1.6 Aggregate size distribution

2.1.6a Soil preparation

Soil was removed from the core as a cylinder and then gently broken up by hand to remove the root system. Fifteen minutes was spent breaking each core apart. Once the soil was extracted it was left to air dry at 16°C for 48 h and weighed.

2.1.6b Methodology

A graded series of sieves with mesh sizes: of 2, 1, 0.71, 0.5, 0.25, 0.106 and 0.045 mm were stacked on top of each other in descending order with a collection tray at the bottom. A sample of soil weighing 200 g was added to the top sieve and a lid was placed on top of the sieve stack to secure the sample. The stack of sieves was then placed onto the mechanical shaker for 2 minutes. Once shaken the remaining soil was removed from each sieve and weighed and used to calculate the % size class distribution of the soil aggregates.

2.2 Plants

2.2.1 Pre germination for non-crop species

2.2.1a Seed vernalisation

Two hundred seeds were placed in separate sealed and labelled plastic bags in a cold store at 5°C for 3 weeks. After this time period a subset of 40 seeds) were then placed on filter paper in Petri dishes and left in specified germination conditions and monitored.

2.2.1b Mechanical scarification

Thirty seeds of each species were mechanically scarified to assess whether breaking down of the seed coat would help induce germination of the wild species. Seeds were placed on a sheet of sandpaper and then covered with a second piece of sand paper and rubbed applying even pressure for 3 minutes (Kimura and Islam 2012). Once scarified seeds were placed on filter paper in Petri dishes and left in specified germination conditions and monitored.

2.2.2 Germination

Two germination methods were used, cover crop seeds were germinated in soil, whereas wild plant species were pre-germinated on filter paper as described below.

2.2.2a Germination of cover crop seeds in soil

Seeds were placed in 1 cm holes premade using a pipette tip and covered with a layer of soil. The columns were monitored twice daily until seedling emergence, at which time 2 out of the 3 seedlings were thinned from the core. During this time period the seeds were subject to glasshouse environmental conditions and were water with an initial 10 mm of water upon planting.

2.2.2b Germination of non-crop species seeds on filter paper

Seeds were placed in Petri dishes (n=20) lined with filter paper and 40 ml of water. The dishes were stacked and placed in a dark room at different temperatures for between 3-5 days until the radical of the plants were visible. Once emerged, seedlings were then transplanted into soil cores.

2.2.3 Growth conditions

2.2.3a Chapter 3

Plants were grown in a glasshouse, the average day/night temperature was 24°/ 18°C. Plants were watered daily, addition of a nutrient spiked (HortiMix Standard 0-36-36 with trace elements) water solution were made weekly.

2.2.3b Chapter 4

Plants were grown in a growth chamber (the day/night temperature of 20˚C/15˚C the humidity was 70 %). The day temperature ran from 05.00-21.00, light duration was 16 h, night duration was 8 h, dawn/dusk duration

was 3 h. The daylight period was from 08.00-18.00 and the night period was from 21.00-05.00. Plants were watered every day with 4 ml of water. Three nutrient applications of 2 mm of solution per core were made over the course of the growth period. The nutrient solution used was HortiMix Standard 0-36-36 (Park Farm, Kettlethorpe, Lincoln, LN1 2LD) with trace elements.

2.2.3c Chapter 5

Growth chamber settings were identical to Experiment 2. The plants were weighed each day and re-watered to a constant weight. Three nutrient applications of 2 mm of solution per core were made over the course of the growth period. The nutrient solution used was HortiMix Standard 0-36-36 with trace elements.

2.2.4 Plant harvesting & biomass storage

Shoots were harvested by cutting the stem of the plant at the point where it protrudes form the soil. Roots were gently washed using a nozzle attachments over a 500 µm sieve. Roots were stored before processing in labelled tubes (50 % ethanol 50% distilled water) at 5°C.

2.2.5 Biomass root and shoot analysis

Harvested (cleaned) fresh shoot weight was recorded and then shoots were dried in tins in an oven at 50°C for 48 h. They were then re-weighed to

provide a dry shoot biomass measurement. Washed roots were dabbed dry using a paper towel and placed in a tin and fresh root biomass was recorded.

Washed roots were placed onto A3 Perspex trays and spread out in a thin layer of water. Roots were scanned using a flatbed EPSON scanner at 800 dpi resolution and analysed using WinRHIZO (Regent Instruments Inc.). Root images were saved as .tiff files. After WinRHIZO analysis, roots were dried at 50°C for 48 h to determine dry root biomass.

2.2.6 Quantifying mycorrhizal roots

Plant roots were cleared and stained using 3% blue Quink ink in vinegar (5% acetic acid) for staining (Vierheilig et al. 1998). The method used to quantify mycorrhizae was adapted from the gridline intersect method (Giovannetti and Mosse 1980). The standard operating procedure for quantifying mycorrhizal roots is given in Appendix 2, A.2.2.

Chapter 3: Investigating cover crop species root architecture responses to soil compaction

This chapter explores the root architecture of selected cover crop plants and how they respond when subjected to varying soil compaction levels. Species were selected via consultation with Frontier Agriculture, Lincolnshire, UK. Preliminary work was undertaken to provide a baseline of root characteristics using 2D analysis methods before a detailed primary investigation was undertaken in 3D (presented in this chapter in the form of a published manuscript). Plants were assessed on their root architecture response to soil compaction and their subsequent potential to remediate soil is discussed.

Aim: To assess how cover crop root architecture responds to changes in soil bulk density using 2D and 3D analysis techniques.

Objectives:

- Select a number of candidate plant species to investigate via consultation with a cover crop expert
- Assess the plant root architecture in 2D for differences in root traits when grown in different soil bulk densities
- Assess plant root architecture in 3D under a single bulk density
- Evaluate plant root architecture in 3D under a dual-phase bulk density treatment to determine root responses to a compacted layer
- Determine changes in soil porosity as a result of root growth

3.1 Consultation with Frontier Agriculture

Frontier Agriculture is a UK based crop production and grain marketing business. In January 2016 Jasmine Burr-Hersey and Karl Ritz met with Paul Brown from Frontier Agriculture at their field site in Nassington, UK. The purpose of the field visit was to assess cover crop plots for potential candidate species that would be assessed to establish cover crop plant roots susceptibility to soil compaction. Paul Brown showed a selection of cover crop species that had a variety of contrasting root system architectures. From this consultation three candidate species were chosen. Each species had a contrasting root system type, the species are outlined in Table 3.1.

Table 3.1: List of cover crop species identified for use from field visit with Frontier Agriculture.

Latin name	Common name	Root type	Plant type
Raphanus sativus	Tillage radish	Tap-root	Non- legume broadleaf
Vicia sativa	Vetch	Shallow rooting	Legume
Avena strigosa	Black oat	Fibrous	Annual grass

3.2 Preliminary trials

A set of preliminary trials were undertaken to assess the root architecture of the chosen species under two compaction treatments. The levels of compaction used were achieved using the dry compaction technique outlined in section (2.1.2a). A bulk density of 1.2 g cm^{-3} was used as an uncompacted treatment, and a bulk density of 1.4 g cm^{-3} was used as a moderately compacted treatment. It was important to have a baseline study of how cover crop roots behaved in uncompacted soils. This study provided a comparison

data set so that when we assessed how the roots responded to abrupt changes in bulk density, it was possible to assess if the traits observed were specifically linked to the treatment effect.

3.2.1 Experimental material and methods for 2D investigation

A total of 36 PVC columns (16 cm height, 7.5 cm diameter), were uniformly packed using the dry compaction technique outlined in Section 2.1.2a using a Dunnington Heath series sandy loam (66.4% sand 18% silt, 15.6% clay) to 1.2 g cm^{-3} (18 columns) or 1.4 g cm^{-3} (18 columns). Cores were saturated for 24 hours and then left to gravimetrically drain for 48 hours before planting. Cores were planted with 3 seeds per core. Once germination had occurred cores were thinned to 1 seedling per core. Cores were placed in a glasshouse with average day night temp 24°C/ 18°C. A total of 18 plants were grown for 20 days and then harvested, the remaining 18 plants grew for 58 days before harvest. Plants were then root washed and WinRHIZO scanned following the methodology in Section 2.2.5.

3.2.2 Results

3.2.2a WinRHIZO image production

Qualitative analysis of the images revealed that there was no obvious differences in root architecture of tillage radish, black oat and vetch between the 1.2 g cm^{-3} and 1.4 g cm^{-3} at day 20 (Figures 3.1, 3.2, 3.3 respectively). All plants developed primary root systems, some with extensive lateral root

development. Notably tillage radish accumulated the greatest root mass at Day 20 and 58. The greatest proportion of this had accumulated by Day 20 as 3rd order fine lateral root mass. The majority of plants had developed a strong straight taproot (Figures 3.1a, 3.1c, 3.1f) however some evidence of root fanging was observed in Figures 3.1b & 3.1d. Vetch plants at Day 20 were of consistent size and morphology (Figures 3.2a-f). All plants exhibited an obvious straight taproot and have multiple branching laterals along the length of the primary root. Black oats at Day 20 also exhibited consistent plant size and root morphology, with evidence of multiple thicker primary roots as well as multiple thinner secondary roots. From these visual observations there was no noticeable difference in the root system architectures of the species between 1.2 g cm^{-3} and 1.4 gm cm^{-3} on Day 20. At Day 58 a level of variation in tillage radish taproots (Figures 3.3g-l) was observed. They had all developed thick primary taproots but there were some instances of this splitting, notably in Replicate i. By this time thicker first-order lateral roots had developed in all replicates and extensive fine lateral root mass was present. Vetch plants were of consistent size and displayed the same morphological traits. Extensive lateral root development was observed, with the primary taproot and laterals thicker than at Day 20. At Day 58 black oats showed less consistency in morphology between replicates. There was substantial fine lateral root development in comparison to Day 20

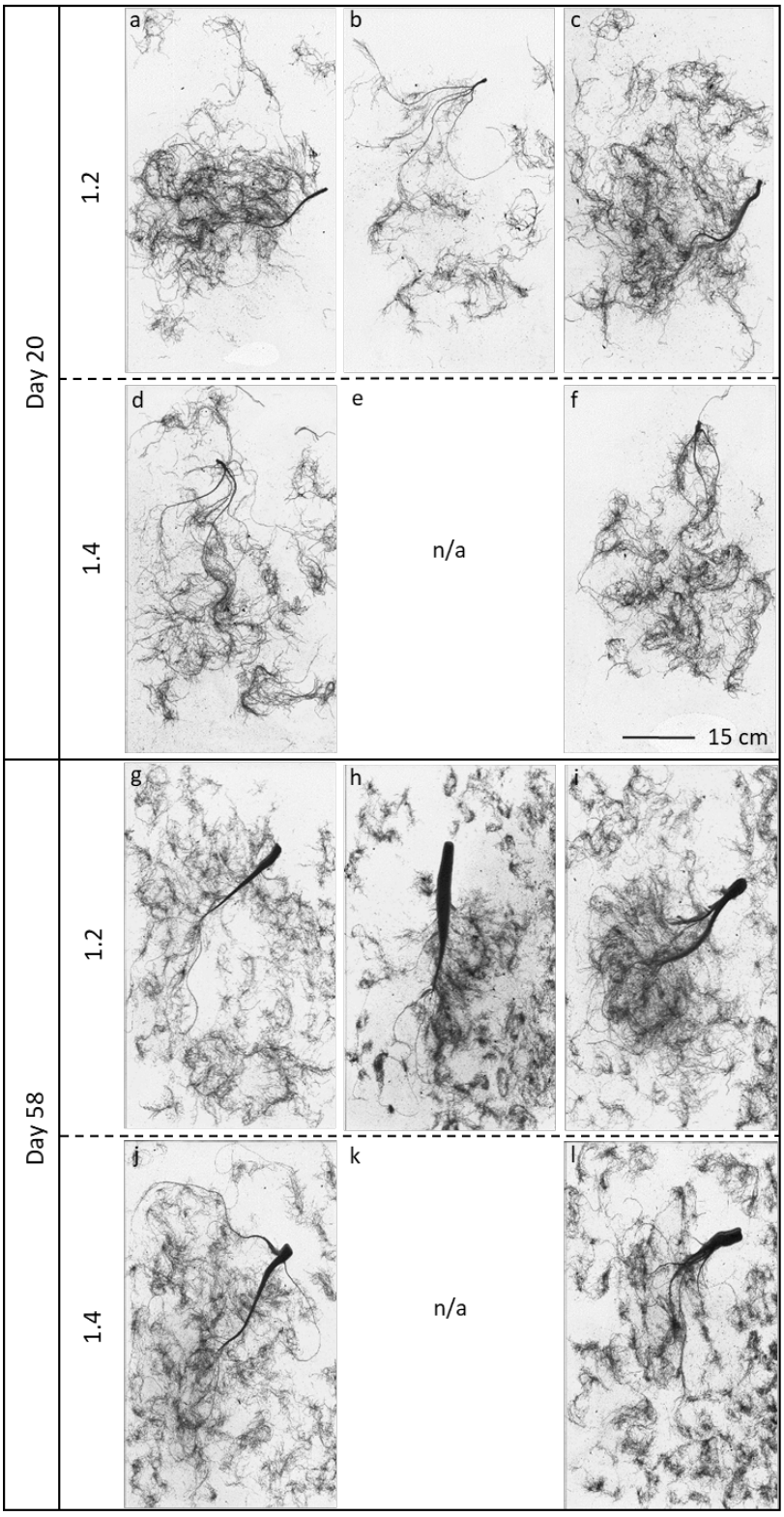


Figure 3.1: Root WinRHIZO scans of tillage radish plants. (a-f) grown for 20 days. Images (a-c) soil bulk density 1.2 g cm^{-3}, images (d-f) soil bulk density 1.4 g cm^{-3}. Images (g-l) grown for 58 days. Images (g-i) soil bulk density 1.2 g cm^{-3}, images (j-l) soil bulk density 1.4 g cm^{-3}.

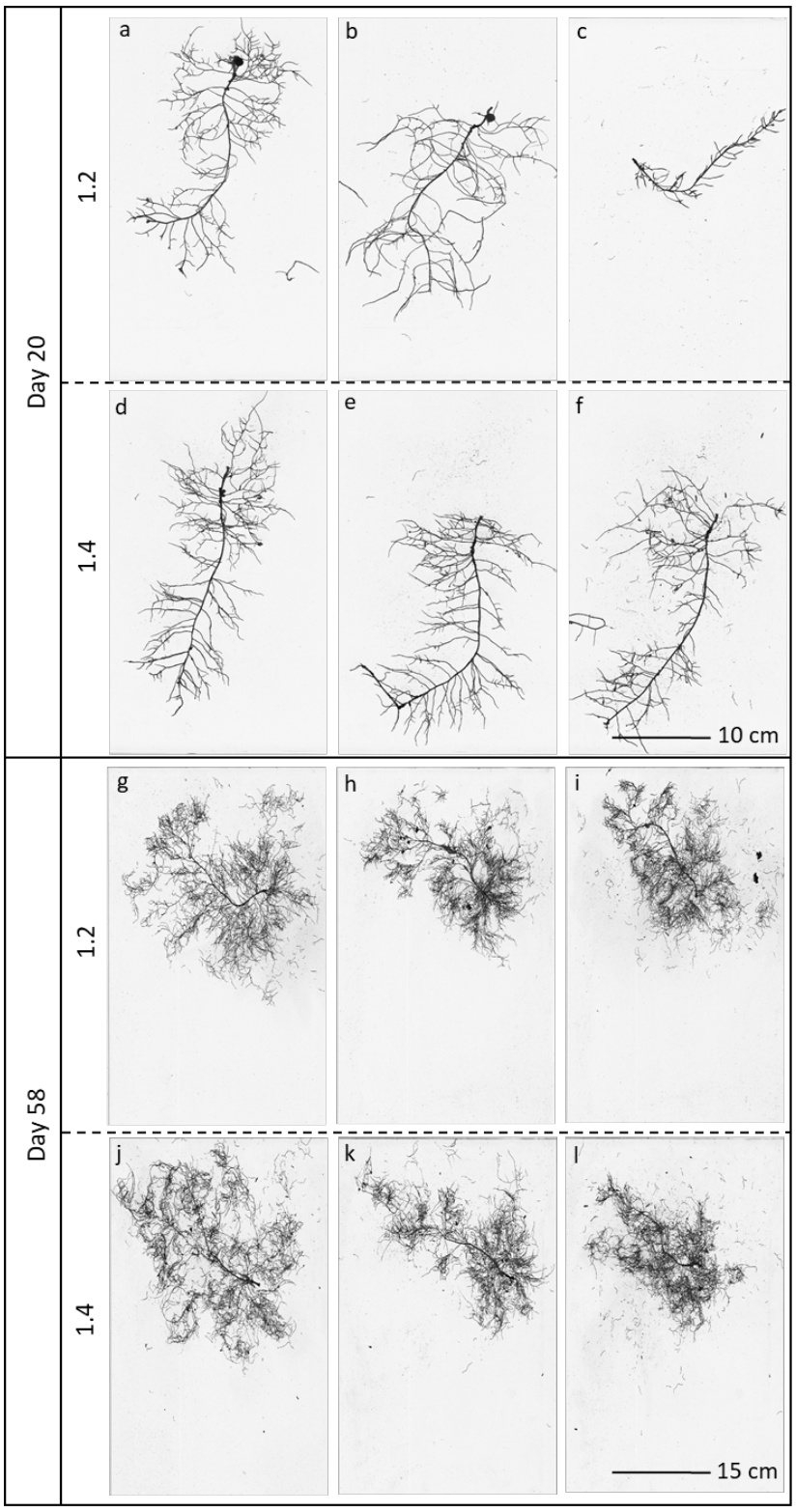


Figure 3.2: Root WinRHIZO scans of vetch plants. (a-f) grown for 20 days. Images (a-c) soil bulk density 1.2 g cm^{-3}, images (d-f) soil bulk density 1.4 g cm^{-3}. Images (g-l) grown for 58 days. Images (g-i) soil bulk density 1.2 g cm^{-3}, images (j-l) soil bulk density 1.4 g cm^{-3}.

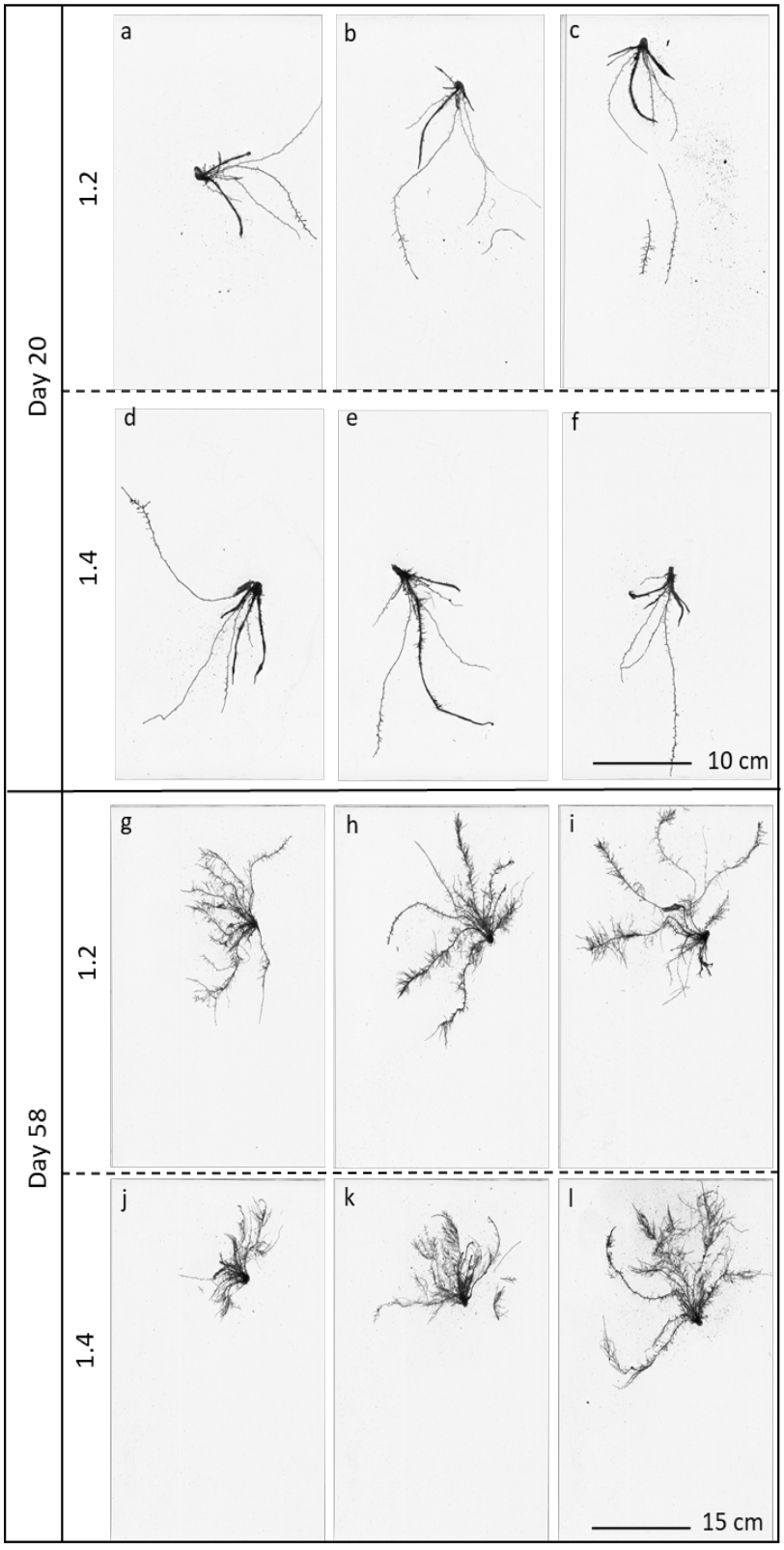


Figure 3.3: Root WinRHIZO scans of black oat plants. (a-f) grown for 20 days. Images (a-c) soil bulk density 1.2 g cm^{-3}, images (d-f) soil bulk density 1.4 g cm^{-3}. Images (g-l) grown for 58 days. Images (g-i) soil bulk density 1.2 g cm^{-3}, images (j-l) soil bulk density 1.4 g cm^{-3}.

3.2.2b WinRHIZO Results

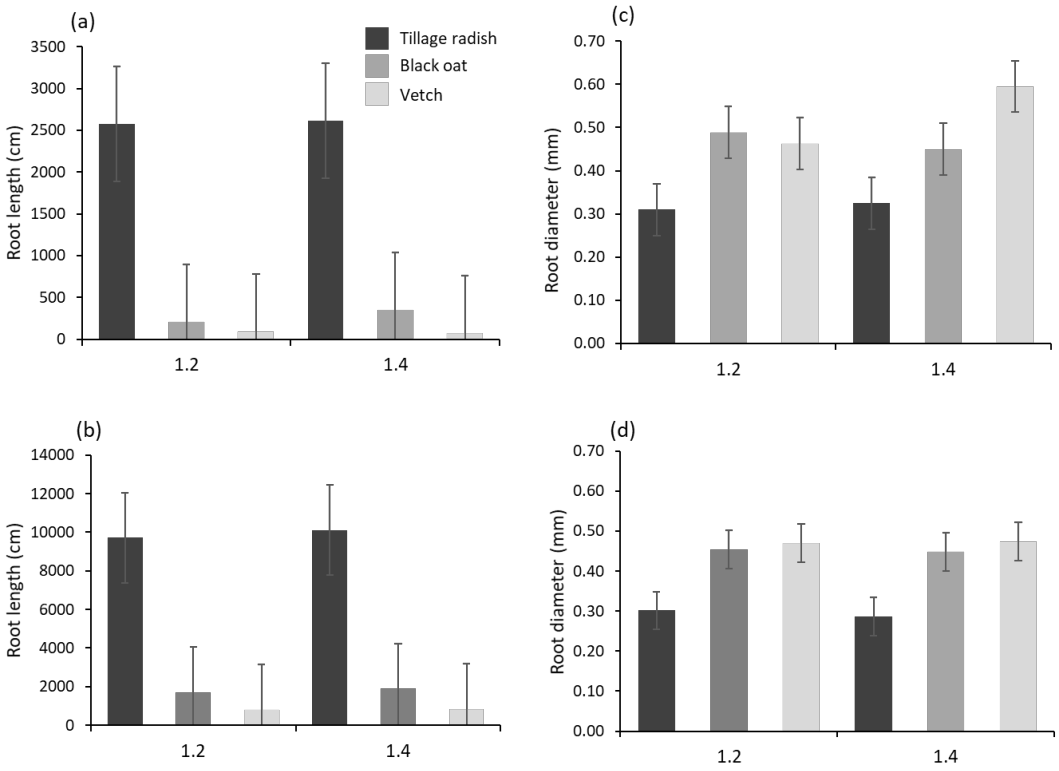


Figure 3.4: (a) Average root length of cover crop species per plant derived from WinRHIZO 2D scan data at day 20. (b) Average root length of cover crop species per plant derived from WinRHIZO 2D scan data at day 58. (c) Average root diameter of cover crop species derived from WinRHIZO 2D scan data at day 20. (d) Average root diameter of cover crop species derived from WinRHIZO 2D scan data at day 58. Bars denote mean whiskers pooled S.E.

To establish whether bulk density or species affected root length and average diameter a two-way factorial analysis of variance (ANOVA) was undertaken. Species significantly affected the amount of root material ($p < .001$) (Figure 3.4a) and average diameter of the roots ($p < .001$) (Figure 3.4c) although no interaction effect was observed. Tillage radish had the lowest average root diameters of the three species, this is likely to be due to the high proportion of fine lateral mass the plants produce out weighing the single larger taproot (Figure 3.1). No interaction was observed for total root length between

species and bulk density at Day 58 (Figure 3.4b). Species significantly affected the total root length within the cores ($p < .001$) (Figure 3.4b) as well as average diameter of the roots ($p < .001$) (Figure 3.4d). Similarly to Day 50, tillage radish had the lowest average root diameters of the three species at Day 58, again this can be attributed to the high proportion of fine lateral roots (Figure 3.1).

ANOVA was undertaken on the total root length found in each individual diameter class for vetch, black oat and tillage radish under the two bulk density treatments after both 20 and 58 days of growth (Figure 3.5). No significant differences ($p > 0.05$) were observed for the distribution of roots under the different compaction treatments for any of the diameter classes apart from for vetch and black oat at Day 20. Specifically for vetch, the diameter classes; 3>3.5, 3.5>4 and 4>4.5 mm had P values of 0.09, 0.02 and 0.03 respectively. For black oat, the diameter classes 1>1.5, 1.5>2 and 2>2.5 mm had P values of 0.04, 0.05 and 0.37 respectively. A table detailing all the calculated significance values can be found in Appendix 3 T.3.1. The data indicates that the increase in bulk density from 1.2 g cm^{-3} to 1.4 g cm^{-3} did not affect the total length of root in each size class in the majority of instances. The imagery in Figures 3.1,3.2 & 3.3 all depict thicker primary roots, graphically in Figure 3.5 these bigger primary roots are represented by the diameter class >4.5 mm as although they represent a large amount of the total mass, the length of these roots is proportionally small in comparison to the length of the finer root mass.

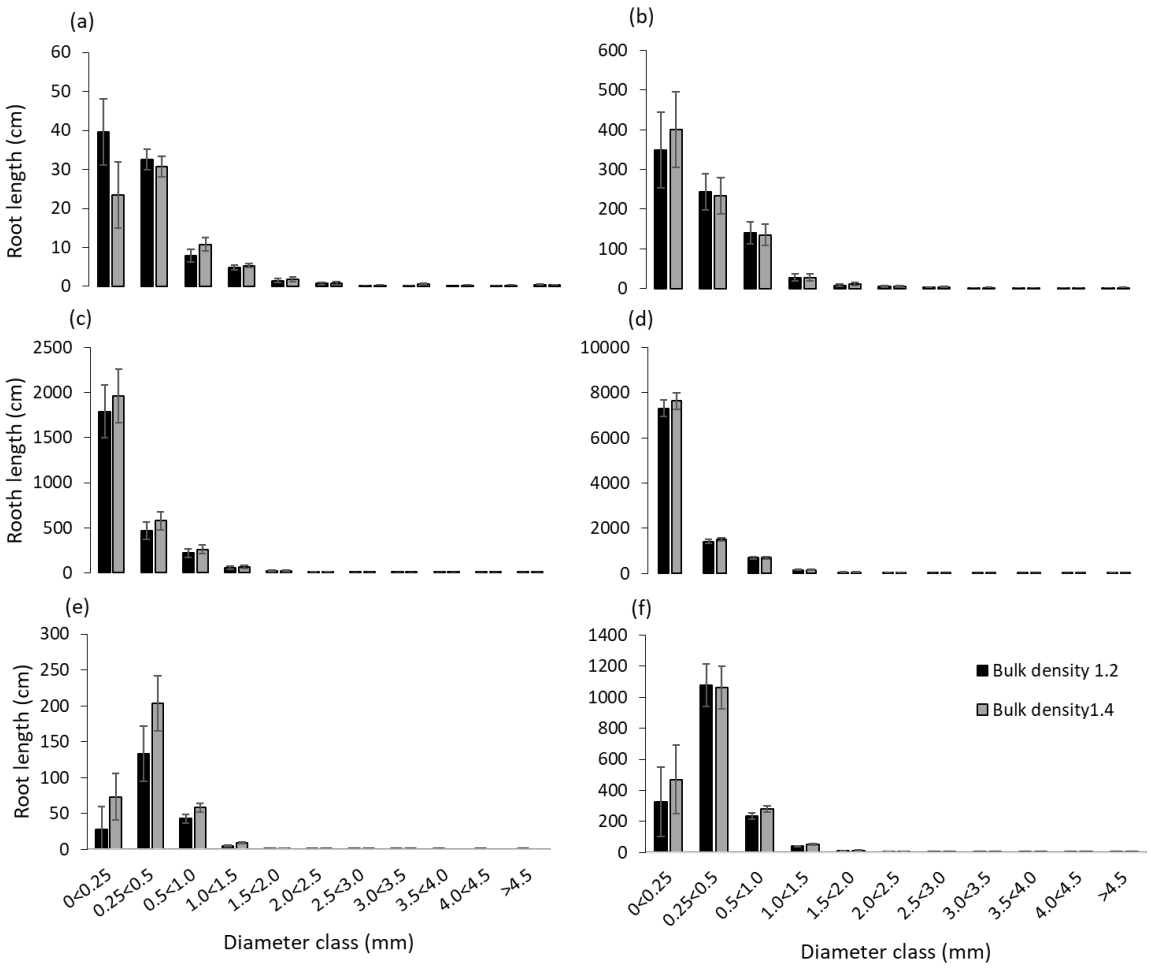


Figure 3.5: Average root length (cm) found within specified diameter classes, derived from WinRHIZO 2D scan data. Black bars indicate plants grown in 1.2 g cm^{-3} bulk density soil. Grey bars indicated plants grown in 1.4 g cm^{-3} soil. (a-b) black oat days 20 and 58 respectively. (c-d) tillage radish days 20 and 58 respectively. (e-f) vetch days 20 and 58 respectively. Bars denote means, whiskers S.E.

3.2.3 Experimental material and methods for 3D investigation

Once the 2D WinRHIZO analysis of the cover crop root architectures had been completed, an X-ray CT study was undertaken. The same experimental set up of cores 16 cm in height and 7.5 cm width filled with sandy loam soil compacted to 1.2 g cm^{-3} using the dry compaction technique. Cores were saturated for 24 hours and left to gravimetrically drain for 48 hours to field capacity. Cores were planted with 3 seeds per core and thinned to 1 seedling

per core once germination had occurred. Cores were placed in a glasshouse with average day night temp 24°C / 18°C. Each plant was grown for 20 days and then X-ray CT scanned.

3.2.3a X-ray CT set up and segmentation

All columns were scanned using a Phoenix V|Tome |X m X-ray 240kV (GE Measurement & Control Solutions, Wunstorf, Germany) at the Hounsfield Facility at the University of Nottingham, with a 0.1 mm copper filter. Scan settings were optimised according to the width of the soil core and time taken for each sample to be processed. The optimum scan resolution for the sample width was determined to be 60 μm resulting in a scan time of 75 minutes per core. Each projection image was an integration of 3 images with a skip setting of 1 discarded image. The potential energy was 180 kV and the current was set at 180 uA. The distance from the sample to the source was 245 mm. A total of 2160 image projections were captured for each column. Images were reconstructed at 32-bit using Phoenix Datosx 2 reconstruction tool to form a 3D volume which was visualised using VG Studio Max 2.2.5 software.

3.2.3b X-ray CT image production

For the purpose of the preliminary investigation, images were segmented in VG Studio Max V 2.2.5. A manual 'region growing' tool was used which relies on the user to identify areas of image known to be root. The tool then uses an

algorithm to identify other areas of the images with the similar greyscales within a predefined range and classifies them as root. The outputs of this initial analysis can be seen in Figure 3.6 which displays the root systems of the three cover crop species after 20 days growth.

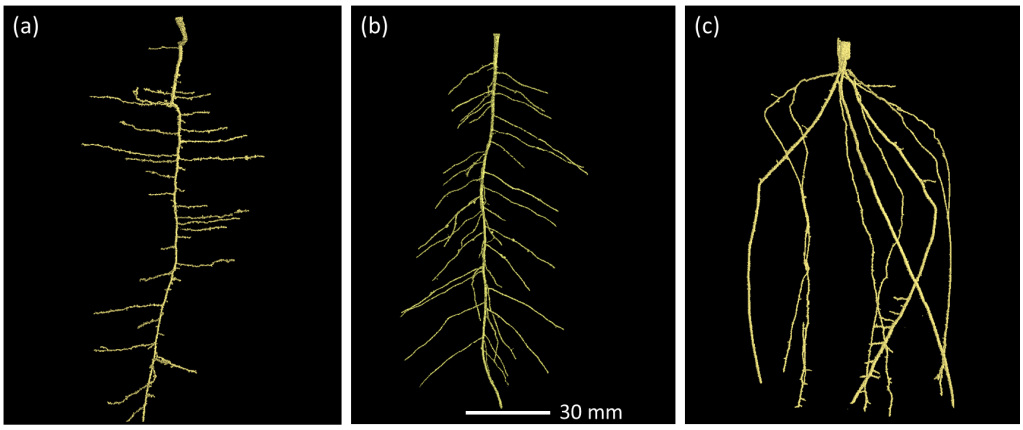


Figure 3.6: X-ray CT visualisations of cover crop plants grown for 20 days scanned at 60 µm. a) Tillage radish, b) Vetch, c) Black oat.

3.2.3c X-ray CT results

Qualitative analysis of the root system architecture in 3D suggests the plants have developed without restriction in the 1.2 g cm^{-3} uncompacted soil. Figure 3.6a depicts tillage radish, revealing the tap-root grew vertically through the soil to the bottom of the core with no change in trajectory, the lateral roots were perpendicular to the taproot and evenly distributed. Figure 3.6b shows a vetch plant, again the fine taproot grew vertically down the core with no deviation and with regularly spaced lateral roots, uniformly angled at approximately 20°. In Figure 3.6c the black oat plant had multiple vertically-oriented primary roots which often grew towards to column wall and followed the edge of the core to depth.

3.3 Summary of preliminary investigations

Preliminary investigation assessing plant root growth in uniform bulk density 1.2 g cm^{-3} and 1.4 g cm^{-3} treatments indicated that the density of the soil did not lead to any obvious or unusual variations in root growth outside of the natural variation (as assessed via the WinRHIZO 2D scans). The greatest variation in root system architecture was observed in the tillage radish replicates where when assessed by eye there was visible variation in lateral branching patterns and thickness between the replicates. The vetch and black oat plants provided relatively uniform replicates in terms of root architectural traits.

X-ray CT imagery of the three species depicted no obvious or unusual root development characteristics when then plants are grown in 1.2 g cm^{-3} uniformly compacted bulk density soil. All data collected in the preliminary investigation into root architectural traits in uniform bulk density environments suggests that the increase in bulk density has no significant difference on the plant. This may be attributed to the relative wetness of the soil.

Section 3.4 details the primary investigation into whether a change in soil compaction within a single core instigates changes in plant root architecture. Plants were grown in a soil core with two levels of soil compaction (1.2 g cm^{-3} overlaying 1.4 g cm^{-3}) and root systems were assessed in 3D. It was hypothesised that an abrupt change in soil bulk density will induce changes in root architecture development within the plant species.

3.4 Authors accepted manuscript

This remainder of this chapter is structured and formatted in accordance with the journal PLoS ONE.

Status: Published.

Citation: Burr-Hersey J.E., Mooney, S.J., Bengough A.G., Mairhofer S., and Ritz K. 2017 Developmental morphology of cover crop species exhibit contrasting behaviour to changes in soil bulk density, revealed by X-ray computed tomography. PLoS ONE 12(7): e0181872. https://doi.org/10.1371/journal.pone.0181872

In accordance with the PLos One submission style, numerical citation format has been used in this chapter. The corresponding reference list is found at the end of this chapter.

Individual replicate 2D WinRHIZO scan imagery and X- ray CT visualisation imagery for cover crop species can be found in A.3.1-A.3.4.

Author contributions

Conceptualisation: J.E. Burr-Hersey, S.J. Mooney, A.G. Bengough, K. Ritz.
Data curation: K. Ritz.
Formal analysis: J.E. Burr-Hersey, S.J. Mooney, K. Ritz.
Funding acquisition: K. Ritz.
Investigation: J.E. Burr-Hersey.
Methodology: J.E. Burr-Hersey, S.J. Mooney, A.G. Bengough, K. Ritz.
Project administration: K. Ritz.
Software: S.J. Mooney, S. Mairhofer.
Supervision: S.J. Mooney, A.G. Bengough, K. Ritz.
Visualization: J.E. Burr-Hersey, S.J. Mooney, S. Mairhofer.
Writing original draft: J.E. Burr-Hersey, K. Ritz.
Writing review & editing: J.E. Burr-Hersey, S.J. Mooney, A.G. Bengough, S. Mairhofer, K. Ritz.

Developmental morphology of cover crop species exhibit contrasting behaviour to changes in soil bulk density, revealed by X-ray computed tomography

Short title: Cover crop root responses to soil bulk density changes

Jasmine E. Burr-Hersey[1,2], Sacha J. Mooney[1], A. Glyn Bengough[2,3], Stefan Mairhofer[4], Karl Ritz[1 *]

[1] Division of Agricultural & Environmental Science, School of Bioscience, University of Nottingham, Sutton Bonington Campus, Leicestershire LE12 5RD, UK

[2] The James Hutton Institute, Invergowrie, Dundee DD2 5DA, UK

[3] School of Science and Engineering, University of Dundee, Dundee DD1 4HN

[4] School of Computer Science, University of Nottingham, Nottingham NG8 1BB

*Corresponding author: karl.ritz@nottingham.ac.uk

3.4.1 Abstract

Plant roots growing through soil typically encounter considerable structural heterogeneity, and local variations in soil dry bulk density. The way the *in situ* architecture of root systems of different species respond to such heterogeneity is poorly understood due to challenges in visualising roots growing in soil. The objective of this study was to visualise and quantify the impact of abrupt changes in soil bulk density on the roots of three cover crop species with contrasting inherent root morphologies, *viz*. tillage radish (*Raphanus sativus*), vetch (*Vicia sativa*) and black oat (*Avena strigosa*). The species were grown in soil columns containing a two-layer compaction treatment featuring a 1.2 g cm^{-3} (uncompacted) zone overlaying a 1.4 g cm^{-3} (compacted) zone. Three-dimensional visualisations of the root architecture were generated via X-ray computed tomography, and an automated root-segmentation imaging algorithm. Three classes of behaviour were manifest as a result of roots encountering the compacted interface, directly related to the species. For radish, there was switch from a single tap-root to multiple perpendicular roots which penetrated the compacted zone, whilst for vetch primary roots were diverted more horizontally with limited lateral growth at less acute angles. Black oat roots penetrated the compacted zone with no apparent deviation. Smaller root volume, surface area and lateral growth were consistently observed in the compacted zone in comparison to the uncompacted zone across all species. The rapid transition in soil bulk density had a large effect on root morphology that differed greatly between species,

with major implications for how these cover crops will modify and interact with soil structure.

3.4.2 Key words

Root growth, RooTrak, Root system architecture, Soil compaction, Soil structure

3.4.3 Introduction

Soil compaction is associated with soil physical stresses of mechanical impedance and hypoxia that often impair the growth of crop plants [1]. Typically, within an agricultural context, the passage of wheeled and tracked machinery, the action of tillage equipment, and the trampling of animals produce compressive forces, which result in the compaction of the soil [2-4]. Compaction decreases the mean size of pores in the soil matrix, and can adversely affect root growth [5]. Roots are immersed in a soil matrix that has a range of inherent properties that affect their structural development, function and anatomy. Root development can be affected by a number of soil factors including texture, structure and degree of compaction [6]. The effect of such compaction can be physically restrictive, impairing the development of the root system and negatively affecting overall plant growth and crop yield [7, 8].

The variation observed between plant species in their capability to penetrate strong soil may be at least partly attributed to the tendency of roots to buckle or deflect, rather than to any inherent difference in root growth pressure or

root elongation rate *per se* [9]. Roots typically follow indirect routes through the soil, seeking out the path of least resistance as they progress, and are able to do so due to their flexible nature [10]. Roots growing through soil experience mechanical impedance to varying degrees of severity. Often this can result in changes in the patterns of lateral root formation as well as considerably decreasing rates of root elongation and increasing root diameter [10, 11]. Roots may be unable to generate the forces required to displace soil particles to allow further extension into the soil profile [5]. Indeed, the strength of many UK arable soils is sufficient to substantially slow root elongation due to mechanical impedance, even when the soil is relatively wet (soil strength is the resistance of soil to deformation by an applied force) [12,13].

The use of plant roots as a tillage tool may offer a novel, practical solution to help remediate soil compaction. The creation of pores by deeply penetrating plant roots results in biologically-created pores, termed biopores. This process has also been termed 'bio-drilling', and allows the subsequent use of such biopores by the roots of succeeding crops as preferential pathways offering low resistance to growth [14]. In soils where crop plants suffer from high levels of mechanical impedance, this is considered to be beneficial [15]. In this context, cover crops (plants grown between harvested crops within rotations) provide a potential means of creating soil biopores which succeeding crop plants can utilise. Where the size of soil pores within the matrix are smaller than the diameter of the penetrating roots, plants species differ in their capability to penetrate the soil [9, 10]. The ability of roots to

preferentially seek out biopores allows roots growing in compacted soil to negotiate otherwise impenetrable soil [16]. Roots clustering within biopores are common in compacted soils [17, 18] and may negatively affect the ability of roots to uptake water and nutrients [19]. Identifying plants that exhibit root architectural and morphological traits that enable them to penetrate soil to produce new pores, is key to determine species which could act as biodrilling cover crops.

Thick primary roots (possessed by many dicotyledonous species) have been shown to maintain faster relative root elongation rates compared to thin (monocotyledon) roots when grown in dense compressed sand [20], and also to penetrate compacted soils to greater depth in the field [21]. Tap-rooted species may exhibit better penetration abilities in compacted soils compared to fibrous rooted species and therefore be more beneficial for use in biological tillage [22]. These findings are also consistent with the use of thick-rooted dicotyledonous crops in rotations, as they may provide more effective penetration of compacted subsoil layers [23]. As well as having better penetration capabilities, crop species with taproots are capable of creating soil biopores >2 mm in diameter [15].

Many factors can affect root morphology and architecture, and it is clear that root systems have an innate plasticity to respond and adapt to their local environment [24]. The incorporation of species with a deep tap root system within crop rotations is desirable to help reduce the effects of soil compaction [25]. Roots of dicotyledonous species (notably lupin, faba bean and medic)

thickened very substantially when grown in compressed sand, and had elongation rates that were relatively less impeded than monocotyledons that thickened less [21]. However, these particular experiments were performed at very large mechanical impedances (sufficient to slow root elongation by 88-97%). Maize plants grown in compacted soil were shown to have fewer lateral roots than plants grown under control conditions [26].

Although there are many studies on the response of crop plants to soil compaction [e.g. 22, 25, 27, 28], relatively few have examined the influence of bulk density p*er se* on root system architecture and response in 3D [11]. Dry bulk density (generally referred to as bulk density in this manuscript) describes the mass of oven-dried soil in a given volume, and generally becomes greater with an increase in compaction pressures and soil depth [29]. A recent study [30] looked at the ability of root tips to deform soil of a low bulk density in 4D, however detailed studies on the effect of compaction on root system architecture of cover crops are lacking. Previous field studies indicated tillage radish had more than twice as many roots per unit volume as rye, and that root counts at depth actually increased for tillage radish with increasing soil strength [22]. The mechanism for this increase in root number was not clear, although the authors hypothesise that it was associated with a substantial change in root system morphology. The development of non-destructive measurement techniques for imaging root architecture *in situ*, makes it possible to determine the geometric properties of root systems [31] which are essential to understand their growth dynamics [32].

The objective of this study was to assess the effects of a sharp transition in bulk density on the root system architecture of three contrasting cover crop species (tillage radish, vetch, and black oats) *in situ*. X-ray computed tomography was used to study root system morphology and trajectory responses to the presence of the compacted layer, with regard to the potential effectiveness of these species for applications in compaction alleviation via bio-drilling.

3.4.4 Materials and methods

3.4.4a Sample preparation

A Dunnington Heath series sandy loam (66.4% sand 18% silt, 15.6% clay) was obtained from the University of Nottingham experimental farm at Sutton Bonington, Leicestershire, UK (52˚50'07"N, 1˚15'04.0"W). The soil was air dried and sieved to <2 mm. Columns (160 mm height x 75 mm diameter) were uniformly packed in a two phase system to provide dry bulk densities of 1.2 g cm^{-3} (uncompacted) overlaying 1.4 g cm^{-3} (compacted). Penetrometer resistance readings were 0.21 (± 0.01) MPa and 0.30 (± 0.03) MPa respectively for the two bulk density layers. These were packed with air-dried soil in *circa* 3 cm deep layers (bottom 10 cm compacted to 1.4 g cm^{-3} / top 6 cm compacted to 1.2 g cm^{-3}). After compacting each layer the surface was lightly scarified to ensure homogeneous packing [33]. Four replicates were prepared for each species plus unplanted controls (originally allowing for two destructive harvests) to give a total of 28 columns. The columns were then

saturated from below for 48 h and allowed to gravimetrically drain to a notional field capacity of approximately 21%. The air-filled porosity at field capacity will have been greater than 20% in both the uncompacted and compacted layers.

Seeds of tillage radish (*Raphanus sativus* L. cv. Early Mino), vetch (*Vicia sativa* L. cv. Buza) and black oat (*Avena strigosa* Schreb cv. Pratex) procured from Frontier Agriculture Ltd, Norfolk, UK, were soaked in water for 12 h before planting. Three seeds of each species were sown in each of 8 replicate columns approximately 1.5 cm below the surface. Once the shoots emerged they were thinned to one plant per column. Columns were placed in a glasshouse in a random block design (four blocks featuring one replicate of each species x harvest; average day/night temperature of 24°/ 18°C) and were watered daily with a nutrient spiked (HortiMix Standard: 15-7-30 +1.6MgO + TE (2: 1: 4)) water solution.

3.4.4b Image processing and analysis

The four unplanted control columns were CT scanned on Day 0. A subset of 12 columns featuring the three species with four replicates was scanned after 20 days and a second subset of 12 columns was scanned after 58 days. Prior to imaging the soil columns were not watered for a period of 48 h to ensure a high level of contrast between soil, organic matter and root material. All columns were scanned using a Phoenix V|Tome |X m X-ray 240kV (GE Measurement & Control Solutions, Wunstorf, Germany) at the Hounsfield

Facility at the University of Nottingham, with a 0.1 mm copper filter. Each projection image was an integration of 3 images with a skip setting of 1 discarded image. Voxel resolution was set at 60 µm, potential energy of 180 kV and current of 180 uA. Columns were scanned in two sections with a total scan time of 75 mins per column. The distance from the sample to the source was 245 mm. A total of 2160 image projections were captured for each column. Images were reconstructed at 32-bit using Phoenix Datosx 2 reconstruction tool to form a 3D volume which was visualised using VG Studio Max 2.2.5 software.

An automated image processing algorithm, 'RooTrak', was used to segment roots from the µCT grey scale images [34]. The method employs a tracking-based strategy which follows the root cross-sections through a sequence of images, with the initial digital processing seed-point being identified manually by the user. As the image stack is traversed, the cross-sections move around the image, reproducing the shape of the scanned root. The tolerance values were adjusted following visual inspection to ensure only root material was included in the region of interest (ROI) produced. Once the root system was successfully extracted from the µCT images it was transferred as a bitmap (.bmp) image stack to VG Studio MAX v. 2.2.5 for editing. The finalised volumetric representation of the root system architecture was analysed to quantify both global and local traits in RooTrak v. 0.3.9.1 [35]. Global traits derived from the entire root system were volume (%), surface area (cm^2), maximum depth (mm), maximum width (mm), convex hull (cm^3) and solidity (mm^{-3}). Local traits were derived from the individual roots or a topical zone of

interest and included the number of lateral roots protruding from the primary root (lateral number) and the angle at which they projected (lateral angle), which were subsequently calculated using VG Studio Max. Global traits were considered for the root systems as a whole for all species. A selection of traits including root volume (%), surface area (mm^2), number and angle of lateral roots were calculated for the uncompacted and compacted zones within the column by splitting the image stacks at the transition zone between the different bulk densities. This allowed a layer comparison over time to be conducted on the individual species.

The root volume provides an estimate of the sum of the cross-sectional areas for all of the voxels in the root system and the total mass of the root system [36], here calculated as a percentage volume of the total soil volume. Root surface area was calculated by summing the representative isosurface of the segmented root system to provide an approximate surface area of root that is in direct contact with the soil [34]. Root depth measurement was calculated as the maximum vertical distance reached by the root system in relation to the first image slice containing a root system voxel [24]. Root system width was calculated as the maximum horizontal width of the whole root system architecture. The convex hull was determined as the smallest convex set of voxels that contain the root system and indicates the effective volume of soil explored by the root system, and allows a formalised geometric analysis of the zone of influence of the root system [35]. Solidity was calculated as the fraction equal to the root volume divided by the convex hull volume in 3D, and partly indicates the relative spatial ability of roots to obtain water and

nutrients. Lateral number was determined by a manual count of the lateral roots protruding from the primary root using the indicator tool in VG Studio Max. Lateral initiation angle was measured using the 3-point angle tool in VG Studio Max and describes the angle of the root at its join to the primary root; an angle of 0 degrees indicates vertical growth and 90 degrees indicates horizontal growth. Once the root systems had been analysed using RooTrak the output image stacks were imported into Blender 2.77 (open source) for image rendering.

The CT resolved air filled pore space (porosity) of the columns was calculated using ImageJ-win64. Due to the resolution of the images in this study only the air filled pore space was included in the soil porosity measurements. This is because the grey scale colouration of water filled pores and organic matter is extremely similar. By discounting water filled pores, porosity measurement is not over-estimated for the scale of the imagery by including unwanted organic matter. Two image stacks of 500 grey scale image slices were extracted separately for the two bulk density layers in each column and the porosity for each sample cube was averaged. A macro was used to automatically crop, enhance brightness/ contrast, apply median filter, radius 1, apply 'minerror' threshold and convert data to 8-bit. Two sample sites were selected with different start coordinates in each layer and an area of 27 cm^3 was analysed.

To establish whether the time, compaction or species effect had interactions as explanatory variables on the global and local root traits, a two-way

factorial analysis of variance (ANOVA) with specified block design was undertaken on the columns as a full system comparing all species and on the two bulk density layers comparing species individually. Soil porosity values were analysed using ANOVA allowing for split plot design for bulk density layers within the cores. Statistical tests were conducted using Genstat 17th edition and included requisite tests for distribution and homogeneity of variance. Treatment effects were considered significant when $p < 0.05$.

3.4.5 Results

3.4.5a Whole root architecture analysis

Whole three-dimensional visualisations of the three species' root systems grown within a two-phase compaction treatment were analysed based on renderings of X-ray CT data. They revealed a marked contrast in the overall root system architecture between the three species, and a substantial effect of soil bulk density on root behaviour was observed (Figs 3.7 and 3.8). Tillage radish developed a taproot system with extensive lateral roots by 20 days with substantial radial tap root expansion by 58 days, entirely confined to the uncompacted zone, and a series of vertically-penetrating finer roots arising from the terminus of the tap root into the compacted zone (Figs 3.7A and 3.7B). Vetch produced a diffuse primary root system largely confined to the uncompacted zone, with very little penetration of the compacted zone and little change between Days 20 and 58 (Figs 3.7C and 3.7D). The root system frequently exhibited a deflection of the taproot towards the column wall

upon encountering the compacted zone (Fig 3.7D). Black oat developed mainly vertically-oriented primary roots which were very prolific in the uncompacted zone, but also penetrated the compacted zone, increasing in frequency between Days 20 and 58 (Figs 3.7E and 3.7F). There was no evidence for any vertically upward growth of roots as a result of encountering the interface between the bulk density phases for any of the species.

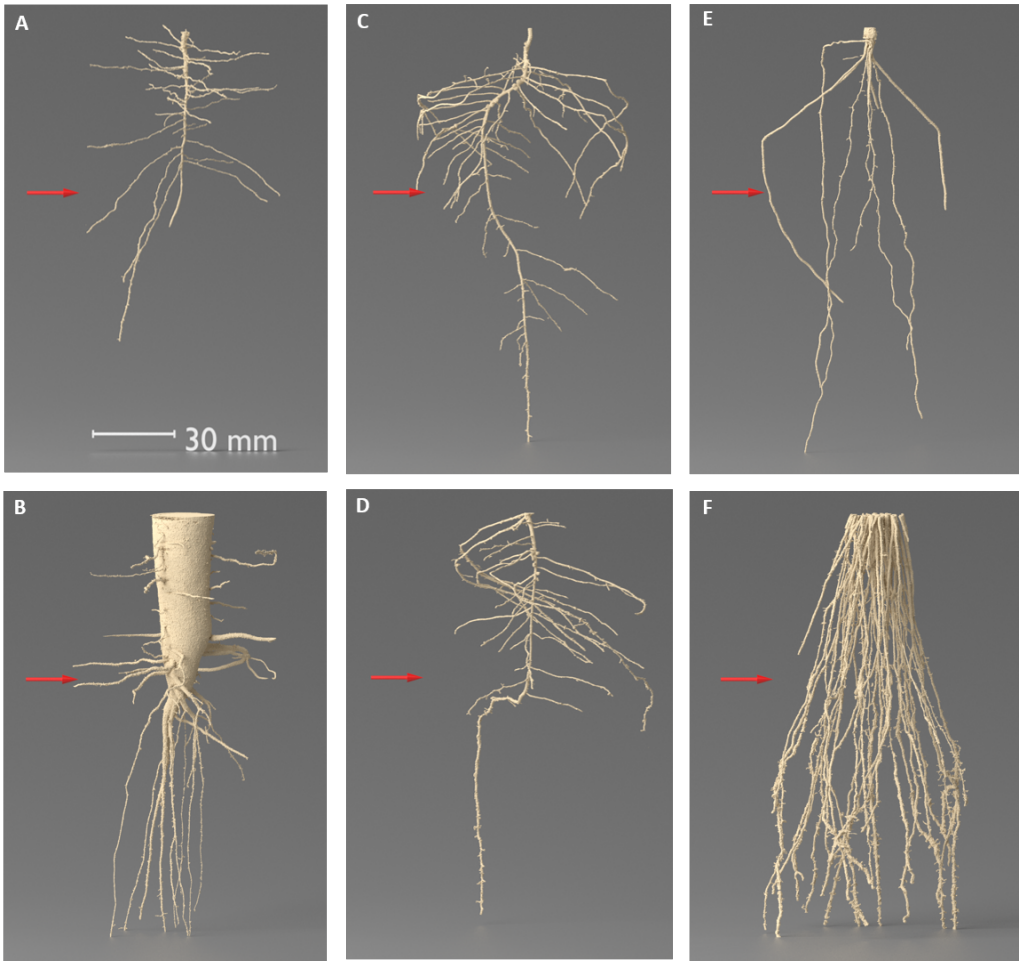


Fig 3.7. Representative 3D renderings of root systems grown in repacked soil columns. (A) tillage radish after 20 days growth; (B) tillage radish after 58 days growth; (C) vetch after 20 days growth; (D) vetch after 58 days growth; (E) black oat after 20 days growth; (F) black oat after 58 days growth. Red arrows indicate location of change in dry bulk density of soil profile from 1.2 to 1.4 g cm^{-3}.

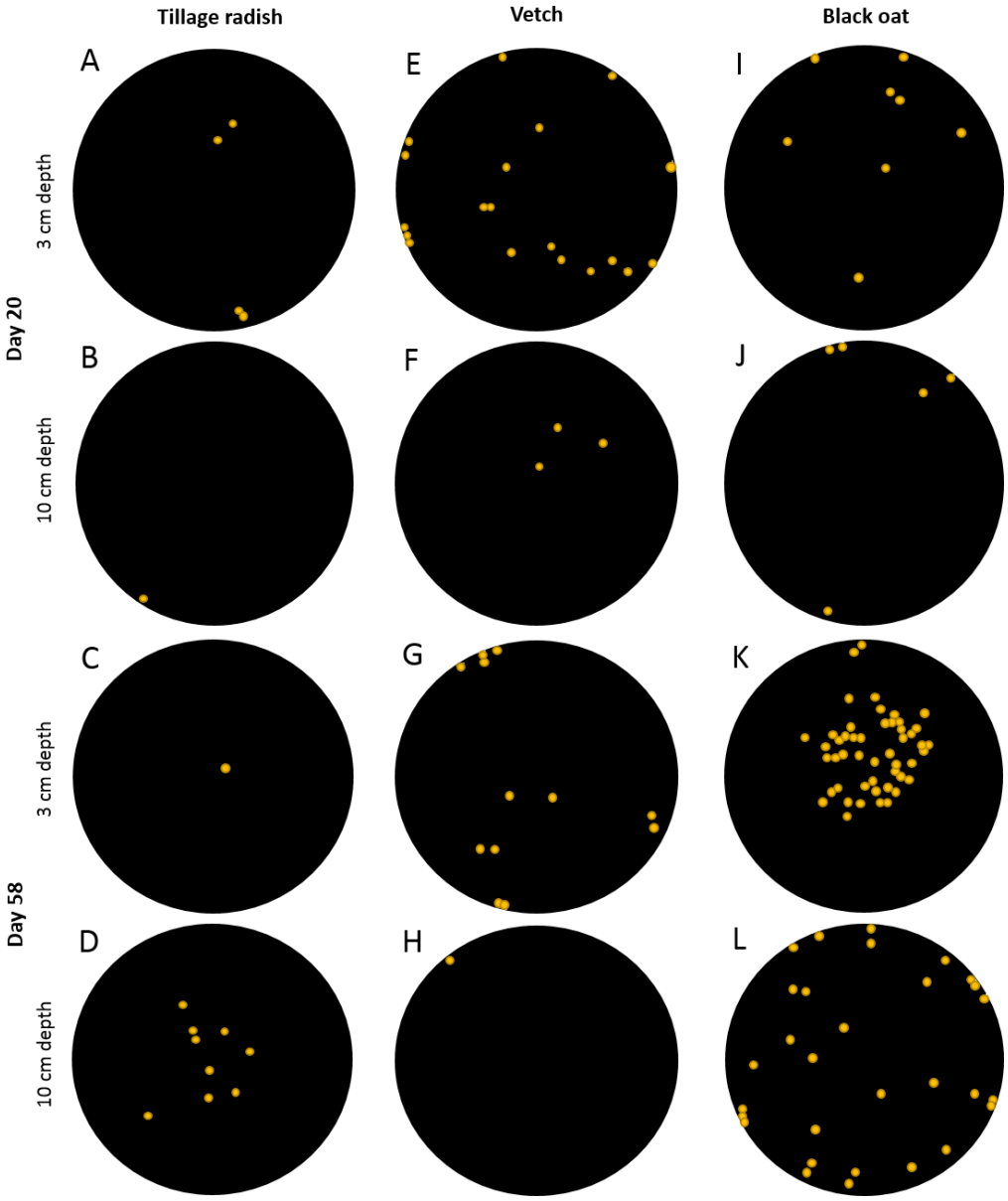


Fig 3.8. Location maps of roots in 2D cross-section representative slices of segmented root systems shown in Fig 3.6. (A-D) Tillage radish: (A-B) Day 20; (C-D) Day 58; (E-H) Vetch: (E-F) Day 20; (G-H) Day 58; (I-L) Black oat: (I-J) Day 20; (K-L) Day 58. Orange circles denote position of root within column and do not relate to root diameter (actual sizes would be indiscernible in many cases at this scale of imaging; diameter of core, here black circles, is 75 mm). For all species 3 cm depth falls within the uncompacted zone and 10 cm depth is within the uncompacted zone.

In all cases, roots that made contact with the edges of the columns subsequently tracked these boundaries by growing vertically downwards (Figs 3.7 and 3.8). Whilst at Day 20 roots of tillage radish and black oat were predominantly located in this peripheral region (Figs 3.8B, and 3.8J), by Day 58 newly formed roots showed little lateral deviation as a result of entering the compacted zone and were subsequently prolific within this layer (Figs 3.8D and 3.8L). Penetration of the compacted zone by vetch was variable between replicates and in most cases roots were confined to the peripheral zone adjacent to the column wall. Where vetch roots penetrated the compacted zone, they tended to grow laterally (Figs 3.7C and 3.8F). Rapid vertical growth was observed with all species penetrating the compacted zone by Day 20, at Day 58 the full depth of the columns had been explored by all root systems. At Day 20 the total surface area of root systems was similar between the three species, increasing significantly between Days 20 and 58 for tillage radish and black oat, but not for vetch (Fig 3.9; species x time interaction $p=< 0.001$, $n = 24$). Similar trends were observed in the root volume data (Fig 3.9B), with tillage radish producing a notably large volume as a result of radial expansion of the tap-root. The relative total volume for tillage radish roots was 48 times greater than for vetch roots, and twice that of black oat roots. Relative total volumes in the compacted zone revealed that mean tillage radish root volumes were 7.3 times greater than vetch root volumes and 1.2 times greater than black oat.

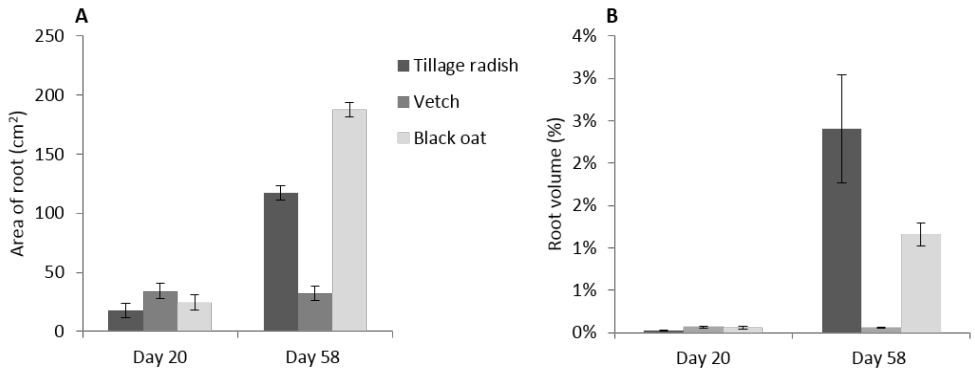


Fig 3.9. Average surface area of root (cm^2) and root volume as % of full soil column. (A) Surface area of root (cm^2) within full soil column for tillage radish, vetch and black oat root systems, derived from X-ray CT data. Bars denote means, whiskers pooled SE. (B) Volume of root as a percentage of the uncompacted and compacted soil zones for tillage radish, vetch and black oat root systems, derived from X-ray CT data. Due to the disproportionately large increase in total root volume for tillage radish the data was not subject to ANOVA. Bars denote means, whiskers individual standard deviation. Data is presented in S1 File.

At Day 20 both tillage radish and vetch plants exhibited extensive lateral proliferation in the uncompacted zone resulting in a wide convex hull tapering into a thin angular hull in the compacted zone as the number of laterals decreased with depth (Figs 3.10A and 3.10B). Black oat roots depicted a thinner convex hull due to the vertical nature of root growth through both the uncompacted and compacted zones (Fig 3.10C). At Day 58 the convex hull volume of tillage radish revealed that the lateral proliferation decreased resulting in a thinner convex hull in the uncompacted zone, observed as a split in the taproot morphology into numerous vertical growing secondary roots, increasing the volume of the hull in the compacted zone (Fig 3.10B). The convex hull of the vetch roots at Day 58 was unchanged from Day 20 (Fig 3.10E). The convex hull of black oats exhibited a thin geometric shape in the lower layer spreading to a wide hull in the compacted zone as the roots

proliferated towards the column walls and started to track down the periphery of the column (Fig 3.10F). Mean convex hull volumes increased significantly over time for tillage radish and black oat plants, whilst they were equal in vetch plants (Fig 3.11A; species x time interaction p=0.031, n=24). Likewise, solidity values increased over time for tillage radish and black oat, but not for vetch (Fig 3.11B).

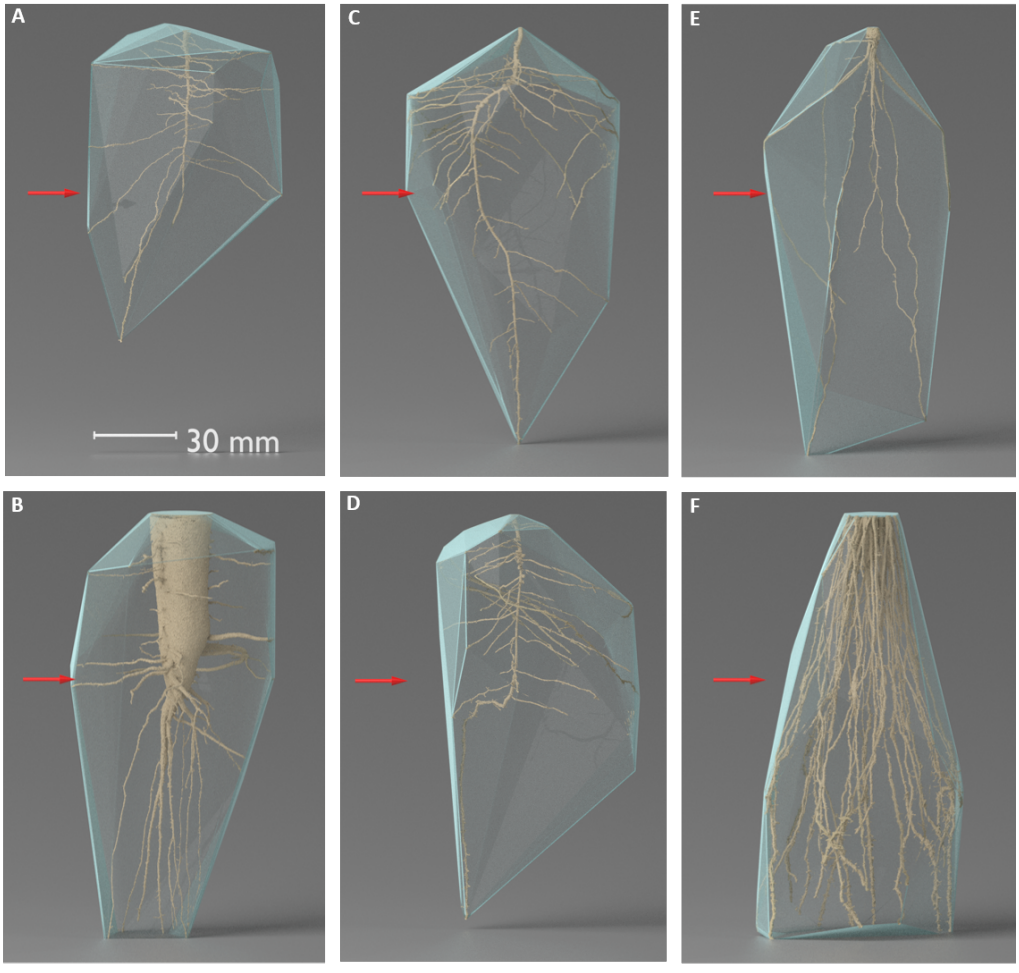


Fig 3.10. Visual representation of convex hull volumes for representative root systems, red arrows indicate change in dry bulk density of soil profile. (A) Tillage radish after 20 days growth. (B) Tillage radish after 58 days growth. (C) Vetch after 20 days growth. (D) Vetch after 58 days growth. (E) Black oat after 20 days growth. (F) Black oat after 58 days growth.

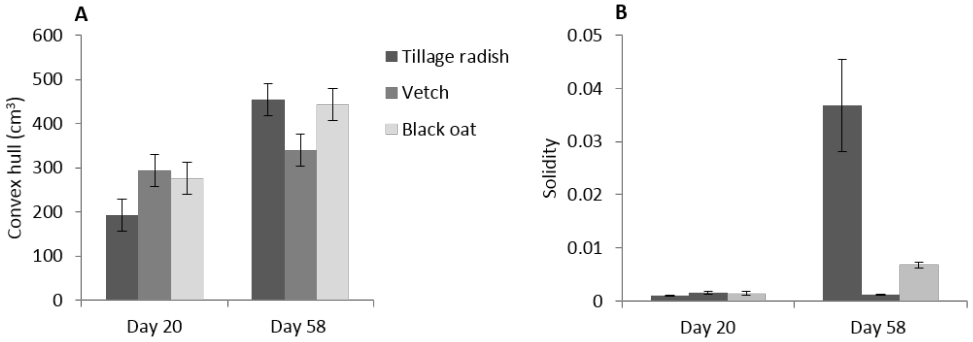


Fig 3.11. Average root systems convex hull (cm^3) and solidity value of full soil column. (A) Convex hull (cm^3) of tillage radish, vetch and black oat root systems. Data represents full root systems, derived from X-ray CT. Bars denote means, whiskers pooled SE. (B) Solidity values of tillage radish, vetch and black oat root systems. Data represents full root systems, derived from X-ray CT data. Due to extreme range of values, tillage radish the data was not subject to ANOVA. Bars denote means, whiskers standard error.

3.4.5b Uncompact versus compact comparison

3.4.5b (i) Tillage radish

Root surface area was similar at Day 20 in both the uncompacted and compacted zones. This increased significantly with time, significantly more so in the uncompacted zone, with 50% greater surface area in comparison to the compacted zone at Day 58 (Fig 3.12A; time x compaction interaction p=0.004, n=16). Root volume of tillage radish increased substantially as a result of tap root expansion by Day 58, which was exclusively confined to the uncompacted zone (Fig 3.12B). Whilst roots subsequently penetrated the compacted zone, their volume was some 30 times smaller than the tap root (Fig 3.12B). Greater numbers of lateral roots were observed in the uncompacted zone compared to the compacted, with means of 35 and 6 respectively (compaction effect p= <0.001, n=16; Fig 3.12C). The number of

lateral roots between the uncompacted and compacted zones did not change over time (Fig 3.12C). Only main effects in ANOVA were apparent with respect to the branch angle of lateral roots (Fig 3.12A). These decreased significantly in the compacted zone in comparison to the uncompacted zone with overall means of 75° and 50° respectively (p=<0.001, n=16). Branch angle also decreased over time in both the uncompacted and compacted zones (overall means 77° and 49° respectively p<0.001, n=16).

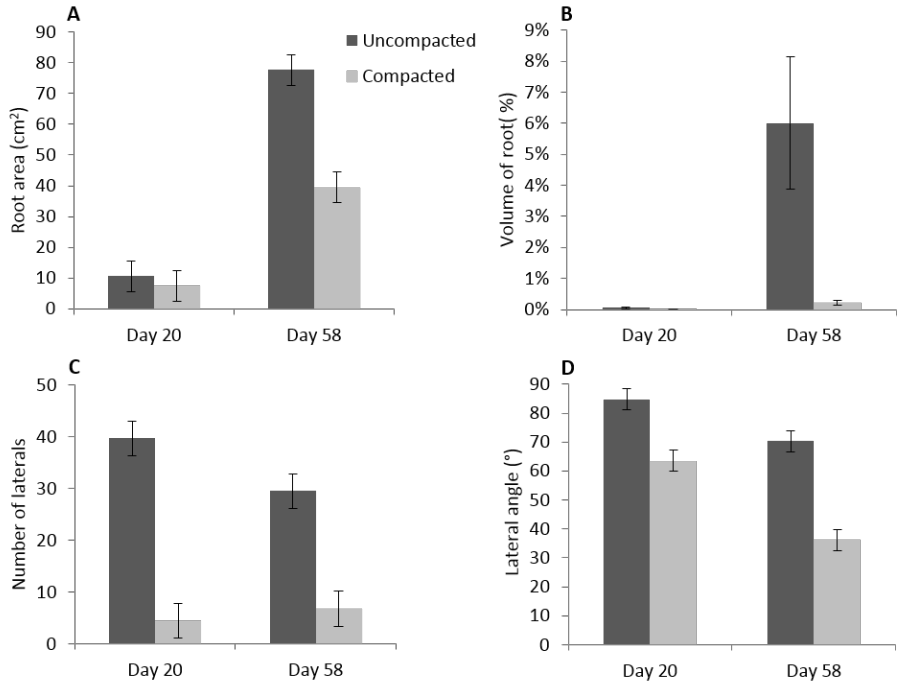


Fig 3.12. Average surface area (cm^2), volume of root (%), number of laterals and lateral angle (°) of tillage radish root systems. (A) Average surface area of tillage radish root (cm^2). (B) Average volume of tillage radish root as a percentage of the soil volumes. Due to extreme range of data values data was not subject to ANOVA. (C) Average number of lateral roots observed protruding from the taproot. (D) Average angle of lateral roots protruding from taproot. For all graphs data is presented for both the compacted and uncompacted zones over two time periods. Bars denote means, whiskers pooled (A, C, D) or individual (B) s.e.

3.4.5b (ii) Vetch

For vetch, there was a significant effect of compaction on root surface area, with overall means of 110 cm^2 and 221 cm^2 for compacted and uncompacted respectively ($p<0.001$, n=16; Fig 3.13A) and hence no significant change over time. This phenomenon was mirrored in the root volume data with a difference of 0.09% between uncompacted and compacted zones (Fig 3.13B; compaction effect p=<0.001, n=16). A 70% reduction in number of lateral roots was observed in the compacted zone compared to the uncompacted zone at both Days 20 and 58 (Fig 3.13C; compaction effect p<.001, n=16). Branch angle was observed to decrease in the compacted zone by 5° (Fig 3.13D; compaction effect p=0.002, n=16).

3.4.5b (iii) Black oat

Root surface area of oats increased significantly between Days 20 and 58 (123 cm^2 and 939 cm^2 respectively; $p<0.001$, n=16), with no effect of compaction or interaction over time (Fig 3.14A). An increase in root volume was observed in both the uncompacted and compacted zones over time, with a substantial volume increase of 0.3% in the uncompacted zone (Fig 3.14B; time x compaction interaction p=0.006, n=16).

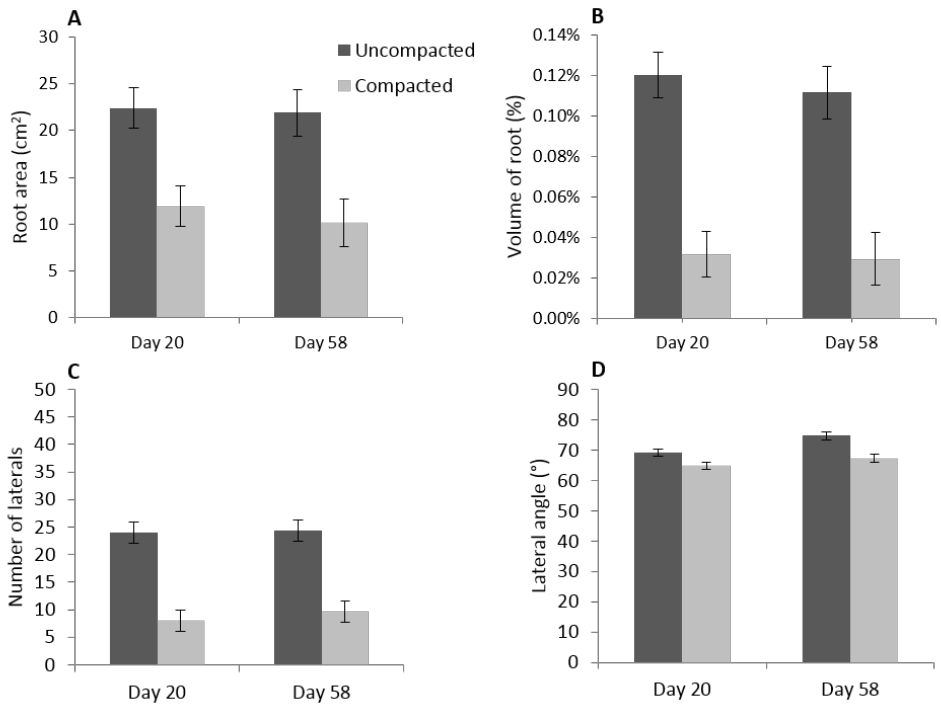


Fig 3.13. Average surface area (cm^2), volume of root (%), number of laterals and lateral angle (°) of vetch root systems. (A) Average surface area of vetch root (cm^2) (B) Average volume of vetch root as a percentage of the soil volumes, (C) Average number of lateral roots observed protruding from the taproot into the soil volumes. (D) Average angle of lateral roots protruding from taproot into the soil volumes. For all graphs data is presented for both the compacted and uncompacted zones over two time periods Bars denote means, whiskers pooled SE.

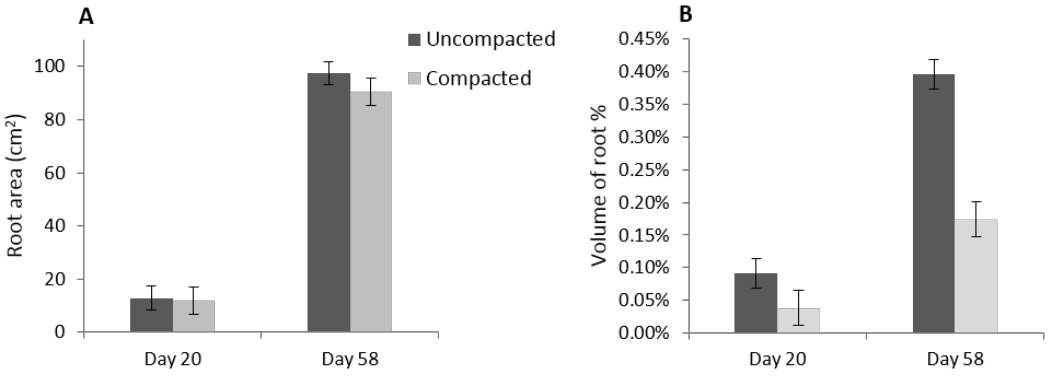


Fig 3.14. Average surface area (cm^2), volume of root (%) of black oat root systems. (A) Average surface area of black oat root (cm^2). (B) Average volume of black oat root as a percentage of the soil volume. For all graphs data is presented for both the compacted and uncompacted zones over two time periods. Bars denote means, whiskers s.e.

3.4.5c Soil porosity

A marginally significant third-order interaction between species, compaction and time was observed in relation to soil porosity (measured at a scale of 60 µm) ($p=0.058$, $n=56$; Fig 3.15). Porosity was of the range 5-6% in the compacted layer, compared to 7-10% in the uncompacted layer. No significant difference in porosity between control columns and vetch or black oat plants was observed in the uncompacted zone at Day 20. However there was a significant difference indicating an increase in porosity between control columns and tillage radish columns at Day 20 in the uncompacted zone. No significant difference in porosity was observed in the compacted zone in any species at either Day 20 or Day 58 in comparison to Day 0. Black oat plants exhibited a significant difference in porosity between the uncompacted and compacted zones at both Day 20 and Day 58. In vetch this significant effect was only exhibited by plants at Day 58, and in tillage radish plants at Day 20.

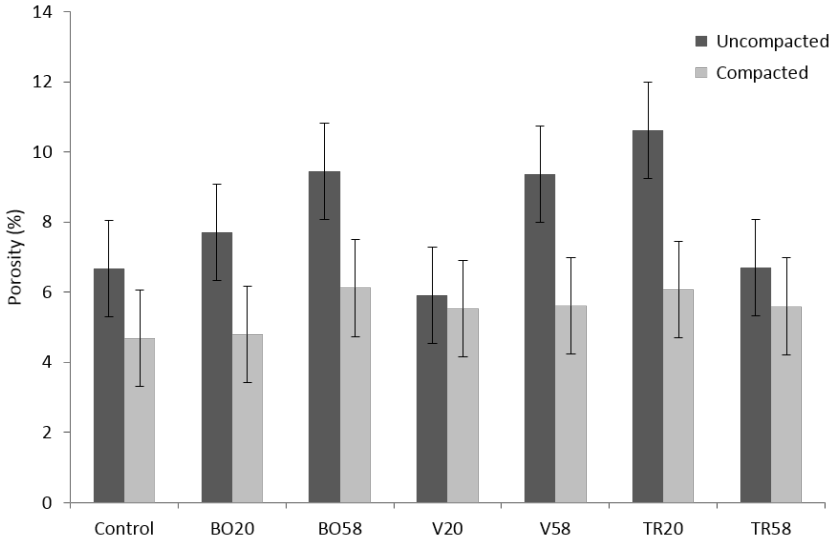


Fig 3.15. Soil porosity of uncompacted and compacted layers with tillage radish, vetch and black oat roots systems growing at three time points. Average percentage of pore space from representative samples within both the uncompacted and compacted soil volumes, bars denote means, whiskers pooled s.e.

3.4.6 Discussion

Soil dry bulk densities typically encountered in the field can range from between 1.1 g cm $^{-3}$ to 1.6 g cm^{-3} with the denser soils restricting plant root development [36]. This study mimicked bulk density transitions which may occur frequently in the field, often as 'plough pans', manifest as a sharp increase in bulk density across a plane at the plough depth (typically *circa* 20 cm), but also more sporadically as a result of general trafficking or soil structural collapse after rainfall [4]. The geometry and scale of bulk density transitions will vary in the field. In our experimental system, the scale of the design was prescribed to optimise the trade-off between the spatial resolution of the CT scanning (smaller volumes providing greater resolution) and a volume of soil that would allow a reasonable development of the plants, whilst providing the key feature of the presence of an interface between relatively low and high soil bulk densities.

The restriction of root growth within compacted soils depends on the species and the age of the plants [1, 22], which is why plants were imaged at both juvenile and more mature growth stages. The roots grown in this experiment will have experienced a decrease in aeration and a small increase in soil penetration resistance (0.21 to 0.30 MPa), and increase in root-soil contact with depth as they enter the more compacted zone. These three changes in soil aeration, soil strength, and root-soil contact represent relatively benign soil physical conditions that would not normally be expected to be a major restriction to root elongation.

At Day 20 both vetch and black oat plants had a mean root volume of 0.06% in comparison to tillage radish 0.03%. Despite having the same mean volume as black oat, vetch plants had the greatest mean solidity, convex hull volume and root surface area values, indicating that at the juvenile growth stage vetch had the greatest ratio between the volume of the column explored in comparison to the volume of the root system. The solidity of the root system is a functionally important indicator in root foraging, and the higher its relative value, the greater the root systems spatial suitability to obtain water and nutrients [37]. Hence at Day 20 the imaged roots of the vetch plants had explored the soil column much better than those of the other two species. Despite this, porosity data indicated that tillage radish plants at Day 20 had significantly increased the air filled porosity within the uncompacted zone. Unlike the other two species, this increase may be attributed to high volumes of fine root mass not accounted for in the 60 µm resolution of the scans. At Day 58 tillage radish root systems exhibited the greatest mean solidity, root volume and convex hull volume; however, in this case of the tillage radish taproot in the upper layer, the bulk of the root volume was contained in one very thick taproot – and so would be relatively ineffective at extracting soil resources as compared with a more finely divided root system – indicating that the concept of solidity cannot be used in isolation. The presence of this large root was reflected in the porosity measurement with tillage radish plants at Day 58 showing a decrease in porosity due to a large volume of the uncompacted zone being comprised by the taproot. The large root system of the tillage radish was mainly concentrated in the tap root, as compared with

the volume of black oat root systems that was widely dispersed by more individual roots within the compacted zone. Under field conditions the ability of roots of various crops to penetrate compacted soils is a reflection of their relative capacity to produce roots under such compacted conditions [21]. The juvenile vetch plants initially produced root volume fastest but, by the mature growth stages, both tillage radish and oat had overtaken the vetch. However, the roots that penetrated into the compacted zone did not significantly increase the porosity of the soil at a resolution of 60 μm.

A number of studies (e.g. [21, 22]) suggest that dicot roots are better able to penetrate compacted subsoil in the field than monocot roots, and species with thicker roots tend to exhibit greater penetration of the subsoil. For tillage radish it was not the thicker roots *per se* which penetrated the compacted layer, but instead the root system architecture response was for the single thick taproot to branch into multiple finer roots ('fanging'; [38]), which penetrated the denser soil. In preliminary studies, when tillage radish was grown in a soil of uniform bulk density, no fanging occurred at depths of up to 83 cm (S1 Fig). Hence it appears to be the transition in bulk density that triggered the morphological changes observed. Similar fanging-style morphological responses of sugar beet and carrots to mechanical impedance has also been observed in compacted field soils [39]. As a result, for tillage radish there was a proliferation of roots within the compacted zone which then grew at an acute angle downward, with no evidence for tracking a path of least resistance towards to edge of the column.

Lateral roots are generally finer than a parent taproot and can penetrate smaller pores [9]. The observed fanging of the tillage radish may increase the exploratory capabilities of the root system. In the field subsoil pans tend to decrease rooting depth, this is commonly associated with an increase in root biomass in the topsoil as a result of increased lateral formation by those roots experiencing impedance at their apices. The thickening of primary roots and increased proliferation of lateral roots in the loose soil located above a high-strength soil layer has been previously reported [40]. It is likely that increased levels of ethylene produced by stressed roots in compacted soil and subsequent higher availability of carbohydrates due to impeded translocation of substrate from the shoot when the growth of the main axis is restricted may results in the increased proliferation of lateral roots above a homogeneous compacted layer [22]. The images of the root systems for vetch and tillage radish at seem at least qualitatively consistent with the concept of increased length of laterals in the upper (uncompacted) layer, although the finest roots will not have been resolved by the CT due to the spatial limit of detection.

A change in tap root morphology at the interface between the two bulk density phases of the vetch plants was observed in the majority of cases; the primary root growth angle was deflected at the compacted phase change to follow the path of least resistance horizontally across the soil profile to the column wall. Roots may not be able to penetrate the subsoil from weaker surface layers if they are very flexible [20]. The trajectories of root tip growth differed markedly between the three species on encountering even the

modest change in soil strength at the interface between the layers. Vetch was most sensitive with its root tip diverting from the vertical to the greatest extent, tillage radish exhibited marked fanging of the taproot, whilst black oat roots were not noticeably diverted. We are not aware that such large differences between species in this characteristic has been reported previously.

Despite tillage radish having the greatest mean root volume in the compacted zone, black oat exhibited the greatest mean root surface area, because the root volume consisted of many thinner roots. A greater root surface area means a higher degree of root:soil surface contact which may be beneficial for nutrient and water uptake [41]. As a result more roots penetrated directly through the compacted zone in black oat plants, indicating the trajectory of root growth was least affected by the bulk density change. The more roots that can penetrate a soil mass, the greater the potential improvement to the soil through changes in soil pore size distribution [21]. In the case of the species studied, the greater number of roots which were able to penetrate into the compacted zone, the greater the potential rate of soil amelioration. Both tillage radish and black oat exhibited evidence of roots penetrating the compacted zone without the aid of the column wall, suggesting that in field realistic conditions they are more likely to have the ability to grow vertically through a compacted soil profile as opposed to deflecting and resulting in high volumes of root in the topsoil. From the data collected at the mature growth stage, both tillage radish and black oat provide contrasting root system architectures each with the ability to consistently penetrate a

compacted zone. Although the porosity of the lower soil layer did not change during this study, the ultimate decay of the roots would leave biopore channels in the soil that subsequent crop roots might exploit. Both tillage radish and black oat may therefore be favourable candidate species for compaction alleviation via bio-drilling.

The three modes of morphological response exhibited by the different species here are complementary in terms of the way the soil volumes in the two soil bulk density layers are exploited, particularly after 58 days. This is apparent in 2-D visualisations, where combined root distributions in both uncompacted (Figs 2C, 2G and 2K) and compacted (Figs 2D, 2H and 2L) zones collectively span the entire plane; and in 3-D visualisations, where the convex hull shells have a highly complementary geometry (Figs 4B, 4E and 4F). These morphological types have here been manifest when the plants are grown in isolation, and it remains to be seen if such trait complementarity would prevail when the plants are grown in combination - and in competition. Were it so, this would offer the potential that such mixtures could be adopted in circumstances where thorough exploration of the soil resource is required. The species prescribed for this study are commonly adopted as cover crops in arable rotations [22, 42, 43], and our study provides evidence as to why tillage radish and black oats in particular are likely effective species in this role where there is soil compaction. It also suggests that a mixture of the three might be more potent, particularly in terms of increasing the porosity of a soil via complementary penetrating and proliferating growth modes.

This study has provided a detailed 3D visualisation using a specialised automated image segmentation method to visualise the impact a change in bulk density of a sandy loam soil had on the root system architecture of three major cover crop species using non-destructive X-ray CT scanning. The spatial resolution of objects imaged by X-ray CT is prescribed by the total volume of the sample being scanned. Here, the limit of resolution was 60 µm and as such the roots visualised were confined to those greater than this dimension. Very fine root mass was not detected and therefore not considered in this study. The size of sample column restricted the maximum rooting width/ depth, convex hull and solidity measurements as the maximum volume of the sample was limited.

3.4.7 Conclusion

Here we revealed the ontogeny of tillage radish, vetch and black oat root formation in 3D and provide insight into changes in root system architecture, specifically changes in taproot morphology and lateral root growth angles upon encountering a compacted soil layer. Smaller root volume, surface area, number of lateral roots and angle values were consistently observed in the compacted zone in comparison to the uncompacted across all species types. This suggests that plant roots can be sensitive to even a relatively small change in bulk density, which can directly inhibit growth and instigate changes in root morphology, particularly in tap-root species. Tillage radish root systems produced the greatest values at the mature growth stage for

root volume, convex hull volume, solidity, lateral number and lateral angle. Black oat root systems produced the greatest root surface area at the mature growth stage and also had the greatest root proliferation within the compacted zone coupled with the least notable change in root morphology. Tillage radish and black oat root systems both appeared better suited for soil structural remediation.

3.4.8 Supporting information

Appendix 3 supplementary data, Table A.3.2, A.3.3 & A.3.4 file contains soil porosity and root characteristic measurements for the 28 columns.

Appendix 3 supplementary data Fig A.3.5 Tillage radish plants, *(Raphanus sativus)* grown in soil columns with dimensions of 85 cm depth, 17 cm width, packed to a bulk density of 1.5 g cm-3 with a soil mixture of Broughton clay loam soil 70%, Tunstall silver sand 30%, for 65 days.

3.4.9 Acknowledgements

This research is supported by the award of a studentship grant to JB-H by the NERC and BBSRC funded STARS (Soils Training And Research Studentships) Centre for Doctoral Training and Research Programme; a consortium consisting of Bangor University, British Geological Survey, Centre for Ecology and Hydrology, Cranfield University, James Hutton Institute, Lancaster University, Rothamsted Research and the University of Nottingham. Grant Ref: NE/M009106/1. The James Hutton Institute receives funding from the Scottish Government. We thank Paul Brown of Frontier Agriculture for

supplying seeds used in this study and useful discussions, and two anonymous reviewers plus the editor for helpful suggestions for improvement to the manuscript.

3.4.10 References

1. Grzesiak S, Grzesiak MJ, Hura T, Marcinska I, Rzepka A. Change in root system structure, leaf water potential and gas exchange of maize and triticale seedlings affected by soil compaction. Journal of Experimental Botany. 2013; 88: 2-10.
2. Taylor HM and Brar GS. Effect of soil compaction on root development. Soil and Tillage Research. 1991; 19: 111-119.
3. Ball BC, Campbell DJ, Douglas JT, Henshall JK, O'Sullivan MF. Soil structural quality, compaction and land management. European Journal of Soil Science. 1997; 48: 593-601.
4. Batey T. Soil compaction and soil management- a review. Soil Use and Management. 2009; 25: 335-345.
5. Tracy SR, Black CR, Roberts JA, Mooney SJ. Soil compaction: a review of past and present techniques for investigating effects on root growth. Journal of Food Science and Agriculture. 2011; 91: 1528-1537.
6. Alameda D, Villar R. Linking root traits to plant physiology and growth in *Fraxinus angustifolia* Vahl. seedlings under soil compaction conditions. Environmental and Experimental Botany.2012; 79: 49-57.
7. Iijima M, Kono Y, Yamauchi A, Paradales JR. Effects of soil compaction on the development of rice and maize root systems. Environmental and Experimental Botany. 1991; 31(3): 333-342.
8. Lipiec J, Hatano R. Quantification of compaction effects on soil physical properties and crop growth. Geoderma. 2003; 116: 107-136.
9. Clark LJ, Whalley WR, Barraclough PB. How do roots penetrate strong soil? Plant and Soil. 2003; 255: 93-104.

10. Bengough AG, Mullins CE. Mechanical impedance to root growth: a review of experimental techniques and root growth responses. Journal of Soil Science. 1990; 41: 341-358.
11. Tracy SR, Black CR, Roberts JA, McNeill A, Davidson R, Tester M, et al. Quantifying the effect of soil compaction on three varieties of wheat (*Triticum aestivum* L.) using X-ray micro computer tomography (CT). Plant Soil. 2012; 353: 195-208.
12. Bengough AG, McKenzie BM, Hallett PD, Valentine TA. Root elongation, water stress, and mechanical impedance: a review of limiting stresses and beneficial root tip traits. Journal of Experimental Botany. 2011; 62: 59-68.
13. Valentine TA, Hallett PD, Binnie K, Young MW, Squire GR, Hawes C, et al. Soil strength and macropore volume limit root elongation rates in many UK agricultural soils. Annals of Botany. 2012; 110: 259-270.
14. Cresswell HP, Kirkegaard JA. Subsoil amelioration by plant roots- the process and the evidence. Australian Journal of Soil Research. 1995; 33: 221-239.
15. Han E, Kautz T, Perkons U, Uteau D, Peth S, Huang N, et al**.** Root growth dynamics inside and outside of soil biopores as affected by crop sequence determined with the profile wall method. Biology of Fertile Soils. 2015; 51: 847-856.
16. Stirzaker RJ, Passioura JB, Wilms Y. Soil structure and plant growth: Impact of bulk density and biopores. Plant and Soil. 1996; 185: 151-162.
17. White RG and Kirkegaard JA. The distribution and abundance of wheat roots in a dense, structured subsoil – implications for water uptake. Plant, Cell & Environment. 2010; 33: 133–148.
18. Tardieu F. Growth and functioning of roots and of root systems subjected to soil compaction. Towards a system with multiple signalling? Soil and Tillage Research. 1994; 30: 217-243.
19. Passioura JB. Soil structure and plant growth. Australian Journal of Soil Research. 1991; 29: 717–728.

20. Jin K, Shen J, Ashton RW, Dodd IC, Parry MAJ, Whalley WR. How do roots elongate in a structured soil? Journal of Experimental Botany. 2013; 64: 4761-4777.
21. Materechera SA, Dexter AR, Alston AM. Penetration of very strong soils by seedling roots of different plant species. Plant and Soil. 1991; 135: 31-41.
22. Chen G. and Weil RR. Penetration of cover crop roots through compacted soils. Plant Soil. 2009; 331(1-2): 31-43.
23. Clark LJ, Barraclough PB. Do dicotyledons generate greater maximum axial root growth pressures than monocotyledons? Journal of Experimental Botany 1999; 50: 1263-1266.
24. Clark RT, MacCurdy RB, Jung JK, Shaff JE, McCouch SR, Aneshansley DJ, et al. three-dimensional root phenotyping with a novel imaging and software platform. Plant Physiology. 2011; 156: 455-465.
25. Ishaq M, Ibrahim M, Hassan A, Saeed M, Lal R. Subsoil compaction effects on crops in Punjab, Pakistan: II. Root growth and nutrient uptake of wheat and sorghum. Soil Tillage Research.2001; 60: 153–161.
26. Hamza MA, and Anderson WK. Soil compaction in cropping systems. A review of the nature, causes and possible solutions. Soil and Tillage Research. 2005; 82**:** 121-145.
27. Iijima M, Kono Y, Yamauchi A, Paradales JR. Effects of soil compaction on the development of rice and maize root systems. 1991; 31: 333-342.
28. Lipiec J, Medvedev VV, Birkas M, Dumitru E, Lyndina TE, Rousseva S, et al. Effect of soil compaction on root growth and crop yield in Central and Eastern Europe. International Agrophysics. 2003; 17: 61-69.
29. White RE. Peds and Pores. In White RE, editors. Principles and Practice of Soil Science. The Soil as a Natural Resource. 4th ed. Blackwell Publishing; 2006. pp. 59-78.
30. Keyes SD, Gillard F, Soper N, Mavrogordato MN, Sinclair I, Roose T. Mapping soil deformation around plant roots using in vivo 4D X-ray

Computed Tomography and Digital Volume Correlation. Journal of Biomechanics. 2016; 49(9): 1802-1811.

31. Dunbabin VM, Postma JA, Schnepf A, Pages L, Javaux M, Wu L, et al. Modelling root-soil interactions using three-dimensional models of root growth, architecture and function. Plant Soil. 2013; 372: 93-124.
32. Mooney SJ, Pridmore TP, Helliwell J, Bennett MJ. Developing X-ray computed tomography to non-invasively image 3-D root systems architecture in soil. Plant Soil. 2012; 352: 1-22.
33. Lewis J, Sjostrom J. Optimising the experimental design of soil columns in saturated and unsaturated transport experiments. Journal of Contaminant Hydrology. 2010; 115: 1-13.
34. Mairhofer S, Zappala S, Tracy SR, Sturrock C, Bennett M, Mooney SJ, et al. RooTrak: automated recovery of three-dimensional plant root architecture in soil from X-Ray microcomputed tomography images using visual tracking. Plant Physiology. 2012; 158: 561-569.
35. Mairhofer S, Sturrock C, Wells DM, Bennet MJ, Mooney SJ, Pridmore TP. On the evaluation of methods for the recovery of plant root systems from X-ray computed tomography images. Functional Plant Biology. 2015; 42: 460-470.
36. Vepraskas MJ. Bulk density values diagnostic of restricted root growth in coarse textured soils. Soil Science Society of America Journal. 1988; 52: 1117-1121.
37. Iyer-Pascuzzi AS, Symonova O, Mileyko Y, Hao Y, Belcher H, Harer J, et al. Imaging and analysis platform for automatic phenotyping and trait ranking of plant systems. Breakthrough Technologies. Plant Physiology. 2010; 152: 1148-1157.
38. Batey T. and McKenzie DC. Soil compaction: identification directly in the field. Soil Use and Management. 2006; 22: 123-131.
39. Lipiec J, Medvedev VV, Birkas M, Dumitru E, Lyndina TE, Rousseva S, et al. Effect of soil compaction on root growth and crop yield in Central and Eastern Europe. International Agrophysics. 2003; 17: 61-69.

40. Atwell BJ. Response of roots to mechanical impedance. Environmental and Experimental Botany. 1993; 33: 27-40.
41. Schmidt S, Bengough AG, Gregory PJ, Grinev DV, Otten W. Estimating root-soil contact from 3D X-ray microtomography. European Journal of Soil Science. 2012; 63: 776-786.
42. Kadziene G, Munkholm LJ, Mutegi JK. Root growth conditions in the topsoil as affected by tillage intensity. Geoderma. 2011; 166: 66-73.
43. Abdollahi L, Munkholm LJ, Garbout A. Tillage system and cover crop effects on soil quality: II. Pore characteristics. Soil Science Society of America Journal. 2013; 78: 271-279.

Chapter 4: Investigating the potential for wild plant roots to modify compacted soil structure in the rhizosphere

This chapter outlines a systematic review undertaken to select wild species for investigation that have a noted ability to grow in compacted soils. Preliminary species screening was undertaken by root washing and scanning in 2D to determine the most favourable candidate species for a more detailed investigation *in situ* using X-ray Computed Tomography (CT) (presented in this chapter as the form of a manuscript, currently under review). Method development of 3D-image processing and analysis techniques are also outlined. Plants were assessed for their ability to grow in a compacted soil. Soil pore formation in the rhizosphere was then quantified *in situ*.

Aim: To identify species able to grow on compacted soil (in 2D) and assess their root archiecture develpoment and subsequent soil pore formation potential in the rhizosphere in 3D.

Objectives:

- Select candidate plant species to investigate further via literature and consultation with experts
- Screen resultant shortlist of species and assess root biomass and architecture characteristics in 2D
- Evaluate image processing techniques for application to primary 3D study
- Evaluate and compare plant root architectures in 3D under a soil compaction treatment

- Calculate changes in soil porosity in both the rhizosphere and full core system as a result of root growth in 3D.

This chapter is structured in two parts. Sections 4.1 and 4.2 describe preliminary investigations into plant species selection. Sections 4.3 and 4.4 details computer based method development for image analsysis. Finally Section 4.5 comprises a manuscript which details the results of the 3D investigation.

4.1 Identification of plant species

A number of sources were consulted to identify potential plant species to investigate with relation to being able to grow in compacted soils. This review comprised a literature search, consultation of an online ecological database, field observations and liaison with experts on wild species. Information was collated and used to prescribe which plant species would be trialed at the seed germination stage and subsequent 2D screen for root and shoot characteristics in compacted soil.

4.**1.1 Literature search**

The following Internet based search engines were used to identify potential literature related to weed species and soil compaction; *Google Scholar (*http://scholar.google.com*), ScienceDirect (*http://www.sciencedirect.com/*),*

*JSTOR (*http://www.jstor.org*).* A systematic literature search was conducted in each of the search engines using specified search terms. Once species had been identified, a secondary search was conducted including specialised search terms. In total 37 documents were collected and reviewed for information.

4.1.2 Database consultation

The Ecological Flora (Ecoflora) project commenced in 1989, based at the University of York, it was started with the intent of producing a comprehensive account of the ecology of British plant species (Fitter & Peat, 1994). The database contains over 120,000 items on 1,777 species from around 1,100 sources relating to the British Flora and is being continually updated. The database can be accessed via an interactive website found at http://www.ecoflora.co.uk which allows the search for specific species via a catalogue based on characteristics. The following characteristics were used as screening parameters for species of interest: deep roots, roots >100 cm depth, taproot, adventitious roots, contractile roots, native species and mycorrhizae. These characteristics were chosen from an extensive catalogue on the Ecoflora database. Helen Peat (Ecoflora, personal communication) gave insight into how the database was originally collated via an extensive literature search, expert opinion and the collection of data by volunteers (A.4.1). An editorial board of 14 ecologists verified the database (Fitter & Peat, 1994), therefore it was deemed an informative tool to aid with the

screening process to identify plant species of interest. Appendix 4, T.4.1 indicates the species identified using the specific traits from the Ecoflora database. Plant species were ranked on presence or absence of the specific traits.

4.1.3 Field observations

A number of species were identified growing on compacted soils from field observations. Dandelion seeds (*Taraxacum officinale* L. Weber ex F.H.Wigg) were collected from Attenborough Nature Reserve, Attenborough, Nottingham, NG9 6DY, May, 2016, and spear thistle (*Cirsium vulgare* (Savi) Ten.) collected from Highfields Park Boating Lake, University Boulevard, Nottingham NG7 2RD, May, 2016. *Equisetum arvense* L. was observed with root systems growing down deeper than 2 metres and were identified during building excavations (Mark Burr-Hersey, personal communication). The plants were subsequently propagated and rhizomes collected for experimentation. *Elymus repens* (L. Gould) was observed in compacted soil in an allotment (Karl Ritz, personal communication) and were subsequently propagated and rhizomes collected for experimentation. *Matricaria discoidea* DC. was identified growing in compacted machinery tracks in agricultural fields, the seeds for this were obtained from Herbiseed (Reading, UK).

4.1.4 Liaison with experts

Experts in weed science from within the UK were contacted via email, the aim and scope of the project was explained to them and they were asked several questions. Their responses were used to help inform the systematic review of which species to investigate. Examples of the email liaison can be found in A.4.2. Bob Froud-Williams (Reading University, personal communication) highlighted a number of weed species with notable taproots as well as some indication of plants that he had observed growing in consolidated soil in the wild. Steve Morton (Herbiseed) (A.4.3) supplied samples of seed for 9 species in the initial screening.

4.1.5 Identification of candidate species

The systematic review resulted in eighteen plant species being screened for potential inclusion in the experiment (Table 4.1).

Table 4.1: Plant species, how seeds were procured and how species were initially identified for inclusion in the study.

Species			
Common name	**Scientific name**	**Seed Provider**	**Identification**
Tillage radish	*Raphanus sativus*	Frontier Agriculture	Observation
Horsetail	*Equisetum*	Self-obtained	Observation
Couch grass	*Elymus repens*	Self-obtained	Observation
Dandelion (D1)	*Taraxacum officinale*	Self-obtained	Expert
Dandelion (D2)	*Taraxacum officinale*	Self-obtained	Expert
Dandelion (D3)	*Taraxacum officinale*	Wild Flowers UK	Expert
Dandelion (D4)	*Taraxacum officinale*	Self-obtained	Expert
Spear thistle	*Cirsium vulgare*	Self-obtained	Literature
Thistle	*Cirsium*	Self-obtained	Observation
Creeping thistle	*Cirsium arvense*	Herbiseed	Literature
Pineapple weed	*Matricaria discoidea*	Herbiseed	Expert
Ribwort plantain	*Plantago lanceloata*	Herbiseed	Literature
Plantain	*Plantago*	Self-obtained	Literature
Greater Burdock	*Arctium lappa*	Herbiseed	Expert
Sow thistle	*Sonchus oleraceus*	Herbiseed	Expert
Broad leaf dock	*Rumex onstusifolius*	Herbiseed	Expert
Curly dock	*Rumex crispus*	Herbiseed	Expert
Dock	*Rumex*	Self-obtained	Expert

4.2 Screening

4.2.1 Germination

The eighteen species (Table 4.1) were germinated under a range of conditions to assess the best conditions for germination. The criteria for inclusion in the experiment was a germination rate of at least 60%, and the conditions used for each species are outlined in Appendix 4, T.4.2. Propagation from seed or rhizome was a challenging aspect of working with wild species. The screen undertaken was extensive with conditions trialled including a range of temperatures, light/ dark conditions, on filter paper or in soil, from seed or from rhizome, vernalisation, scarification and location. From these

germination trials, 7 species were selected for the first round of growth trials in soil.

4.2.2 Screening trial

4.2.2a Species

The species selected were; *Plantago lanceloata*, *Sonchus oleraceus*, *Raphanus sativus*, *Cirsium* arvense and *Taraxacum officinale*, *Equisetum arvense* and *Elymus repens*. In the early growth stages, the plants produced very different amounts of above-ground biomass. Plants were grown for 5-10 and 9-14 days depending on the species and the amount of shoot material produced.

4.2.2b Experimental set up & growth conditions

Cores, 5 cm in diameter and 10 cm in height, were uniformly packed with sandy loam soil (66.4% sand, 18.0% silt and 15.6% clay) to a depth of 8 cm at dry bulk densities of 1.6 g cm^{-3} and 1.8 g cm^{-3} with penetrometer resistance of 0.85 and 1.55 MPa respectively. Columns were compacted using the wet soil compaction method outlined in Section 2.1.2b, the moisture content at the time of packing was 16%. The penetration resistance of the soil was measured using the method specified in Section 2.1.4. Plants were grown in batches to three different time points since emergence, Point A: 5 days after emergence, Point B: 10 days after emergence days and Point C: 58 days after emergence. Days since emergence was used instead of days since planting as the different species took varying amounts of time to emerge. This is reflected in the time

categories in Table 4.3. Plants were grown in the University of Nottingham Hounsfield Glass House with sodium lights with an average day night temperature of 20˚C /15˚C. Plants were watered with 4 ml of water each day.

4.2.2c Results

Data on specific plant traits including; shoot fresh weight (g), shoot dry weight (g), root dry weight (g), root: shoot ratio (%), total root length (cm), average root diameter (mm) and root area (cm^2) was collected for each species grown in 1.6 g cm^{-3} or 1.8g cm^{-3} bulk density soil at three time points. The propagation of both *Equisetum* and *Elymus* species was unsuccessful so they were no longer used.

To establish whether bulk density, time or plant species affected biomass and 2D root characteristics a three-way factorial analysis of variance (ANOVA) was undertaken in R. Table 4.2 indicates the output of the statistical analysis.

Table 4.2: Details the results of the three way ANOVA conducted. The factors were Time, Species and Bulk density. The ANOVA was conducted in Rstudio.

Measured characteristic	**Interaction**	**p value**
Shoot fresh weight (g)	Time	<0.001
	Species	<0.001
	Time x Species	<0.001
Shoot dry weight (mg)	Time	<0.001
	Species	<0.001
	Time x Species	<0.001
Root dry weight (mg)	Time	<0.001
	Species	<0.001
	Bulk density	=0.01
	Time x Species	<0.001
	Time x Bulk density	<0.001
	Species x Bulk density	<0.001
	Time x Species x Bulk density	<0.001
Root length (mm)	Time	<0.001
	Species	<0.001
	Time x Species	<0.001
Average root diameter (mm)	Time	<0.001
	Species	<0.001
	Bulk density	=0.1
	Time x Species	=0.01
	Time x Bulk density	=0.05

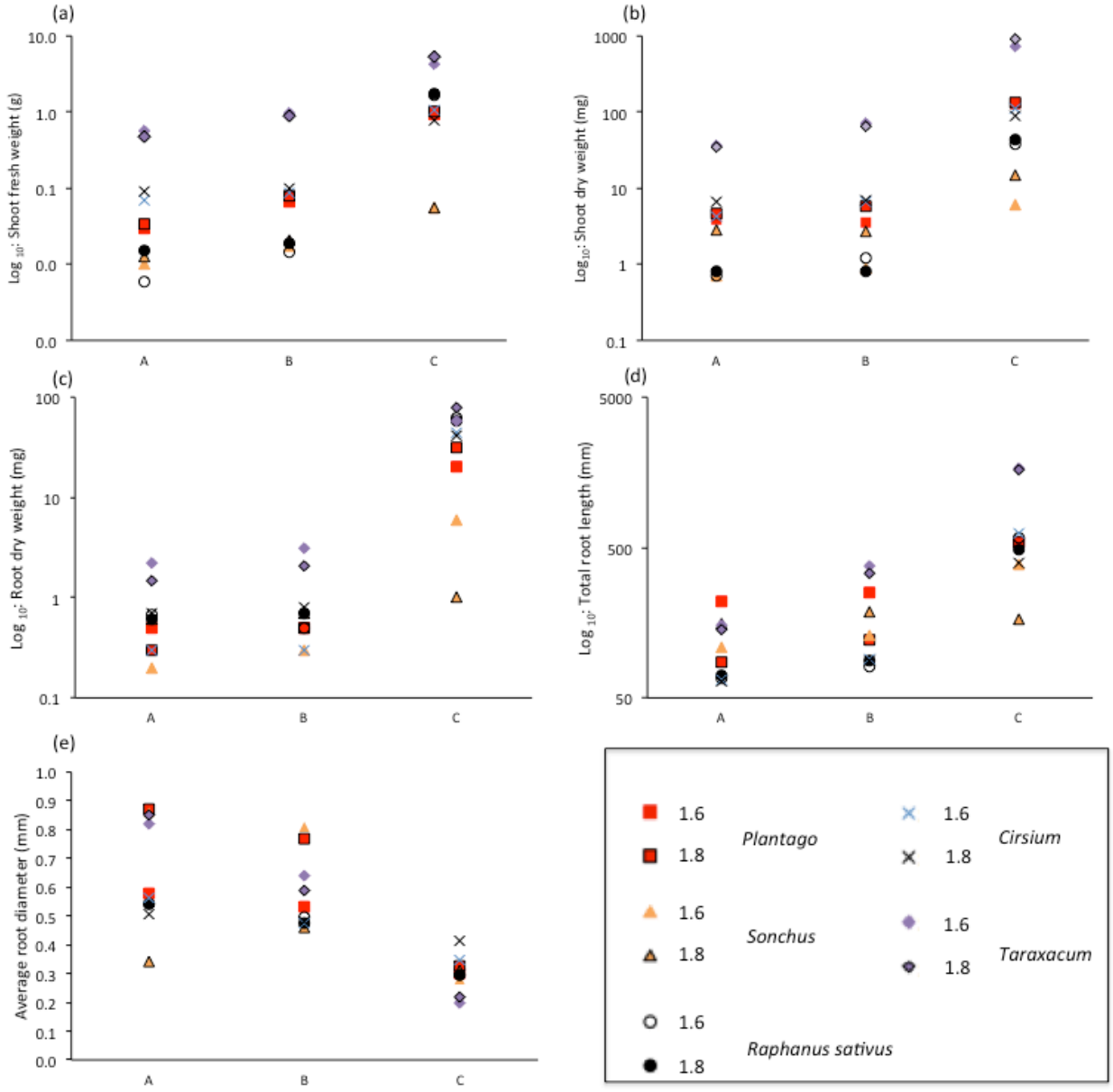


Figure 4.1: Biomass and WinRHIZO characteristic graphs for *R. sativus*, *Plantago*, *Taraxacum*, *Sonchus* and *Cirsium*. (a) Shoot fresh weight (g), (b) Shoot dry weight (mg), (c) Root dry weight (mg), (d) Total root length (mm), (e) Average root diameter (mm). Lines denote means, whiskers denote pooled s.e. (negative error bars not displayed below 0 on Log scale graphs).

4.2.2d Growth analysis

Time point A (5 days after emergence)

Plantago plants had greater dry root weight and total root length in the lower compaction treatment and significantly greater root average diameters in the 1.8 g cm^{-3} treatment (Figure 4.1d&e). *Sonchus* plants favoured the 1.8 g cm^{-3} bulk density treatment producing greater dry shoot weights, dry root weights and total root length at this growth stage (Figure 4.1b, c, d). The average root diameter of the plants was significantly greater in the 1.6 g cm^{-3} treatment. There was no difference between any of the measured characteristics for *Taraxacum* plants grown to Time Point A. *Cirsium* plants favoured the 1.8 g cm^{-3} compaction treatment producing greater dry shoot and root weights compared to in the 1.6 g cm^{-3} treatment (Figure 4.1b&c).

Time point B (10 days after emergence)

Plantago had significantly greater average root diameters in the 1.8 g cm^{-3} treatment and could produce greater total root length in the 1.6 g cm^{-3} treatment (Figure 4.1d&e). *Sonchus* plants favoured the 1.8 g cm^{-3} bulk density treatment producing greater dry shoot weights, dry root weights and total root length at this growth stage (Figure 4.1b, c, d). The average root diameter of the plants was significantly greater in the 1.6 g cm^{-3} treatment. There was no difference between any of the measured characteristics for *Taraxacum* plants grown to time point B. For *Cirsium* dry root weight was significantly greater in the 1.8 g cm^{-3} treatment and the shoot biomass

produced at this growth stage was significantly greater than any other species (Figure 4.1c&a).

Time point C (58 days after emergence)

There was no difference between any of the measured characteristics for *Plantago, Sonchus* or *Taraxacum* plants grown to Time Point C. Out of the four species, *Plantago* had consistently greater dry shoot biomass (Figure 4.1a). For *Cirsium*, total root length was observed to be greater in the 1.6 g cm^{-3} treatment and average root diameter was greater in the 1.8 g cm^{-3} treatment (Figure 4.1d&e). Indicating that more root was able to grow in the lower compaction but the average root thickness was greater in the higher compaction.

4.2.3 Database creation (from physical biomass quantification)

All physical biomass characterisitcs were averaged and tabulated for each of the five species at three diferent growth stages (Table 4.3). *R. sativus* was excluded from the comparison calculations for which species to use for the X-ray CT study due to it being a deemed a 'cultivated control' which acted as a baseline of what root development was achivable by a cover crop root system. The remaining four species were ranked against each other, considering individual traits, the best performing of each species within each trait group was marked with yellow and given a score of +1. This ranking

system determined that the species best able to reproduce biomass in compacted treatments were in order; *Cirsium* (9 points), *Taraxacum* (4 points), *Plantago* (4 points) and *Sonchus* (2 points).

4.2.4 Final species selection

From this screening trial, data was collated and each species ranked using the database shown in Table 4.3. From this, four candidate species for further investigation using X-ray CT were determined. These species were selected on their ability to produce below and above ground biomasss under compacted treatments in comparision to each other. The four candidate species selected were: *R. sativus, Plantago*, *Cirsium* and *Taraxacum.*

Table 4.3: Average biomass and WinRHIZO characteritcs for the five screened species at 3 measured time points. Yellow highlight indicates greatest measurement in each category. Total column idicates tallied number of greatest measurements and subsequnetly best performing plants at each time point.

Species	Sample point	Growth (days)	BD	Shoot fresh (g)	Shoot dry (mg)	Root dry (mg)	R:S ratio	Root length (mm)	Average diam (mm)	Total
R. sativus	A	5	1.6	0.56	36.3	2.2	0.1	152	0.82	*
R. sativus	A	5	1.8	0.48	34.1	1.5	0.0	143	0.85	*
Plantago	A	6	1.6	0.03	3.8	0.5	0.1	217	0.58	1
Plantago	A	6	1.8	0.03	4.7	0.3	0.1	86	0.87	1
Sonchus	A	10	1.6	0.01	0.7	0.2	0.4	108	0.86	1
Sonchus	A	10	1.8	0.01	2.8	0.6	0.2	156	0.34	0
Taraxacum	A	9	1.6	0.01	0.7	0.68	0.6	68	0.54	1
Taraxacum	A	9	1.8	0.02	0.8	0.6	0.6	70	0.54	0
Cirsium	A	8	1.6	0.07	4.3	0.3	0.1	66	0.56	0
Cirsium	A	8	1.8	0.09	6.7	0.7	0.1	64	0.51	3
R. sativus	B	9	1.6	0.98	69.7	3.1	0.0	373	0.64	*
R. sativus	B	9	1.8	0.91	66.0	2.1	0.0	335	0.59	*
Plantago	B	11	1.6	0.07	3.5	0.5	0.1	250	0.53	1
Plantago	B	11	1.8	0.08	5.8	0.5	0.1	121	0.77	0
Sonchus	B	14	1.6	0.02	0.9	0.3	0.4	130	0.81	1
Sonchus	B	14	1.8	0.02	2.7	0.7	0.3	189	0.46	0
Taraxacum	B	14	1.6	0.01	1.2	0.5	0.7	81	0.50	0
Taraxacum	B	14	1.8	0.02	0.8	0.7	0.8	89	0.47	1
Cirsium	B	14	1.6	0.09	6.7	0.3	0.0	91	0.48	1
Cirsium	B	14	1.8	0.10	7.0	0.8	0.1	88	0.48	3
R. sativus	C	58	1.6	4.28	719.7	58.3	0.1	1702	0.20	*
R. sativus	C	58	1.8	5.43	914.7	78.7	0.1	1646	0.22	*
Plantago	C	58	1.6	0.93	130.0	20.3	0.2	545	0.30	0
Plantago	C	58	1.8	1.00	131.0	31	0.2	547	0.32	1
Sonchus	C	58	1.6	0.06	6.0	6	0.9	385	0.28	0
Sonchus	C	58	1.8	0.06	15.0	1	0.1	168	0.31	0
Taraxacum	C	58	1.6	1.67	37.7	61.7	1.6	585	0.30	2
Taraxacum	C	58	1.8	1.73	44.3	57.3	1.3	483	0.29	1
Cirsium	C	58	1.6	1.06	111.3	44.3	0.4	628	0.35	1
Cirsium	C	58	1.8	0.76	89.7	41.7	0.5	391	0.41	1

4.3 Computer based method development

This section outlines the variety of computer based method development regarding image processing and root/ soil system analysis that was undertaken. It compares and summarises different approaches and details which were chosen for analysing the 3D data set for this chapter.

4.3.1 Root segmentation methodologies

4.3.1a VG Studio & RooTrak

Two primary methods were identified that could be used to extract plant root data from the greyscale X-Ray CT images. These were manual segmentation using VG Studio Max software or a semi-automated segmentation using a tracking program RooTrak, the method used for running each program can be found in Appendix 4 A.4.4 & A.4.5. A trial was implemented to determine which image segmentation process was the most appropriate to use on the generated data set. The aim was to provide the most consistent and repeatable segmentations of the root systems. The following sets of images detail the 2D WinRHIZO scan of the washed root systems alongside the 3D root segmentations processed using VG Studio Max (grey) and RooTrak (Red). Figures 4.2 and 4.3 depict these images for Cirsium, *Plantago, Taraxacum* and *R. sativus* respectively. Table 4.4 indicates the length of time taken to produce each of the segmentations. This time period was taken into account when deciding on the segmentation method. The outputs generated indicated that RooTrak had the ability to correctly identify the taproot of all plant species

and some instance some lateral development. As RooTrak provides a semi-automated way of tracking the root systems the output generated, it is more readily repeatable. For this reason, the initial analysis was run through RooTrak. The segmented systems were then exported into VG Studio to verify the output against manually segmented root systems and to undergo modification by adding in lateral roots that RooTrak was unable to trace. Combining the methods ensured the repeatability of the taproot identification from RooTrak as well as capturing the lateral root details.

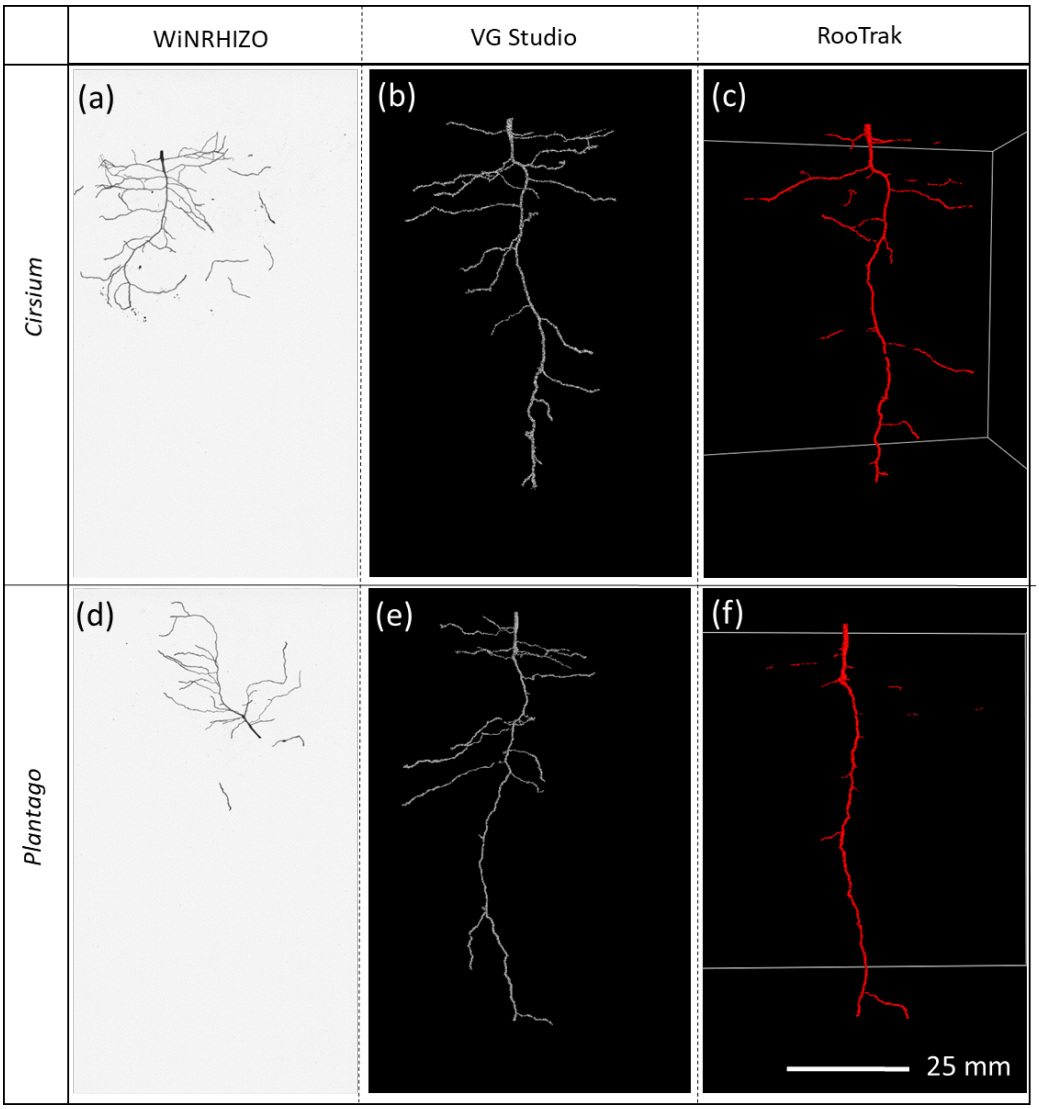


Figure 4.2: *Cirsium* plants at 28 days growth. (a) 2D WinRHIZO scan of washed roots, (b) 3D VG Studio Max root segmentation, (c) 3D RooTrak root segmentation. *Plantago* plants at 28 days growth. (d) 2D WinRHIZO scan of washed roots, (e) 3D VG Studio Max root segmentation, (f) 3D RooTrak root segmentation.

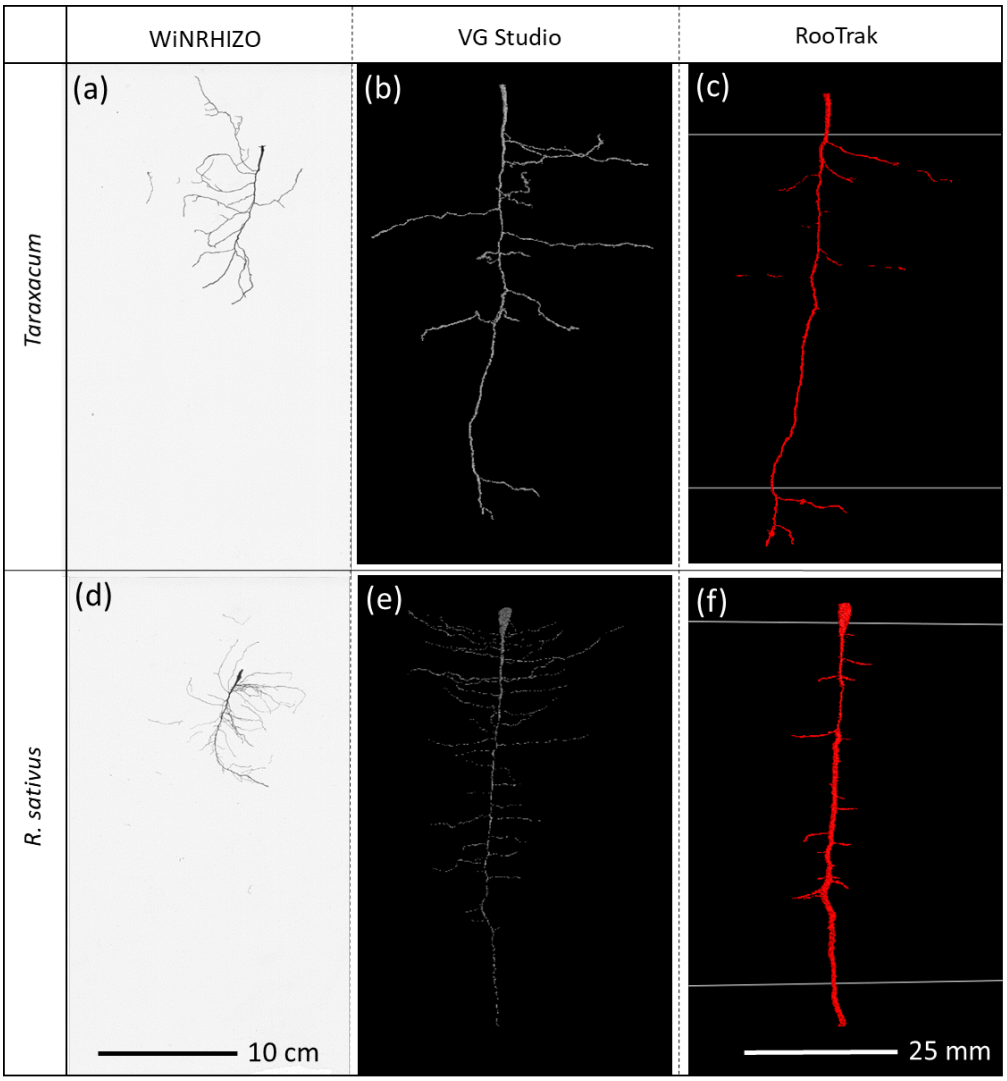


Figure 4.3: *Taraxacum* plants at 28 days growth. (a) 2D WinRHIZO scan of washed roots, (b) 3D VG Studio Max root segmentation, (c) 3D RooTrak root segmentation. *Raphanus sativus* at 28 days growth. (d) 2D WinRHIZO scan of washed roots, (e) 3D VG Studio Max root segmentation, (f) 3D RooTrak root segmentation.

Table 4.4: Time taken for operator to segment root systems at 28 days old, using the two segmentation techniques, VG Studio and RooTrak.

	Segmentation time (h)	
Species	**VG Studio**	**RooTrak**
Cirsium	4	7
Plantago	6	4
R. sativus	10	3.5
Taraxacum	7	3.5

It is important to note that Figure 4.3e depicts a very fine *R. sativus* root system. Over the course of the 28 day growth period it was observed that the *R. sativus* plants were not well adapted to the growth environment. Plant malnutrition/ stress was observed, such as the yellowing of the leaves and the plants began to die halfway through the experiment. Cores were treated in the same way as the other species and were continued to be watered until day 28. For observation purposes a sample scan of the *R. sativus* plants was taken at day 28 even though they had largely died. The images in Figure 4.4 indicate the *R. sativus* root system (a) at Day 14 and (b) at Day 28. It is clear to see that as the plant started to die, the root system has started to decay/shrink, leaving only a very fine skeleton of the original root system being able to be segmented from the greyscale images. Image (c) shows 2D slices of the *R. sativus* root system within the soil. The black arrows indicate those areas of pore space that have most likely been formed by the expansion of the root system and then its subsequent decay. These images verify that planted cores of *R. sativus* plants would not be able to be considered for comparison to the other three plant species as the observed pore space created in the rhizosphere was a result of root death. For this reason, the *R. sativus* plants were not considered as part of this investigation going forward.

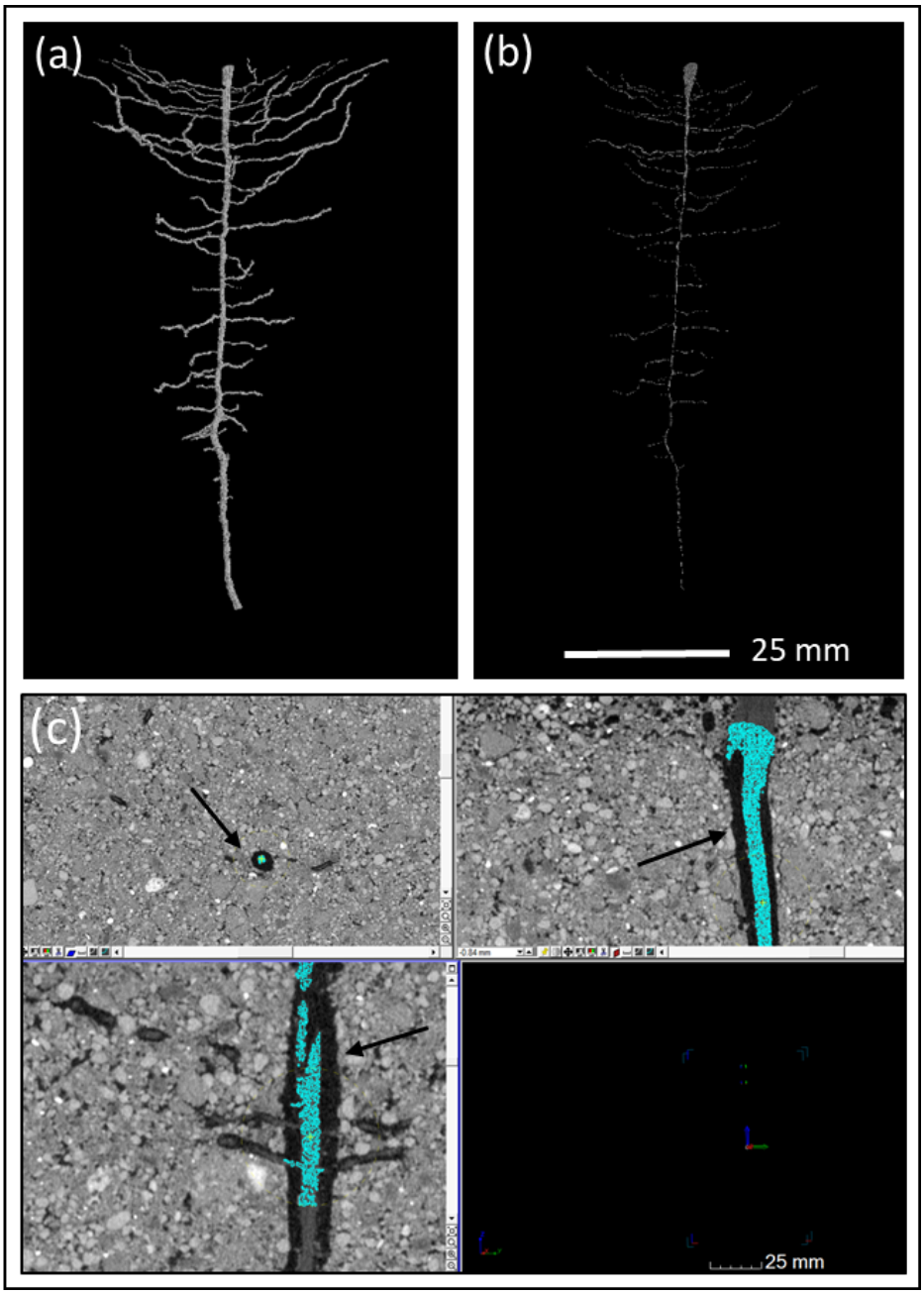


Figure 4.4: Example of root death (a) *R. sativus* 14 days growth, (b) *R. sativus* 28 days growth. (c) Screenshots from VG Studio Max indicating pore formation due to root die back.

4.3.2 Root analysis

Three different software programs were used to measure the root system characteristics for this experiment. These were: VG Studio Max, RooTrak and RooTh. Each software programme provides quantification of different characteristics, outlined in the following sections. In some instances methods for obtaining characteristics were trialled but ultimately were not implemented on the whole dataset set. These trials are also included here.

4.3.2a VG Studio

The functional methodology for the use of VG Studio Max to segment root systems can be found in Appendix A.4.4. Here, the root area measurements from 3D segmentations in VG Studio Max are compared with the root area measurements derived from WinRHIZO at 28 days growth. A strong positive relationship between the two comparative data sets was observed, with an R^2 value 0.86. This indicates that the 3D segmentations are able to visualise 86 % of the actual root in the soil cores. The remaining 14 % may be accounted for by being comprised of fine root mass that is below that of the spatial resolution of the scan preformed. Root capture using WinRHIZO will not account for 100% of root material in the core as some may be lost during the washing process. Additionally the calculations the root area value are derived from assume that all roots scanned are of perfectly cylindrical geometry so the value can only be used as a guide to estimate root area.

For this experiment VG Studio was used to modify and verify the root system output (primarily lateral roots) generated by RooTrak. VG Studio was used to compare the root area (cm^2) characteristics identified using WinRHIZO (Figure A.4.4) additionally it was used to verify the root area (cm^2) and volume (cm^3) characteristics from the initial RooTrak analysis. VG Studio max was also used to measure the maximum root depth and width explored by the root systems within the cores. Visualisations of root architecture development over time by overlaying root systems segmented at the different time points were also generated, allowing visual identification of where new root growth had occurred over time (Figure 4.5).

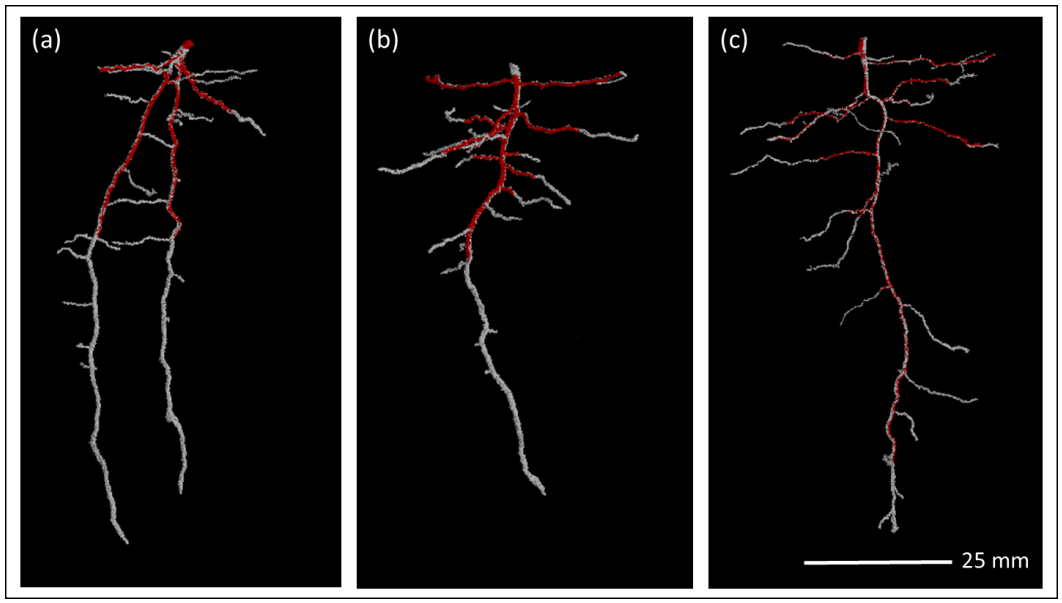


Figure 4.5: *Cirsium* root segmentations produced using VG Studio Max indicating root growth. Red roots represent 14 days growth, white roots represent 28 days growth. (a) Replicate 1, (b) Replicate 2 and (c) Replicate 3.

4.3.2b RooTrak

The functional methodology for the use of RooTrak to segment root systems can be found in Appendix A.4.5. In this experiment the parameters measured using RooTrak include; root area (cm^2), root volume (cm^3), maximum rooting width (cm), maximum rooting depth (cm) and convex hull (cm^3).

4.3.2c RooTh

Following root segmentation from the soil, root skeletonisation software, RooTh (Johnson et al. unpublished, https://github.com/rootth/rooth) was used to process the segmented root volume into a nested root system skeleton (Figure 4.6). This allows structural description of the root system architecture to be obtained including the distinction between primary and lateral roots to be made. The method presented in Appendix A.4.6 provides a basic guide on implementing the RooTh analysis software. Specific details are given in the method section of Mairhofer et al. (2017). RooTh was identified as an accurate and useful tool for defining root characteristics however due to the nature of the data set collected, it was not possible to apply the use of the software to all of the root samples being analysed in this experiment. Due to the complexity of the program, a number of the samples were misclassified due to the nature of roots touching each other. When roots touched the program could not distinguish them from one another causing them to appear as a single root section. As a result this greatly increased apparent individual root lengths and affected the overall data set. For this reason the

trial was not undertaken on all samples and the data generated does not appear as part of the manuscript.

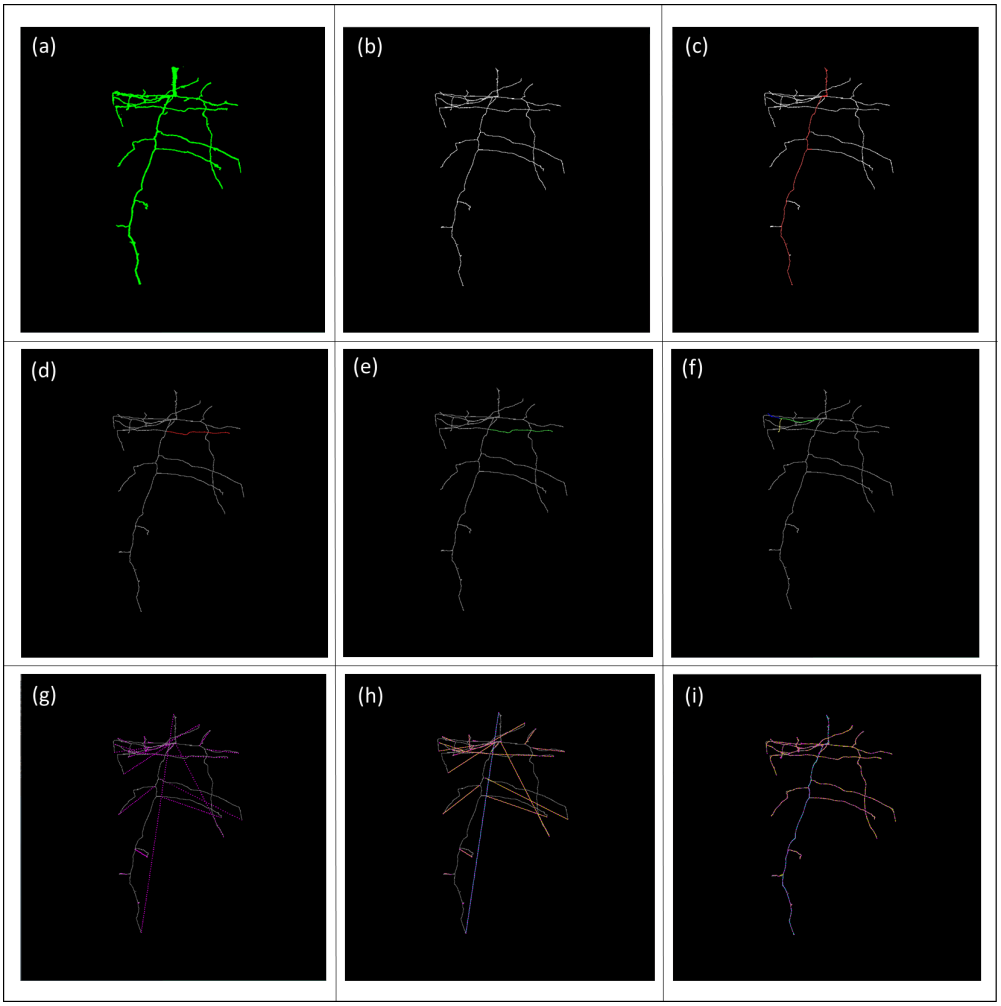


Figure 4.6: Example of root system processing using RooTh. (a) Input root wall, (b) Root skeleton, (c) indicates selection of primary root (in red), (d) indicates selection of secondary root (in red) (e) indicates confirmation of secondary root choice (in green) (f) indicates choosing root pathway (yellow/ blue), (g) indicates allocated root snake points, (h) indicates calculated root splines and i) depicts fitted root system. All images generated using RooTh.

4.3.3 Soil porosity analysis

Soil porosity analysis was assessed using a number of methods at different local scales, each of which are outlined in this section.

4.3.3a VG Studio

Initial soil porosity analysis was undertaken using VG Studio Max. The arrangement of slices in 2D provides a quick and effective way of visually assessing changes in pore space across a sample. Traversing through the image stacks enabled observations in the change in pore space developing over time (Figure 4.7). This initial observation prompted investigation of the pore space change in more detail across the whole core system using systematic analysis technique in QuantIm.

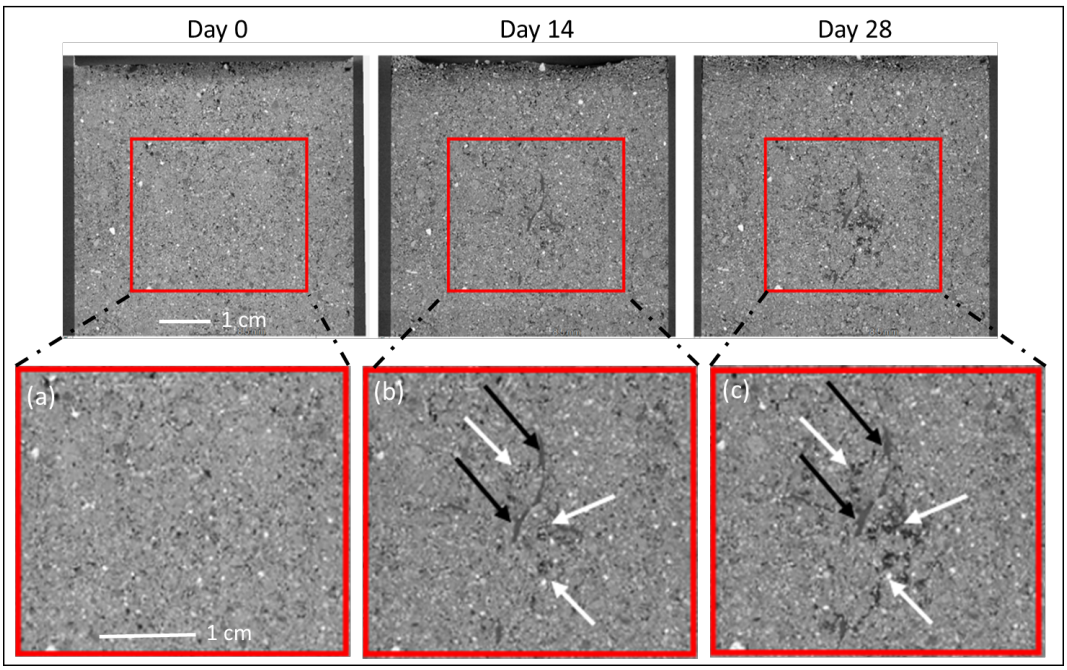


Figure 4.7: *Cirsium* Replicate 3 indicating soil pore formation in vicinity of root growth from Day 0, 14 and 28. Black arrows indicate root growth, white arrows indicate soil pore formation.

4.3.3b Image J

Image stacks of each soil column overlaid with a root mask derived from the RooTrak segmentations were exported as .tiff files and imported into ImageJ, which was used to manipulate the data sets for analysis in QuantIm.

The image stacks were cropped to form new regions of interest within the column with the dimensions of 1000 pixels by 1000 pixels (3.5 cm x 3.5 cm). 2000 images were exported to give the output data set a representative depth of 7 cm (7 cm out of the 9 cm core was used as a representative proportion of the soil columns). Once the dimensions of the area to be analysed had been set the image stack was prepared by: (i) enhance brightness and contrast, (ii) apply median filter with a radius of 2 pixels, (iii) convert the image stack to 8-bit data, (iv) save image stack and export. The final exported volume for analysis was 3.5 x 3.5 x 7 cm, a total of 86 cm^3. This equated to 48.5 % of the total soil volume within the experimental columns 5 cm x 5 cm x 9 cm (177 cm^3). Once the image stacks had been prepared, a manual range threshold was determined in ImageJ by applying the Li Threshold method, this was adapted to each image sequence to determine two threshold values for each image stack (T_1 and T_2; (Vogel et al. 2010), the rationale for which is described below. This process was repeated for the 15 scanned columns across three times points totalling 45 sampled cores and 90 individual sections.

4.3.3c QuantIm

Once the threshold values had been determined for each image stack, they were applied using the method Bin-bilevel threshold developed by (Vogel et al. 2010). The threshold calculation method consists of converting greyscale imagery into binary imagery and is available within the open source

software, QuantIm, which allows 3D analysis of the prepared image stack. The Bin-bilevel method employs two values (T_1 and T_2) of the grey histogram to process the conversion. QuantIm screens all the greyscale image voxels (T_i): (i) if $T_i < T_1$, the voxel is attributed to the pore space, (ii) if $T_i > T_2$ the voxel is attributed to the solid phase and (iii) if $T_1 < T_i < T_2$ the voxel is allocated to the fuzzy region. When all voxels are allocated to a group, the software re-assigns the voxel from the fuzzy region by looking at their neighbouring voxels: for example, if the majority of voxels surrounding are air space then the voxel will be attributed to airspace. The step is repeated until no further modification of the voxel statement is possible. QuantIm analyses the pore system by using a digital pore surface which is intersected by a spherical structure element. Each step consists of increasing the diameter of the spherical structure element and intersecting it with the digital pore surface, as a result only the surface that is included in the spherical structure is kept (Vogel et al. 2010). The output variables from the QuantIm analysis include the soil porosity measured as a % of the total area, the connectivity of the system described by a Euler number and the pore size distribution of the analysed region. Once processed the binary images were reimported into ImageJ and the BoneJ plug in was used to visualise pore thickness in 3D (Figure 4.8).

4.3.3d Soil porosity characteristics

The soil porosity characteristics of each column were analysed at Day 0, 14 and 28. The overall porosity of the soil columns decreased over time from 1.3 % at Day 0 to 0.7 % at Day 28 ($p = <.001$). This highlights the impact plants are

having is at a localised distance from the plant roots as indicated by Figure 4.7, as the increase in pore space visualised here is not reflected in the whole core. Time had a very significant effect on porosity (%) of columns (p= <.001) across all treatment types, with the general trend of porosity decreasing with time (Figure 4.9a-d). Both the control columns and those planted with *Cirsium* exhibited a steady decrease in porosity at each time point. For the control this decreased from 1.25% at Day 0, to 0.93% at Day 14 to 0.62% at Day 28. For *Cirsium* this decreased from 1.52% at Day 0, to 1.24% at Day 14 to 0.09% at Day 28. *Taraxacum* plants maintained the overall porosity in the columns between Day 0 and Day 14 at 1.07% and this then decreased at Day 28 to 0.69%. *Plantago* exhibited opposite characteristics with the porosity of the columns dropping sharply between Day 0 1.51% to Day 14 at 0.77% and then maintaining at an approximate constant porosity till Day 28 at 0.78%. Time had a very significant effect on the pore size distribution (PSD) of the columns (p= <.001). The graphs show a decrease in the proportion of pores of the smaller pore classes from Day 0 to Day 28 (Figure 4.9e-h). This trend was more prominent in the columns containing plant species than the control columns. Time had a very significant effect on the connectivity of the pore systems (p= <.001) described by an Euler number- normalised to total volume. The graphs represent an unconnected pore system which increases in connectivity over time due to the reduction of smaller pores (Figure 9i-l).

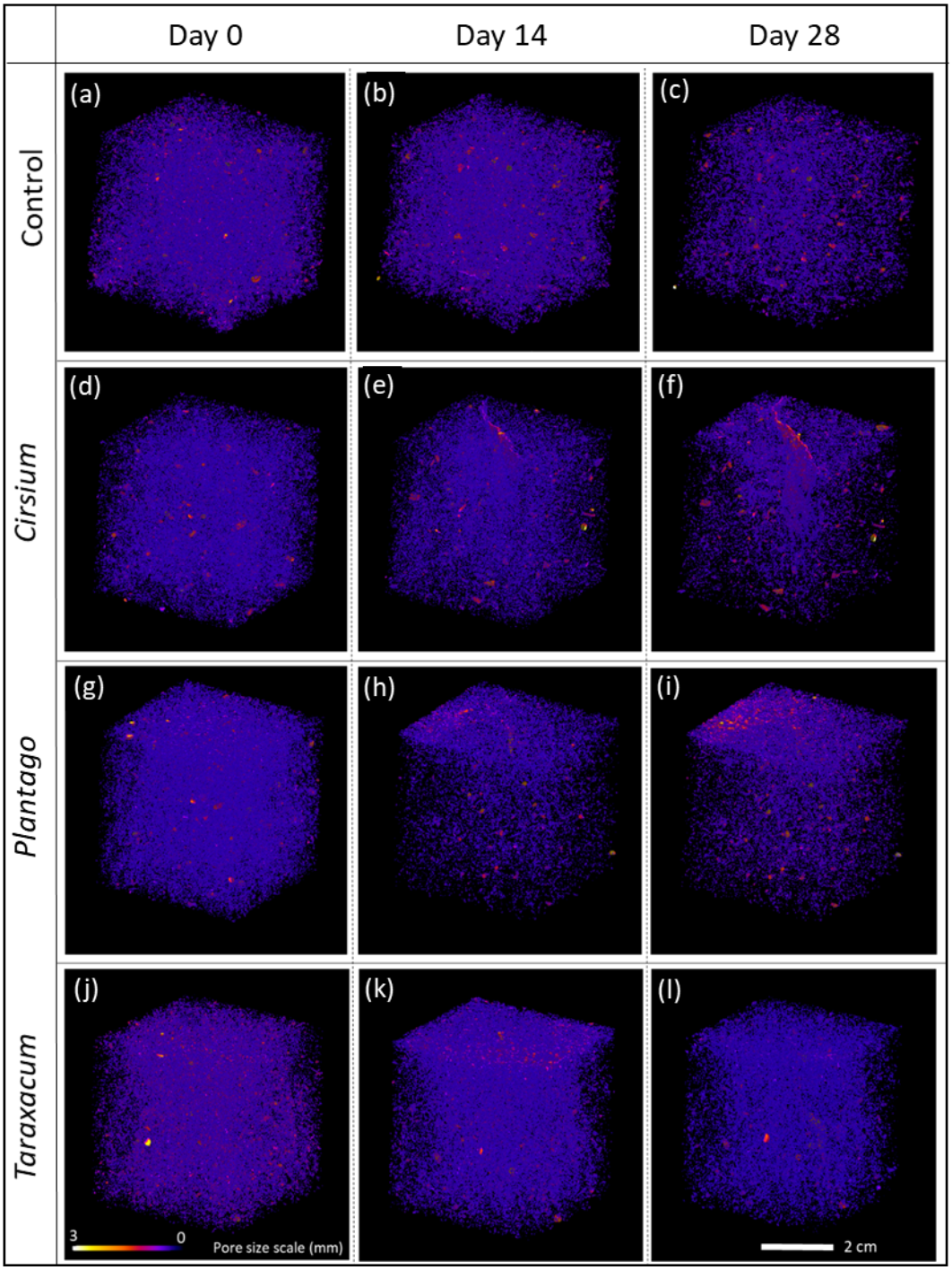


Figure 4.8: Representative 3D renderings of the top 3.5 cm^2 column pore space determined from thresholding. (a-c) Unplanted control columns at Days 0, 14 and 28. (d-f) Planted with *Cirsium* at Days 0, 14 and 28. (g-i) Planted with *Plantago* at Days 0, 14 and 28. (j-l) Planted with *Taraxacum* at Days 0, 14, and 28. Colouring represents a pore size heat map produced in ImageJ. Dark purple colouration represents the smaller pores- warmers yellow white and pink represents larger pores. Images produced using VG Studio Max 2.2.5.

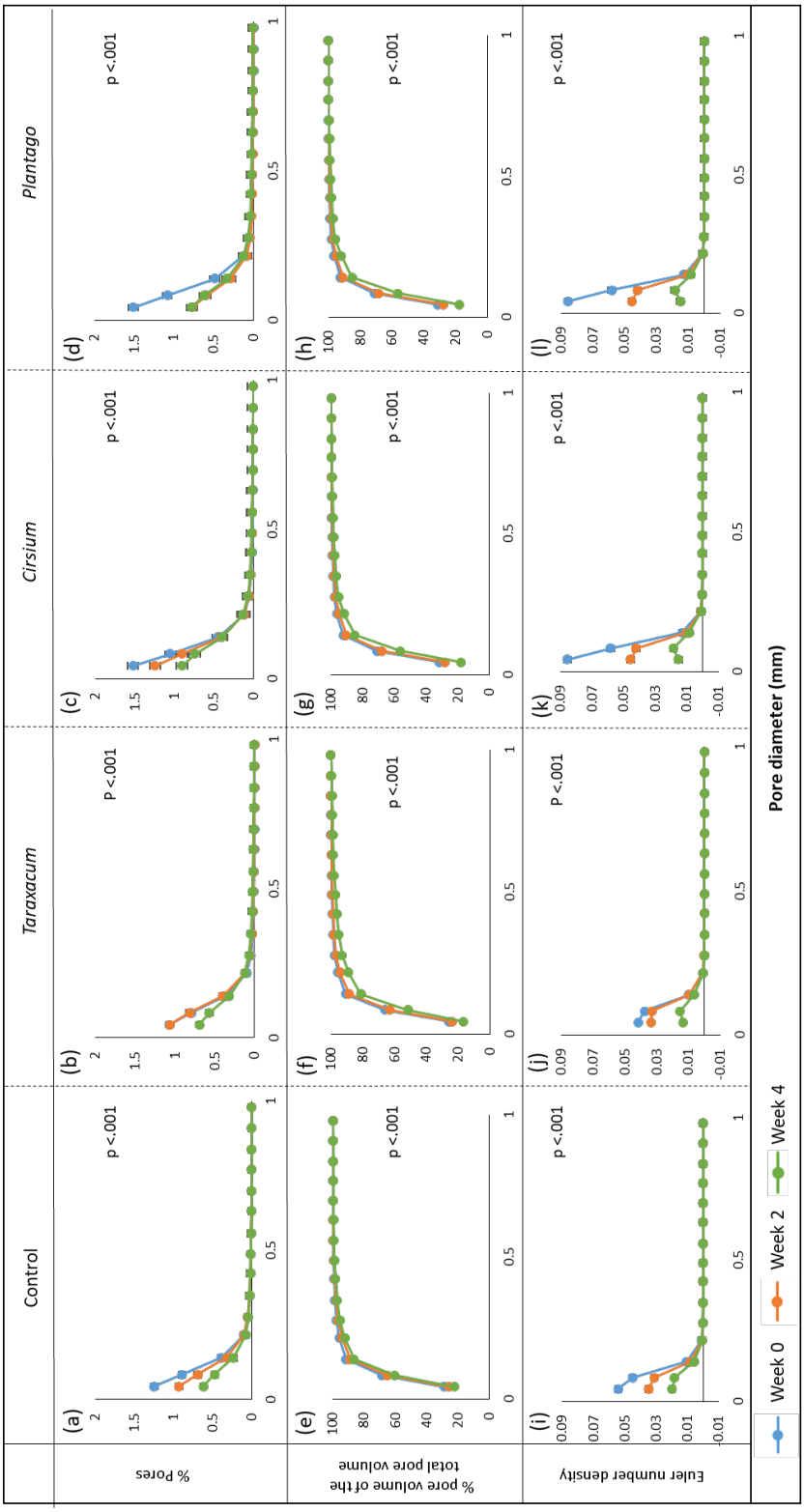


Figure 4.9: Soil pore characteristics of sandy loam soil under different species growth. (a-d) percentage of pores (e-h) Cumulative distribution of pores (i-l) connectivity of soil pore network. Control cores (a, e ,i). *Taraxacum* cores (b, f, j). *Cirsium* cores (c, g, k). *Plantago* cores, (d, h, l). Points indicate means, whiskers pooled s.e.

4.3.4 Rhizosphere porosity analysis

Soil porosity was assessed in the rhizosphere with distance away from the root surface using a method similar in approach to Helliwell et al. (2017) in VG Studio Max. For each sample a surface determination tool was applied to the soil column to identify air space and material. The surface determination tool was calibrated by user defined examples areas within each sample. Once the pore space had been identified, 'rhizosphere zones' were created for analysis. The segmented root system (ROI) (Figure 10b) was dilated by +2, +4, +8 and +12 pixels. This pixel dilation is equivalent to the resolution (1 pixels = 35 μm). The rhizosphere zones created were 70, 140, 280 and 420 μm distance from the root surface (Figure 4.10 c, d, e, f). This resulted in 4 incremental sections of 0-70, 70-140, 140-280 and 280-420 μm. For each zone, around each individual root system, the total area (mm^3) was measured. The porosity of each zone was also calculated (mm^3). To allow comparison between different zone sizes, the porosity was calculated as a percentage of the total incremental zone volume. Once identified these pore volumes were then false-coloured for visualisation.

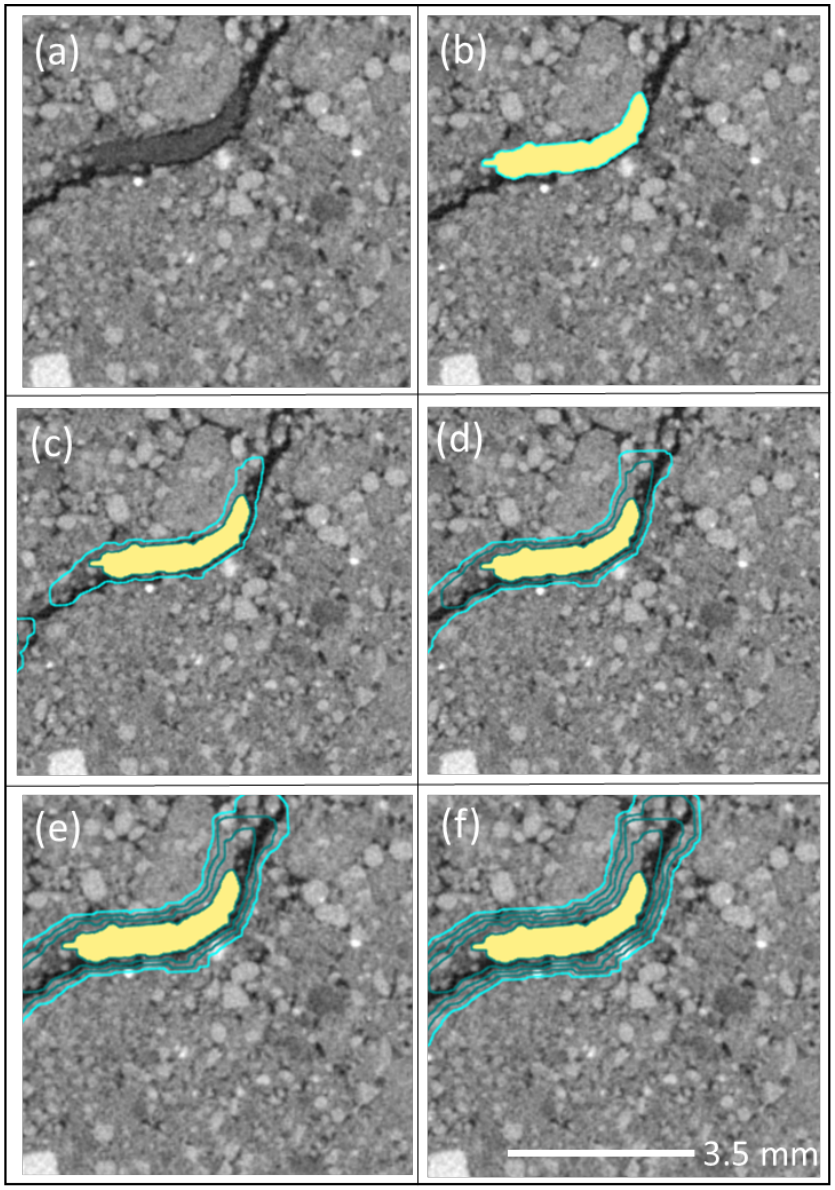


Figure 4.10: Example rhizosphere zone of *Cirsium* created from original plant root ROI. (a) original grey scale root, (b) segmented root system shown in yellow, (c) segmented root system with first rhizosphere zone 0-70 um, (d) rhizosphere zone 70-140 um, (e) rhizosphere zone 140-280 um, (f) rhizosphere zone 280-420 um from root surface. All zones boundaries highlighted by light blue line. All images generated using VG Studio Max.

4.4 Summary of computer based method development

Extensive trials using numerous soil pore and plant root segmentation techniques have been trialled in this chapter. Each trial was designed to understand how the software tools available could be implemented to generate data for analysis at a larger project scale. From this preliminary investigation using X-ray CT techniques, a full scale analysis was undertaken on *Plantago, Taraxacum* and *Cirsium* plants grown for 28 days in a sandy loam soil back to bulk density of 1.8 g cm^{-3}.

Section 4.5 details the full investigation into whether different plant species are better adapted to grow in soils of such high bulk density. Subsequently their root traits are characterised and their ability to produce air filled pores in the rhizosphere is assessed using methods trialled and developed in this section.

4.5 Authors manuscript

This remainder of this chapter is structured and formatted in accordance with the Journal of Experimental Botany. Status: Under review

Individual replicate 2D WinRHIZO scan imagery and X-ray CT root and rhizosphere porosity visualisation imagery for wild plant species can be found in A.4.7-A.4.13.

Author Contributions

Conceptualisation: J.E. Burr-Hersey, S.J. Mooney, A.G. Bengough, K. Ritz.
Data curation: K. Ritz.
Formal analysis: J.E. Burr-Hersey, S.J. Mooney, K. Ritz.
Funding acquisition: K. Ritz.
Investigation: J.E. Burr-Hersey.
Methodology: J.E. Burr-Hersey, S.J. Mooney, A.G. Bengough, K. Ritz.
Project administration: K. Ritz.
Software: J.E. Burr-Hersey**,** S.J. Mooney,
Supervision: S.J. Mooney, A.G. Bengough, K. Ritz.
Visualization: J.E. Burr-Hersey, S.J. Mooney,
Writing original draft: J.E. Burr-Hersey, K. Ritz.
Writing review & editing: J.E. Burr-Hersey, S.J. Mooney, A.G. Bengough, K. Ritz.

Reorganisation of rhizosphere soil structure by wild plant species in compacted soils

Author names

Jasmine E Burr-Hersey [1,2] Jasmine.burr-hersey@nottingham.ac.uk

Sacha J Mooney [1] Sacha.mooney@nottingham.ac.uk

A Glyn Bengough [2,3] A.bengough@dundee.ac.uk

Karl Ritz [1] Karl.ritz@nottingham.ac.uk

Institution addresses

[1] Division of Agricultural & Environmental Science, School of Bioscience, University of Nottingham, Sutton Bonington Campus, Leicestershire, LE15 2RD, United Kingdom

[2] The James Hutton Institute, Invergowrie, Dundee, DD2 5DA, United Kingdom

[3] School of Science and Engineering, University of Dundee, Dundee, DD1 4HN, United Kingdom,

*Corresponding author: **jasmine.burr-hersey@nottingham.ac.uk**

Reorganisation of rhizosphere soil structure by wild plant species in compacted soils

Running title

Wild plant roots modify compacted soil structure in the rhizosphere

Highlight

Wild plant species increase soil porosity locally within the rhizosphere, with notable differences between species.

4.5.1 Abstract

We analysed the root growth patterns of three non-cultivated plant species often found growing in heavily compacted soils in the wild. Ribwort plantain (*Plantago lanceolata*), dandelion (*Taraxacum officinale*) and spear thistle (*Cirsium vulgare)* plants were grown for 28 days in a sandy-loam soil compacted to 1.8 g cm^{-3} with a penetration resistance of 1.55 MPa. X-ray Computed Tomography was used to observe root architecture *in situ* and visualise changes in rhizosphere porosity (at a resolution of 35 µm) at 14 and 28 days after sowing. Porosity of the soil was analysed within four incremental zones up to 420 µm from the root surface. In all species the porosity of the rhizosphere was greatest closest to the root and decreased with distance from the root surface. There were significant differences in the rhizosphere porosity between the three species, with *Cirsium* plants exhibiting the greatest structural genesis across all rhizosphere zones. This

creation of pore space indicates that plants can self-remediate compacted soil via localised structural reorganisation in the rhizosphere, which has potential functional implications for both plant and soil.

4.5.2 Key words

Cirsium vulgare, dandelion, *Plantago lanceoloata*, porosity, ribwort plantain, roots, soil compaction, spear thistle, *Taraxacum officianale*, X-Ray Computed Tomography

4.5.3 Introduction

Pioneer vascular plant species often face particular challenges in colonising new habitats if the topsoil is impoverished with respect to nutrient or water supply, or if the subsoil is compacted and resistant to root penetration and development. Soil compaction is common in agricultural soils, arising as a result of trafficking (Soane et al. 1981; Hamza and Anderson, 2005) or livestock trampling (Mulholland and Fullen, 1991; Mohseni Saravi et al. 2005), and is acknowledged as a major constraint to crop root growth (Rosolem et al. 2002; Tracy et al. 2011) and productivity (Iijima et al. 1991; Oussible et al. 1992; Chen and Weil, 2011). The phenomenon also occurs in natural ecosystems, for example as a result of wild animal trampling (Thomas 1943; Cumming and Cumming 2003; Lei, 2003; Hosokawa 2010), even by relatively small mammals (Pascual et al. 2017), via wallowing (Gutterman 2003; McMillan et al. 2011; Ozan & Borrero 2018), or as a result of human activities

such as walking and bicycle riding (Lei, 2004). Naturally compact soil horizons can also be formed as a result of glaciation (Fitzpatrick, 1956). Vegetation which develops on such compacted soils is typically distinct from that which prevails in adjacent zones in both natural (Gibson 1989; Trager et al. 2004; Alberti et al. 2010) and human-induced contexts (Scott et al. 2005). However, few studies consider the extent to which plants are able to colonise such soils or carry traits which enable them to grown in such dense substrata, such as via aerenchyma formation (Engelaar et al. 1993). Adapting to grow in adverse conditions such as compacted tyre tracks in agricultural fields or roadside verges likely requires specialised root traits. These may be manifest as the ability to radially expand under high levels of mechanical impedance and quickly and effectively occupy a soil volume during establishment (Hettiaratchi, 1990). The ability to outcompete other species due to their adaptive traits enables them to grow in suboptimal conditions. For example, it has been shown that deeper root penetration within a soil profile improves a plants ability to compete for soil resources in conditions where resource availability is limited (Place et al. 2008). It has been suggested that roots with greater diameter may be better able to penetrate compacted soils (Materechera et al. 1991; Clark et al. 2003; Chen and Weil, 2009), hence tap-rooted species could be well adapted to grow in such circumstances. In a study investigating root growth of 22 crop species in a highly compacted soil, root extension of all species was severely inhibited, but the roots of dicots seemed to be less restricted than monocots (Materechera et al. 1991). Actively growing crop plant roots have been shown to have the ability to

significantly alter the environment in the immediate vicinity of their surface, for instance they have the potential to ameliorate soil in poor physical condition (Cresswell and Kirkegaard 1995). To what extent wild species are able to do this is essentially unknown.

Recently, X-ray Computed Tomography (CT) has been used to investigate the undisturbed rhizosphere with a focus on root-soil contact (Schmidt et al. 2012) and soil pore formation (Helliwell et al. 2017; Koebernick et al. 2019; Rabbi et al. 2018; Schluter et al. 2018; Helliwell et al. 2019). These studies examine the impact crop plants such as wheat, barley, tomato, pea, bean and chickpea have on soil structure, but to date no study has investigated the formation of microscale pore space at the root surface created by wild plant species. It has been suggested previously that the growth of crops may be more sensitive to levels of soil resistance in the rhizosphere zone compared to non-cultivated plants (Cook et al. 1996). Crop plants have generally been selected for their ability to grow in a loosely-structured seedbed and as such may be poorly adapted to develop in compacted soils. Wild plants which are able to grow on compacted soils may carry intrinsic traits which enable them to achieve this, but little is known about the *in situ* root architecture of such species. We investigated three wild dicot plant species *viz*. *Plantago lanceolata* (ribwort plantain), *Cirsium vulgare* (spear thistle) and *Taraxacum officinale* (dandelion). All species exhibit the same basic root architectural development patterns, having a primary taproot with secondary lateral root development. We hypothesise that the different species will produce varying amounts of root biomass under a high compaction treatment and

subsequently have varying effects on the soil porosity of the columns over time. We grew each species in highly compacted soil, analysed their root architecture in 3D via X-ray CT, and quantified soil porosity at pot and rhizosphere scales.

4.5.4 Materials and methods

4.5.4a Soil core preparation and planting

A Dunnington Heath series sandy loam (66.4% sand, 18% silt and 15.6% clay) was obtained from The University of Nottingham experimental farm at Sutton Bonington, Leicestershire, UK (52˚50'07"N, 1˚15'04.0"W). Soil was air-dried and sieved to <2 mm. Columns (100 mm height x 51 mm diameter) were uniformly packed with soil at a moisture content of 16% to a dry bulk density of approximately 1.8 g cm^{-3} and a penetrometer resistance reading of 1.55 ± MPa (1 mm diameter 30˚ semi-angle cone with 0.8 mm relieved shaft, driven at 4 mm/min^{-1}). Columns were packed in two 4 cm layers, after compacting each layer the surface was lightly scarified to ensure homogenous packing and hydraulic continuity within the columns (Lewis and Sjostrom 2010). Once packed columns were weighed and stored in airtight polythene wrap for 2 days before X-ray CT scanning to prevent moisture loss and to allow the cores to equilibrate. Seeds of ribwort plantain (*Plantago lanceolata* L.) (procured from Herbiseed, W End, Reading RG10 0NJ), dandelion (*Taraxacum officinale* L. Weber ex F.H. Wigg) were collected from Attenborough Nature Reserve, Attenborough, Nottingham, NG9 6DY, May 2016, and spear thistle (*Cirsium*

vulgare (Savi) Ten.) collected from Highfields Park Boating Lake, University Boulevard, Nottingham NG7 2RD, May 2016. Six soil columns were planted, each with one pre-germinated seed of each of the three plant species. Three of these replicates were scanned and three remained unscanned planted controls, with a further three columns remaining as unplanted controls (n=3). This allowed a comparison to be undertaken on the effect of X-rays on plant development of the species investigated. Once planted all 21 columns were placed in a growth chamber in a randomised block design (three blocks featuring one replicate each of the seven treatments) with a day/night temperature of 20˚C /15˚C. The light duration was 16 hours and night duration was 8 hours. The daylight period was from 08.00-18.00 and the night period was from 21.00-05.00. The growth chamber was kept at 70% humidity. Plants were grown for 28 days and the subset of 12 columns initially scanned on Day 0 were rescanned on Days 14 and 28 providing three times points. All columns were watered with 4 mg of water each day.

4.5.4b X-ray CT scanning

Columns were scanned using a Phoenix V|Tome |X m X-ray 240kV (GE Measurement & Control Solutions, Wunstorf, Germany) at the Hounsfield Facility at the University of Nottingham. Voxel resolution was set at 35 µm, potential energy of 160 kV and current of 180 uA, with a 0.1 mm copper filter. Projection image averaging and skip were set to 3 and 1 respectively. Columns were scanned in two sections with a total scan time of 1 h 15 m. The distance

from the sample to the source was 135 mm. For each column, 3000 image projections were captured. Scanned images were optimised to correct for any movement of the sample during the scan and noise was reduced using the beam hardening correction algorithm set at 8. Images were reconstructed at 32 bit using Phoenix Datosx 2 reconstruction tool to form a 3D volume which was visualised as 18 bit data using VG Studio Max 2.2.5 software.

4.5.4c Destructive harvest

After 24 days all shoot material was removed and placed in an oven at 50°C for 48 h to determine dry mass. Roots were washed from the soil over a 500 µm sieve and fresh mass determined, then stored in 1:1 water: ethanol prior to WinRHIZO (Regent Instruments Inc) scanning. For WinRHIZO scanning, roots were separated as far as was practically possible in water on A3 plastic trays and then imaged using an EPSON Expression 11000XL flatbed scanner at 800 dpi to determine total root length (cm) and average root diameter (cm). After scanning roots were dried at 50°C for 48 h and dry mass determined.

4.5.4d 3D Image processing, segmentation and analysis
Root analysis

An automated image processing algorithm, 'RooTrak' (Mairhofer et al. 2012), was used to segment roots from the µCT grey scale images. The method employs a tracking-based strategy which follows the root cross-sections through a sequence of images, with the initial digital processing seedpoint

being identified manually by the user. As the image stack is traversed, the cross-sections move around the image, reproducing the shape of the scanned root (Mairhofer et al. 2015). The tolerance values were adjusted following visual inspection to ensure only root material was included in the region of interest (ROI) produced. Once the root system was successfully extracted from the µCT images it was transferred as a bitmap (.bmp) image stack to VG Studio Max V 2.2.5 for cleaning and manual editing. This ensured the full root system from within each of the columns had been identified. The finalised volumetric representation of the root system architecture was analysed to quantify traits in RooTrak v. 0.3.9.1 (Mairhofer et al. 2012). Global traits derived from the entire root system were root volume (cm^3), root surface area (cm^2), maximum root exploration depth (mm; limited by the length of the core) and maximum root exploration width (mm) (limited by the width of the core). Additional traits were derived from the individual roots and included the number of lateral roots protruding from the primary root (lateral number) and the length of the taproot (mm), which were subsequently calculated using VG Studio Max V 2.2.5.

Soil porosity analysis

Image stacks of each soil column overlaid with a root mask derived from the RooTrak segmentations (Supplementary Figure A.4.14) were exported as .tiff files and imported into ImageJ (Schneider et al. 2012), which was used to manipulate the data sets for subsequent thresholding and analysis using the bin bi-level approach in open access software QuantIm

(http://www.quantim.ufz.de/)(Vogel & Kretzschmar, 1996). The image stacks were cropped to form new regions of interest within the column with the dimensions of 1000 pixels by 1000 pixels (3.5 cm x 3.5 cm). Two thousand images were exported to give the output data set a representative depth of 7 cm (7 cm out of the 9 cm core length was used as a representative proportion of the soil columns). Once the dimensions of the area to be analysed had been set the image stack was prepared by: (i) enhancing brightness and contrast, (ii) applying median filter with a radius of 2 pixels, (iii) converting the image stack to 8-bit data, (iv) saving image stack and exporting. The final exported volume for analysis was 3.5 x 3.5 x 7 cm, a total of 85.8 cm^3. Once the image stacks had been prepared a manual range threshold was determined in ImageJ by applying the Li Threshold method, to each image sequence to determine two threshold values for each image stack (T_1 and T_2; Vogel et al. 2010). This process was repeated for the 15 scanned columns across three times points totalling 45 sampled cores and 90 individual sections.

Rhizosphere porosity analysis

A method adapted from Helliwell et al. (2017) was used to assess local changes in porosity with distance from the root surface. The surface determination tool based on greyscale levels was applied to each column to identify both air space and soil material. Calibrations of the tool were used by defining material from example areas. Once the pore space had been

identified four new regions of interest (ROI) were created that encompassed incremental zones with distance from the originally segmented root system in 3D (Figure 4.11 a-e). The segmented root (ROI) was dilated by +2, +4, +8, +12 pixels (equivalent to 70,140, 280 and 420 µm distance from the root) across the entire root system. This resulted in four incremental section volumes 0-70, 70-140, 140-280 and 280-420 µm distal from the root surface which we term 'mantles', for which the total pore volume (mm^3) was identified (Figure 4.11 f-j). The volume of each mantel varied due to the unique structure of each root system; the incremental zone sizes were based on Helliwell et al, (2017). Porosity (%) was determined using an automated threshold approach in VG Studio Max V2.2.2 and the porosity (%) of each mantle was expressed as pore volume as a % of the total incremental mantle volume. These pore volumes were then false-coloured for visualisation of the pore locations within each mantle layer (Figure 4.11 k-o). This process was undertaken on each of the nine scanned plants at two time points, resulting in 72 individual rhizosphere porosity mantles for analysis. All volume manipulation and analysis was performed in VG Studio Max V 2.2.5.

4.5.5 Statistical analysis

A one-way factorial analysis of variance (ANOVA) was conducted on the 2D WinRHIZO data. A two-way ANOVA with specified block design was conducted on the X-ray CT scanned plants to assess whether time or species had the greatest effect on the root characteristics of the plants. A regression analysis

was performed on X-ray CT and WinRHIZO root area data. To assess the soil characteristics including porosity, connectivity and pore size distribution a 2-way ANOVA was performed with a treatment structure of time x pore diameter classification with a specified nested block structure. To assess the porosity of the rhizosphere mantles a 2-way ANOVA was performed with a treatment structure of species x time with a specified nested block structure.

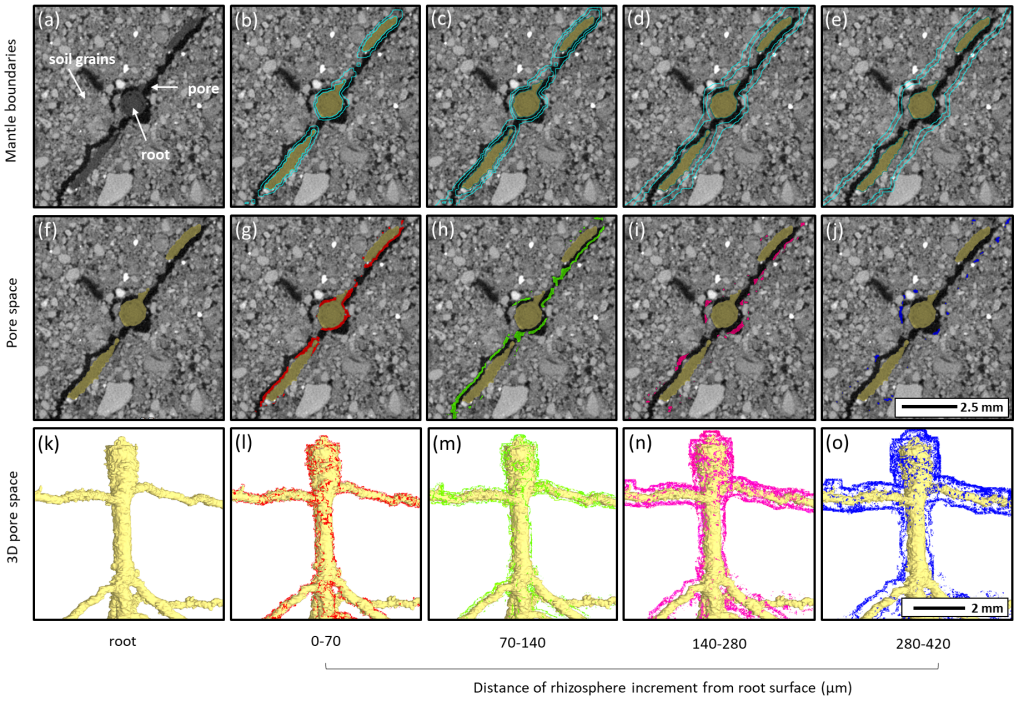


Figure 4.11: Delineation of rhizosphere zones, and example of 2D & 3D pore space identification and visualisation. Panels (a) depicts original greyscale imagery with root, pore space and soil indicated at Day 28. In all additional images segmented root system shown in yellow at Day 28. (b-e) indicate incremental mantle zone boundaries with distance from the roots surface up to 420 um (depicted by blue lines). Panels (f-j) indicate segmented pore space from specified mantle zone depicted by colour gradient. Panels (k-o) show 3D representation of soil porosity in specified mantle zones depicted by a colour gradient. Figure produced using VG Studio Max V.2.2.

4.5.6 Results

4.5.6a 3D root characteristics

3D visualisations of the three species root systems were analysed based on renderings of X-ray CT data at Days 14 & 28. There was a marked similarity in the species root architecture, all producing vertical primary taproots with subsequent lateral root formation. At Day 14 there was a distinguishable morphological difference between *Cirsium* and the other two species. The root systems explored a smaller volume of the soil core and produced more lateral root mass than *Taraxacum* or *Plantago* (Figure 4.12a, c, e). By Day 24 *Cirsium* had extended deeper into the soil core and produced a great number of thicker lateral roots, whilst the roots of *Taraxacum* and *Plantago* were notably finer in comparison (Figure 4.12b, d, f). The total area of roots for all species increased significantly over time ($p<.001$; Figure 4.13a). *Cirsium* had the greatest root area on both Day 14 and 28, whilst *Taraxacum* had approximately half the root area compared to *Cirsium* by Day 28, and *Plantago* intermediate ($p=0.004$; Figure 4.13a). The root volume of *Cirsium* was greater than the other species on both Days 14 and 28 ($p<.001$; Figure 4.13b). Within each time, there was no significant difference in root volume between *Taraxacum* and *Plantago* (Figure 4.13b). The maximum depth of the root system increased significantly over time for all species ($p=0.006$), with the maximum depth of 8 cm being reached at Day 28 in the majority of circumstances. Subsequently, there was no significant difference in the length of the primary taproot between the species although they were observed to

increase in length over time (6.35 ± 1.39 and 10.3 ± 5.80 cm mean ± s.e. for Days 14 and 28 respectively).

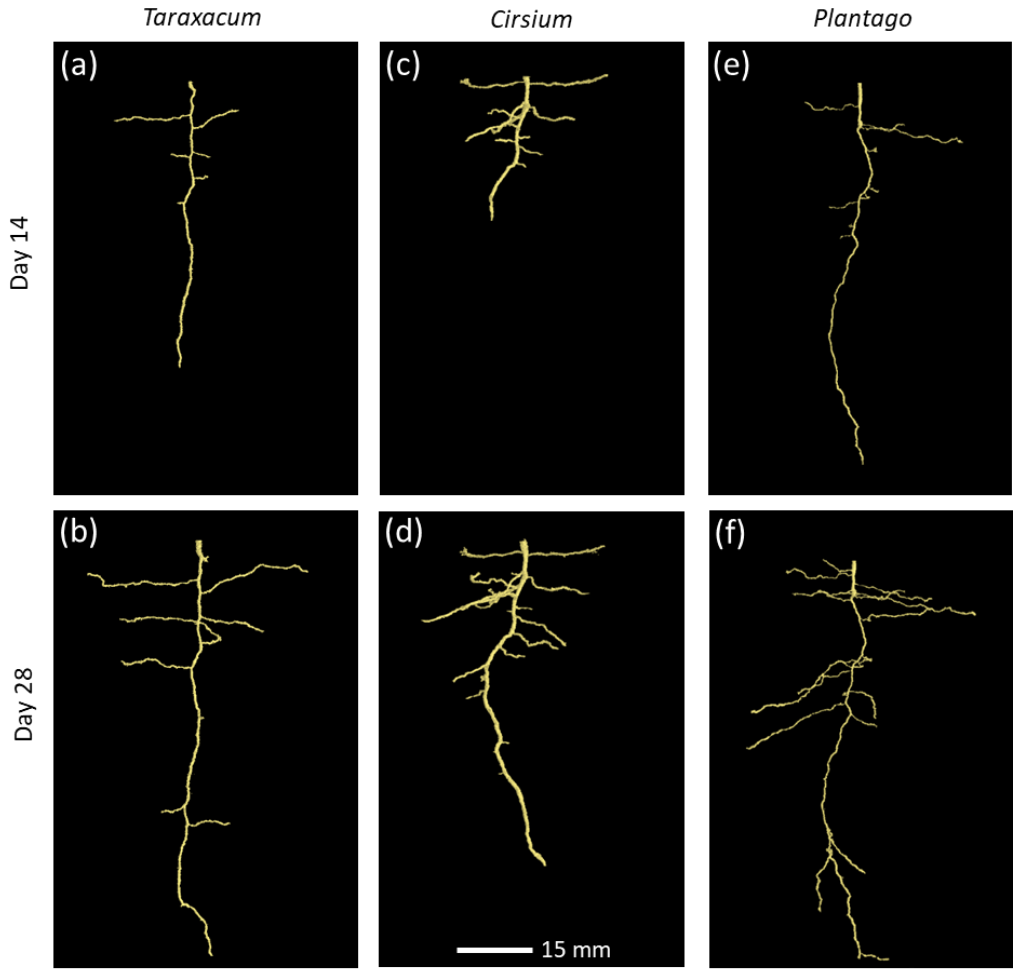


Figure 4.12: Representative 3D renderings of root systems grown in repacked soil columns with bulk density 1.8 g cm^{-3}. (a, b) *Taraxacum*, (c, d) *Cirsium* and (e, f) *Plantago* at 14 and 28 days growth respectively. Images produced using VG Studio Max V.2.2.

The maximum exploration width of the root systems significantly increased over time (p=0.006). At Day 14 *Cirsium* had significantly greater exploration width (mean 4.9 cm) in comparison to *Taraxacum* and *Plantago* (mean 3.4 and 4.4 cm respectively, pooled s.e. 0.37; p=0.007). There was a difference in the number of number of lateral roots produced between species, *Taraxacum*

produced notably fewer roots in total (average 9) in comparison to *Plantago* and *Cirsium* (average 18 and 19 respectively, s.e. 19.4; p=0.023).

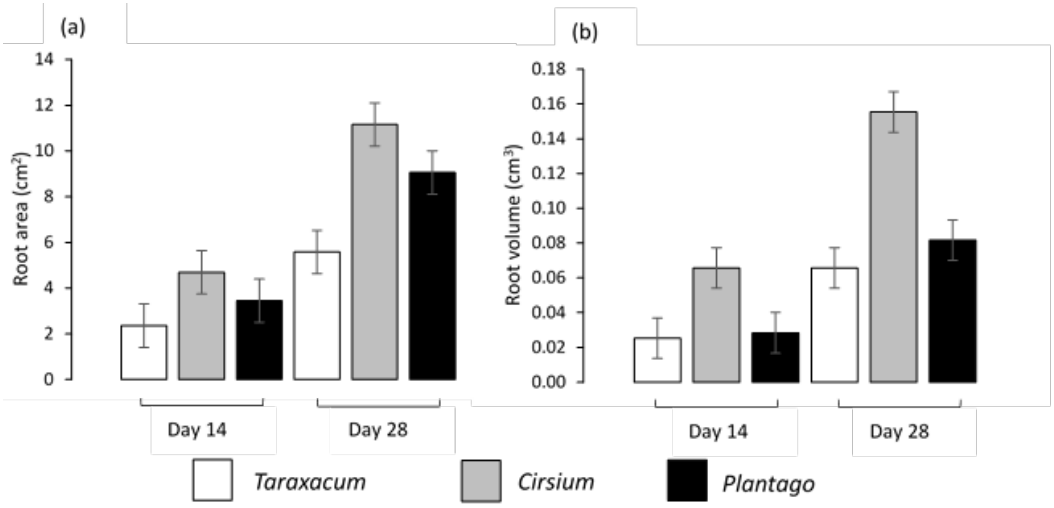


Figure 4.13: Average surface area of roots (cm^2) and root volume (cm^3) of plant species derived from X-Ray Computed Tomography segmentation. (a) Root area (cm^2), (b) Root volume (cm^3). Bars denote means, whiskers pooled SE.

4.5.6b Biomass

The use of X-ray CT did not affect the shoot or dry root weight (p= 0.341, p=0.991 respectively). *Cirsium* produced significantly greater root biomass than both *Taraxacum* and *Plantago*, the latter being similar (mean 0.007, 0.002 & 0.005 g respectively; pooled s.e. 0.0008; p<.001).

Table 4.5: Details dry biomass weights (g) and 2D WinRHIZO parameters average diameter (mm) and total root length (cm) for control and X-ray exposed plants.

		Biomass dry weight		WinRHIZO	
Species	Treatment	Shoot (g)	Root (g)	Average diameter (mm)	Total root length(cm)
Plantain	Control	0.04	0.006	0.28	71.57
Plantain	X-Ray Exposure	0.04	0.005	0.27	54.11
Thistle	Control	0.03	0.008	0.29	89.05
Thistle	X-Ray Exposure	0.04	0.007	0.29	51.32
Dandelion	Control	0.06	0.003	0.27	51.50
Dandelion	X-Ray Exposure	0.03	0.002	0.25	30.65

4.5.6c 2D WinRHIZO parameters and visual assessment

Total root length was not significantly different between the species (overall mean 58 cm pooled s.e. 13.35; p=0.110). However, X-ray exposure reduced total root lengths irrespective of all species by 35% (p=0.020), but did not affect the average root diameter. *Cirsium* produced significantly thicker roots than both *Plantago* and *Taraxacum* (mean 0.29, 0.27 and 0.26 mm respectively, pooled s.e. 0.013; p=0.080) (Table 4.5). It was noted upon visual assessment that *Cirsium* plant roots had a substantial rhizosheath when washed from the soil cores, that was well adhered to the root system. Comparatively *Taraxacum* and *Plantago* had relatively few soil aggregates attached to their roots. Due to the extremely small weights of the dried root mass (g) and total root length there appears to be no significant difference between x-ray exposed or control from the table however when expressed to further significant figures the effect x ray has on the total root length becomes significantly different.

4.5.6d Soil porosity characteristics

The total visible pore space of the columns at 33 µm resolution decreased over time from 1.3 % at Day 0 to 0.7 % at Day 28 (pooled s.e. = 0.19 p<.001). Pore size distribution and pore connectivity were significantly different between treatments (p>0.05 in all cases; Supplementary Fig 2).

4.5.6e Rhizosphere porosity

Visualisation of the porosity associated with the rhizosphere showed that there was generally greater rhizosphere porosity around the roots closer to the soil surface, i.e. the older roots, at both 14 and 28 days (Figure 4.14). In the case of all species the porosity within the incremental rhizosphere mantles was greatest with immediate proximity to the roots and decreased with distance from the root surface (p<.001; Figure 4.15). However, *Cirsium* exhibited consistently greater rhizosphere porosities at both Days 14 and 28 in comparison to *Taraxacum* and *Plantago,* and at Day 14 *Taraxacum* exhibited greater porosity than *Plantago* (p<0.001). For all species, the incremental rhizosphere mantle zones had a greater porosity at Day 14 and this decreased with time to Day 28 (p<.001), particularly for *Cirsium* and *Taraxacum*, and less so for *Plantago*. For *Taraxacum* the biggest decline in rhizosphere pore space occurred in the first mantle 0-70 µm from the root surface, with the average porosity decreasing from 6.9 % to 3.9 % from Day 14-28. *Cirsium* saw a decrease of 2% pore space in the 0-70 and 70—140 µm zones, however even with this decrease the total porosity of the 0-70 µm

zone remained higher than either of the other two species. Plantago consistently had the lowest observed rhizosphere porosity values, which decreased by less than 1% in each mantle zone from Day 14-28. Interestingly the porosity of the furthest mantle from the root surface measured 350-420 µm for *Cirsium* was greater than the porosity of the first incremental mantle 0-70 µm from the root surface for *Plantago*.

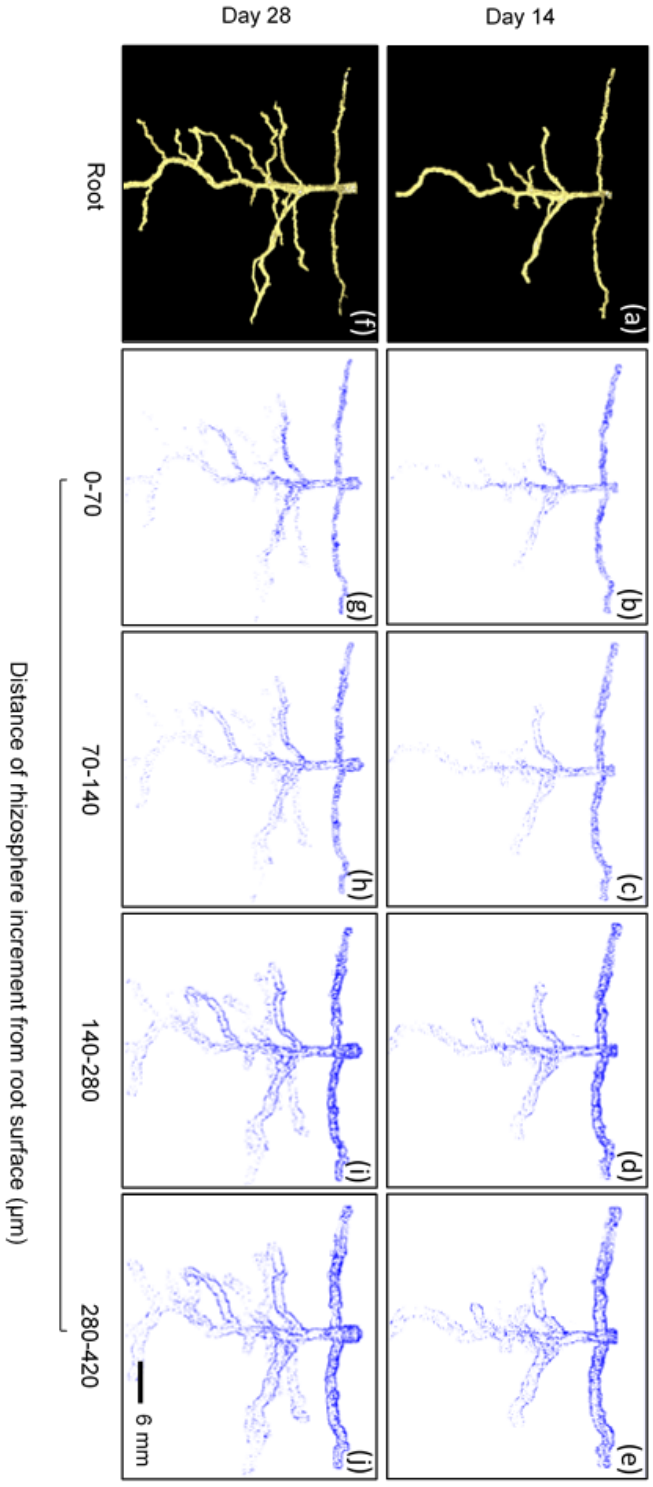


Figure 4.14: Example renderings of 3D segmented pore space incremental rhizosphere zones with distance from the root surface. Example segmented root system displayed in yellow at day 14 and 28 (a, f). Pore space depicted in blue for both days 14 (b, c, d, e) and 28 (g, h, I, j) respectively. Visualisations produced using VG Studio Max V 2.2.5

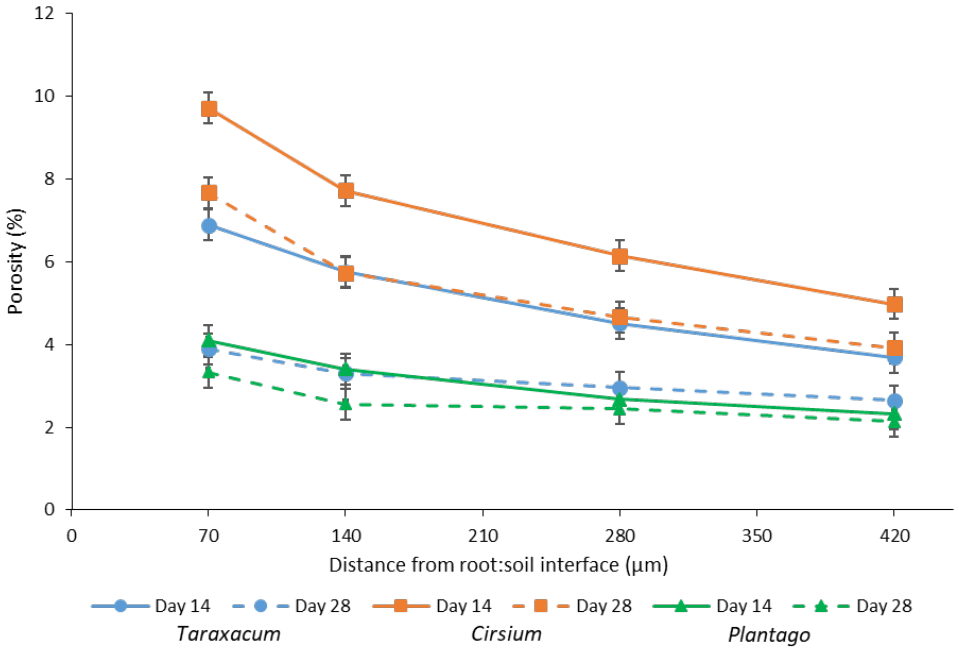


Figure 4.15: Porosity of incremental rhizosphere zones over time with distance from root surface. Values represent mean, whiskers pooled S.E.

4.5.7 Discussion

The volume of soil that can be explored by a root system is directly determined by its architecture (Morris et al. 2017). In principle, certain complex architectures may acquire soil-based resources efficiently, but the force required to penetrate compacted soil is often constraining (Bizet et al. 2016), restricting the 3D topology of the root system (Tracy et al. 2012; Burr-Hersey et al. 2017). In our study the individual species' response to compaction was varied, despite no difference in overall taproot length. It has previously been observed in barley plants that when the main axis is impeded, compensatory growth of lateral roots can occur (Goss, 1977). The length and shape of the primary root axis of the species indicates how readily

it was able to displace the soil. The straighter the taproot, the less it has buckled and deflected as it grows downward. An increase in root diameter such as was observed in *Cirsium* roots may indicate a response to the mechanical impedance of the soil, resulting in slower root elongation rate (Bengough and MacKenzie, 1994). *Cirsium* exhibited similar characteristics producing a shorter taproot in the first instance and notably more lateral root mass compared to the other two species. The difference in the way in which the species produce different types of root reinforces the utility of visual assessment of the systems. For example, it is clear that *Cirsium* developed a shallower, thicker root system in comparison to the deeper finer systems exhibited by *Taraxacum* and *Plantago*.

Traits that enable roots to modify their surroundings when conditions are sub-optimal is important, especially when considering their ability to advantageously modify their environment and colonise physically dense subsoils. For example, thick roots buckle less under mechanical stress (Clark et al. 2003). Our study features an experimentally-compacted sandy soil system, with few large pores and no previously extant biopores. As a result the packed cores presented a dense, granular environment which the roots must physically displace to grow. As soil bulk density increases, the connectivity of the pore system usually decreases (Udawatta et al. 2016), resulting in increased mechanical impedance to the root system (Bengough, 2012). A plant root's ability to overcome these constraints necessarily allows for structural alteration of the soil. Here we observed a significant increase in porosity but only in the direct vicinity to the plant roots, as previously shown

by Helliwell et al. (2017). This trend was observed across all species but was substantially different between them, with the greatest increases in rhizosphere porosity being manifest by *Cirsium*. In all species this porosity subsequently decreased with time, which we attribute to the continued radial expansion of the taproot systems into the newly-created pore space. We do not attribute this pore space creation to thigmotropism, as the moisture content of the columns was maintained over the course of the experiment. These findings suggest similar fundamental mechanisms of structural reorganisation at the root surface, but with greater potential for the phenomenon in the case of *Cirsium*. This experiment was designed to determine if specific plants had the ability to grow in compacted soils, and if so how they modified their local environment. The rhizosphere porosity data for this investigation has been averaged across the entire root system, therefore we consider the pore space as a function of distance from the root surface and not as a function of depth within the core, which would be concomitantly associated with the age of the roots. Analysis was undertaken in this way to directly compare the total resolved pore space of different plant species across their entire root network opposed to within the root network of different plants as comparisons concerning the ability of plants to generate pore space were being considered.

Our study further highlights that although changes in porosity were not observed at the larger (core) scale, they were manifest at a scale of certain significance to the plant, i.e. the rhizosphere. Soil porosity in this zone was inherently greater up to 2.8 mm distance from the root surface than that of

the bulk soil. Rabbi et al. (2018) observed a zone of hydraulic influence of approximately 3 mm in an oxic soil. Helliwell et al. (2019) notes the rhizosphere zone of structural influence is variable and both related to plant species (with contrasting root systems), soil type (loamy sand *versus* clay loam) and level of soil compaction. Kirby and Bengough (2002), Bengough et al. (2006) and Chen and Weil (2009) all observed that radial expansion of a root helps to relieve stress at the root apex, thus decreasing the likelihood of the root buckling. In our experiment *Cirsium* plants developed notably thicker root systems than *Taraxacum* or *Plantago* indicating that it possesses a trait that enables it to potentially utilise this mechanism more so than the other species. Subsequently *Cirsium* was the species identified that produced the greatest proportion of modified pore space in the rhizosphere. The increase in localised pore space adjacent to plant roots modifies the liquid and gas phase of the soil system the roots are in contact with. Studies by Oleghe et al. (2017) show that there are differences in root exudate composition which can result in changes to soil physical properties. For example, the presence of mucigel, along with root hairs and fungal hyphae is responsible for the agglutination of soil particles to roots (Moreno-Espíndola et al. 2007). This may also be the case for the species we studied, and is worthy of further investigation. Work by Bao et al. (2014) suggests that a porous rhizosheath may hold significantly more water at the root-soil contact zone. The overall greater diameter roots, greater rhizosphere pore space and presence of rhizosheath indicate that the presence of the rhizosheath may have positively impacted lateral root emergence. There are many root-soil interaction processes occurring and the

structural alteration of soil particles, in the context of this study to increase pore space, is one of the by-products of such activities. Our study indicates that root-induced soil structural changes in high bulk-density soils appears to be confined to the rhizosphere, at least during the first 28 days of growth. The development of pore space along lateral roots (Fig 1) may later contribute to more substantial structural generation of the soil.

This investigation involved the use of plant species not previously studied using X-ray CT technology. Blaser et al. (2018) investigated the effects of cumulative X-ray dosage on *Vica faba* and *Hordeum vulgare* over a 17 day period. They observed significant decreases in total root length in *V. faba* and no significant effect on *H. vulgare*. Their study highlights that susceptibility to X-ray dosage varies between plant species, and that for investigations involving temporal resolution an unscanned treatment is required for baseline comparison of root parameters observed in 2D. In our experiment the x-ray dosage was less than the one used in Blaser et al. (2018). Due to this a subset of plants were grown and not subject to X-ray CT analysis to determine if the use of this technique had a significant effect on the plants root and shoot characteristics. It was previously observed by Zappala et al. (2013) that in comparison to plants exposed as seeds, vegetative tissues appear less susceptible if exposed to X-rays post germination. In our experiment plants were first exposed to X-rays 14 days after germination. The only X-ray induced effect that we observed was the reduction in overall total root length of all plant species measured using WinRHIZO. Since the effect was consistent across all species we surmise this reduction does not interfere

with the determination of relative differences between species. There is insufficient data as yet in order to establish if there is an inherent difference in susceptibility to X-rays between wild and cultivated species, but these preliminary observations suggest that cultivated monocots at least may be more resistant.

4.5.8 Conclusions

We have demonstrated the ability of selected wild plant species to grow in extremely compacted soils, and illustrate their ability to create and modify soil pore space likely to their advantage as the phenomenon provides increased access to both water and air during the early stages of growth. However, this is confined to the rhizosphere zone. This has implications for the development of successional series where compacted soils are involved, and informs about advantageous root traits that enable colonisation of such habitats. Such factors are also of relevance in the context of the potential for using plants to remediate compacted soils in agricultural contexts. Our study was confined to the first 4 weeks of plant growth, hence further investigation into the changes in the rhizosphere zone over extended time periods are warranted. The precise mechanisms and associated traits in species better able to penetrate extremely compacted soils such as *Cirsium* is also worthy of elucidation.

4.5.9 Acknowledgments

This research is supported by the award of a studentship grant to JB-H by the NERC and BBSRC funded STARS (Soils Training And Research Studentships) Centre for Doctoral Training and Research Programme; a consortium consisting of Bangor University, British Geological Survey, Centre for Ecology and Hydrology, Cranfield University, The James Hutton Institute, Lancaster University, Rothamsted Research and the University of Nottingham. Grant Ref: NE/M009106/1. The James Hutton Institute receives funding from the Scottish Government. We thank Dr Brian Atkinson for 3D visualisation support and Dr Aurelie Bacq-Labreuil for technical guidance using QUANTIM.

4.5.10 Supplementary information

Appendix 4 supplementary data, Figure A.4.11. Example or Root Mask for *Cirsium* at Day 14 overlaying greyscale soil imagery for soil porosity calculation.

4.6 Mycorrhizae association

Plant roots were cleared and stained using the method developed by Vierheilig et al. (1998). The method used to quantify mycorrhizae was adapted from the gridline intersect method (Giovannetti and Mosse 1980). The standard operating procedure for quantifying mycorrhizal roots is given in Appendix 2, A.2.2. We observed the presence of mycorrhizae in all the plant root systems. The infection rate was calculated at less than 1% for Plantago, Cirsium and Taraxacum for this experiment (Figure 4.16).

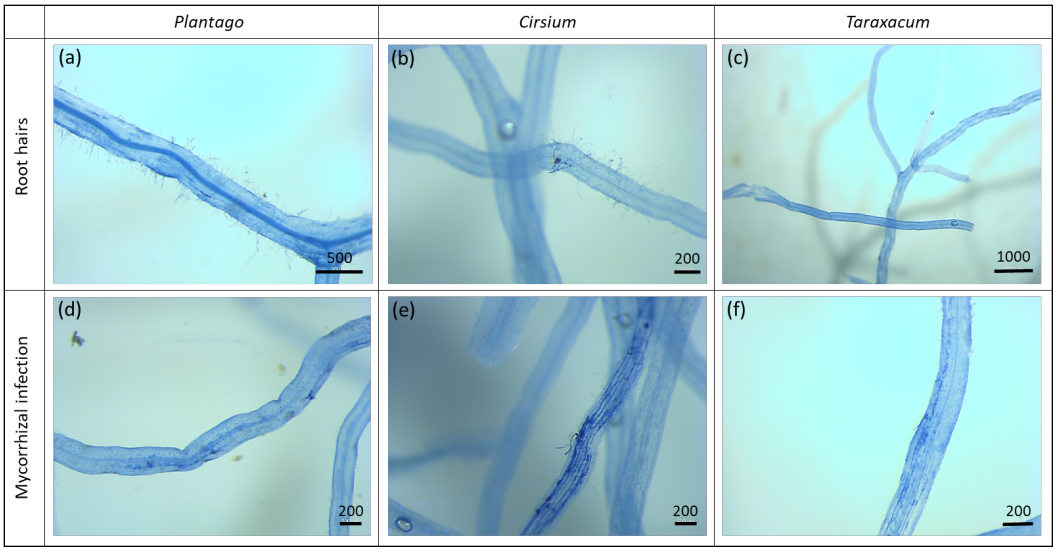


Figure 4.16: Identification of root hairs and mycorrhizal infection. (a-c) Root hairs Plantago, Cirsium and Taraxacum. (d-f) Mycorrhizae Plantago, Cirsium, Taraxacum. Images generated using a compound microscope.

4.7 Further analysis

All the data was collated encompassing root and shoot biomass, 2D and 3D root parameters and the soil porosity analysis for the system at the core scale

and rhizosphere scale. This data was then subject to further statistical testing via principle component analysis to help determine potential relationships between the measured parameters.

4.7.1 Principal component analysis

A principal component analysis (PCA) was undertaken which included 13 plant parameters and 6 soil porosity parameters (Figure 4.17). The results of this analysis showed some strong groupings of measured parameters including the grouping of rhizosphere soil characteristics (S3, S4, S5 & S6) and the grouping of plant characteristics (P1, P4, P12).

4.7.2 Final species selection

Once the data set had been subject to PCA testing, straight ordination between the two parameters was undertaken that were deemed to be the most important for demonstrating soil porosity formation in the rhizosphere. These two parameters were: 1) the amount of pore space (%) in the 0-70 µm increment from the root surface and 2) the volume of root within the soil core (cm^3). It is clear that *Cirsium* stands out as a species as having considerably greater overall root volumes and porosity in the rhizosphere (Figure 4.18). On this basis *Cirsium* was the plant species identified to take forward and investigate further to assess its ability to generate pore space in different compacted soil textures.

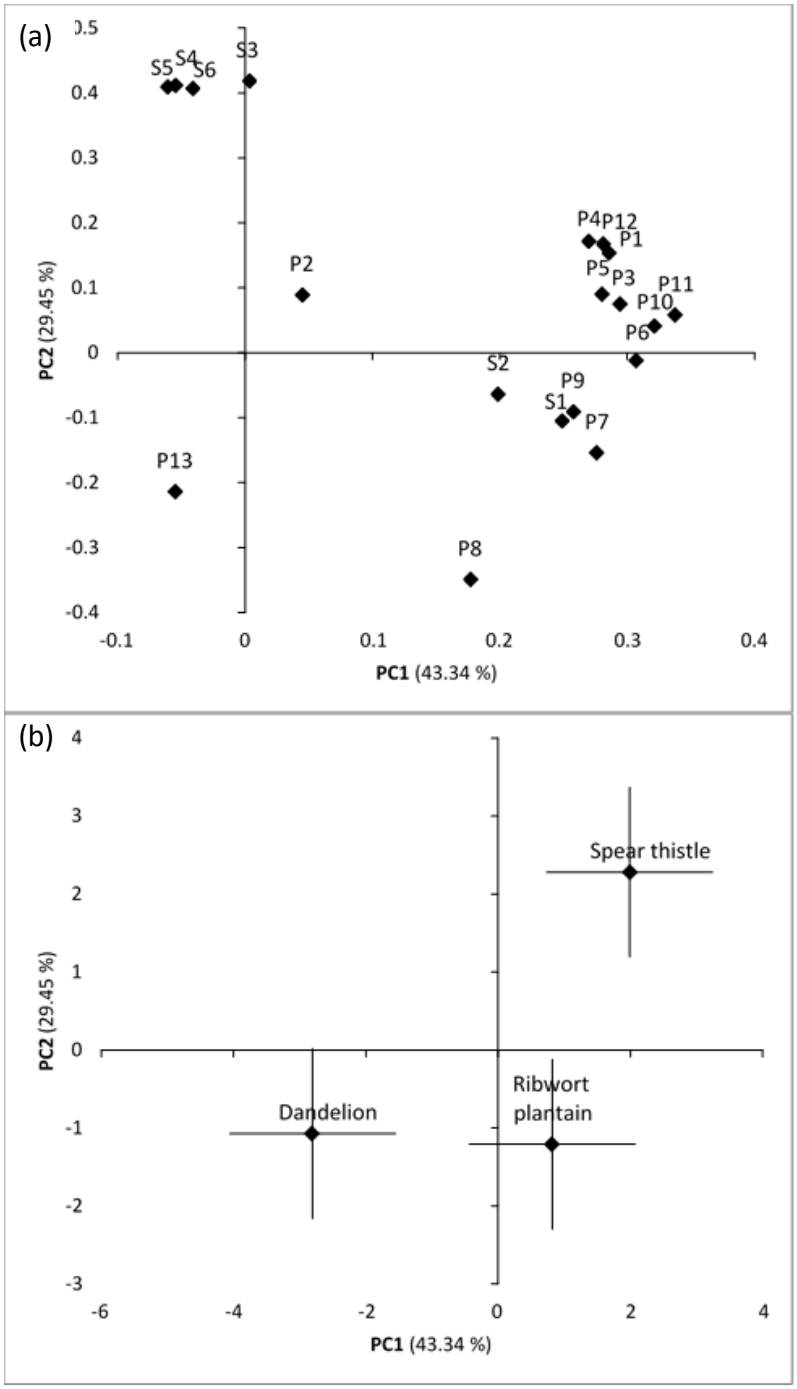


Figure 4.17: Principal component plots (PC) based on plant root and shoot characteristics with relation to soil and rhizosphere porosity measurements. (a) Plots denote loadings of PC1 & PC2. (b) Plots denote means, whiskers pooled S.E. Percent variance accounted for by PC's shown in parentheses on axis label.

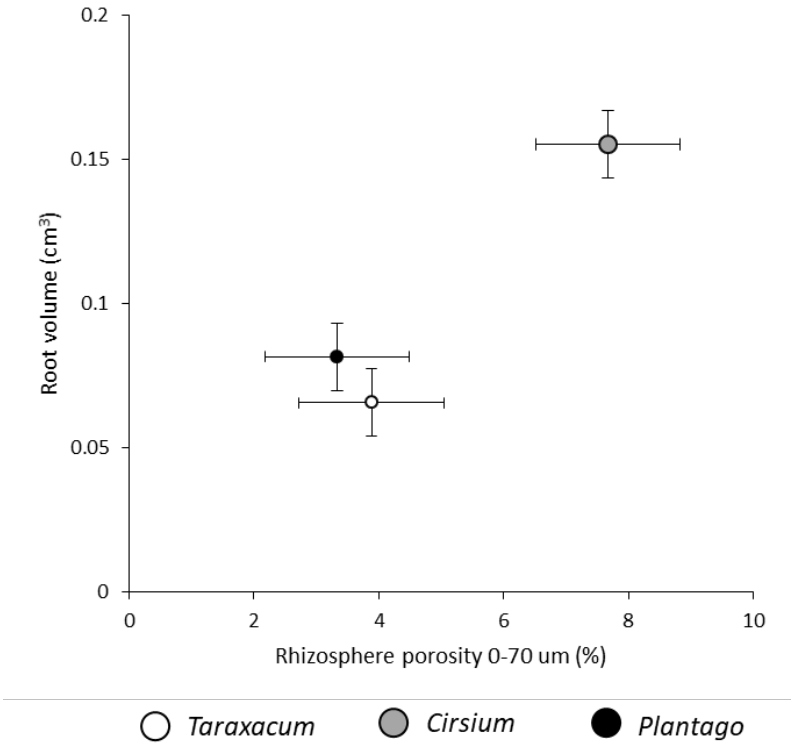


Figure 4.18: Straight ordination between root volume cm^3 and rhizosphere porosity (%) for the 0-70 µm incremental zone.

4.8 Chapter summary

This chapter outlined the systematic review undertaken to initially identify plant species of interest that had the ability to grow on heavily compacted soils. The preliminary trial work undertaken with regards to seed germination and initial screenings of plants in soil was reviewed and data collected contributed to a full scale screen experiment of five plant species using 2D analysis methods. This data was analysed and a plant trait database generated which allowed the four species to be used in the 3D X-ray CT experiment to be determined. Image analysis method trials are explained and the full 3D experiment presented in the form of a manuscript. Further

statistical analysis was completed to identify relationships between plant and soil characteristics measured. This analysis forms the basis of justification to identify which plant species was able to generate root mass in a compacted soil and subsequently alter to soil pore network within the soil cores. This species will form the basis of the study presented in Chapter 5.

Chapter 5: Assessing the impact of soil texture on *Cirsium vulgare* root architectural development and soil porosity formation in the rhizosphere

This chapter explores how roots of *Cirsium vulgare* plants developed in different soil textures under a high soil compaction treatment. *Cirsium* was selected from a number of species as described in Chapter 4. Preliminary work focused on categorising the soils used, and determining the most appropriate soil conditions for long-term monitoring. Novel image processing techniques were evaluated and applied to the 3D data set (presented in this chapter in the form of a manuscript). Plants were assessed on the basis of responses of their root architecture to both soil compaction and soil texture, and associated effects on soil pore formation in the rhizosphere were analysed.

Aim: To determine the ability *Cirsium vulgare* to grow in heavily compacted soil of different textures, and assess plant root architecture and associated pore formation in the rhizosphere in 3D.

Objectives:

- Categorise soils of different textures and determine appropriate soil matric potential for long term growth via tension table experiments
- Evaluate novel greyscale equalisation and plant root segmentation techniques

- Assess plant root architecture in 3D to establish if there are differences in root traits under different soil textures
- Calculate changes in 3D soil porosity in the rhizosphere as a result of root growth

The chapter is structured in two parts. Sections 5.1-5.5 describe preliminary investigations to establish appropriate image analysis methodologies. Section 5.6 comprises a manuscript which details the results of the experiment.

5.1 Soil classification

5.1.1 Soil texture

Soil was collected and processed using the methods outlined in Section 2.1.1 *Soil preparation*. Once air-dried and sieved to < 2 mm the texture of the soil was determined using the method outlined in Section 2.1.5 *Soil texture (quantitative analysis by hydrometer).* Results were generated and texture was classified using the soil textural triangle for England and Wales (Hodgson, 1997; Table 5.1).

Table 5.1: Textural characteristics of soil adopted for studies described in Chapter 5.

Sample	% Clay	% Silt	% Sand
Clay loam	31.62	30.52	37.86
Clay	43.32	28.45	28.23
Sandy loam	9.52	26.12	64.35

5.1.2 Soil core preparation

Soil cores were packed to 1.2 g cm^{-3} and 1.8 g cm^{-3} using the wet compaction technique outlined in Section 2.1.2b at a gravimetric soil moisture content of 16 %. Saturated moisture was then equilibrated over 96 hours (Figure 5.1a). Once saturated the water release curve of the soil was calculated using the method outlined in Section 2.1.3b *Soil equilibrium and water release characteristics.* The results from the tension table experiment demonstrate the relative moisture holding capacity for the three soil types at soil bulk densities of 1.2 g cm^{-3} and 1.8 g cm^{-3}. Measurements were collected under two bulk density treatments to demonstrate the soil's moisture holding characteristics in both uncompacted compacted and heavily compacted states (Figure 5.1b).

The cores were considered equilibrated when they had been at 5 kPa for 24 hours. At this time the average gravimetric moisture contents for the three soils was as follows: sandy loam 13.0%, clay loam 16.5% and clay 18.3%. These were the moisture content percentages that the soils were subsequently maintained at for the duration of the experiment.

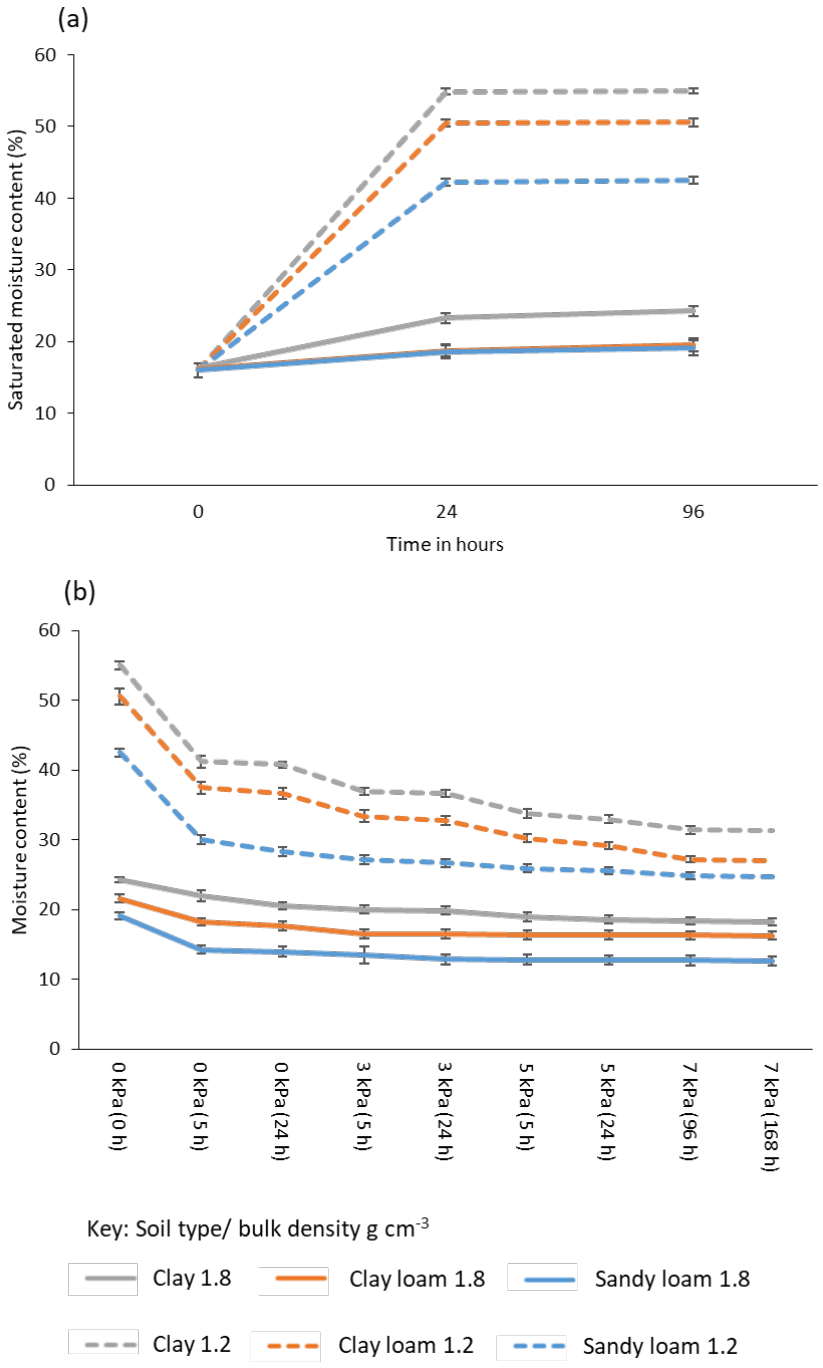


Figure 5.1: (a) Saturated moisture contents of soil cores of different textures packed to different bulk densities (g cm^{-3}) at 0, 24 and 96 hours. (b) Relative soil moisture contents of cores subject to different levels of suction across a time course.

5.1.3 Soil penetration resistance

Soil cores (5 cm diameter x 10 cm height) were uniformly packed using the wet compaction technique (Section 2.1.2b) to specified moisture contents determined from the water equilibration experiment. Once packed, cores were individually wrapped in polythene film and stored in a cold store for 3 days at 5°C before measuring penetrometer resistance. The method is outlined in Section 2.1.6. The recorded penetrometer resistances for the three soils at 1.8 g cm^{-3} were: sandy loam 3.64 MPa, clay loam 3.83 MPa and clay 4.54 MPa.

5.1.4 Growth conditions

Plants were grown in a growth chamber with settings prescribed as follows: day/night temperature of 20˚C/15˚C; day temperature ran from 05.00-21.00, light duration was 16 h; night duration was 8 h; dawn/dusk duration was 3 h. The daylight period was from 08.00-18.00 and the night period was from 21.00-05.00. The growth chamber was kept at 70% humidity. The cores were weighed each day and re-watered to a constant weight. Three nutrient applications of 2 mm of solution per core were made over the course of the growth period. The nutrient solution used was HortiMix Standard 0-36-36 with trace elements (Hortifeeds, Lincoln, UK).

5.2 Primary imaging processing

5.2.1 Reconstructing X-ray data

All image data was reconstructed using the PCA file in DATOS REC, VG Studio Max V2.2.2. The images were optimised using an auto feature to adjust for any movement that may have occurred during the scan. The region of interest (ROI) was determined using the auto ROI function to reduce the size of the image area for analysis. Once cropped the region was reconstructed for use in the greyscale equalisation trial using VG Studio Max.

5.2.2 Greyscale equalisation

The purpose of the greyscale equalisation trial was to assess whether unifying the input files greyscale range would enhance the potential for consistent pore space and root segmentations from the data set.

5.2.2a Data preparation

The minimum and maximum greyscale values for each individual scanned section of all soil cores were collected from the original .pcr files from Volume Graphics (VG). This data served as the raw input data for the greyscale equalisation trail. The change in these data over time are given in Figure 5.2. All of these values were collated in a thresholding document in excel. Here the minimum and maximum 32 bit greyscale values from the .pcr file are collated in columns. The spreadsheet was configured to search for the

smallest minimum value and the largest maximum value (providing the two extremes for the data set). The difference between the two values was then calculated and divided to produce a 16-bit greyscale range instead of the original 32-bit. The two centre points of the data set were then identified (the highest minimum value and the lowest maximum value) and divided by the 16-bit greyscale range. This process equalised the greyscale values, providing a new minimum and maximum range across the replicates as well as converting the values from 32-bit to 16-bit. For the purpose of this investigation a number of equalisation combinations were investigated for each soil type at each time point (Table 5.2).

5.2.2b Image preparation

The chosen trial input threshold was applied to both the top and bottom sections of the same core in VG Studio Max. An image stack of the core was then exported from VG studio and saved as a greyscale image stack. The number of images the trial was conducted on was set at 200 image slices per core. The start and end location of each trial section was noted in mm and was consistent between replicates and across time. The greyscale image stacks were imported into ImageJ and converted into 8-bit. They were then cropped to specific width x height of 1000 x 1000 pixels and the x and y coordinates within the core were set as 425, 435 for consistency across all stacks analysed (Figure 5.3). The scale of the image stack was set 1 pixels = 33 unit length (µm).

A threshold was then applied to the image (a number of automated thresholds were investigated but were all found to over- or under- estimate the proportion of pore space in the image). The threshold was initially selected via the default tab and then manually modified. From the analysis undertaken It was determined that the soil cores could be equalised across soil type within a time frame i.e. Sandy loam Week 0 or Clay loam Week 4.

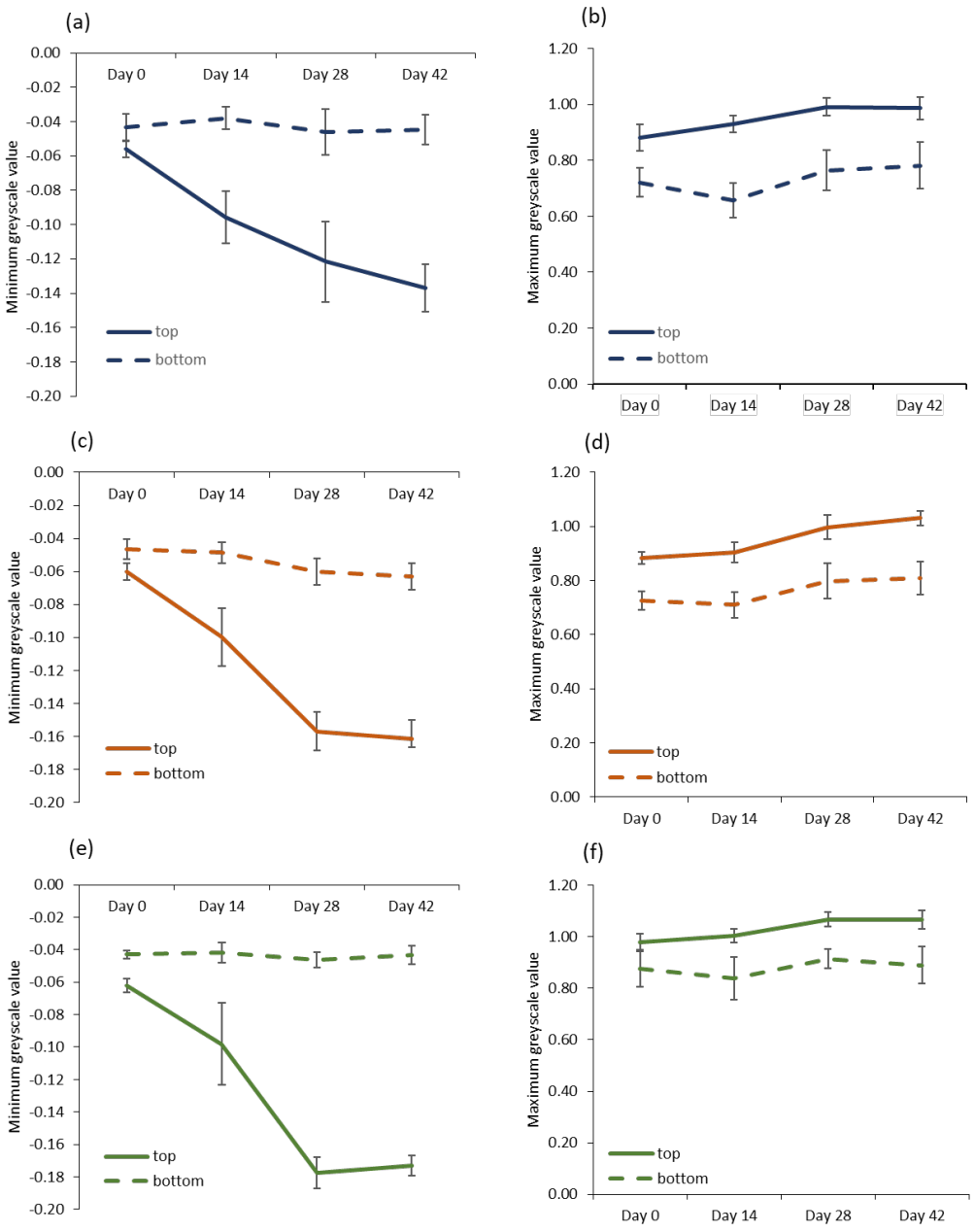


Figure 5.2: Average minimum and maximum greyscale values recorded over a 42 day period for: (a), (b) clay, (c), (d) sandy loam, (e), (f) clay loam. Top and bottom refer to the scanned top 4 cm and bottom 4 cm of the soil cores. Bars denote means, whiskers SE.

Table 5.2: Table of equalised greyscale input 32-bit and output 16-bit values for each soil type at each scan time point.

Soil type	Week	VG Studio Max	32bit	16 bit
Sandy loam	0	Lower Limit	-0.03441	2283
Sandy loam	0	Upper Limit	0.66215	43929
Sandy loam	2	Lower Limit	-0.02703	1610
Sandy loam	2	Upper Limit	0.60527	36056
Sandy loam	4	Lower Limit	-0.03051	1600
Sandy loam	4	Upper Limit	0.66101	34670
Sandy loam	6	Lower Limit	-0.0325	1704
Sandy loam	6	Upper Limit	0.67547	35413
Clay	0	Lower Limit	-0.03204	2086
Clay	0	Upper Limit	0.66879	43534
Clay	2	Lower Limit	-0.02964	1765
Clay	2	Upper Limit	0.57697	34353
Clay	4	Lower Limit	-0.03517	1948
Clay	4	Upper Limit	0.64675	35826
Clay	6	Lower Limit	-0.0348	1923
Clay	6	Upper Limit	0.67742	37438
Clay loam	0	Lower Limit	-0.03954	2340
Clay loam	0	Upper Limit	0.79793	47222
Clay loam	2	Lower Limit	-0.03235	1820
Clay loam	2	Upper Limit	0.74477	41899
Clay loam	4	Lower Limit	-0.04139	2099
Clay loam	4	Upper Limit	0.87237	44245
Clay loam	6	Lower Limit	-0.03708	1879
Clay loam	6	Upper Limit	0.82327	41721

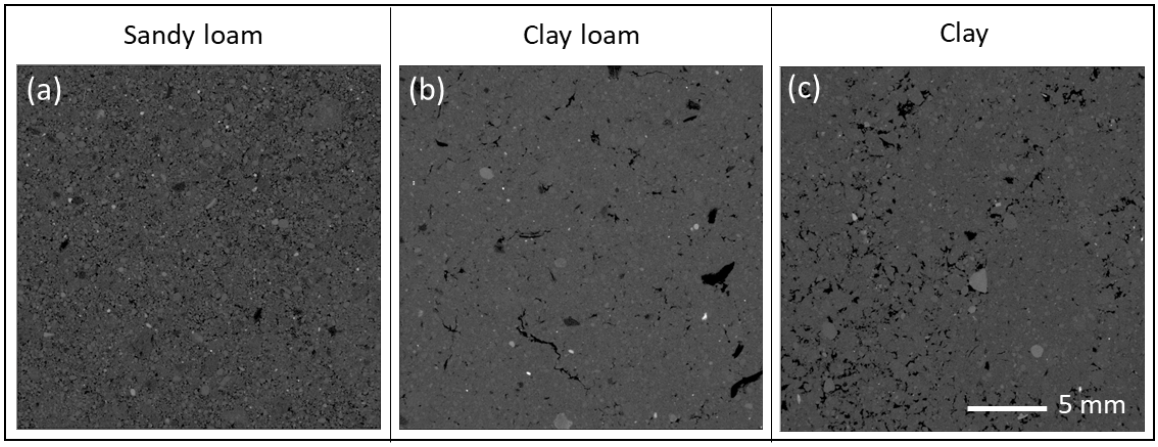


Figure 5.3: Example greyscale imagery taken from image stack produced by X-ray CT scanning of three different soil types: (a) sandy loam, (b) clay loam and (c) clay compacted to a bulk density of 1.8 g cm^{-3}.

This method was deemed to provide the most representative estimate of pore space across the 200 slice image stack. This specific threshold was then routinely used for the same soil type when classifying soil porosity for this trial (different thresholds were necessary for the different soil types due to the inherent difference in pore structure). Once the images were thresholded, the results were saved and analysed in Microsoft Excel to generate 2D soil porosity values.

5.2.2c Outcome of greyscale equalisation trial

The equalisation of greyscale allows the consistent application of segmentation thresholds between samples that contribute to the original equalisation. It was established that there were three different levels of equalisation worthy of trial for the three soil types. The first of these was to include all original greyscale values from all cores at each time point

regardless of the soil type. This would provide one all-encompassing equalisation of the greyscale for the experiment. The second was to include replicates of all three soil types within a single time point. The third was to consider each soil type individually at each time point.

The location of the core (top scanned section 0-4 cm or bottom scanned section 4-8 cm) consistently had a statistically significant effect on the minimum greyscale value recorded ($p < 0.001$) at Days 0, 14, 28 and 42. The soil type had a significant effect on the minimum greyscale values at Days 28 and 42 ($p<0.001$). Both the location of the core and soil type had an effect on the maximum greyscale recorded at all time points ($p<0.001$).

From this investigation it was determined that the equalisation of greyscales could be applied to successive scans from within the same soil type and scan time period. For example, all the scanned clay soil replicates from Day 0 could have their grey scales equalised by the same approach. This equalisation ensures consistency and comparability with subsequent root and pore segmentations within each specific treatment x time replicate. When conducting this approach a number of factors were considered such as the relative moisture content of each core (this was consistent across soil type).

5.3 Root segmentation methodologies

Three different root segmentation techniques were investigated to determine which methodology would provide the most rigorous and repeatable results. The first of these was a manual segmentation methodology which relies solely

on user-discretion within VG Studio Max (Appendix 4, A.4.4). This technique has been widely applied across numerous studies (Gregory, 2003; Ahmed et al. 2016) and is based on region-growing that relies on thresholding small sections of image into a greyscale denoted by the user as root. The second method investigated was utilising 'RooTrak', an automated image processing algorithm (Mairhofer et al. 2015; Appendix 4, A.4.5). The method employs a tracking-based strategy which follows the root cross-sections through a sequence of images, with the initial digital processing seed-point being identified manually by the user. As the image stack is traversed, the cross-sections move around the image, reproducing the shape of the scanned root. Finally an ImageJ based auto thresholding macro (Root1) was tested (Flavel et al. 2017; Figure 5.4). The method employs a number of filtering, thresholding and erosion techniques to classify root material via a user-identified threshold value range. The full method and the adopted macro is given in Appendix 5, A.5.11 & A.5.12.

5.3.1 Results of segmentation trial

Each of the three segmentation methodologies was tested on each of the three soil types in relation to Day 14 data (providing simple root systems to provide a straightforward check as to whether the methods were effective; (Figure 5.5)). This was necessary due to the difference in greyscale and texture of the soils meaning that each of the three segmentation methods would have varying levels of accuracy. By testing the different methods on different soil types, an assessment of the appropriateness of each method against each soil

type could be made, including an estimated segmentation time for the plant species at different growth stages (Table 5.3). Once the young root systems had been investigated, a single Day 42-plant grown in clay soil was studied, to assess how well the segmentation methods picked up complex root systems (Figure 5.6).

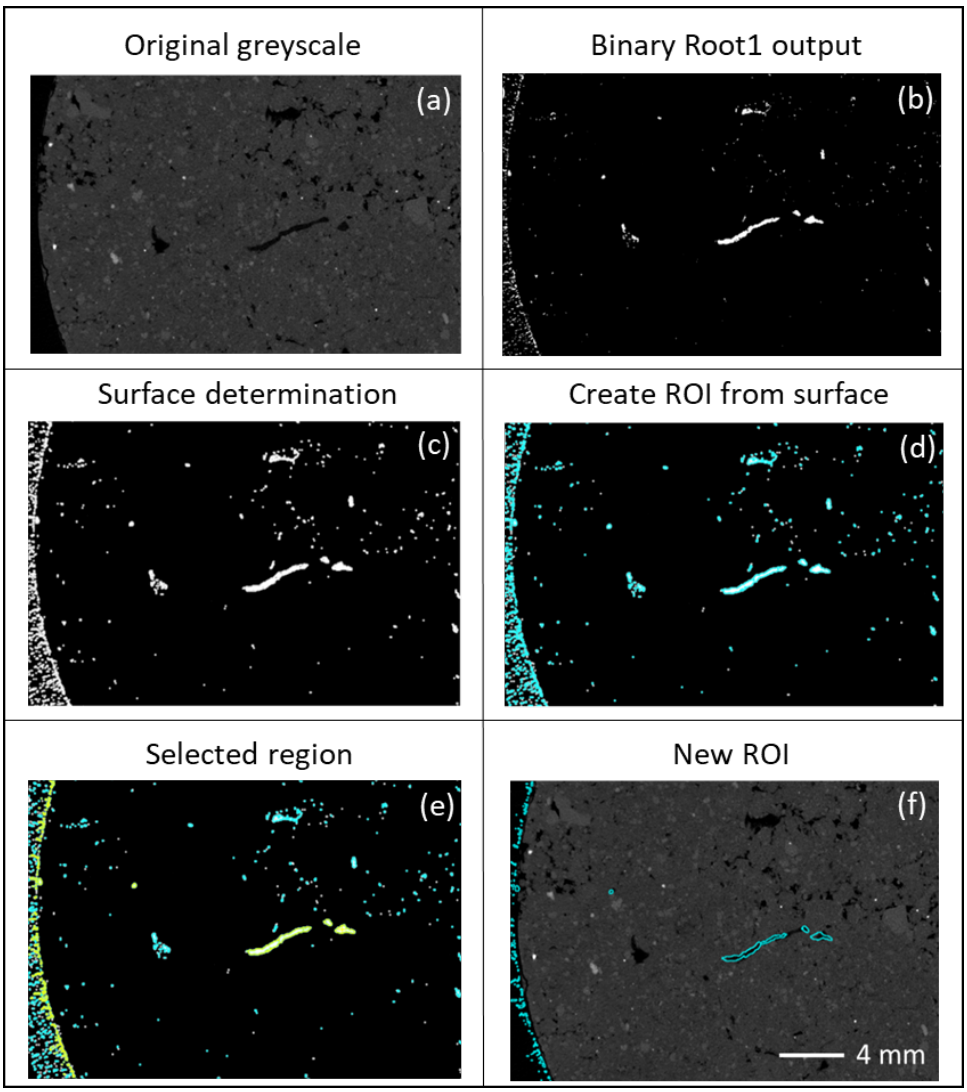


Figure 5.4: Example Images detailing Root1 image import into VG Studio Max. (a) original greyscale image, (b) binary Root1 output, (c) surface determination classification, (d) region of interest creation from surface, (e) region selected for creation, (f) new region of interest created. Images generated using VG Studio Max V 2.2.5.

Table 5.3: Root segmentation times of *Cirsium* plants from different soil textures using different segmentation techniques at 14 and 28 days growth.

		Segmentation time (h)		
Soil type	Day	Manual	RooTrak	Root1
clay	14	2	2.5	3.5
clay loam	14	1	3	3
sandy loam	14	1.5	3	3.5
clay	28	5	4	3.5

Each segmentation method was graded on three attributes, *viz*. time to produce output, accuracy of output and repeatability of segmentation. The most important attributes were deemed as accuracy of output segmentation and the repeatability of segmentation. The accuracy was determined by how similar the output root systems were to the manually segmented system. The repeatability was determined by how easy the method would be to reproduce. The methods were scored 1 for best performer and 3 for worst, with resultant grades presented in Table 5.4. From this initial analysis it was determined that the most appropriate root segmentation methodology was the Root1 thresholding macro. From the scoring assessment we can say that the most accurate segmentation was produced by the Root1 macro as this thresholding segmentation was able to pick out areas of root features within the cores that were not possible to determine by eye using the manual segmentation, due to subtle changes in greyscale. RooTrak had the lowest accuracy score as the example imagery in Figures 5.5 & 5.6 demonstrates that the in all instances only partial root systems were constructed from the segmentation technique. From the analysis of the root segmentation types

the Root1 segmentation method was used to obtain root related data for this experiment. When undertaking this comparision of root segmentation methodologies it was noted that there was a variance in the average root thickness between the methods. This is commented on in the discussion of this chapter. Each root system was fully extracted, cleaned and checked using VG Studio Max 2.2.5.

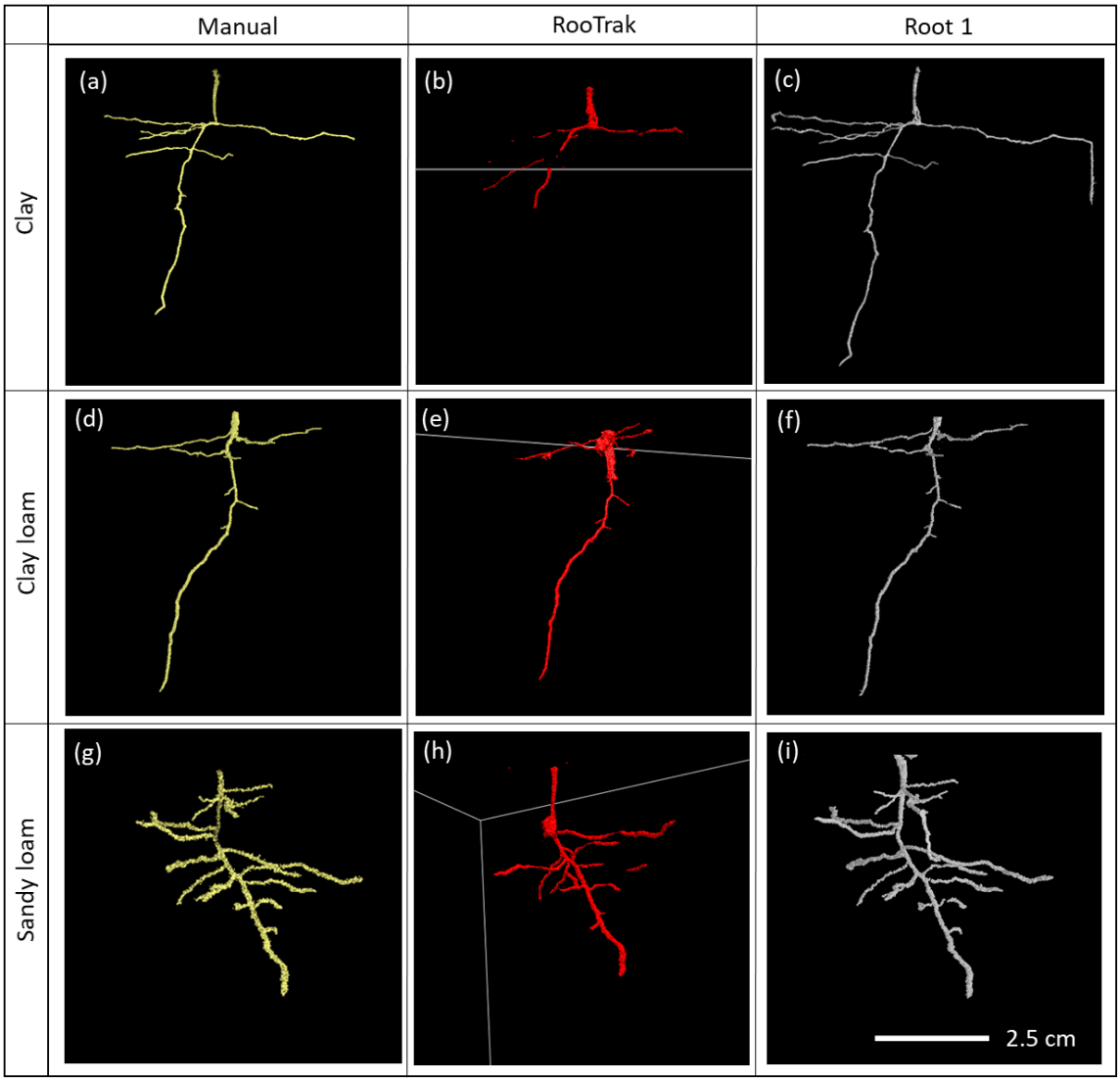


Figure 5.5: Root imagery of three different segmentation methodologies for *Cirsium* plants grown for 14 days in three contrasting soil types. (a) Manual segmentation in clay soil, (b) RooTrak segmentation in clay soil, (c) Root1 segmentation in clay soil, (d) Manual segmentation in clay loam soil, (e) RooTrak segmentation in clay loam soil, (f) Root1 segmentation in clay loam soil, (g) Manual segmentation in sandy loam soil, (h) RooTrak segmentation in sandy loam soil, (i) Root1 segmentation in sandy loam soil.

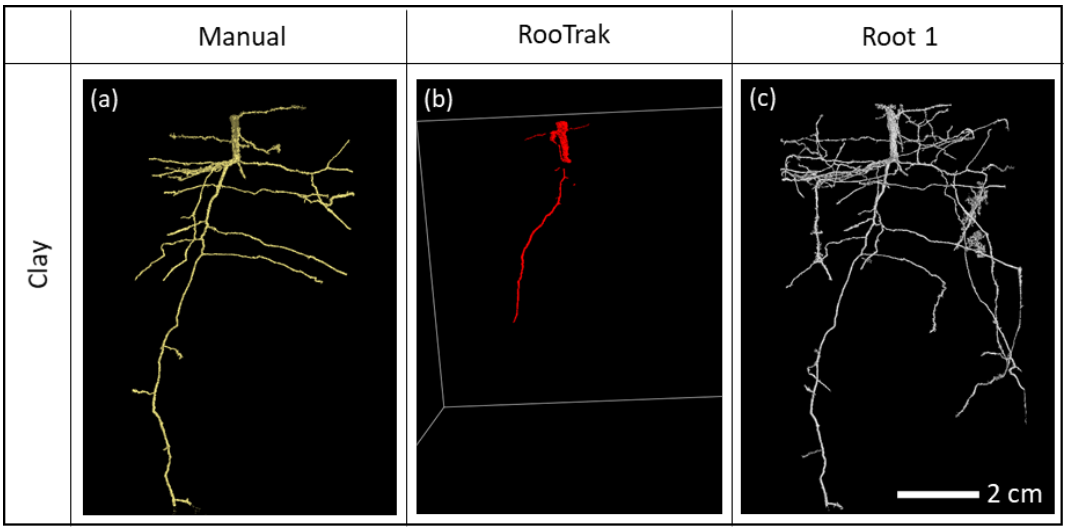


Figure 5.6: Root imagery of three different segmentation methodologies for *Cirsium* plants grown for 28 days in clay soil. (a) Manual segmentation in clay soil, (b) RooTrak segmentation in clay soil, (c) Root1 segmentation in clay soil.

Table 5.4: Results of root segmentation method grading. A score of 1 is high and 3 is low; lowest overall score determines the best-ranked method

	Segmentation method		
Attribute	Manual	RooTrak	Root1
Time	1	2	3
Accuracy	2	3	1
Repeatability	3	2	1

5.4 X-ray CT analysis methods

5.4.1 Root analysis VG Studio

Once the root systems were segmented, resultant data was duplicated and the copied set modified by visual interpretation to display the taproot and lateral roots as separate entities for analysis. This was achieved by using the erase tool to remove small sections of root protruding from the taproot to the

laterals roots, causing the two root types to become disjointed (Figure 5.7 c&d). This enabled specific volume and surface area characteristics to be obtained for the different root types within the same core (Figure 5.6b) Total root length of the taproot was subsequently measured using the polyline tool in VG Studio Max.

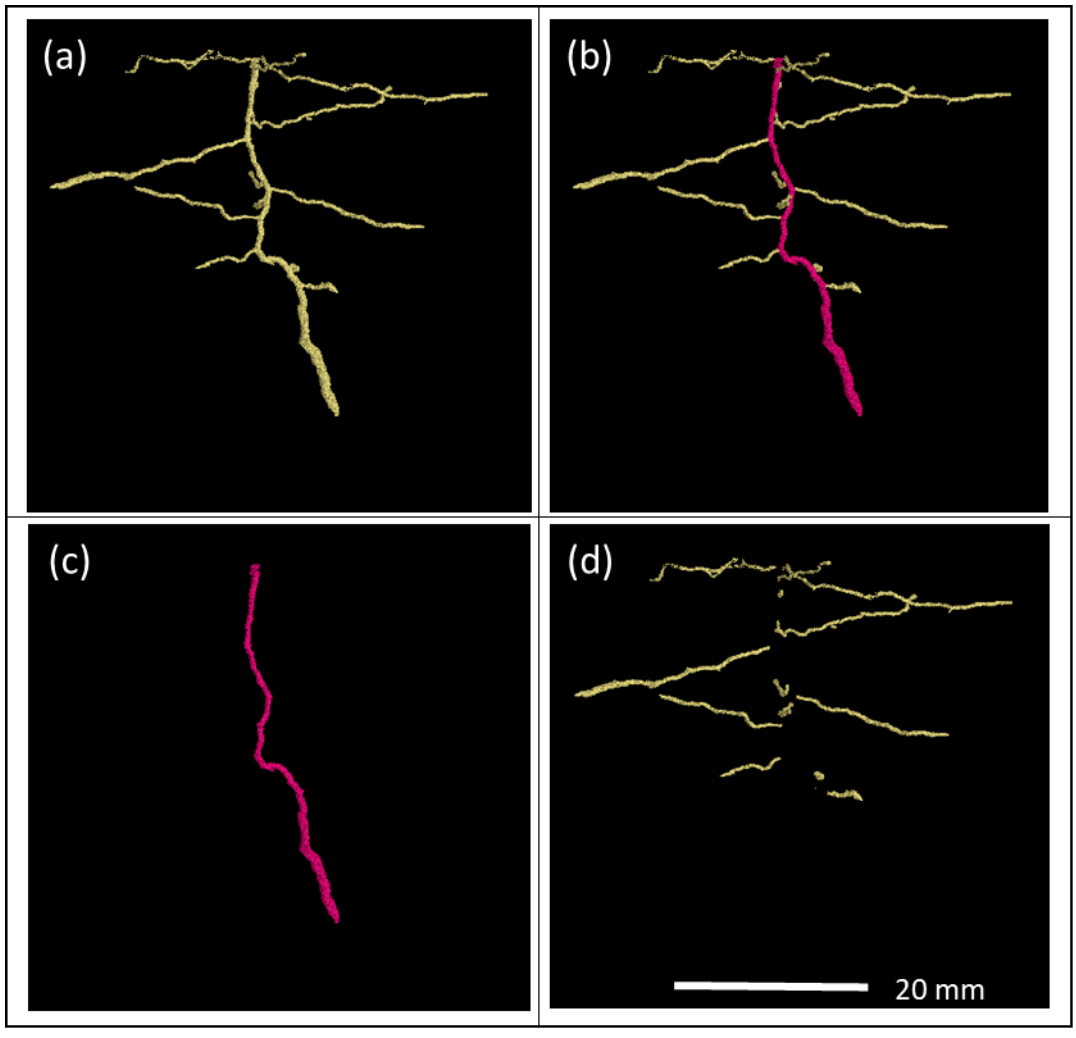


Figure 5.7: Example Root1 segmentation of Spear thistle roots grown in sandy loam soil for 14 days and root classification. (a) Cleaned Root1 segmentation, (b) Root system split into taproot ROI (pink) and lateral roots ROI (beige), (c) Taproot ROI, (d) Lateral root ROI. Images generated using VG Studio Max 2.2.5.

5.4.2 Poly angle measurement tool (PAM)

The software tool PAM (Mairhofer et al. unpublished) was used to obtain specific taproot characteristics. The segmented .vgl files were loaded into the program and visualised as polylines. Specific values including the total length of the root (mm), the angle of root growth (°) along 10-mm increments of the root and the taproot convex hull (mm^3) were generated (Figure 5.8).

5.4.4 Rhizosphere porosity analysis

5.4.4a Defining rhizosphere pore space and pore thickness

Rhizosphere porosity was defined using same the method employed in Chapter 4. Here the pore space change around the taproot with increasing distance from its surface is investigated using the incremental zones with the following distances from the root surface; 0-70, 70-140, 140-280 and 280- 420 µm (Figure 5.9). The image stack was threholded for pore space and then each incremental zone was classified and the pore space was exported to ImageJ as a binary file. The BoneJ plugin from ImageJ was used to run a pore thickness assessment on the rhizosphere porosity (Figure 5.9f). This allowed further descriptive characteristics concerning the pore space to be determined including mean pore thickness (mm) and maximum pore thickness (mm) (Figure 5.10).

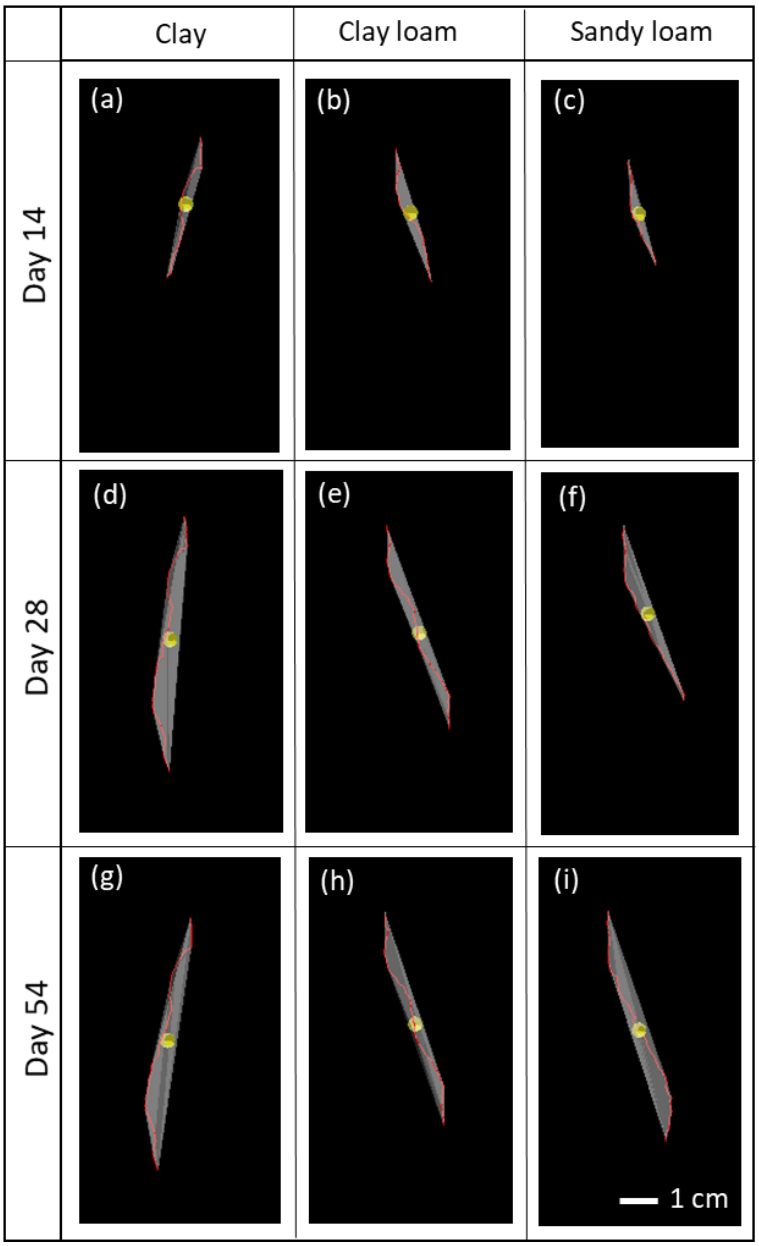


Figure 5.8: Example visualisation via Poly angle measurement tool (PAM) of *Cirsium* taproot Convex hull's (mm^3), grown in (a) clay, (b) clay loam, (c) sandy loam for 14 days. (d) clay, (e) clay loam, (f) sandy loam for 24 days. (g) clay, (h) clay loam, (i) sandy loam for 42 days.

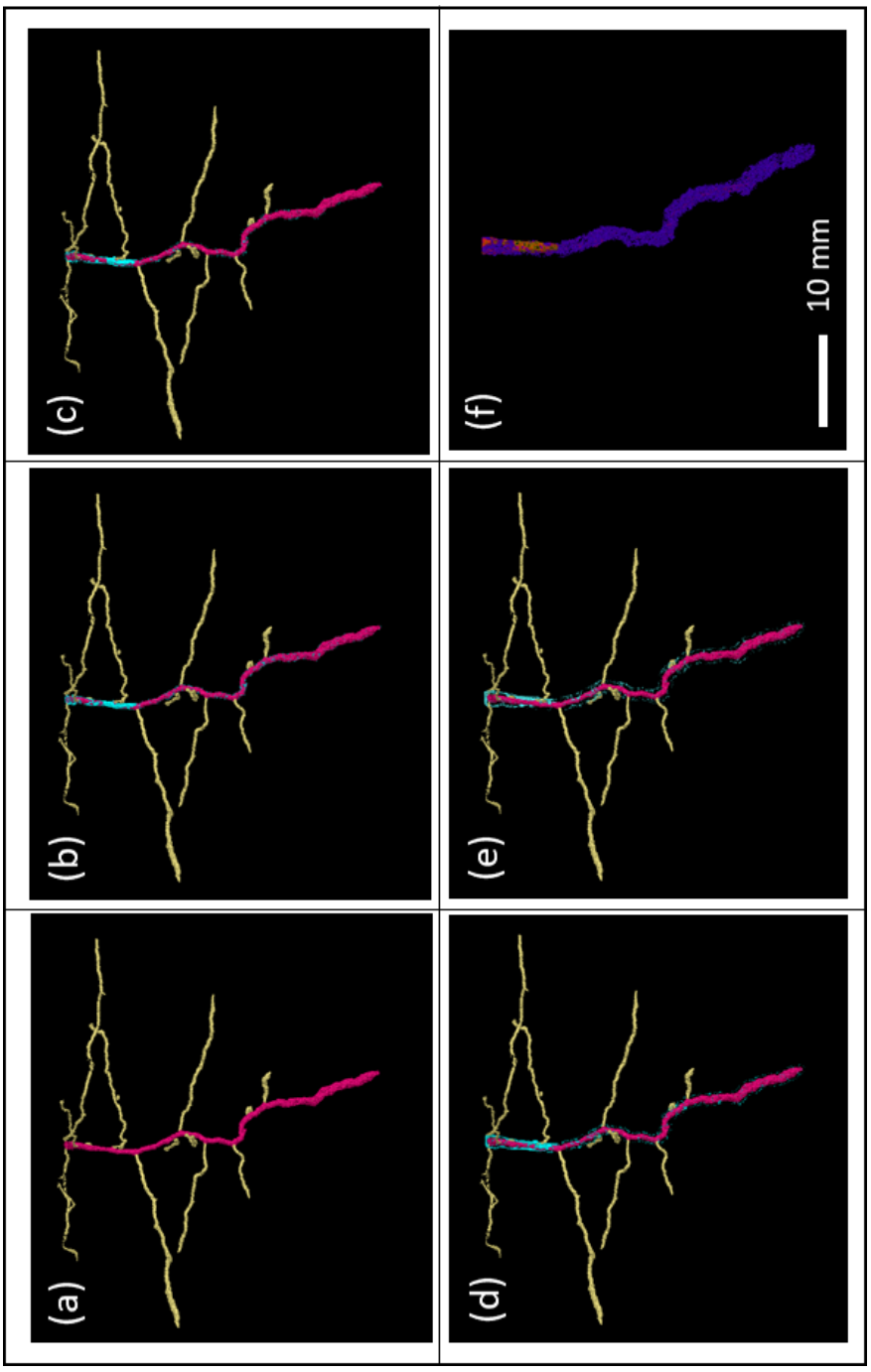


Figure 5.9: Example Root1 segmentation of *Cirsium* roots grown in sandy loam soil for 14 days and root/ rhizosphere porosity classification. (a) Cleaned Root1 segmentation split into taproot ROI (pink) and lateral roots ROI (beige); (b) root system and pore space (blue) within rhizosphere zone 0-70 um, (c) Root system and pore space (blue) within rhizosphere zone 70-140 um, (d) Root system and pore space (blue) within rhizosphere zone 140-280 µm, (e) Root system and pore space (blue) within rhizosphere zone 280-420 um, (f) Pore thickness map for rhizosphere 0-420 um from root surface. Images generated using VG Studio Max 2.2.5.

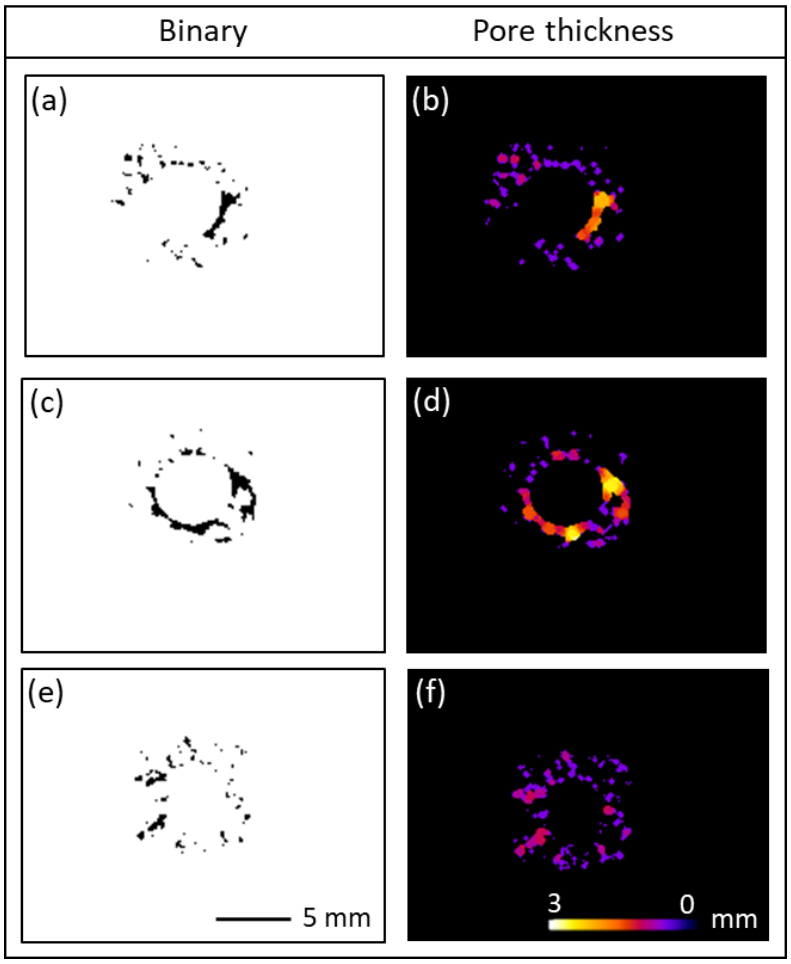


Figure 5.10: Indicates example input binary imagery (a, c, e) generated in ImageJ from VG Studio rhizosphere pore space classifications and subsequent pore thickness classification (b, d, f). Colour gradient indicates relative thickness of pores.

5.5 Biomass and 2D characteristics analysis

5.5.1 Shoots

Shoot fresh and dry weights were measured after 42 days growth using the method outlined in Section 2.2.5. Images of X-ray CT scanned *Cirsium* shoots day 14 Figure 5.11: (a-c) day 14 (d-e) day 28 (g-i) day 42 were used to quantify shoot area (cm^2) in ImageJ. Original images were thresholded to classify leaf material as black and background as white. These binary images were then

processed using the 'analyse particles' function to provide a value of the overhead shoot area.

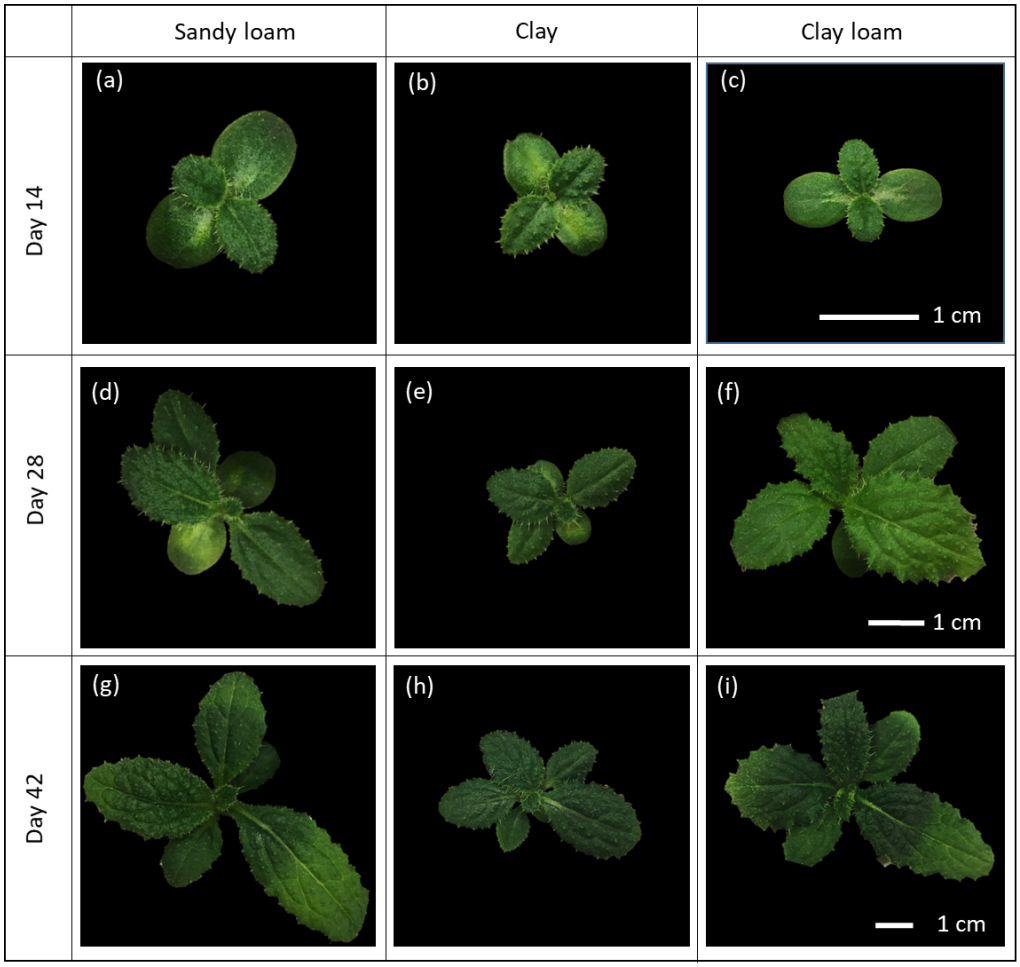


Figure 5.11: Images of *Cirsium* plant shoots subject to X-ray CT after 14 days growth. Plants grown in (a) sandy loam, (b) clay, (c) clay loam. After 28 days growth (d) sandy loam, (e) clay, (f) clay loam. After 42 days growth (g) sandy loam, (h) clay, (i) clay loam. Images cropped and modified using ImageJ.

5.5.2 Roots

At Day 42 plants were destructively harvested and roots removed from the soil. Control and X-ray CT scanned plant roots were scanned in 2D using WinRHIZO (Section 2.2.5). Images of root systems grown in clay, sandy loam and clay loam at 1.8 g cm^{-3} bulk density are shown in Figure 5.12.

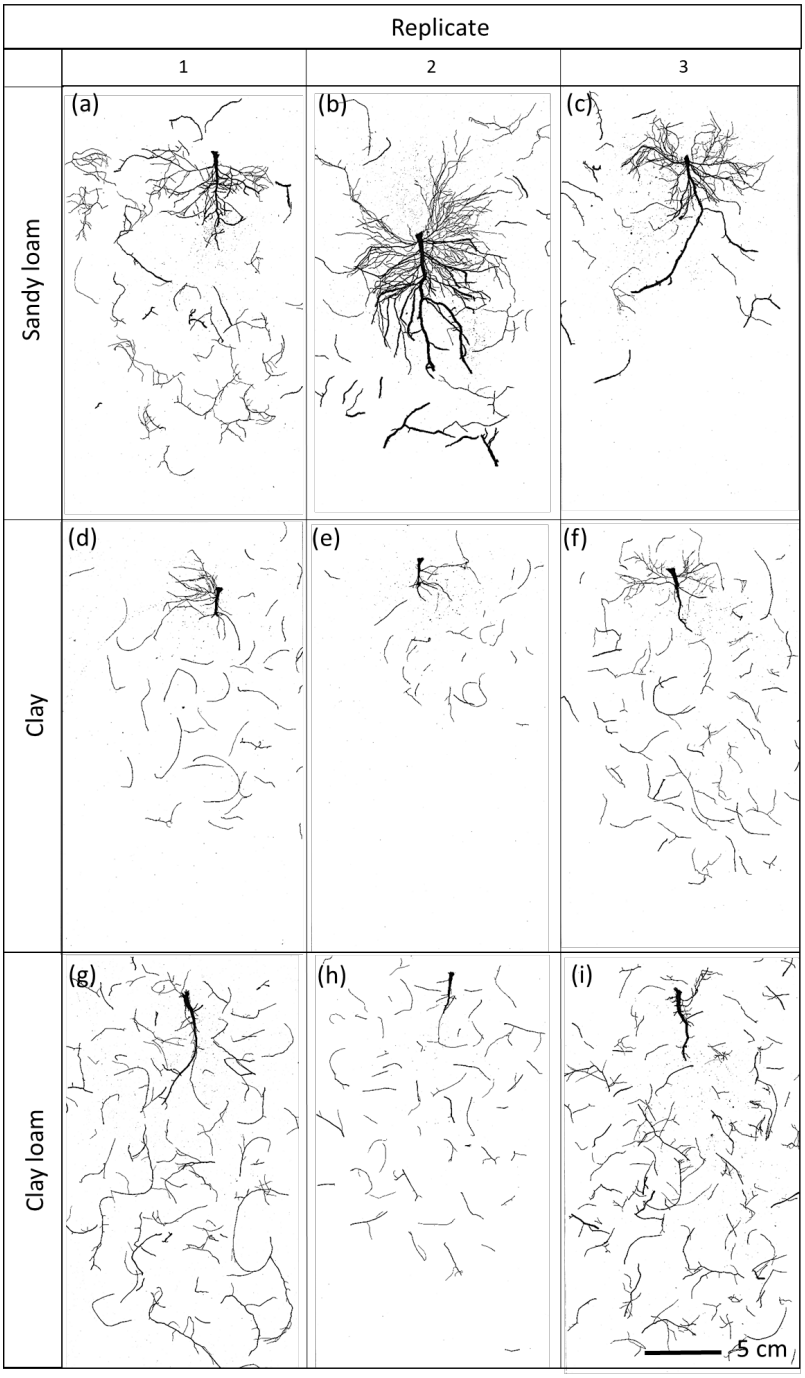


Figure 5.12: WinRHIZO 2D scans of *Cirsium* grown to 42 days compacted to 1.8 g cm^{-3}. (a,b,c) in sandy loam soil, (d,e,f) in a clay soil, (g,h,i) in clay loam soil.

5.6 Physical soil characteristics

5.6.1 Aggregate size distribution

The aggregate size distribution of the cores was measured using the method outlined in Section 2.1.6 from samples at two time points. Three unplanted replicates of each soil type were sampled on day 0 giving a representation of the initial aggregate size distribution of the compacted cores. A further three unplanted and six planted replicates were measured on Day 42. This allowed the change in aggregation within the core systems under the influence of plant root development to be assessed.

5.7 Authors manuscript

The remainder of this chapter is structured and formatted in accordance with the journal Plant and Soil. Status: For submission

Individual replicate 2D WinRHIZO scan imagery and X- ray CT root imagery and plant shoot photographs for *Cirsium* plants can be found in A.5.1-A.5.9.

Author Contributions

Conceptualisation: J.E. Burr-Hersey, S.J. Mooney, A.G. Bengough, K. Ritz.
Data curation: K. Ritz.
Formal analysis: J.E. Burr-Hersey, S.J. Mooney, K. Ritz.
Funding acquisition: K. Ritz.
Investigation: J.E. Burr-Hersey.
Methodology: J.E. Burr-Hersey, S.J. Mooney, C. Sturrock, A.G. Bengough, K. Ritz.
Project administration: K. Ritz.
Software: J.E. Burr-Hersey**,** S.J. Mooney, C. Sturrock, B. Atkinson.
Supervision: S.J. Mooney, A.G. Bengough, K. Ritz.
Visualization: J.E. Burr-Hersey, S.J. Mooney,
Writing original draft: J.E. Burr-Hersey, K. Ritz.
Writing review & editing: J.E. Burr-Hersey, S.J. Mooney, A.G. Bengough, K. Ritz.

Soil texture affects root system architecture and soil structural dynamics in the rhizosphere of *Cirsium vulgare*

Author names

Jasmine E Burr-Hersey [1,2] Jasmine.burr-hersey@nottingham.ac.uk

Sacha J Mooney [1] Sacha.mooney@nottingham.ac.uk

A Glyn Bengough [2,3] A.bengough@dundee.ac.uk

Craig Sturrock[1] Craig.sturrock@nottingham.ac.uk

Brian Atkinson[1] Brian.atkinson@nottingham.ac.uk

Karl Ritz [1] Karl.ritz@nottingham.ac.uk

Institution addresses

[1] Division of Agricultural & Environmental Science, School of Bioscience, University of Nottingham, Sutton Bonington Campus, Leicestershire, LE15 2RD, United Kingdom

[2] The James Hutton Institute, Invergowrie, Dundee, DD2 5DA, United Kingdom

[3] School of Science and Engineering, University of Dundee, Dundee, DD1 4HN, United Kingdom,

Soil texture affects root system architecture and soil structural dynamics in the rhizosphere of *Cirsium vulgare*

5.7.1 Abstract

Soil compaction is a serious form of soil physical degradation that results in destruction of soil pore networks leading to suboptimal conditions for plant growth. We assessed the impact growing spear thistle (*Cirsium vulgare),* a pioneer plant species often found growing on compacted soils in the wild, had on soil porosity development in three contrasting soil types. *Cirsium* plants were grown for 42 days in sandy loam, clay loam and clay soils compacted to 1.8 g cm^{-3} with a penetration resistance of 3.6, 3.8, 4.5 MPa respectively. X-ray Computed Tomography was used to observe root architecture *in situ* and visualise changes in rhizosphere porosity (at a resolution of 35 µm) at 14, 28 and 42 days after sowing. Porosity of the soil was analysed within four incremental zones up to 420 µm from the root surface. Soil texture was observed to significantly affect plant growth with notably less root and shoot development by plants grown in clay soils in comparison to the clay loam and sandy loam treatments. In all soil textures the porosity of the rhizosphere was greatest closest to the root and decreased with distance from the root surface. There were significant differences in the rhizosphere porosity between the three soil textures, with *Cirsium* plants grown in sandy loam exhibiting the greatest structural genesis across all rhizosphere zones. We

demonstrate the soil texture has a significant impact on plant root system architecture development and subsequent localised pore space creation in the rhizosphere.

Key words
Soil compaction, X-Ray Computer Tomography, Sandy loam, Clay, Clay loam

5.7.2 Introduction

Soil compaction is a form of physical degradation whereby the structure is partly destroyed through compressive forces, and as a result there is an associated increase in soil strength (Van den Akker and Soane, 2005). It occurs via the rearrangement of soil particles into closer contact, resulting in decreased pore space and increased bulk density, typically from the impact of heavy farm traffic machinery and animal trampling in agricultural settings (Hamza and Anderson, 2005; Mohseni Saravi et al. 2005). Such compaction can extend to the subsoil, and it has been acknowledged by the European Union as a serious form of soil degradation due to its persistence once established (Jones et al. 2003).

Soil compaction has been shown to negatively influence soil pore networks via the reduction of macropores (Kim et al. 2010) resulting in pore systems that are less well connected. Poorly-connected systems hinder the movement of water and air through the soil (Hamamoto et al. 2008) which subsequently

has a detrimental effect on plant root growth. To grow effectively, plant roots require a continuous network of appropriately sized pores to facilitate their growth through the soil matrix (Gregory, 2006). The architecture of root systems produced by plants is remarkably plastic, and shaped by the local soil environment such as the soil microbiome, localised nutrient and water availability (Kano-Nakata et al. 2012) as well as the physical properties of the soil (Tracy et al. 2011). The activity of roots impacts both the physiochemical and biological status of the surrounding soil, with root development and pore space being closely linked (Mooney et al. 2012). For example roots release exudates which bind soil particles, resulting in higher levels of aggregate stability and pore space modification (Bronick and Lal, 2005). In compacted soils the connectivity of the pore network is severely reduced meaning that the root must deform the soil by exerting sufficient penetrative force (Bengough and Mullins, 1990; Gregory et al. 2006) to displace or break soil aggregates. White (2006) suggests that soils with a higher proportion of clay particles are likely to have stronger aggregates which are larger and more difficult to break, in compassion to aggregates in sandy soil which can be more easily broken.

Plants have the ability to alter soil pore networks and subsequently soil aggregate size distribution, depending on the soil texture (Bacq-Labreil et al. 2019). As soil texture underpins the composition of the pore network it directly influences root growth. Root growth strategies are influenced by their immediate surroundings and therefore an interdependent relationship exists between plant roots and soil structure. The effect of soil texture on plant root

development and subsequently soil structural dynamics is not well understood (Rogers et al. 2016). Previous work identified *Cirsium vulgare* as a plant species that was able to generate larger quantities of root (cm^3) which resulted in the subsequent increase in rhizosphere porosity in heavily compacted sandy soils, in comparison to *Plantago lanceolata* and *Taraxacum officinale* (Burr-Hersey et al. 2019; Submitted Manuscript, Section 4.5).

We investigated this potential of plants to induce changes in soil porosity in three different soil textures, specifically sandy loam, clay loam and clay soils with controlled water contents. We employed X-ray computed tomography to non-destructively assess the root growth patterns of *Cirsium* plants grown in contrasting soil textures, and determined the effect root growth had on early stage soil structural genesis around the taproot at a rhizosphere scale. Direct measurements of soil structural changes such as pore space creation and soil aggregation via plant root development can be obtained at a microscale using X-ray CT (Mooney, 2002; Helliwell et al. 2013). Understanding these structural formation and deformation processes at these small scales is crucial to advance the understanding behind soil stabilisation processes and the subsequent development of pore networks (Peth et al. 2010). We hypothesised that the different soil textures would result in varied amounts of root biomass being produced and that the subsequent soil pore formation in the rhizosphere will reflect this over time.

5.7.3 Materials and methods

5.7.3a Soil core preparation and planting

A Dunnington Heath series sandy loam (66.4% sand 18% silt, 15.6% clay), clay loam (37.8% sand 30.5% silt 31.6% clay) and clay (43.3% clay 28.4% silt 28.2% sand) soil were obtained from the University of Nottingham experimental farm at Sutton Bonington, Leicestershire, UK (52.836394, -1.243231). The soil was air dried and sieved to <2 mm. Columns (100 mm height x 51 mm diameter) were uniformly packed with soil to provide bulk densities of approximately 1.8 g cm^{-3}. Columns were packed in 2 cm incremental layers, after compacting, each layer the surface was lightly scarified to ensure homogenous packing and hydraulic continuity within the columns (Lewis and Sjostrom, 2010). Each soil texture was pre-mixed with a prescribed amount of water to ensure the relative suction of -5 kPa and thus the amount of water available to the plants within the cores was equal. The respective moisture contents were; sandy loam 13%, clay loam 16.5% and clay 18.3% and these were maintained over the course of the experiment. The penetrometer resistance readings for the different soil textures at the prescribed moisture contents were; sandy loam 3.6 ± MPa, clay loam 3.8 ± MPa and clay 4.5 ± MPa. Three replicates were prepared for each of the nine treatment types resulting in 27 columns. Once packed, columns were weighed and stored in airtight polythene wrap for 2 days before X-ray CT scanning.

Seeds of spear thistle (*Cirsium vulgare* (Savi) Ten.) were collected from Highfields Park Boating Lake, University Boulevard, Nottingham, (52.934655, -

1.199113), May, 2016. These were pre-germinated and planted to one seedling per column. As planting introduces disturbance to the soil profile the tops 1.5 cm of the core was excluded from analysis. Eighteen columns were planted with the plant species with nine columns remaining unplanted controls. Due to investigating previously un-scanned plant species nine out of the eighteen replicates remain un-scanned controls, to determine if X-ray exposure had an effect on root and shoot growth. Once planted, all 27 columns were placed in a growth chamber in a random block design (three blocks featuring one replicate each of the nine treatments) with a day/ night temperature of 20˚C /15˚C. The day temperature ran from 05.00-21.00, light duration was 16 hours, night duration was 8 hours, dawn/dusk duration was 3 hours. The daylight period was from 08.00-18.00 and the night period was from 21.00-05.00. The growth chamber was kept at 70 % humidity. Plants were grown for 42 days and the subset of 18 columns initially scanned on day 0 (Figure 5.13) were rescanned on days 14 and 28 and 42 providing four times points for analysis. All columns were individually weighed and watered to a constant weight each day.

5.7.3b X-ray CT scanning

A subset of 18 columns were scanned on Day 0, 14, 28 and 42 using a Phoenix V|Tome |X m X-ray 240kV (GE Measurement & Control Solutions, Wunstorf, Germany) at the Hounsfield Facility at the University of Nottingham, with a 0.1 mm copper filter. Projection image averaging and skip were set to 3 and 1

respectively. Voxel resolution was set at 33 µm, potential energy of 160 kV and current of 180 UA. Columns were scanned in two sections with a total scan time of 1 h 15 m. The distance from the sample to the source was 135.085 mm. 3000 image projections were captured for each column. Images were reconstructed at 32 .bit using Phoenix Datosx 2 reconstruction tool to form a 3D volume which was visualised as 18 .bit data using VG Studio Max 2.2.5 software. Example greyscale imagery of the three soil textures can be seen in Fig 5.13.

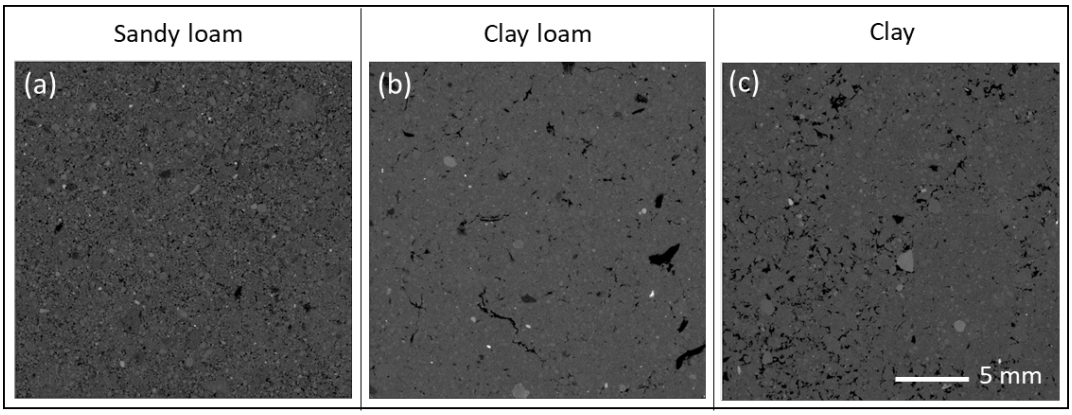


Figure 5.13: Example greyscale image slice of each soil texture at Day 0. (a) sandy loam, (b) clay loam, (c) clay, compacted to a bulk density of 1.8 g cm^{-3}. Images generated using VG Studio Max.

5.7.4 Destructive harvest

5.7.4a Root & shoot material

Plant shoots were photographed at Days 14, 28 and 42 using a Canon DSLR camera. The images were used to quantify the shoot areas (cm^2) in ImageJ. Original images were thresholded classifying leaf material as black and background as white. These binary images were then processed using the

'analyse particles' function to provide a value of shoot area. After 42 days the shoots were removed from the columns and weighed. They were then placed in an oven at 50°C for 48 h and reweighed to give the dry shoot weight. Roots were washed from the soil over a 500 µm sieve and weighed to provide fresh root weight, then stored in 50 % distilled water 50 % ethanol prior to WinRHIZO scanning. For WinRHIZO scanning roots were carefully spread out in water on A3 plastic trays to avoid roots overlaying. Once WinRHIZO scanned roots were placed in an oven at 50°C for 48 h and weighed to calculate dry root weight.

5.7.4b Aggregate size distribution

At Day 0 a subset of 9 unplanted control columns (3 replicates for each soil texture) were destructively harvested and the soil was collected and air-dried. Aggregate size distribution was determined by passing 200 g of air dry soil through a series of sieves of 4000, 2000, 1000, 710, 500, 425, 300, 212 and 53 µm via horizontal shaking for 2 minutes 30 seconds at 300 rotations per minute. The mass of aggregates retained on each sieve was determined and calculated as a percentage of the total mass. After 42 days the both the remaining 9 control and 9 planted columns were destructively harvested using the outlined method.

5.7.5 3D Image processing segmentation and analysis

5.7.5a Equalisation of greyscale images

The minimum and maximum greyscale values for each individual scanned section of all soil cores were collected from the original .pcr files from Volume Graphics (VG) and imported into Microsoft Excel. The spreadsheet was configured to search for the smallest minimum value and the largest maximum value (this provides the two extremes for the data set). The difference between the two values was then calculated and divided to produce a 16 bit greyscale range instead of the original 32 bit. The two centre points of the data set were then identified (the highest minimum value and the lowest maximum value) and were also divided by the 16 bit greyscale range. This process equalised the greyscale values providing a new minimum and maximum range across the replicates as well as modifying the values from 32 bit to 16 bit. For the purpose of this investigation greyscale values were equalised across the three replicates of each soil texture at each sample time point, resulting in 12 sets of newly-equalised grey values (pers. comm. Craig Sturrock). This equalisation provided consistency with subsequent root and pore segmentations within the specific treatment and time replicates.

5.7.5b Root system analysis

An automated macro code 'Root1' was used to segment root material from the greyscale imagery in ImageJ (Supplementary Figure 1). The macro written by Flavel et al. (2017) works by separating non-root features and isolating

root structure based on connectivity of the system. The macro works by employing an edge detection filter at the air:soil-phase boundary. A mask was produced that excludes the partial volume effect at the root edge via a semi-automated local adaptive threshold range defined by the user. This allowed the detection of both fine and coarse roots and a 3D median filter was then applied to the data set to remove any noise consisting of fine pores included in the network. From this process a binary image stack was created. The stack was then imported into VG Studio Max where it was manipulated as a region of interest and cleaned to remove any remaining unconnected pore space. Quantification of total root area (cm^2), volume (cm^3), lateral root area (cm^2), lateral root volume (cm^3), taproot area (cm^2), taproot volume (cm^3), taproot length (cm), taproot convex hull (cm^3), taproot growth angle (°) and number of lateral roots were subsequently made using VG Studio Max and PAM.

5.7.5c Taproot rhizosphere porosity analysis

A method adapted from Helliwell et al. (2017) and previously reported by Burr-Hersey et al. (2019)(Submitted Manuscript, Section 4.5) was used to assess local changes in porosity with distance from the taproot surface. The surface determination tool based on greyscale levels was applied to each column to identify both air space and soil material. Calibrations of the tool were used by defining material from example areas. Once the pore space had been identified four new regions of interest (ROI) were created that encompassed incremental zones with distance from the originally segmented

root system in 3D (Figure 5.14 a-e). The segmented taproot (ROI) was dilated by +2, +4, +8, +12 pixels (equivalent to 70,140, 280 and 420 µm distance from the root). This resulted in four incremental section volumes 0-70, 70-140, 140-280 and 280-420 µm distal from the root surface which we term 'mantles', for which the total pore volume (mm^3) was identified. The porosity (%) of each mantle was expressed as pore volume as a % of the total incremental mantle volume. These pore volumes were then false-coloured for visualisation of the pore locations within each mantle layer (Figure 5.14 a-e). This process was undertaken on each of the nine scanned plants at the three time points, resulting in 108 individual taproot rhizosphere porosity mantles for analysis. All volume manipulation and analysis was performed in VG Studio Max 2.2.5.

5.7.5d Statistical analysis

A one-way factorial analysis of variance (ANOVA) was conducted on the 2D WinRHIZO data and dry/fresh shoot weight data. A two-way ANOVA with specified block design was conducted on the X-ray CT scanned plants to assess whether time or soil texture had the greatest effect on root characteristics. To assess the soil aggregate distribution a 1-way ANOVA was performed with a treatment structure of size class with a specified nested block structure. To assess the porosity of the rhizosphere mantles a 2-way ANOVA was performed with a treatment structure of soil texture x time with

a specified nested block structure. Statistical analysis was preformed using Genstat.

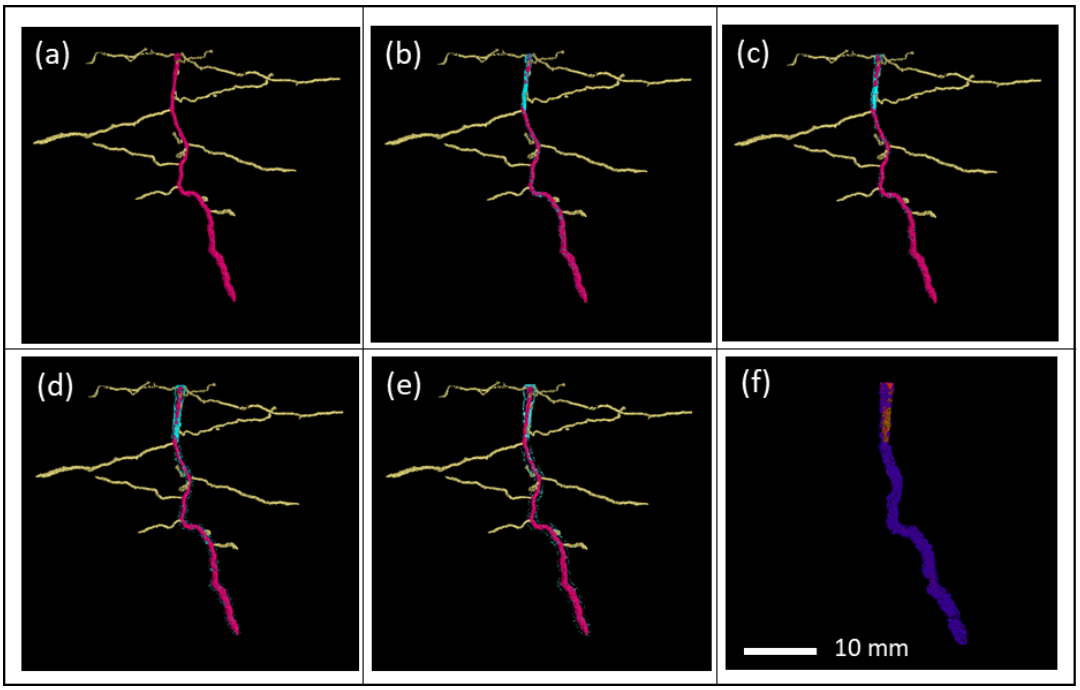


Figure 5.14: Example Root1 segmentation of *Cirsium vulgare* roots grown in sandy loam soil for 14 days and root/rhizosphere porosity classification. (a) Cleaned Root1 segmentation split into taproot ROI (pink) and lateral roots ROI (beige), (b) Root system and pore space (blue) within rhizosphere zone 0-70 um, (c) Root system and pore space (blue) within rhizosphere zone 70-140 um, (d) Root system and pore space (blue) within rhizosphere zone 140-280 um, (e) Root system and pore space (blue) within rhizosphere zone 280-420 um, (f) Pore thickness map for rhizosphere 0-420 um from root surface. Images generated using VG Studio Max 2.2.5.

5.7.6 Results

5.7.6a Biomass and 2D root measurements

Soil texture significantly affected the total root length (p=0.018; Figure 5.15d) and average root diameter (p=0.010; Figure 5.15e) of the plant roots, visually confirmed via WinRHIZO imagery (Figure 5.15a-c). No X-ray effect was observed on plant root 2D characteristics. Soil texture significantly affected both the amount of fresh shoot (p=0.014; Figure 5.16j) and dry shoot

produced (p=0.025; Figure 5.16k), confirmed by visual observation (Figure 5.16a-i). Soil texture significantly affected shoot surface area (p=0.026; Figure 5.16l) as did time (p<.001).

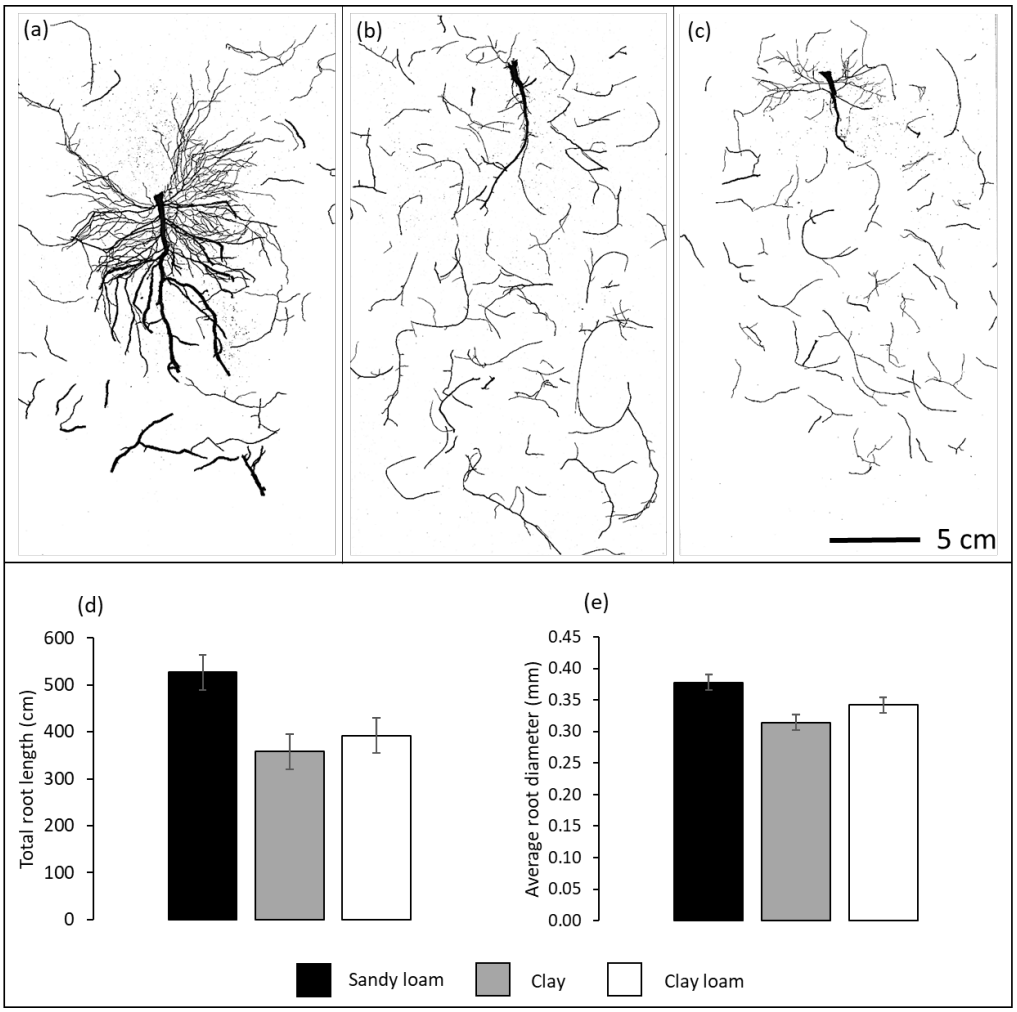


Figure 5.15: Example 2D WinRHIZO scans of *Cirsium vulgare* root systems grown for 42 days. (a) Sandy loam, (b) Clay, (c) Clay loam, (d) Total root length (cm), (e) Average root diameter (mm) of plants grown to 42 days. Bars denote means, whiskers pooled s.e.

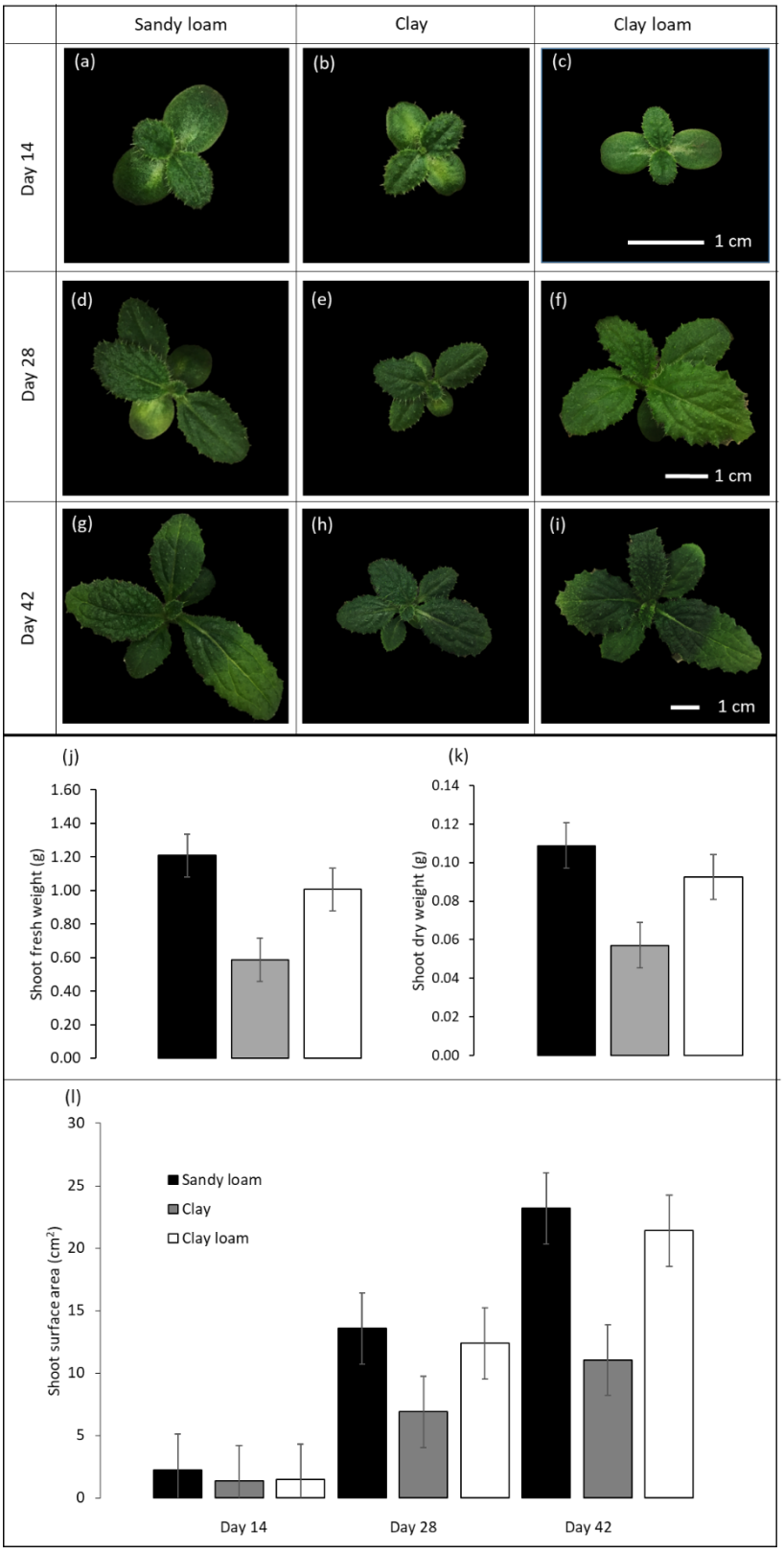


Figure 5.16: (a-i) Photographs of plant shoot material. (a-c) Plants grown for 14 days in sandy loam, clay and clay loam soil. (d-f) Plants grown for 28 days in sany loam, clay and clay loam soil. (g-i) Plants grown for 42 days in sandy loam, clay and clay loam soil. (j) Shoot fresh weight (g), (k) Shoot dry weight (g), (l) Shoot surface area (cm^2) measured using ImageJ for *Cirsium* plants grown for 14, 24 and 42 days. Bars denote means, whiskers pooled s.e.

5.7.6b Soil physical characteristics

At Day 0, the aggregate size distribution of the sandy loam, clay loam and clay soil all showed the greatest proportion of aggregates were in the size class >4000 µm (Figure 5.17a, c, e). For the clay and clay loam soil this proportion accounted for over 92% and 90% of the total soil mass respectively, in the sand loam the proportion was closer to 40%. The sandy loam had the most dispersed range of aggregate size classification with a further 40% of the aggregates falling into classes between 106-500 µm. At Day 42 the sandy loam soil saw no significant difference in aggregate size distribution between control or plant cores (Figure 5.17f). In comparison to Day 0 there had been a decrease in the proportion of aggregates in the smallest size class <45 µm resulting in an increase in aggregates in the size classes 2000 and 4000 µm. The clay and clay loam soils followed an almost identical trend in aggregate distribution with less than 15% of each sample accounting for the classification range of <45- 4000 µm. By Day 42 for the clay loam treatment the percentage of aggregates in the greatest size class had dropped to 86% for the control cores and 82% for the planted cores (Figure 5.17b&d). This is reflected by a notable increase in aggregates size 2000-4000 µm in comparison to Day 0. This trend was identical in the clay loam treatment. In both instances the redistribution of aggregates to smaller size classes was greater in the presence of plant roots but was not statistically significant in this case.

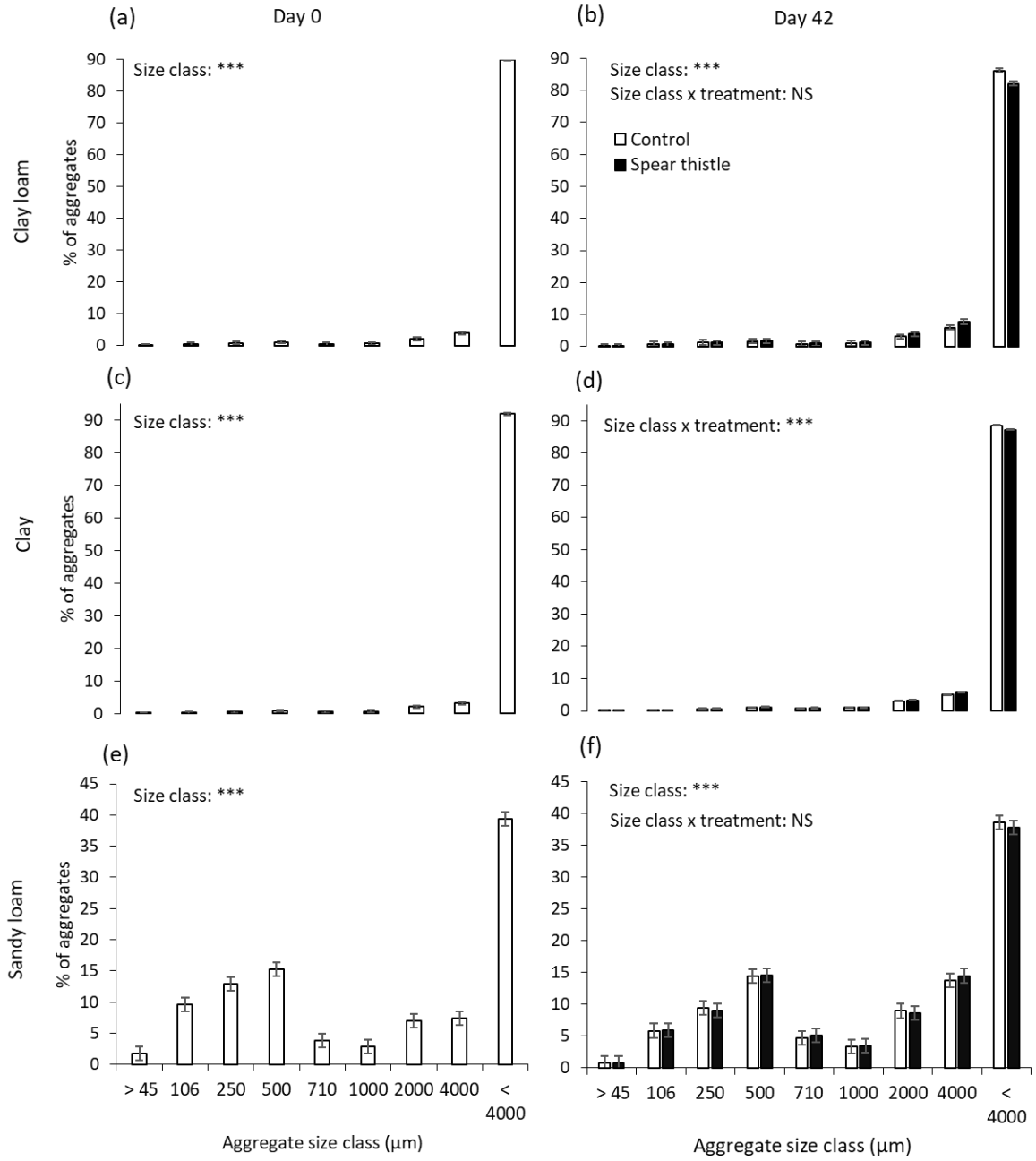


Figure 5.17: Aggregate size distribution showing that starting condition at Day 0 (a,c,e) and the effects of plants at Day 56 (b,d,f) for a Clay loam soil (a-b), Clay soil (c-d) and Sandy loam soil (e,f). Bar chart, means expressed as the percentage of aggregates relative to the total volume, whiskers: pooled standard errors

5.7.6c Root 3D architectural analysis

3D visualisations of *Cirsium* root systems were analysed based on renderings of X-ray CT data at Days 14, 28 and 42 (Figure 5.18). There was a consistent similarity in the root morphology despite the different soil textures. All plants generated vertical primary taproots with subsequent lateral root formation to varying degrees over time. At Day 14 *Cirsium* grown in sandy loam soil (Figure 5.18g) had generated more lateral roots than those plants grown in clay (Figure 5.18a) or clay loam (Figure 5.18d). This trend continued at Day 28 with substantially greater root mass being produced in the sandy loam, which was generally located in the upper section of the soil core as a fine root mesh, with the presence of some thicker roots developing at depth (Figure 5.18h). By Day 28 the taproots of plants grown in the clay and clay loam treatments had extended to the base of the core. The lateral root development in the clay was still notably sparse, with few very thin lateral roots having emerged (Figure 5.18b). At Day 42 the root systems of plants grown in the clay loam and sandy loam soils were well established (Figure 5.18f&i), for the clay loam there was good root proliferation through all areas of the column depicting an even root distribution. For the sandy loam a larger proportion of this mass was localised in the top section where increased amount of thinner roots had developed contrasting the multiple thicker roots that now occupied the lower sections of the core. The root systems in the clay treatment at Day 42 were notably under-established in comparison to the other two treatments (Figure 5.18c).

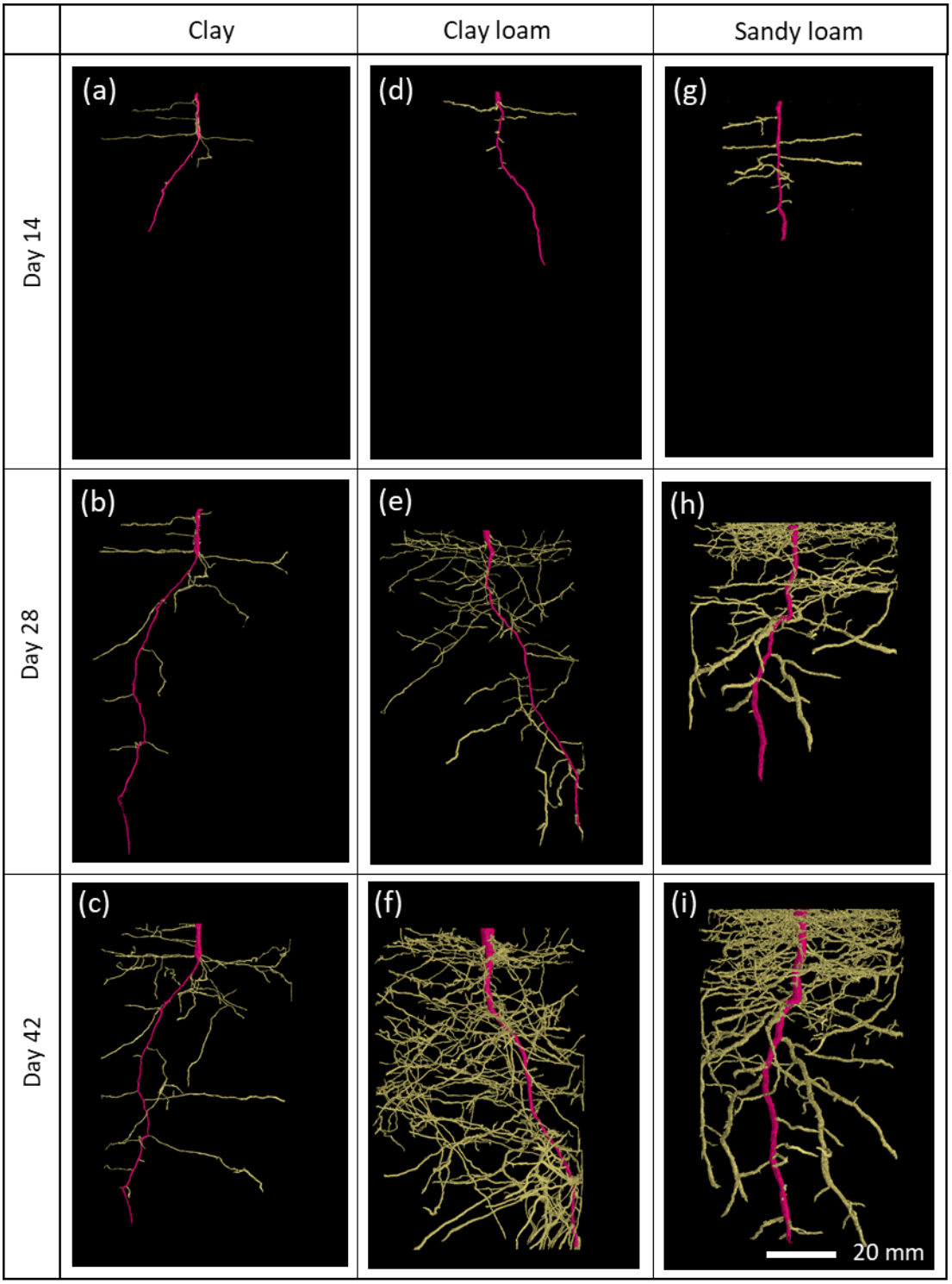


Figure 5.18: Example 3D visualisations of *Cirsium vulgare* root systems. Pink indicates taproot, yellow indicates lateral roots. Plant grown in clay soil (a) 14 days, (b) 28 days, (c) 42 days. Plants grown in clay loam soil (d) 14 days, (e) 28 days, (f) 42 days. Plants grown in sandy loam soil (g) 14 days, (h) 28 days, (i) 42 days. All images generated using VG Studio Max V 2.2.5.

5.7.6d Root 3D analysis

Soil texture significantly affected the total root system volume (p=0.021) with greater root volumes being observed consistently in the sandy loam and clay loam treatments (Figure 5.19a). Soil texture had a significant effect on the total root surface area (cm^2) (p=0.003), with notably greater surface areas in the sandy loam and clay loam treatments in comparison to the clay (Figure 5.19b). Soil texture significantly affected the volume of the plant taproots (p=0.047) with the greatest volumes being observed in the sandy loam treatment (Figure 5.19c). Soil texture had a significant effect on the taproot surface area cm^2 (p=0.002), by Day 42 the taproot surface area of *Cirsium* grown in the sandy loam was almost twice as large as those grown in clay loam or clay (Figure 5.19 d). Soil texture significantly affected lateral root volume (p=0.019) with plant grown in sandy loam and clay loam having lateral root volumes of 49 cm^3 and 44 cm^3 respectively at Day 42 in comparison to roots grown in clay which had volumes of 19 cm^3 on average (Figure 5.19e). Figure A.5.10 indicates the distribution of plant roots into either lateral root or taproot as a percentage of the total root system over time. It indicates that at Day 14 the lateral vs taproot growth was at around 50% for each soil texture, over time this distribution decreased rapidly of the plants grown in the clay loam and sandy loam treatment and more gradually for the clay treatment. Soil texture was observed to affect for lateral root surface area (p=0.004) (Figure 5.19f) with significantly great surface areas being observed in the sandy loam and clay loam treatments in compassion to the clay soil. A soil texture x time interaction was observed for the taproot length (cm)

(p=0.065) (Figure 5.20a) with the plants grown in sandy loam having notably shorter taproots at all growth stages in comparisons to those grown in clay and clay loam soil. There was a significant time effect on the development of taproot convex hull exploration area (p<0.001; Figure 5.20b).

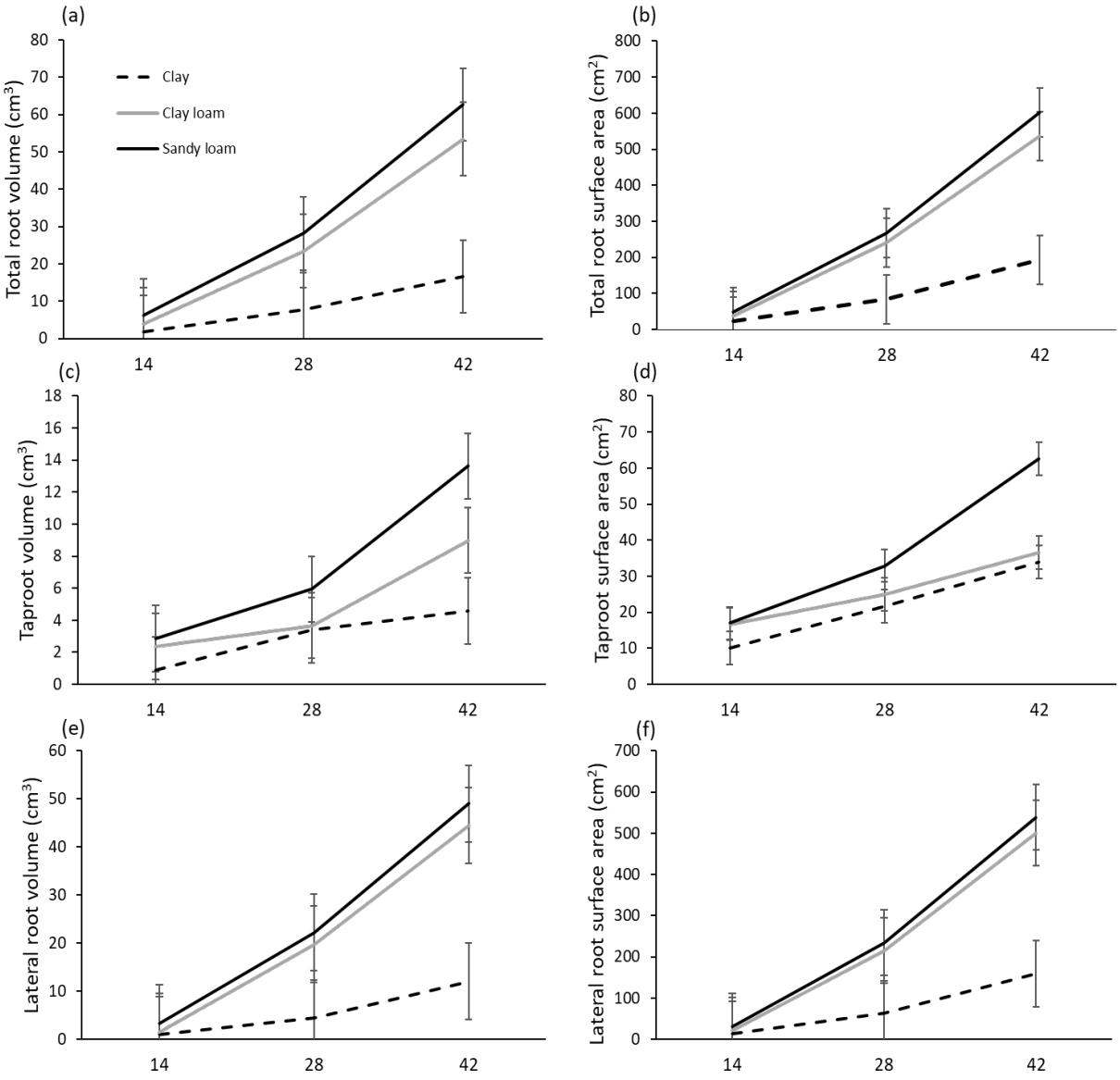


Figure 5.19: 3D root system characteristic of *Cirsium vulgare* plants grown for 14, 28 and 42 days. (a) Total root system volume (cm^3), (b) Total root system area (cm^2), (c) Taproot volume (cm^3), (d) Taproot surface area (cm^2), (e) Lateral root volume (cm^3), (f) Lateral root surface area (cm^2). Lines denote means, whiskers pooled s.e.

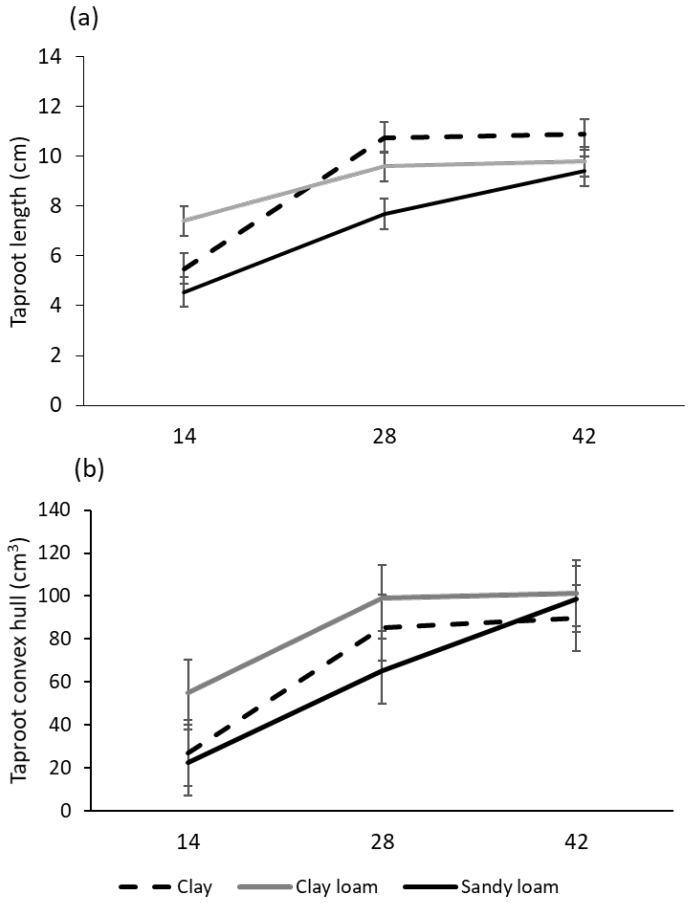


Figure 5.20: (a) Average taproot length (cm) and (b) Average taproot convex hull (cm^3) of Cirsium plants grown in clay, clay loam and sandy loam soils for 14, 28 and 42 days. Lines denote means, whiskers pooled s.e.

5.7.6e Rhizosphere porosity analysis

Visualisation of the porosity associated with the taproot rhizosphere showed that there was generally greater rhizosphere porosity around the top of the root closer to the soil surface, i.e. the older section of the roots, at days 14, 28 and 42 (Figure 5.14). The results from the 3 –way ANOVA indicate that soil texture has a significant effect on taproot rhizosphere porosity ($p<.001$; Fig 5.21), with the greatest porosity being generated in the sandy loam soil. Time also had a significant effect on the porosity ($p=0.01$) with the greatest values

being manifest at Day 14, these then decreased by Day 28, and then subsequently increased again by Day 42, a trend apparent for all three soil textures. In the case of all soil textures the porosity within the incremental rhizosphere mantles was greatest with immediate proximity to the roots and decreased with distance from the root surface ($p<.001$; Figure 5.21). There was a soil texture x time interaction for maximum pore width recorded within the taproot rhizosphere when considering the whole 0-420 µm distance from the root surface significant to a factor of 10% ($p=0.067$). For the clay the maximum recorded pore width increased over time, the opposite was observed for the clay loam with maximum pore thickness decreasing on average over days 12, 28 and 42.

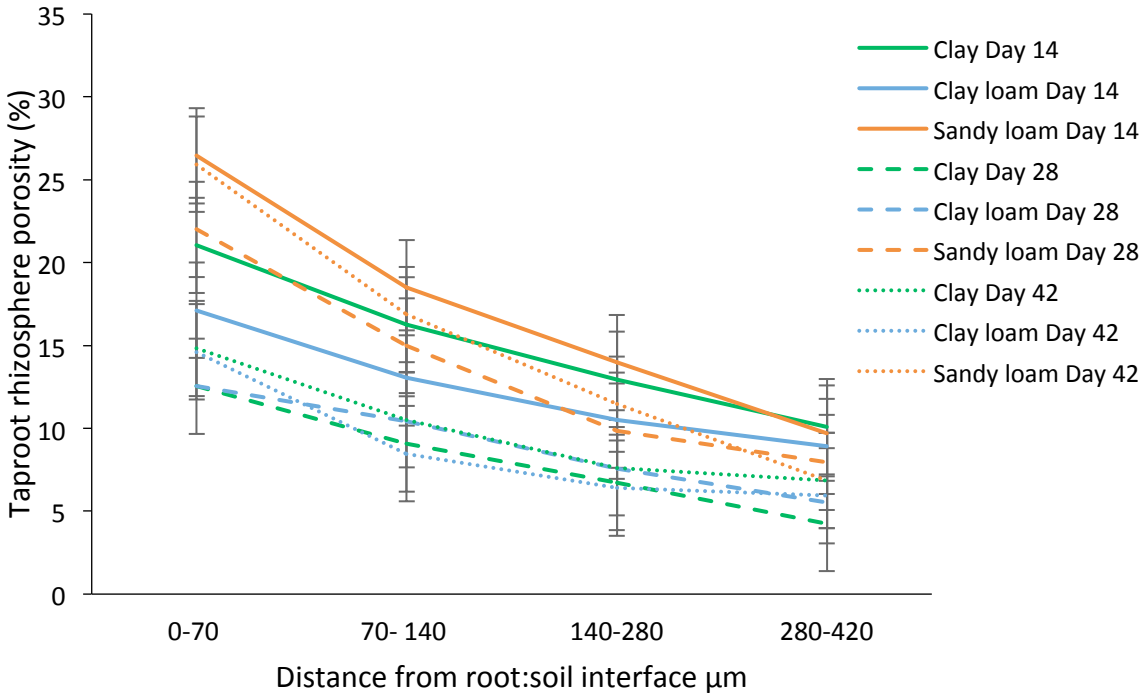


Figure 5.21: Porosity of incremental taproot rhizosphere zones of *Cirsium vulgare* plants over time (Days 14, 28 and 42) with distance from root surface grown in clay, clay loam and sandy loam soils at 1.8g cm^{-3}. Values represent mean, whiskers pooled S.E.

5.7.7 Discussion

We used non-destructive X-ray computed tomography to study the response of *Cirsium* root system architecture to changes in the physical properties of different soil substrates. Our results indicate that the texture of the soil and its strength have a direct impact on *Cirsium* root system architecture. The soil with the highest penetration resistance (clay 4.5 MPa) having the greatest level of restriction on the root growth, with substantially less total root mass as well as notably thinner roots being produced by the plants. In direct comparison, the plants grown in sandy loam soil (penetration resistance of 3.5 MPa) produced the greatest root mass and root diameters. Soil texture has previously been shown by Helliwell et al. (2017) to affect developing root architectures of tomato (*Solanum lycopersicum*) in sandy loam and clay loam soils at a bulk density of 1.2 g cm^{-3}, with thicker roots being seen in the sandy treatment in comparison to the clay. Our findings complement this and highlight that this response is just as prominent in highly compacted soils. A study by Rogers et al. (2016) into the development of rice roots found that coarse beads were easier to penetrate than fine beads and that sand was the most difficult medium to penetrate. Our results show that *Cirsium* roots certainly shows this greatest morphological response to the sand treatment with thicker and shorter root development in comparison to the other soil textures. This indicates that the heterogeneity of stress at a granular level may be an important factor defining root system architecture response to soil texture, particularly taproot elongation rate.

The management of soil structure is essential for the growth and stability of plants, equally a change in soil structure involves particle rearrangement via the presence of plant roots developing in a soil profile. We have observed changes in soil structure occurring at a rhizosphere scale, localised to within 420 µm distance from the root soil interface. The greatest changes in soil porosity in all three soil textures was observed in the 0-70 µm distance from the root surface. We posit that as roots secrete mucilage it is likely that this is stabilising aggregates by increasing cohesion (Czarnes et al. 2000) and inducing localised wet-dry cycles at the root soil interface resulting in microscale pore space formation. *Cirsium* roots grown in sandy loam had higher levels of taproot rhizosphere porosity compared to the other soil textures, this may be due to thicker roots contributing to increased levels of soil deformation at the root: soil interface as previously demonstrated by Helliwell et al. (2019). Alternatively it may be a result of the sandy loam soil having weaker characteristics due to decreased levels of clay particles resulting in higher deformation rates. We attribute the interim decrease in taproot rhizosphere porosity to the subsequent radial expansion of the plant roots into the pore space that they have created, with this process reoccurring over time. The changes to maximum pore thickness within the rhizosphere zone were related to the zones of influence, which in this case extended to 420 µm distance from the root surface. Here we saw fluctuation of pore size across the course of the experiment suggesting that aggregate displacement was taking place at a microscale. We note the effect that the chosen root segmentation technique can have on the subsequent analysis

due to the thickness of root produced. To counteract the effect this may have when calculating rhizosphere porosity a further dilation of one voxel from the root surface was undertaken, in order to account for any potential mis-segmentation of the root section associated with partial volume effects.

Soil strength is governed by the microstructural nature of the soil skeleton and influences the response of the soil to deformation by growing roots (Hettiaratchi, 1990). As shown in Figure 5.13 the variation in the pore network between the three soil textures at 1.8 g cm^{-3} was quite contrasting. Sandy loam has virtually no macropores and its pore network is extremely fractured consisting mainly of mesopores. The clay loam soil did contain some macropores but these were extremely disjointed and the soil also featured a sparse distribution of mesopores. In comparison the clay appeared to have a reasonably well distributed network of pores. Our study investigates soil compacted to an extremely high bulk density. To achieve this the medium was subject to a high level of physical deformation via compaction forces which may have resulted in forced aggregation of particles and subsequent low levels of soil porosity and lack of macropores (particularly in the sandy loam treatment) within the columns. The presence of plants did not significantly impact the aggregate size distribution in the sandy loam soil over a 42 day period. This indicates that the composition of the soil texture had more of an effect on the stability of the aggregates than the presence of root material in these cores. As the samples were maintained at a constant water potential this may be due to a lack of any substantial wet:dry cycles imparted, which is known to stabilise aggregates (Bronick and Lal 2005), similar

observations were made in a study Bacq-Laburiel et al. (2019) when observing the impact of *Phacelia tanacetifolia* in modifying soil structure in un-compacted soils. For the clay and clay loam soils the presence of plants reduced the number of larger aggregates <4000 µm and a subsequent increase in the mass of aggregates in the 2000-4000 µm size classes, however this trend was not statistically significant over the 42 day period. As roots grow through soil they have three options when encountering aggregates: they may penetrate the aggregate, displace the aggregate from its path, or the root may bend to avoid the obstruction (Whiteley et al. 1984). The reduction in larger-sized aggregates suggests that as the roots grew through the soil they were penetrating or displacing aggregates thus changing the structure of the soil. These data do suggest that if the plants were able to grow for a longer time period then their presence may have an effect on the aggregation of the soil cores, as smaller aggregates means an increase in cracks and voids and therefore an increase in the potential for air and water to move through the soil system. This structural modification and change in rhizosphere environment may lead to increased levels of microbial activity leading to subsequent structural genesis.

5.7.8 Conclusion

Soils with contrasting textures are deformed by roots in different ways, depending on initial soil bulk density and plant species. This results in a feedback cycle between soil and roots, with texture governing plant root

system architecture and the root system architecture effecting the soil structural genesis. We observed that *Cirsium* roots were better able to penetrate clay loam and sandy loam, generating greater root mass soil in comparison to clay, where the resistance of the clay was substantially greater than the sandy loam and clay loam soils. Taproot rhizosphere porosity changed coherently over time with root growth. Our study was confined to the first 42 days of plant growth, hence further investigation into the changes in the rhizosphere zone over extended time periods are warranted. The use of confocal imagery techniques to assess internal root cell structures may highlight physical changes to the plant roots which may further our understanding into the plant roots response and ability to overcome soil compaction in certain soil textures.

5.7.9 Acknowledgments

This research is supported by the award of a studentship grant to JB-H by the NERC and BBSRC funded STARS (Soils Training And Research Studentships) Centre for Doctoral Training and Research Programme; a consortium consisting of Bangor University, British Geological Survey, Centre for Ecology and Hydrology, Cranfield University, James Hutton Institute, Lancaster University, Rothamsted Research and the University of Nottingham. Grant Ref: NE/ M009106/1. The James Hutton Institute receives funding from the Scottish Government.

Chapter 6: General discussion

6.1 Introduction

The overall aim of this research was to investigate the interdependent relationships between root system architecture and soil structural development in compacted soils, with specific interest in understanding the capability of plant roots to generate pore space at micro-scales. Root system architecture was quantified over time and linked to changes in soil structure.

This investigation was performed through controlled experimental pot studies using a variety of plant species and soil textures compacted to a range of bulk densities. A range of image processing techniques were implemented and trialled over the course of the project as new software programmes became available.

6.2 Application of novel image analysis techniques

The accuracy of root and pore segmentation procedures are ultimately determined by the quality of the original scan data, as this determines the fundamental contrast between the different densities of materials within the soil core. In this study a number of root and pore segmentation techniques were implemented employing different software programmes. Image analysis procedures described in Chapters 3 & 4 tested the use of the RooTrak

(Mairhofer et al. 2012), an automated tracking algorithm and it was found to be effective at increasing the repeatability of the root systems generated as it identifies root material based on a nearest-neighbour greyscale pixel allocation approach. The software had a high level of accuracy when identifying the primary taproot and origin of lateral roots. However, the software struggled to pick out entire lateral roots due to fluctuations in root growth angle (particularly upward growth). This resulted in a hybrid approach being developed which combined the use of the automated RooTrak approach to initially identify roots, followed by the manual segmentation of the remaining sections of the lateral roots. This combined approach enabled a full accurate root system segmentation to be produced for each plant in the experiments.

As the application of using X-ray CT analysis to investigate root and soil systems increases, associated methods for analysis have also developed (Gregory et al. 2009; Morris et al. 2017). The use of Root1 (Flavel et al. 2017) for plant root segmentation, as described in Chapter 5, is an example of one of these advances. Working using a thresholding approach on the original greyscale imagery in ImageJ, the root systems' segmentation is generated as a binary stack for import into VG Studio Max. This approach was observed to be extremely accurate, in some cases it was able to identify a greater amount of plant root from the greyscale imagery than a manual segmentation by eye. Due to the complex nature of the mature plant systems this technique meant that large quantities of root material could be accurately segmented with only minor need for cleaning. This method significantly reduced the amount of

time taken to generate the same data using localised region growing manual segmentation techniques in VG Studio Max. Furthermore the software was notably effective at identifying root material within different soil textures, with the texture of the soil not affecting the accuracy or quality of the outputs. The implementation of semi-automated, open access image segmentation software reduces the rate of human error when determining areas of root from grey scale imagery.

6.3 Response of root system architecture to soil bulk density

A variety of root responses to different soil bulk densities were observed in different experimental configurations, such as single-phase and split-phase compaction treatments. In the single-phase compaction treatments at bulk densities of 1.2 g cm^{-3} or 1.4 g cm^{-3} (Chapter 3), the difference in bulk density was not observed to affect the total root length or average root diameter of tillage radish, vetch or black oat plants in 2D. This indicates that the relatively low-level compaction treatments did not restrict the ability of these plant root systems to develop when grown in soils of a uniform bulk density. This observation was further confirmed in the investigative X-ray CT scans performed on each of the three species at compaction levels of 1.2 g cm^{-3}. Here the plant species exhibited 'model' root growth, with well distributed primary, secondary and lateral roots throughout the soil cores. The visualisation of the root system architecture in 3D suggested the plants were not restricted by the low level compaction and were able to axially and

radially expand at a sufficient rate to facilitate root growth (Bengough, 2012; Jin et al. 2013). Conversely the split-phase compaction study into cover crops in 3D (Chapter 3) identified that different species with contrasting inherent root architectural traits respond differently to a change in soil bulk density within a system. In this instance, the fibrous root systems of black oat was not restricted by the change in soil compaction. Plant roots grew comparatively well in the 1.2 / 1.4 g cm^{-3} sections of the split phase treatment compared to the 1.2 g cm^{-3} single phase treatment. They produced well-distributed root system throughout the extent of the core, with no morphological response to the induced soil compaction layer. This absence of a recognisable morphological response suggests that the black oat roots were able to generate a great enough penetrative force to deform to soil at 1.4 g cm^{-3}. This may be attributed to the thickness of the plant roots. Although not directly measured using X-ray CT in this experiment the visual imagery in Figure 3.7 alludes to the plant having well-developed thick roots especially by Day 58. A number of studies suggest that dicots may be more able to penetrate compacted soil, as they generally have roots with greater diameters (Clark, 1999; Clark, 2003; Chen and Weil, 2011). However in these experiments, both of the tap-rooted plant species exhibited severe morphological responses to the change in bulk density that resulted in changes in the plant roots inherent root morphology. For the vetch, the change in bulk density resulted in restriction to plant root growth in the lower 1.4 g cm^{-3} section of the core, with the deflection of the primary root along the compacted layer towards the column wall being observed consistently between the replicates. Previous

work has shown that, in some instances, when the bulk density of the medium is greater than the penetrative ability of the plant root that they may deflect or buckle (Kolb et al. 2017). The apparent presence of this trait means that the plant species may not possess the phenotypic ability to penetrate harder soils and therefore this species would not be an appropriate candidate for the amelioration of soil compaction in the field, where zones of localised compaction are common.

Roots have evolved to be extremely adaptable and responsive to their local environment (Grossman and Rice, 2012). For the tillage radish plants this was particularly evident as there was a profound morphological response to the compacted soil layer, demonstrated by fanging of the primary taproot into multiple finer roots. This change in root architecture is likely to be due to the greater initial size of the primary taproot, in this instance it appears the size of the root tip was too great to be able to penetrate available soil pores in the 1.4 g cm^{-3} compacted layer. The result was the development of multiple finer roots which in turn were able to punch their way down through the soil to the bottom of the cores without restriction. The adaptive nature of the plant in these circumstances suggests that it readily adjusts to its local environment and is able to overcome physical restrictions posed by growth media to enable development. Increases in root proliferation in soil above compacted layers has previously been linked to increased levels of ethylene production by stressed roots (Kays et al. 1974). Root stress signals may explain why there were lower numbers of lateral roots recorded in the 1.4 g cm^{-3} bulk density section of the core. The roots that did develop had steeper growth angles for

both the vetch and tillage radish plants. This root response to soil compaction has previously been observed in maize crown roots, and is thought to be a beneficial trait for root foraging (Lynch, 2013). In compacted agricultural and natural systems this change in root angle may result in more effective nutrient and water acquisition by plants in restricted systems.

Compacted layers occur frequently in agricultural soils as plough pans, and are notably restrictive to plant root growth. The split-core system was designed to provide a controlled environment that mimicked this restriction (Chapter 3). The root systems of the cover crops used indicate that in the field both the black oat and tillage radish plant would likely be able to overcome the environmental restriction a plough pan compacted at 1.4 g cm^{-3}. This is an important characteristic as the morphology of a plant root system directly influences its ability to anchor itself within a soil profile (Downie et al. 2015). Although it may result in the morphological change to the tillage radish plant roots, it would be unlikely to detrimentally affect the subsequent growth of the plant.

This assessment indicates that both black oat and tillage radish plants may be beneficial at instigating soil structural change as cover crops. All three of the cover crop species investigated have been identified in a recent review by Storr et al. (2019) as being currently used in cover crop rotations by farmers in the UK. The insight provided in this thesis into their specific root morphology and growth characteristics in 3D can be used to inform how plants grown in the field may interact with compacted soil conditions. The same review

highlighted that 70% of UK-based farmers who responded to a survey used cover crops and reported numerous benefits after 2 years since their implementation into cropping regimes including improvements to soil structure, increased earthworm numbers and less soil erosion (Storr et al. 2019). This survey indicated that cover crops are having observed beneficial impacts to soil condition and that the time period for changes in physical characteristics of the soil may take multiple growing seasons to have impact at larger scales.

The wild plant species investigated in Chapter 4 were trialled in high compaction treatments of 1.6 g cm^{-3} and 1.8 g cm^{-3} bulk densities. The aim was to directly compare specific plant root traits within the two compaction treatments to assess the species ability to generate root mass. In these conditions plants that had greater average mean root diameters were generally able to generate greater root mass. In this instance the specific plant species and the length of time they were grown for were observed to generate the greatest differences in the measured root and shoot parameters not the bulk density of the soil. This suggests that the increase in restrictive nature of the system at high bulk densities from 1.6 g cm^{-3} to 1.8 g cm^{-3} did not significantly affect the ability of the plants to grow. This may indicate that plant root development was already severely hindered by the reduced macropore network at 1.6 g cm^{-3} soil bulk density, and the further relative reduction in pore space in the 1.8 g cm^{-3} treatment concomitantly reduced the number of smaller mesopores in the soil matrix. As these were not

accessible to the plant roots to facilitate growth in the 1.6 g cm^{-3} their further reduction did not affect the measured plant root characteristics.

Similarities in root system architectural development were observed for the three tap-rooted plant species, *Cirsium*, *Plantago* and *Taraxacum* (Chapter 4). The latter two species were more efficient at taproot extension, with the primary root almost reaching the bottom of the core at Day 14, in comparison to *Cirsium* which took 28 days to penetrate to this depth. This indicates that the penetrative force and rate of axial extension of *Plantago* and *Taraxacum* was greater than *Cirsium*, suggesting that those roots were able to displace soil particles to facilitate a pathway for root growth more efficiently than *Cirsium*. However, *Cirsium* developed a greater number of lateral roots and the tap and lateral roots were thicker than those of *Taraxacum* and *Plantago* resulting in greater root areas and volume at both time points. The process of radial root expansion was less repressed in the *Cirsium* than the other two species indicating that its radial growth pressure was sufficient to deform its local soil environment. Previously it has been shown that plants with roots of greater diameter are favourable for penetration as they have to overcome less friction pressure from the soil and less tension in the cell wall, compared to thinner roots (Kirby and Bengough, 2002). The difference in result observed in this experiment may be attributed to the development of a more substantial lateral root network for the *Cirsium* in comparison to *Taraxacum* and *Plantago*. Root foraging and resource capture is an equally important root system architecture trait, which in this instance appears to have been

beneficial in aiding greater plant root development overall in the *Cirsium* plants.

The root system architecture of *Cirsium* was observed in three contrasting soil textures, *viz.* sandy loam, clay loam and clay at 1.8 g cm^{-3} (Chapter 5). The plant root architectures that developed were inherently different but the response is more likely to be attributed to the soil texture not the high level of soil compaction and therefore this response is discussed in the following section.

6.4 Response of root system architecture to soil texture

Sandy loam soil was initially identified as an appropriate soil texture for use in these experiments, the texture provided a good level of contrast between plant root and soil material required for image segmentation at the resolutions studied in this thesis. As the soil was sieved to <2 mm before packing it provided a repacked soil core environment with no presence of macropores. Due to this absence of macropores, plant roots had to displace the soil in their path to extend within the soil core. This means that the roots were not able to use preferential pathways of least resistance that macropore networks would provide in field structured soils.

In the cores packed to a low bulk density of 1.2 g cm^{-3} in the X-ray CT scanning trial experiment in Chapter 3 the sandy loam soil was not observed to induce any unusual response in root system architecture development across the

three species (tillage radish, vetch and black oat) investigated. At these relatively low compaction levels there would have been greater volumes of pore space within the core system. This means that the soil particles being displaced by root growth would have had a greater volume of space to move freely into, resulting in a reduced level of restriction to the roots. As a result roots did not need to radially thicken to such a high degree as they did not require high levels of penetrative force to move through the soil. This idea is supported by the observation of generally thin roots with small diameters in the trial experiment. The lateral root development was also not hindered by the single phase low compaction treatment with even root distributions coming from the primary root in both the tillage radish and vetch plants. For the split phase compaction treatment the significant differences in lateral root number and growth angle are attributed to the change in bulk density not the specific soil type as discussed in the previous section.

The root development of *Cirsium*, *Plantago* and *Taraxacum* plants in the sandy loam soil at 1.8 g cm^{-3} was not observed to alter the inherent root architecture (Chapter 4). All species were able to axially extend both tap and lateral roots, however these processes occurred at different rates. The response of *Cirsium* to this high bulk density treatment resulted in thicker roots being produced with greater root diameters than the other two species resulting in greater root area and root volume measurements at both Days 14 and 28. This thickening response of roots was also observed in *Cirsium* when grown in three contrasting soil textures (clay, clay loam and sandy loam) at a compaction of 1.8 g cm^{-3} (Chapter 5). Here the root system architecture of

Cirisum plants was strongly affected by the different soil textures, with the sandy loam inducing the least level of restriction to the root system architecture in comparison to the clay soil which proved highly restrictive. The soil texture was observed to have an effect on both the root and shoot biomass characteristics and subsequent creation of rhizosphere porosity. Clay soil proved to be the most restrictive growth environment with the plants producing consistently less shoot and root material than the clay loam and sandy loam treatments. *Cirsium* roots were thinnest in the clay, thicker in the clay loam and thickest in the sandy loam soils which directly corresponded to the soils penetration resistance which was 4.5 MPa in the clay, 3.8 MPa in the clay loam and 3.6 MPa in the sandy loam respectively. This indicates that the clay soil provided an environment that was harder to penetrate, this may be due to the cohesion between clay particles, meaning that soil aggregates require a greater relative root growth pressure to deform (Kemper and Rosenau, 1984). The thinner roots also indicate that the plants were not able to effectively radially expand in comparison to the clay loam and sandy loam treatments. The ability of *Cirsium* roots to radially and axially expand resulted in thicker roots, this was clearly advantageous for the plants development as they were able to generate significantly greater root mass compared to the plants grown in clay soil. The higher levels of root observed in the clay loam in comparisons to the clay may be attributed to the more plastic nature of the soil, which may have resulted in the formation of localised microscale cracks during root growth further enabling the roots to develop (Helliwell et al. 2019). The contrast in root system architecture highlights that roots are highly

responsive to soil texture, with significant differences being observed in plant at a young growth stage. In the field different soil textures are extremely variable and depend on local conditions within a soil profile, the same is also observed for a soil's bulk density and penetration resistance. These changes to the physical components of the soil, will directly affect the pore network and movement of air throughout the soil profile. It is clear that a plant that is able to penetrate through soil compaction to depth must be able to readily alter its environment to improve its condition as the effects of soil bulk density and soil type on root growth are interconnected. Considering only one of these variables limits the understanding into how soil physical properties affect root growth (Alameda and Villar, 2012).

6.5 Generation of soil porosity via plant root development

Changes in soil porosity were measured at both a core and rhizosphere scale. The porosity of the core systems exhibited a trend of decreased pore space over time regardless of the soil bulk density (Chapters 3 & 4). An exception to this trend was where the presence of tillage radish lateral root mass increased the soil porosity in the un-compacted section of the split core experiment at day 28 (Chapter 3). This change was attributed to the high volume of fine lateral root mass that the plant develops modifying the microscale structure and subsequently instigating soil aggregation. The overall decrease in porosity was attributed to the loss of the smallest mesopores over time due to the natural compression of the soil profile as it settled a phenomena reported by

Koestel and Schluter, (2019), facilitated by wet dry cycles. The decrease in total core porosity despite the presence of plant roots may be attributed to the young age of the plants investigated here, in field studies cover crops have been shown to improve soil structure over multiple growing seasons (Chen and Weil, 2011). It also indicates that the potential these plant species have to structurally ameliorate soil maybe happening at more localised scales.

Investigation into the porosity of the rhizosphere showed a positive impact on soil structure was observed at localised scales in close proximity to plant roots (Chapters 4 & 5). Significant increases in porosity were observed, but only directly adjacent to the plant roots, as previously shown by Helliwell et al. (2017). This trend was observed across all species and soil types but was substantially different between them, with the greatest increases in rhizosphere porosity being manifest by *Cirsium* in Chapter 4 and in the sandy loam soil in Chapter 5. In all species the porosity subsequently decreased with time, which is attribute to the continued radial expansion of the taproot systems into the newly-created pore space. Secondary increases in the porosity of the rhizosphere zones at Day 42 were observed in Chapter 5, demonstrating continued pore space creation after radial expansion had occurred. The porosity gradient decreased with distance from the root surface, again this trend was manifest in all species and soil types. The gradient from the root surface indicates that the pore space creation is most likely of plant origin, and the volume of structural reorganisation subsequently differs between species and soil types. This root:soil contact zone provides a dynamic environment that generates localised ‘breathing

space' for roots, increasing the localised air and water flow to and from the root surface, with the generation of pore networks being revealed in this work to be a temporally dynamic process. The work undertaken highlights that once plant roots occupy a new soil volume, they structure their local microenvironment, and this is likely to have functional consequences for rhizosphere-based phenomena. Although not investigated in the scope of this study, changes in soil structure in the rhizosphere zone occur through the combination of multiple processes. These include plant roots physically moving soil particles as they grow through the soil (Gregory and Nortcliff , 2013; Koestel and Schluter, 2019), the release of exudates from plant roots facilitating localised wetting and drying cycles that increase the strength of bonds between soil particles (Czarnes et al. 2000), the influence of fungi (Ritz and Young, 2004), and the potential for longer temporal dynamic and higher-order interactions with microbes that are influencing the rate of soil particle cohesion (Barea et al. 2005). Plants with thicker roots were observed to have greater rhizosphere porosity in the first incremental zone of measurement with distance from the root surface (Chapter 4 & 5). This finding is promising from a soil remediation perspective: the development of thick roots is a direct response of plants growing through compacted soils. Thick roots have been identified as a desirable trait, as the subsequent microscale reorganisation of the soil structure to create new pore space is also greatest in these plants. This suggests that root thickness is a phenotypic trait that should be considered adventitious for soil remediation purposes in the instances of the plants and soil types investigated in this thesis.

6.6 Implications in the field

The findings in this thesis focus on plant root development and soil porosity formation in artificial systems. The theory behind these development could be applied to plants growing in the wild. We would expected to see plant root architectures develop without restriction, reaching to further maximum widths and depths. The process behind creation of soil pore space in the rhizosphere is likely to be significantly alter in field soils due to the presences of pre existing marcopore and mesopore networks. We have previously stated that the results of this thesis are based on 'model' homogenous soil systems. To further the work undertaken here it would be beneficial to undertake similar experiments using soil cores collected form the field that have existing pore networks. This would enable understanding about how plant roots develop into pores to be better understood and what implication this has on further changes in soil porosity at the rhizosphere scale.

6.7 Limitations to the study

A number of limitations of the conducted studies have been identified by the author. The implication these limitations may have on applying information about methods, results and theories developed in this thesis to field scale experimentation is discussed in this section.

6.7.1 System size

The size of sample columns restricted the maximum rooting width and depth of the plant species. The size of the core used has a direct effect on the achievable resolution at which the samples could be scanned, with smaller sample cores able to achieve higher resolutions. The size of the cores was carefully considered before each experiment and was linked to the aim of the experiment. With the experiments in Chapter 4 & 5 requiring smaller cores due to the higher level of soil compaction restricting plant root development and the objective of look at pore space creation at smaller scales. In the case of all three experiments, the cores plants were grown in provided an artificially limited growth environment that is not representative of field conditions and that is why roots that hit the column wall were not segmented or considered for analysis as they represented an artefact of the experimental design.

6.7.2 Length of experiments

The length of time plans where grown for was directly related to the time they take to become pot bound within the soil columns they are growing in. The bulk density of the soil also has an effect on how long it takes the plants to become pot bound, with soils of high bulk density restricting plant root development for longer time periods than soils of low bulk densities. For the experiments in this thesis we wanted to let plants grow to mature growth stages before they became pot bound and started to exhibited root characteristics that where artefacts of the soil column size and shape. This was reflected in the higher bulk density compaction treatments being

implemented in the smaller cores and lower bulk density in the larger cores. This allowed the plants to be grown to maturity at a growth period of 58 days. In natural systems plants would typically grow for extended time periods and the termination of the experiments at this stage was a limitation of the project. Further studies into plants that have been growing for longer times periods are warranted as they will explore how maturing plant root systems continue to influence soil pore architectures.

6.7.3 Scan resolution

The spatial resolution of objects imaged by X-ray CT is prescribed by the total volume of the sample being scanned. Here, the limit of resolution was either 60 or 35 µm and as such the roots visualised were confined to those greater than this dimension. At both experimental scales very fine root mass was not detected and therefore not considered in the 3D analysis. 2D WinRHIZO sans were also conducted of the root systems to provide an estimate of the total amount of root mass in the core. This allowed some assumptions to be drawn about how the additional root mass not imaged by the 3D technique may have been influencing the porosity of the soil cores. Due to the destructive way of collecting the 2D data no assumptions about where the very fine root mass was located in relation to larger roots could be made. To assess very fine root mass the overall size of the samples investigated would need to be reduced, this has a knock on effect on the age the plants can be grown to as they would become pot bound faster than in larger core systems. This is a trade off between scan resolution, root system maturity and amount of root

resolved by the 3D analysis technique that has to be contemplated when setting up these style of experiments.

6.7 Conclusions

The following key conclusions can be drawn from this research:

(i) Different root system types respond differently to changes in soil bulk density. Species with taproots were observed to have a diverse response to the zones of induced compaction in comparison to fibrous root systems. The evidence suggests that this response is likely to be linked to the thickness of the extending roots and the relative growth pressures they are able to exhibit. Their root response is directly linked to the soil pore matrix and the presence of meso *versus* macro pores will contribute to the changes in root system architecture.

(ii) Soil texture has a significant effect on plant root architectural development of tap-rooted species in highly compacted soils and results in a morphological response, as demonstrated here in the case of *Cirsium arvense*. Soils with increased proportion of clay particles have a more restrictive growth environment in comparison to soils with more sand particles. This results in a gradient of plant performance developing more established root systems in the sandy loam and clay loam soils in comparison to the clay soil.

(iii) Plants with thicker roots appear able to generate greater rhizosphere porosity in high bulk density soil systems. *Cirsium* plants were observed to have thicker roots in comparison to *Plantago* and *Taraxacum* and subsequently generated greater volumes of pore space in the rhizosphere. This phenomenon was also observed in the sandy loam soil with *Cirsium* developing thicker roots and producing greater rhizosphere porosity in comparisons to the clay loam and clay soils.

(iv) Rhizosphere-induced soil porosity is consistently greatest at the zone in immediate contact with the root and decreases with distance from the root surface. This increase was consistent across three different tap-rooted plant species and three widely contrasting soil textures. This indicates that the modification is a result of plant growth and that the phenomenon occurring is not particularly affected by soil texture.

(v) Several methods are now available to segment root systems from X-ray CT data. The greater the level of manual intervention in the segmentation process the greater the room for operator error and bias. Semi-automated segmentation techniques reduce the occurrence of these problems. The implementation of the Root1 macro in ImageJ demonstrated the ability for a semi-automated approach that reduces this level of manual interference as well as providing a high quality root segmentation output. Its level of accuracy in comparison to RooTrak and the manual segmentation process

demonstrated that it has the potential to greatly reduce segmentation times and therefor increasing the throughput of image analysis.

Plant root responses to both soil compaction and texture are strongly dependant on the inherent root system architecture and phenotypic traits of individual species. However the observed impact roots have on soil structure at microscales are fundamentally similar.

6.6.1 Overarching conclusion

Plant root responses to both soil compaction and texture are strongly dependent on the inherent root system architecture and phenotypic traits of the species. However, the observed impact that roots have on soil structure at microscales are fundamentally similar. All plant roots instigate structural reorganisation of the rhizosphere, possibly as an inevitable consequence of the nature of root growth, with the rate of occurrence linked to both the specific root system characteristics and wider biotic processes within the soil environment.

6.7 Further work

The studies described in this thesis demonstrate that different wild plant species have varying abilities to generate root mass and subsequent

rhizosphere porosity in heavily compacted soils, and that soil texture significantly influences root architectural traits.

These studies were undertaken over short experimental time periods. Increasing the time scale over which plant species are analysed, allowing them to develope mature root systems and implementing increased scanning time points would help to enhance the understanding of the dynamics of root growth through the life-cycle of plants. Assessment of the impact root death and decay has on the soil pore networks in 3D would be similarly insightful as the lifetime of soil pore networks developed by plant roots once they have decayed is very poorly documented. Studies have shown that plants grown after cover crops typically use old root channels as paths of least resistance through the soil (Williams and Weil, 2004; Lynch and Wojciechowski, 2015). Investigating how subsequent cohorts of plant growth is aided by root channels formed by the species investigated in this thesis would give a novel insight into the potential for cover crop and wild species to act as soil structural primers over the course of the their life cycle. Furthermore, this work has demonstrated how different plant species with different architectural traits respond to both bulk density and soil compaction. The studies all involved growing plants in isolation, which is not the circumstance in the field, even for monocultures. Understanding how species interact with each other in these conditions also needs to be taken into consideration. In field conditions plants are unlikely to grow without competition from neighbours of the same or different species. Particularly in agricultural conditions where cover crops are often grown as mixtures, understanding

how plants with different traits interact with each other and both aid or hinder the subsequent pore space development in their localised region is of importance when devising effective plant mixes for improving soil structure.

The impact of hard soil, such as in a subsoil, on plant root anatomy and subsequent plant behaviour and function is not fully understood. A greater understanding into the mechanisms behind root response to compaction and texture could be achieved by assessing root anatomy:

(i) *Quantify anatomical traits such as cortical cell number and aerenchyma diameter from roots grown in compacted soil conditions employing laser ablation technology (LAT) and confocal microscopy techniques.*

These techniques allow the 2D and 3D structure of root anatomy to be captured, subsequently images can be analysed to identify specific root cell structures. Generally the ability of a root to penetrate hard soil is associated with its phenotype or 'phenes' which reduce the likelihood of root buckling when compacted layers are encountered (Chimungu et al., 2015). Differences between species in their phenotypic ability to penetrate compacted soil may be attributed to variation in root diameter and the tendency of roots to deflect or buckle as opposed to differences in the pressure exerted by growing roots (Tracy et al., 2011). Some examples of root phenes include; root cortical aerenchyma, cortical cell file number and cortical cells (Chimungu et al., 2015). In general the growth rate of root cells in any soil environment is controlled by the balance of the internal and external pressures together with the rheological properties of the cell wall (Bengough

and Mullins, 1990). These pressures will have a direct impact on the ability of plant roots to extend through the soil and analysing them can give insight into why plant roots are behaving in certain ways in different soil and compaction conditions.

Greater insight into how the presence of plant roots modifies soil structure could also be obtained by conducting a study looking at the porosity of both rhizosphere and bulk soil aggregates. Rhizosphere aggregates are expected to have increased levels of porosity in comparison to bulk soil aggregates demonstrating the presence of the plant roots has induced soil structural changes via the increase in micropores. The formation of pores at this scale is of importance as it directly impacts the transfer of water and nutrient to the plant roots from the soil.

(ii) Assess aggregate porosity and pore connectivity from rhizosphere and bulk soil aggregates of different soil textures compacted to high bulk densities using X-ray computed tomography at the nano scale.

Finally the focus of this thesis surrounded the physical changes in soil structural dynamics instigated by plant roots. Many other biological processes occur simultaneously to, and as a result of, root growth. For example, the relationship between arbuscular mycorrhiza and plant roots, where the mycorrhiza hyphae help to bind soil particles along with bacteria to produce microaggregates and subsequently macroaggragtes, (Barea et al. 2005), thus changing the inherent pore network of a soil system. A study addressing the microbial impact of plant root development linked to soil structural analysis

may help further understand how these microscale changes in pore space are occurring over time and what impact the relationship between plant, soil and its microbiome has on these structural forming processes.

References

Abdollahi, L., Munkholm, L.J., Garbout, A. (2013) Tillage system and cover crop effects on soil quality: II. Pore characteristics. Soil Science Society of America Journal. 78, 271-279.

Ahmed, S., Klassen, T.N., Keyes, S., Daly, M., Jones, D.L., Mavrogordato, M., Sinclair, I. (2016) Imaging the interaction of roots and phosphate fertiliser granules using 4D X-ray tomography. Plant and Soil. 401, 125-134.

Alameda, D. and Villar, R. (2012) Linking root traits to plant physiology and growth in *Fraxinus angustifolia* Vahl. seedlings under soil compaction conditions. Environmental and Experimental Botany. 79, 49-57.

Alberti, J., Casariego, A.M., Daleo, P., Fanjul, E., Silliman, B., Bertness, M., Iribarne, O. (2010) Abiotic stress mediates top-down and bottom-up control in a Southwestern Atlantic salt marsh. Oecologia. 163, 181-191.

Aravena, J.E., Berli, M., Ghezzehei, T.A., Tyler, S.W. (2011) Effects of Root-Induced compaction on rhizosphere hydraulic properties- X-ray microtomography imaging and numerical simulations. Environmental Science and Technology. 45, 425.431.

Arnaud, C., Bonnot, C., Desnos, T., Nussaume, L. (2010) The root cap at the forefront. Comptes Rendus Biologies. 333, 335-343.

Atkinson, J.A., Pound, M.P., Bennett, M.J., Wells, D.M. (2019) Uncovering the hidden half of plants using new advances in root phenotyping. Current Opinion in Biotechnology. 55, 1-8.

Atwell, B.J. (1993) Response of roots to mechanical impedance. Environmental and Experimental Botany. 99, 27-40.

Bacq-Labreuil, A., Crawford, J., Mooney, S.J., Neal, A.L., Ritz, K. (2019) Phacelia (*Phacelia tanacetifolia* Benth.) affects soil structure differently depending on soil texture. Plant and Soil. https://doi.org/10.1007/s11104-019-04144-4.

Bacq-Labreuil, A., Crawford, J., Mooney, S.J., Neal., A.L., Akkari, E., McAuliffe, C., Zhang, X., Redmile-Gordon, M., Ritz, K. (2018) Effects of cropping systems upon three-dimensional architecture of soil systems are modulated by texture. Geoderma. 332, 73-83.

Bailey, P.H.J., Currey, J.D., Fitter, A.H. (2002) The role of root system architecture and root hairs in promoting anchorage against uprooting forces in *Allium cepa* and root mutants of *Arabidopsis thialiana*. Journal of Experimental Botany. 55, 333-340.

Bais, H.P., Weir, T.L., Perry, L.G., Gilroy, S., Vivanco, J.M. (2006) The role of root exudates in rhizosphere interactions with plants and other organisms. The Annual Review of Plant Botany. 57, 233-266.

Ball, B.C., Campbell, D.J., Douglas, J.T., Henshall, J.K. and O'Sullivan, M.F. (1997) Soil structural quality, compaction and land management. European Journal of Soil Science. 48, 593-601.

Bao, Y., Aggarwal, P., Robbins, N.E., Sturrock, C.J., Thompson, M.C., Tan, H.Q., Dinneny, J.R. (2014) Plant roots use a patterning mechanism to position lateral root branches toward available water. Proceedings of the National Academy of Sciences of the United States of America. 111, 9319-9342.

Barea, J.M., Pozo, M.J., Azcon, R., Azcon-Aguilar, C. (2005) Microbial co-operation in the rhizosphere. Journal of Experimental Botany. 56, 417, 1761-1778.

Barlow, P.W. (1975) The root cap. In: Torrey JG, Clarkson DT, editors. The development and function of roots. London: Academic Press. 21–54.

Barrios, E. (2007) Soil biota, ecosystem services and land productivity. Ecological Economics. 269-285.

Barzegar, A.R., Nadian, H., Heidari, F., Herbert, S.J., Hasemi, A.M. (2006) Interaction of soil compaction, phosphorus and zinc on clover growth and accumulation of phosphorus. Soil and Tillage Research. 87, 155-162.

Batey, T. (2009) Soil compaction and soil management-a review. Soil use and management. 335-345.

Batey, T., and McKenzie, D.C. (2006) Soil compaction: identification directly in the field. Soil Use and Management. 123-131.

Baumert, V.L., Vasilyeva,N.A.,Vladimirov, A.A., Meier, I.C., Kogel-Knabner, I., Mueller, C.W. (2018) Root exudates induce soil macroaggragation facilitated by fungi in the subsoil. Frontiers in Environmental Science. 6, 140-157.

Bengough, A.G. (2012) Root elongation is restricted by axial but not by radial pressures: so what happens in field soil? Plant Soil. 360, 15-18.

Bengough, A.G., and MacKenzie C.J. (1994) Simultaneous measurements of root force and elongation for seedling pea roots. Journal of Experimental Botany. 45, 270, 95-102.

Bengough, A.G., Bransby, M.F., Hans, J., McKenna, S.J., Roverts, T.J., Valentine, T.A. (2006) Root response to soil physical conditions; growth dynamics from field to cell. Journal of Experimental Botany. 57, 2, 437-447.

Bengough, A.G., McKenzie, B.M., Hallet, P.D., Valentine, T.A. (2011) Root elongation, water stress, and mechanical impedance: a review of limiting stresses and beneficial root tip traits. Journal of Experimental Botany. 62, 59-68.

Bengough, A.G., Mullins, C.E. (1990) Mechanical impedance to root growth: a review of experimental techniques and root growth responses. Journal of Soil Science. 41, 341-358.

Bizet, F., Bengough, A.G., Hummel, I., Bogeat-Triboulot, M.B., Dupuy, L.X. (2016) 3D deformation field in growing plant roots reveals both mechanical and biological responses to axial mechanical forces. Journal of Experimental Botany. 67, 9, 5605-5614.

Blaser, S.R.G.A., Schluter, S., Vetterlein, D. (2018) How much is too much? - Influence of X-ray dose on root growth of faba bean (*Vica faba*) and barley (*Hordeum vulgare*). PLoS ONE. 13, 3: e0193669.

Bowen, H.D. (1981) Alleviating mechanical impendence. In: Modifying the root environment to reduce crop stress (eds. Arkin, G.F., Taylor, H.M.), pp. 21-57. American Society of Agricultural Engineers. Michigan, USA.

Bronick, C. J., and Lal, R. (2005) Soil structure and management: A review. Geoderma. 124, 3-22.

Brussard, L., DeRuiter, P.C., Brown, G.G. (2007) Soil biodiversity for agricultural sustainability. Agricultural Ecosystem Environment. 233-244.

Burr-Hersey. J.E., Mooney, S.J., Bengough, A.G., Mairhofer, S., Ritz, K. (2017) Developmental morphology of cover crop species exhibit contrasting behaviours to changes in soil bulk density, revealed by X-ray computed tomography. PLoS ONE 12(7): e0181872.

Carminati, A., Vetterlein, D., Koebernick, N., Blaser, S., Weller, U., Vogel, H-J. (2013) Do roots mind the gap? Plant and Soil. 367, 1-2, 651-661.

Chaparro, J.M., Sheflin, A.M., Manter, D.K., Vivanco, J.M. (2012) Manipulating the soil microbiome to increase soil health and plant fertility. Biology and Fertility of Soils. 48, 489-499.

Chen, G., and Weil, R.R. (2009) Penetration of cover crop roots through compacted soils. Plant and Soil. 331, 1, 31-43.

Chen, G., and Weil, R.R. (2011) Root growth and yield of maize as affected by soil compaction and cover crops. Soil and Tillage Research. 117, 17-27.

Chen, G., Weil, R.R., Hill, R.L. (2014) Effects of compaction and cover crops on soil least limiting water range and air permeability. Soil and Tillage Research. 136, 61-69.

Chimungu, J.G., Loades, K.W., Lynch, J.P. (2015) Root anatomical phenes predict root penetration ability and biomechanical properties in maize (*Zea mays*). Journal of Experimental Botany. 66, 3151-3162.

Clark, R.T., MacCurdy, R.B., Jung, J.K., Shaff, J.E., McCouch, S.R., Aneshansley, D.J., Kochian, L.V. (2011) A three-dimensional root phenotyping with a novel imaging and software platform. Plant Physiology. 156, 455-465.

Clark, L.J., and Barraclough, P.B. (1999) Do dicotyledons generate greater maximum axial root growth pressures than monocotyledons? Journal of Experimental Botany. 50, 1263-1266.

Clark, L.J., Whalley, W.R., Barraclough, P.B. (2003). How do roots penetrate strong soil? Plant and Soil. 255, 93-104.

Colombi, T., Braun, S., Keller, T., Walter, A. (2017) Artificial macropores attract crop roots and enhance plant productivity on compacted soils. Science and the Total Environment. 574. 1283-1293.

Cook, A., Marriott, C.A., Seel, W., Mullins, C.E. (1996) Effects of soil mechanics on root and shoot growth of *Lolium perenne* L., *Agrostis capillaris* and *Trifolium repens* L. Journal of Experiment Botany. 47, 301, 1075-1084.

Cresswell, H.P., and Kirkegaard, J.A. (1995) Subsoil amelioration by plant roots- the process and the evidence. Soil Physics and Hydrology. 33, 221-239.

Cumming, D.H.M., and Cumming, G.S. (2003) Ungulate community structure and ecological processes: body size, hoof area and trampling in African savannas. Oecologia. 134, 560-568.

Czarnes, S., Hallett, P.D., Bengough, A.G., Young, I.M. (2000) Root- and microbial- derived mucilages affect soil structure and water transport. European Journal of Soil Science. 51, 435–443

Day, P.R. (1965) Particle fractionation and particle size analysis. In: Black, C.A. (ed.) Methods of Soil Analysis. Part 1. American Society of Agronomy and Soil Science Society of America, Madison, USA. 545–567.

Defra (2007) Scoping study to assess soil compaction affecting upland and lowland grassland in England and Wales. Project BD2304. Final report to the Department for Environment, Food and Rural Affairs.

Dexter, A.R., Horn, R., Kemper, W.D. (1988) Two mechanisms for age-hardening of soil. European Journal of Soil Science. 39, 2, 163-175.

Diaz-Zorita, M., Perfect, E., Grove, J.H. (2002) Disruptive methods for assessing soil structure. Soil and Tillage Research. 64, 3-22.

Downie, H., Holden, N., Otten, W., Spiers, A.J., Valentine, T.A., Dupuy, L.X. (2012) Transparent soil for imaging the rhizosphere. PLOS ONE. 7, 9, 1-6.

Downie, H.F., Adu, M.O., Schmidt, S., Otten, W., Dupuy, L.X., White, P.J., Valentine, T.A. (2015) Challenges and opportunities for quantifying roots and

rhizosphere interactions through imaging and image analysis. Plant Cell Environment. 38, 7, 1213-1232.

Dunbabin, V.M., Postma, J.A., Schnepf, A., Pages, L., Javaux, M., Wu, L., Leitner, D., Chen, Y.L., Rengel, Z., Diggle, A.J. (2013) Modelling root-soil interactions using three-dimensional models of root growth, architecture and function. Plant Soil. 372, 93-124.

Edwards, A.P., and Bremner, J.M. (1967) Microaggregates in soils. European Journal of Soil Science. 18, 1, 64-73.

Ehrmann, J., and Ritz, K. (2014) Plant soil interactions in temperate multi-cropping production systems. Plant Soil. 376, 1, 1-29.

Engelaar, W.M.H., Jacobs, M.H.H.E., Blom, C.W.P.M. (1993) Root growth of *Rumex* and *Plantago* species in compacted waterlogged soils. Acta Botanica Neerlandica. 42, 1, 25-35.

Enriqueta Arias, M., Gonzalez-Perez, J.A., Gonzalez-Vila, F.J., Ball, A.S. (2005) Soil health- a new challenge for microbiologists and chemists. International Microbiology. 8, 13-21.

Evans, S.D., Lindstrom, M.J., Voorhees, W.B., Moncrief, J.F., Nelson, G.A. (1996) Effect of subsoiling and subsequent tillage on soil bulk density, soil moisture and corn yield. Soil and Tillage Research. 38, 35-46.

Feeney, D.S., Crawford, J.W., Daniell, T., Hallett, P.D., Nunan, N., Ritz, K., Rivers, M., Young, I.M. (2006) Three-dimensional microorganisation of the soil-root-microbe system. Microbial Ecology. 52, 151-158.

Ferris, H, and Tuomisto, H. (2015) Unearthing the role of biological diversity in soil health. Soil Biology and Biochemistry. 85, 101-109.

Fitter, A.H. and Peat, H. J. (1994) The Ecological Flora Database. Journal of Ecology. 82, 415-425. Available at: http://www.ecoflora.co.uk

Fitzpatrick, E.A. (1956) An indurated soil horizon formed by permafrost. Journal of Soil Science. , 248–254.

Flavel, R.J., Guppy, C.N., Rabbi, S.M.R., Young, I.M. (2017) An image processing and analysis tool for identifying and analysing complex plant root systems in 3D using non-destructive analysis: Root1. PLoS One. 3, 12, (5): e0176433

Gao, W., Ren, T., Bengough, A.G., Auneau, L., Watts, C.W., Whalley, W.R. (2011) Predicting penetrometer resistance from the compression characteristics of soil. Soil Science Society of America Journal. 76, 2, 361-369.

Gibson, D.J. (1989) Effects of animal disturbance on tallgrass prairie vegetation. American Midland Naturalist. 121, 144-154.

Giovannetti, M. and Mosse, B. (1980) Evaluation of techniques for measuring vesicular arbuscular mycorrhizal infection in roots New Phytologist. 84, 489-500.

Goss, M.J. (1977) Effects of mechanical impedance on root growth in barley (*Hordeum vulgare* L.) I. Effects on elongation and branching of seminal roots. Journal of Experimental Botany. 28, 96-111.

Gregory, P.J., Bengough, A.G., Grinev, D., Schmidt, S., Thomas, W.T.B., Wojciechowski, T., Young, I.M. (2009) Root phenomics of crops: Opportunities and challenges. Functional Plant Biology. 36, 922–929.

Gregory, A.S., Watts, C.W., Whalley, W.R., Kuan, H.L., Griffiths, B.S., Hallett, P.D., Whitmore, A.P. (2007) Physical resilience of soil to field compaction and the interactions with plant growth and microbial community structure. European Journal of Soil Science. 1221-1232.

Gregory, P.J., Hutchison, D.J., Read, D.B., Jenneson, P.M., Gilboy, W.B. & Morton, E.J. (2003) Non-invasive imaging of roots with high resolution X-ray micro-tomography. Plant & Soil. 255, 351–359.

Gregory, P.J., and Nortcliff, S. (2013) Soil conditions and Plant Growth. Blackwell Publishing Ltd. Print ISBN:9781405197700

Grossman, J.D., and Rice, K.J. (2012) Evolution of root plasticity responses to variation in soil nutrient distribution and concentration. Evolutionary Applications. 5, 8, 850-857.

Grzesiak, S., Grzesiak, M.T., Hura, T., Marcinska, I., Rzepka, A. (2013) Changes in root system structure, leaf water potential and gas exchange of maize and triticale seedlings affected by soil compaction. Environmental and Experimental Botany. 2-10.

Gutterman, Y. (2003) The influences of animal diggings and runoff water on the vegetation in the Negev Desert of Israel. Israel Journal of Plant Sciences. 51, 161-171.

Hahn, A., Zimmermann, R., Wanke, D., Harter, K., Edelmannn, H.G. (2008) The root cap determines ethylene-dependent growth and development in maize roots. Molecular Plant. 1, 359-367.

Haling, R.E., Brown, L.K., Bengough, A.G., Young, I.M., Hallett, P.D., White, P.J., George, T.S. (2013) Root hairs improve root penetration, root-soil contact, and phosphorus acquisition in soils of different strength. Journal of Experimental Botany. 64, 12, 3711-3721.

Hamamoto, S., Moldrup, P., Kawamoto, K., Komatsu, T. (2009) Effect of particle size and soil compaction on gas transport parameters in variably saturated, sandy soils. Vadose Zone Journal. 8, 4, 986-995.

Hamza, M.A., and Anderson, W.K. (2005) Soil compaction in cropping systems; A review of the nature, causes and possible solutions. Soil and Tillage Research. 82, 2, 121-145.

Han, E., Kautz, T., Perkons, U., Uteau, D., Peth, S., Huang, N., Horn, R., Ulrich, K. (2015) Root growth dynamics inside and outside of soil biopores as affected by crop sequence determined with the profile wall method. Biology of Fertile Soils. 51, 847-856.

Haygarth, P.M., and Ritz, K. (2009) The future of soils and land use in the UK: Soil systems for the provision of land-based ecosystem services. Land Use Policy. 5187-5197

Helliwell, J.R., Sturrock, C.J., Grayling, K.M., Tracy, S.R., Flavel, R.J., Young, I.M., Whalley, W.R., Mooney, S.J. (2013) Applications of X-ray computed tomography for examining biophysical interactions and structural development in soil systems: a review. European Journal of Soil Science. 64, 279-297.

Helliwell, J.R., Sturrock, C.J., Mairhofer, S., Craigon, J., Ashton, R.W., Miller, A.J., Whalley, W.R., and Mooney, S.J. (2017). The emergent rhizosphere: imaging the development of the porous architecture at the root-soil interface. Scintific Reports. 7, 14875.

Helliwell, J.R., Sturrock, C.J., Miller, A.J., Whalley, W.R., Mooney, S.J. (2019) The role of plant species and soil condition in the physical development of the rhizosphere. Plant, Cell and Environment. 1-13.

Hettiaratchi, D.R.P. (1990) Soil compaction and plant root growth. Philosophical Transactions of the Royal Society. 329, 35-47.

Hettiaratchi, D.R.P., Goss, M.J., Harris, J.A., Hague Nye, P., Smith, K.A., Greenwood, D.J., Walker, S.A. (1990) Soil compaction and plant root growth. Philosophical Transactions of the Royal Society of London. Series B: Biological Sciences. 329, 343-355.

Hiltner, L. (1904) Uber neuere erfahrunger und probleme auf dem gebiete der bodenbakteriologie unter besonderer berucksichtigung der grundungung und brache. Arbeiten der Deutschen Landwirtschafts-Gesellschaft. 98, 59–78.

Hodge A. (2004) The plastic plant: Root responses to heterogeneous supplies of nutrients. New Phytologist. 162, 9–24.

Hodgson, J.M. (1997) Soil Survey Field Handbook. Cranfield University.

Hosokawa, Y. (2010) Characteristics of tracks formed by wild deer in Natsumushi-yama pasture of Sanriku town. Bulletin of the Faculty of Agriculture Miyazaki University. 56, 63-71.

Houston, A.N., Otten, W., Baveye, P.C., Hapca, S. (2013) Adaptive- window indicator kriging: A thresholding method for computed tomography images of porous media. Computers and Geoscience. 54, 239-248.

Hu, L., Robert, C.A.M., Cadot, S., Zhang, X., Ye, M., Li, B., Manzo, D., Chervet, N., Steinger, T., van der Heijden, M.G.A., Schlaeppi, K., Erb, M. (2018) Root exudates metabolites drive plant-soil feedbacks on growth and defense by shaping the rhizosphere microbiota. Nature Communications. 9, 2738.

Iijima, M., Kono, Y., Yamauchi, A., Pardales Jr, J.R. (1991) Effects of soil compaction on the development of rice and maize root systems. Environmental and Experimental Botany. 31, 3, 333-342.

Ishaq, M., Ibrahim, M., Hassan, A., Saeed, M., Lal, R. (2001) Subsoil compaction effects on crops in Punjab, Pakistan: II. Root growth and nutrient uptake of wheat and sorghum. Soil Tillage Research. 60, 153–161.

Iyer-Pascuzzi, A.S., Symonova, O., Mileyko, Y., Hao, Y., Belcher, H., Harer, J., Weitz, J.S., Benfey, P.N. (2010) Imaging and analysis platform for automatic phenotyping and trait ranking of plant systems. Plant Physiology. 152, 1148-1157.

Jin, K., Shen, J., Ashton, R.W., Dodd, I. C., Parry, M.A.J., Whalley, W.R. (2013) How do roots elongate in a structured soil? Journal of Experimental Botany. 64, 4761-4777.

Jones, R.J.A., Spoor, G., Thomasson, A.J. (2003) Vulnerability of subsoils in Europe to compaction: a preliminary analysis. Soil and Tillage Research. 73, 131-143.

Kadziene, G., Munkholm, L.J., Mutegi, J.K. (2011) Root growth conditions in the topsoil as affected by tillage intensity. Geoderma. 166, 66-73.

Kano-Nakata, M., Inukai, Y., Wade, L.J., Siopongco, J.D.L.C., Yamauchi, A. (2011) Root development, water uptake, and shoot dry matter production under water deficit conditions in two CSSLs of rice: functional roles of root plasticity. Plant Production Science. 14, 307–317

Kays, S.J., Nicklow, C.W., Simons, D.H. (1974) Ethylene in relation to response of roots to physical impedance. Plant Soil. 40, 565–571

Kemper, W.D., Rosenau, R.C. (1984) Soil cohesion as affected by time and water content. Soil Science Society of America Journal. 48, 5, 1001-1006.

Keyes, S.D., Gillard, F., Soper, N., Mavrogordato, M.N., Sinclair, I., Roose, T. (2016) Mapping soil deformation around plant roots using in vivo 4D X-ray Computed Tomography and digital volume correlation. Journal of Biomechanics. 49, 9, 1802-1811.

Kibblewhite, M.G., Ritz, K., Swift, M.J. (2008) Soil health in agricultural systems. Philosophical Transactions of the Royal Society B. 685-701.

Kim, H., Anderson, S.H., Motavalli, P.P., Gantzer, C.J. (2010) Compaction effects on soil macropore geometry and related parameters for an arable field. Geoderma. 160, 2, 244-251.

Kimura, E., and Islam, M.A. (2012) Seed scarification methods and their use in forage legumes. Research Journal of Seed Science. 1-13.

Kirby, M., and Bengough, A.G. (2002) Influence of soil strength on root growth: Experiments and analysis using a critical-state model. European Journal of Soil Science. 53, 1, 119-127.

Knappett, J.A., and Craig, R. F. (2012) Craig's soil mechanics. Eighth Edition. CRC Press. https://doi.org/10.1201/b12841

Koebernick, N., Daly, K.R., Keyes, S.D., Bengough, A.G., Brown, L.K., Cooper, L.J., George, T.S., Hallett, P.D., Naveed, M., Raffan, A., Roose, T. (2019) Imaging microstructure of the barley rhizosphere: particle packing and root hair influences. New Phytologist. 221, 4, 1878-1889.

Koestel, J., and Schluter, S. (2019) Quantification of the structure evolution in a garden soil over the course of two years. Geoderma. 338, 597-609.

Kolb, E., and Hartmann, C. (2012) Radial force development during root growth measured by photoelasticity. Plant Soil. 360, 19-35.

Kolb, E., Legué, V., Bogeat-Triboulot, M. (2017) Physical Root-Soil Interactions. Physical Biology, Institute of Physics: Hybrid Open Access. 1-40.

Kuhn, N.J. (2014) Soil Loss. In Churchman, G.J., Landa, E.R. (2014) The Soil Underfoot. Infinite Possibilities for a Finite Resource. CRC Press. Taylor & Francis Group. 37.

Kumi, F., Hanping, M., Jianping, H., Ullah, I. (2015) Review of applying X-Ray computed tomography for imaging soil-root physical and biological processes. International Journal of Agricultural and Biological Engineering. 8, 5, 1-14.

Kuzyakov, Y., and Razavi, B.S. (2019) Rhizosphere size and shape: temporal dynamics and spatial stationarity. Soil Biology and Biochemistry. 135, 343-360.

Lal, R. (2016) Soil health and carbon management. Food and Energy Security. 5, (4), 212-222.

Lamont, B.B. (2003) Structure, ecology and physiology of root clusters- a review. Plant and Soil. 248, 1-19.

Lei, S.A. (2003) Soil compaction and moisture status from large mammal trampling in Coleogyne (blackbrush) shrublands of southern Nevada. Bulletin Southern California Academy of Sciences. 102, 119-129.

Lei, S.A. (2004) Soil compaction from human trampling, biking and off-road motor vehicle activity in a blackbrush (*Coleogyne ramosissima*) shrubland. Western North American Naturalist. 64, 1, 125-130.

Lewis, J. and Siostrom, J. (2010) Optimising the experimental design of soil columns in saturated and unsaturated transport experiments. Journal of Contaminant Hydrology. 115, 1-13.

Lipiec, J., Medvedev, V.V., Birkas, M., Dumitru, E., Lyndina, T.E., Rousseva, S., Fulajtar, E. (2003) Effect of soil compaction on root growth and crop yield in Central and Eastern Europe. International Agrophysics. 17, 61-69.

Lipiec, J., and Hatano, R. (2003) Quantification of compaction effects on soil physical properties and crop growth. Geoderma. 116, 107-136.

Lynch, J.P. (2013) Steep, cheap and deep: an ideotype to optimize water and N acquisition by maize root systems. Annals of Botany. 112, 347-357.

Lynch, P.J. Wojciechowski, T. (2015) Opportunities and challenges in the subsoil: pathways to deeper rooted crops. Journal of Experimental Botany. 66, 8, 2199-2210.

Maenhout, P., Sleutel, S., Xu, H., Van Hoorebke, L., Cnudde, V., De Neve, S. (2019) Semi-automated segmentation and visualization of complex undisturbed root systems with X-ray µCT. Soil and Tillage Research. 192, 59-65.

Mairhofer, S., Sturrock, C., Wells, D.M., Bennett, M.J., Mooney, S.J., and Pridmore, T.P. (2015) On the evaluation of methods for the recovery of plant root systems from X-ray computed tomography images. Functional Plant Biology. 42, 460–470.

Mairhofer, S., Zappala, S., Tracy, S.R., Sturrock, C., Bennett, M., Mooney, S.J. et al. (2012) RooTrak: Automated recovery of three dimensional plant root architecture in soil from X-ray microcomputed tomography images using visual tracking. Plant Physiology. 158, 561–569.

Materechera, S.A., Dexter, A.R., Alston, A.M (1991) Penetration of very strong soils by seedling roots of different plant species. Plant Soil. 135, 31–41

McCully, M. (1999) Roots in soil: unearthing the complexities of roots and their rhizospheres. Plant Physiology and Plant Molecular Biology. 50, 695-718.

McMillan, B.R., Pfeiffer, K.A., Kaufman, D.W. (2011) Vegetation responses to an animal-generated disturbance (Bison wallows) in tallgrass prairie. American Midland Naturalist. 165, 60-73.

Mohseni Saravi, M., Chaichi, M.R., Attaeian, B. (2005) Effects of soil compaction by animal trampling on growth characteristics of *Agropyrum repens* (Case study: Lar Rangeland, Iran). International Journal of Agriculture and Biology. 7, 6, 909-914.

Mooney, S.J., Pridmore, T.P., Helliwell, J., Bennett, M.J. (2012) Developing X-ray computed tomography to non-invasively image 3-D root systems architecture in soil. Plant Soil. 352, 1-22.

Moreno-Espindola, I.P., Rivera-Becerril, F., Ferrara-Guerrero, M.J., Leon-Gonzalez, F.D. (2007) Role of root-hairs and hyphae in adhesion of sand particles. Soil Biology and Biochemistry. 39, 10, 2520-2526.

Morgan, R.P.C. (2005) Soil Erosion and Conservation. Oxford: Blackwell Publishing.

Morris, E.C., Griffiths, M., Golebiowska, A., Mairhofer, S., Burr-Hersey, J., Goh, T., Wangenheim, D., Atkinson, B., Sturrock, C.J., Lynch, J.P., Vissenberg, K., Ritz, K., Wells, D.M., Mooney, S.J., Bennett, M.J. (2017) Shaping 3D root system architecture. Current Biology. 27, 919-930.

Motavalli, P.P., Stevens, W.E., Hartwig, G. (2003) Remediation of subsoil compaction and compaction effects on corn N availability by deep tillage and application of poultry manure in a sandy textured soil. Soil and Tillage Research. 71, 121- 131.

Mulholland, B., Fullen, M.A. (1991) Cattle trampling and soil compaction on loamy sands. Soil Use and Management. 7, 4, 189-193.

Naveed, M., Moldrup, P., Arthur, E., Wildenschild, D., Eden, M., Lamande, M., Vogel, H-J., Wollesen de Jonge, L. (2012) Revealing soil structure and functional macroporosity along a clay gradient using X-ray Computed Tomography. Soil Science Society of America. 77, 403-411.

Negi, S., Ivanchenko, M.G., Muday, G.K. (2008) Ethylene regulates lateral root formation and auxin transport in *Arabidopsis thaliana*. The Plant Journal. 55, 175-187.

Nimmo, J.R. (2004) Porosity and pore size distribution. In: D. Hillel (Ed.) Encyclopedia of Soils in the Environment. Vol. 3. London, Elsevier. 295–303.

Olanrewaju, O.S., Ayangbenro, A.S., Glick, B.R., Babalola, O.O. (2019) Plant health: Feedback effect of root exudates-rhizobiome interactions. Applied Microbiology and Biotechnology. 103, 3, 1155-1166

Oleghe, E., Naveed, M., Baggs, E.M., Hallett, P.D. (2017) Plant exudates improve the mechanical conditions for root penetration through compacted soils. Plant and Soil. 421, 19-30.

Otsu, N. (1979) A thresholding selection method from gray-scale histogram. IEEE Transactions on System, Man, and Cybernetices. 9, 62-66.

Oussible, M., Crookston, R.K., Larson, W.E. (1992) Subsurface compaction reduces the root and shoot growth and grain yield of wheat. Agronomy Journal. 84, 34-38.

Ozan, I.L., Borrero, L.A. (2018) About the circular depression origin placed along the Tres Arroyos Talus, Tierra Del Fuego. Magallania. 46, 167-185.

Pascual, J., Alberti, J., Daleo, P., Iribarne, O. (2017) Herbivory and trampling by small mammals modify soil properties and plant assemblages. Journal of Vegetation Science. 28, 1028-1035.

Passioura, J.B. (1991) Soil structure and plant growth. Australian Journal of Soil Research. 29, 717–728.

Passioura, J.B. (2002) Soil conditions and plant growth. Plant, Cell and Environment. 25, 311-318.

Peret, B., Larrieu, A., Bennett, M. (2009) Lateral root emergence: a difficult birth. Journal of Experimental Botany. 60, 3637-3643.

Peth, S., Nellesen, J., Fischer, G., Horn, R. (2010) Non-invasive 3D analysis of local soil deformation under mechanical and hydraulic stresses by mu CT and digital image correlation. Soil and Tillage Research. 111, 3–18.

Pierret, A., Capowiez, Y., Belzunces, L., Moran, C.J. (2002) 3D reconstruction and quantification of macopores using x-ray computed tomogrpahy and image analysis. Geoderma. 106, 247-271.

Place, G., Bowman, D., Burton, M., Rufty, T. (2008) Root penetration through a high bulk density soil layer: differential response of a crop and weed species. Plant and Soil. 307, 179-190.

Power, A.G. (2010) Ecosystem services and agriculture: tradeoffs and synergies. Philosophical Transactions of the Royal Society. 365, 2959-2971.

Rabbi, S.M.F., Tighe, M.K., Flavel, R.J., Kaiser, B.N., Guppy, C.N., Zhang, X., Young, I.M. (2018) Plant roots redesign the rhizosphere to alter the three-dimensional physical architecture and water dynamics. New Phytologist. 219, 542-550.

Ritz, K., and Young, I.M (2004) Interactions between soil structure and fungi. The Mycologist. 18, 52-59.

Rogers, E.D., Manaenkova, D., Mijar, Medhavinee, Nori, A., Goldman, D.I., Benfey, P.N. (2016) X-Ray computed tomography reveals the response of root system architecture to soil structure. Plant Physiology. 171, 2028-2040.

Rosolem, C.A., Foloni, J.S.S., Tiritan, C.S. (2002) Root growth and nutrient accumulation in cover crops as affected by soil compaction. Soil and Tillage Research. 65, 1, 109-115.

Rowell, D.L. (1994) Soil Science: Methods and applications. Longman Scientific and Technical, UK.

Schluter, S., Blaser, S.R.G.A., Weber, M., Schmidt, V., Vetterlein, D. (2018) Quantification of root growth patterns from the soil perspective via root distance models. Frontiers in Plant Science. 9, 1084.

Schmidt S, Bengough AG, Gregory PJ, Grinev DV, Otten W. (2012) Estimating root-soil contact from 3D X-ray microtomography. European Journal of Soil Science. 63, 776–786.

Schmidt, S., Gregory, P. J., Grinev, D., Bengough, A.G. (2013) Root elongation rate is correlated with the length of the bare root apex of maize and lupin roots despite contrasting responses of root growth to compact and dry soil. Plant Soil. 372, 609-618.

Schneider, C.A., Rasband, W.S., Eliceriri, K.W. (2012) NIH image to ImageJ: 25 years of image analysis. Nature Methods. 9, 671-675.

Scott, D.I., Tams, A.R., Berry, P.M., Mooney, S.J. (2005) The effects of wheel-induced soil compaction on anchorage strength and resistance to root lodging of winter barley (*Hordeum vulgare* L.) Soil and Tillage Research. 82, 2, 147-160.

Soane, B.D. and Ouwerkerk, van, C. (1995) Implications of soil compaction in crop production for the quality of the environment. Soil and Tillage Research. 35, 55-22.

Soane, B.D., Blackwell, P.S., Dickson, J.W., Painter, D.J. (1981) Compaction by agricultural vehicles: a review. I. Soil and wheel characteristics. Soil and Tillage Research. 1, 207-237.

Soffe, R.J. (2003) The Agricultural Notebook, 20th edition. Blackwell Science, Oxford.

Spoor, G. (2006) Alleviation of soil compaction: requirements, equipment and techniques. Soil Use and Management. 113-122.

Spoor, G., Tijink, F.G.J., Weisskopf, P. (2003) Subsoil compaction: risk avoidance, identification and alleviation. Soil and Tillage Research. 73, 175-182.

Stirzaker, R.J., Passioura, J.B., Wilms, Y. (1996) Soil structure and plant growth: Impact of bulk density and biopores. Plant and Soil. 185, 151-162.

Stokes, A., Atger, C., Bengough, A.G., Fourcaud, T., Sidle, R.C. (2009) Desirable plant root traits for protecting natural and engineered slopes against landslides. Plant Soil. 324, 1-30.

Storr, T., Simmons, R.W., Hannam, J.A. (2019) A UK survey of the use and management of cover crops. Annals of Applied Biology. 174, 179-189.

Tardieu F. (1994) Growth and functioning of roots and of root systems subjected to soil compaction. Towards a system with multiple signalling? Soil and Tillage Research. 30, 217-243.

Taylor, H.M., and Brar, G.S. (1991) Effect of soil compaction on root development Soil and Tillage Research. 19, 111-119.

Thomas, A.S. (1943) The vegetation the Karamoja district, Uganda - An illustration of biological factors in tropical ecology. Journal of Ecology. 31, 149-177.

Tisdall, J.M., and Oades, J.M. (1982) Organic matter and water-stable aggregates in soils. European Journal of Soil Science. 33, 141-163.

Tracy, S.R., Black, C.R., Roberts, J.A., Mooney, S.J. (2011) Soil compaction: a review of past and present techniques for investigating effects on root growth. Journal of Science Food and Agriculture. 91, 1528-1537.

Tracy, S.R., Black, C.R., Roberts, J.A., Sturrock, C., Mairhofer, S. Craigon, J., Mooney, S.J. (2012) Quantifying the impact of soil compaction on root system architecture in tomato (*Solanum lycopersicum*) by X-ray micro-computed tomography. Annals of Botany. 110, 511-519.

Trager, M.D., Wilson, G.W.T., Hartnett, D.C. (2004) Concurrent effects of fire regime, grazing and bison wallowing on tallgrass prairie vegetation. American Midland Naturalist. 152, 237-247.

Travlos, I.S., Karamanos, A. J. (2006) Effects of soil texture on vegetative growth of the tropical legume Marama Bean (*Tylosema esculentum*). Journal of Agronomy. 5, 609-612.

Tubeileh, A., Groleau-Renaud, V., Plantureux, S., Guckert, A. (2003) Effect of soil compaction on photosynthesis and carbon partitioning within a maize-soil system. Soil and Tillage Research. 71, 151-161.

Udawatta, R.P., Gantzer, C.J., Anderson, S.H., Assouline, S. (2016) Synchrotron microtomographic quantification of geometrical soil pore characteristics affected by compaction. SOIL. 2, 211-220.

Valentine, T.A., Hallet, P.D., Binnie, K., Young, M.W., Squire, G.R., Hawes, C., Bengough, A.G. (2012) Soil strength and macropore volume limits root elongation rates in many UK agricultural soils. Annals of Botany. 110, 259-270.

Van Den Akker, J.J.H., Saone, B. (2005) Compaction. Encyclopaedia of soils in the environment. Elsevier Ltd. 285-293.

Vepraskas, M.J. (1988) Bulk density values diagnostic of restricted root growth in coarse textured soils. Soil Science Society of America Journal. 52, 1117-1121.

Vierheilig, H., Coughlan, A.P., Wyss, U., Piche, Y. (1998) Ink and vinegar, a simple staining technique for arbuscular-mycorrhizal fungi Applied and Environmental Microbiology. 64, 5004-5007

Vogel, H.J., and Kretzschmar, A. (1996) Topological characterization of pore space in soil- sample preparation and digital image processing. Geoderma. 73, 23-28.

Vogel, H.J., Weller, U., Schlüter, S., (2010) Quantification of soil structure based on Minkowski functions. Computer Geoscience. 36, 1236–1245.

Walker, T.S., Baid, H.P., Grotewold, E., Vivanco, J.M. (2003) Root exudation and rhizosphere biology. Plant Physiology. 132, 44-51.

Whalley, W.R., Dumitru, E., Dexter, A.R. (1995) Biological effects of soil compaction. Soil and Tillage Research. 35, 53-68.

White, R.E. (2006) Peds and Pores. In White RE, editors. Principles and Practice of Soil Science. The Soil as a Natural Resource. 4th ed. Blackwell Publishing. 59-78.

White, R.G. and Kirkegaard, J.A. (2010) The distribution and abundance of wheat roots in a dense, structured subsoil – implications for water uptake. Plant, Cell & Environment. 33, 133–148.

White, R.E. (2006) Principles and Practice of Soil Science. The Soil as a Natural Resource. Oxford: Blackwell.

Whiteley, G.M., and Dexter, A.R. (1984) Displacement of soil aggregates by elongating roots and emerging shoots of crop plants. Plant and Soil. 77, 131-140.

Williams, S.M., and Weil, R.R. (2004) Crop cover root channels may alleviate soil compaction effects on Soybean Crop. Soil Science Society of America Journal. 68, 4, 1403-1409.

York, L.M., Carminati, A., Mooney, S.J., Ritz, K., Bennett, M.J. (2016) The holistic rhizosphere: integrating zones, processes, and semantics in the soil influenced by roots. Journal of Experimental Botany. 67, 12, 3629-3643.

Zappala, S., Helliwell, J.R., Tracy, S.R., Mairhofer, S., Sturrock, C.J., Pridmore, T., Bennett, M.J., Mooney, S.J. (2013) Effects of X-Ray dose on rhizosphere

studies using X-Ray Computed Tomography. PLoS ONE 8(6): e67250. doi:10.1371/journal.pone.0067250

Ziyaee, A., and Roshani, M.R. (2012) A survey study on soil compaction problems for new methods in agriculture. International Research Journal of Applied and Basic Sciences. 3, 1787-1801.

Appendix Chapter 2

A.2.1 Soil texture (quantitative analysis by hydrometer) SOP.

Reagents

- Hydrogen peroxide: 6% H_2O_2. Dilute 200 ml of 30% H_2O_2 to 1000 ml. Use gloves and safety glasses as H2O2 is corrosive and oxidising

Sodium hexametaphosphate –$(NaPO_3)_6$, 5%: Dissolve 50 g sodium hexa metaphosphate and 7g sodium carbonate in 1 litre of distilled water.

- Hydrometer

Soil preparation

Weight 50 g of <2 mm sieved air dry soil into a 500 ml beaker. Slowly add 100 ml of 6% H2O2 and leave the solution to stand for 12 hours. Separately weigh 10-50 g of soil into a crucible, place in an oven at 105 °c for 12 hours. Record the oven dry weight.

Soil dispersion

Add 100 ml of sodium hexametaphosphate to the soil and hydrogen peroxide solution and mix well. Leave for 12 hours. Pour the solution into a measuring cylinder. Fill the cylinder with distilled water to the 1 litre mark. Record the temperature of the suspension. Using a plunger mix the content of the cylinder thoroughly (hold the cylinder whilst using the plunger to avoid spilling any liquid. Finish the agitation with 2-3 slow smooth stroke and remove the plunger). Slowly lower the hydrometer into the solution and read the number in line with the solution liquid at 32 second. This gives the value for silt and clay. Next repeat the mixing of the cylinder with the plunger and then allow the solution to stand for 8 hours. Take an additional reading from the hydrometer after this time to get the clay content reading.

Calibration of the hydrometer

Calibration of the hydrometer is required as not all hydrometers read 0 g/L when there is no soil in suspension. Calibration of the hydrometer was undertaken using the following method: Add 100 ml of sodium hexa meta phosphate and 100 ml of hydrogen peroxide to a measuring cylinder. Add 800 ml of distilled water to the cylinder. Mix the solution thoroughly, record the temperature of the solution. Take a hydrometer reading if the calibration reading is greater than zero then you must subtract the read number from your hydrometer reading for the soil solution. If the calibration reading is less than zero you should add the read number to your hydrometer reading for the soil solution (Day, 1965; Rowell, 1994).

Correction of hydrometer reading

The density correction is calculated by subtracting the density of the control at each reading from the corresponding density readings for the soil solution samples. Add 0.2 units to the reading of the sample for every 1°C above 20°C and subtract 0.2 units for every 1°C below 20°C. The equations to calculate clay % and silt % contents of the samples are outlined below:

$$silt\ \% = \left(\frac{corected\ hydrometer\ reading\ at\ 32\ sec}{weight\ of\ oven\ dried\ soil} \times 100\right) - clay\ \%$$

$$clay\ \% = \frac{corrected\ hydrometer\ reading\ at\ 8\ hrs}{weight\ of\ oven\ dried\ soil} \times 100$$

$$sand\ \% = 100 - (\ silt\ \% + clay\ \%)$$

A.2.2 Quantifying mycorrhizal roots SOP.

Equipment and reagents

The following equipment and regents were prepared for clearing and staining roots:

- Freshly collected and washed root samples, chopped into 1 cm segments (labelled with Sample name)
- Tubes with perforated base for samples
- Water baths at 70°C containing vessels of:

-10% KOH (w/v potassium hydroxide) solution

-water (v/v) solution for washing after clearing

-3% ink in vinegar (5% acetic acid) for staining

-5% acetic acid for washing after staining

- Forceps and dissecting needles to transfer roots to Petri dishes
- Petri dishes containing 50% glycerol-water (v/v) solution

The following equipment was prepared for quantifying mycorrhizal roots:

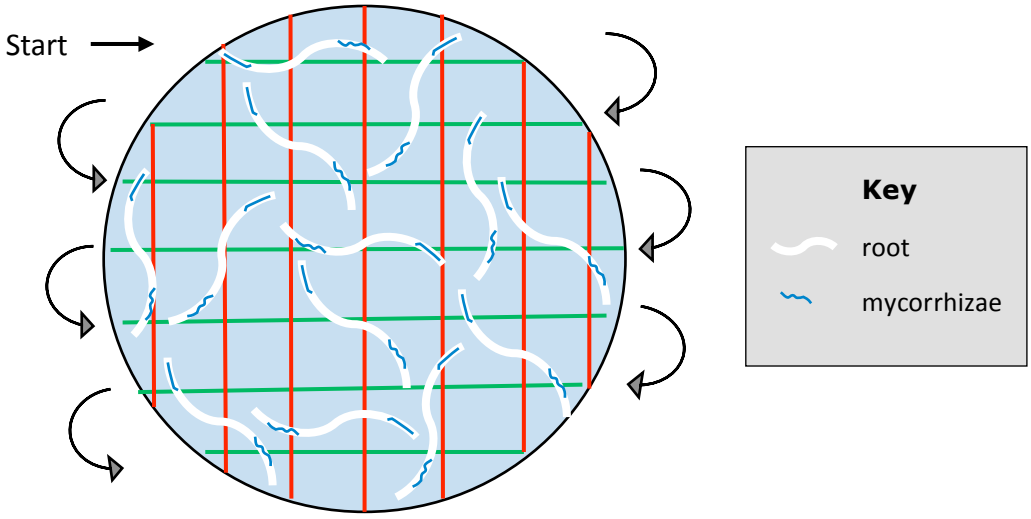
- The Dissecting microscope
- Petri dishes containing 50% glycerol-water (v/v) solution marked with 1 cm grid
- Forceps and dissecting needles to move roots around

Clearing and staining roots

Place the root sample loosely to a depth of around 1 cm in each tube. Place the tubes into the 10% KOH solution in the water bath. Leave samples in the KOH solution for 90 mins to clear. Remove tubes from KOH and wash in water for 2 mins. Next place tubes containing cleared and washed root samples into the stain solution in the water bath. Leave samples to stain for 6 mins. Remove tubes from stain and wash in acetic water bath for 10 mins. Use forceps to carefully place cleaned, stained roots into a petri dish with gridlines marked on the bottom containing 50% glycerol- water solution (Vierheilig et al., 1998).

Quantifying mycorrhizae

The method used to quantify mycorrhizae is adapted from the gridline intersect method (Giovannetti and Mosse 1980). Each set of prepared root samples were placed into 9 cm diameter petri dishes with gridlines marked on the bottom (Figure A.2.1). To observe the mycorrhizae population, scan along the gridlines using a dissecting microscope to quantify intersections between gridlines and roots. These are designated as either colonised (mycorrhizal) or non- mycorrhizal. Scan along the gridlines systematically. At each point where a root intersects a gridline record whether there is mycorrhizal infection present or not. This process was repeated until 100 such intersections had been scored. Where there were not sufficient crossing points to give 100 intersections the rots were rearranged in the dish and the survey was continued from the new position. There percentage colonisation of the sample was then calculated.



A.2.1: Schematic of mycorrhiza identification using petri dish method.

T.2.1: Outlines the amount of water needed to obtain to pack soil cores to specific moisture contents

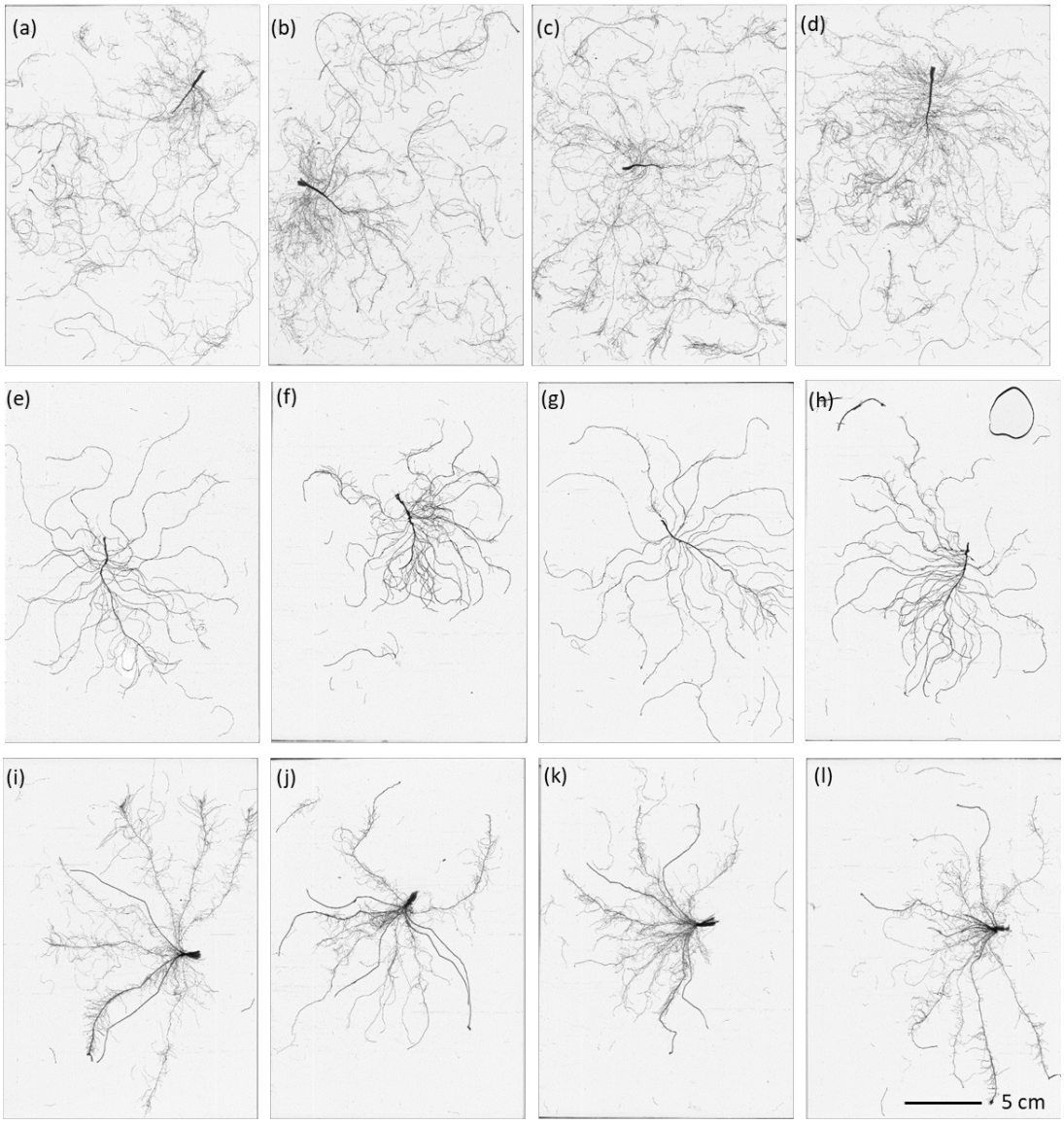
Compaction level	Soil (g)	Water (g)	Moisture content (%)
1.6	228.67	50.2	22
1.6	228.67	48	21
1.6	228.67	45.7	20
1.6	228.67	43.4	19
1.6	228.67	41.1	18
1.6	228.67	38.8	17
1.6	228.67	36.6	16
1.6	228.67	34.3	15
1.8	257.25	56.5	22
1.8	257.25	54	21
1.8	257.25	51.4	20
1.8	257.25	48.8	19
1.8	257.25	46.2	18
1.8	257.25	43.7	17
1.8	257.25	41.1	16
1.8	257.25	38.5	15

Appendix Chapter 3

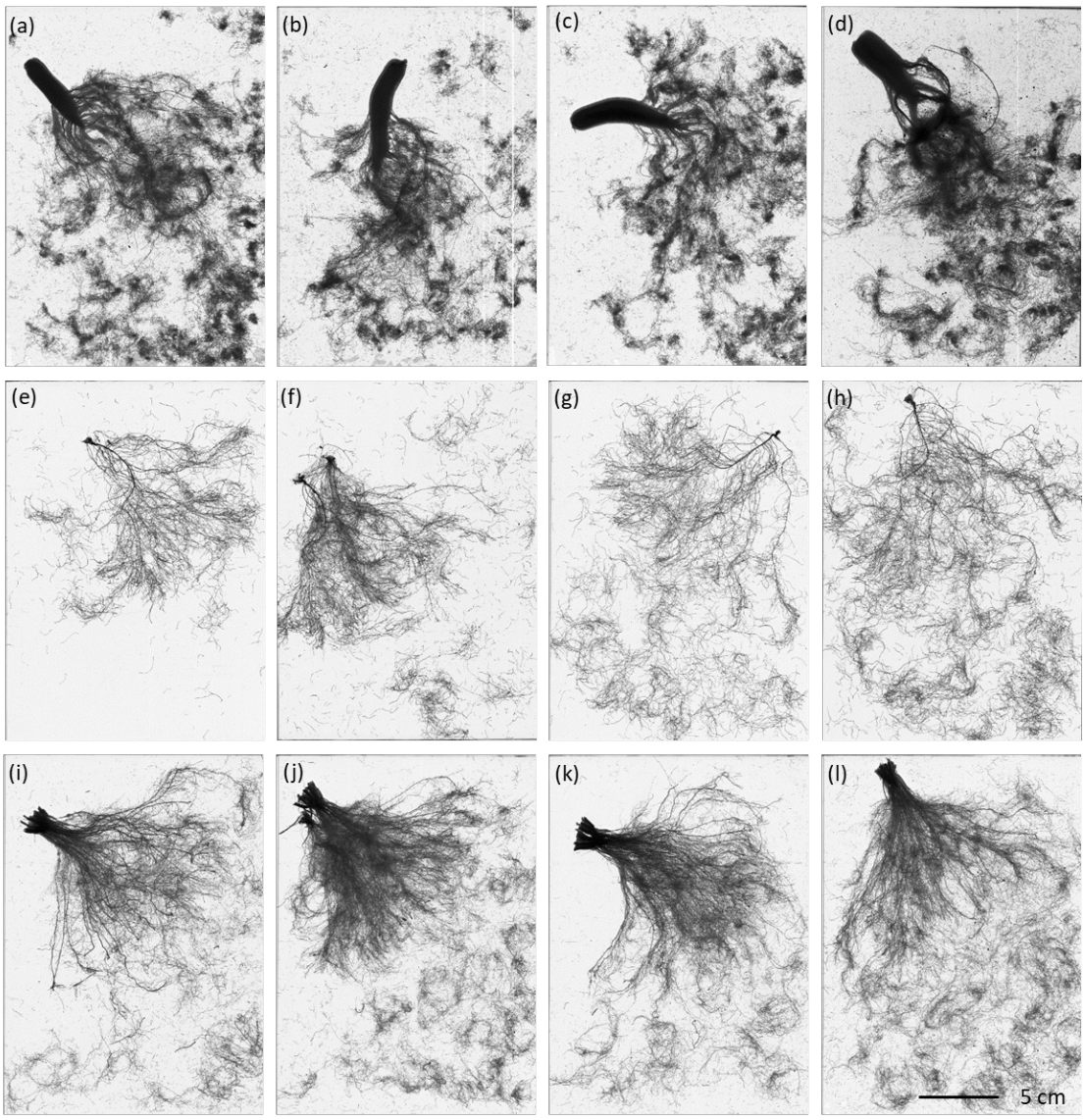
T.3.1: Table detailing the p values of individual ANOVA's calculating the significance of plant root diameters between plants being grown in 1.2 gm cm-3 or 1.4 g cm-3 soil.

Species	Time	Diameter class	p value
Black oat	Day 20	0<0.25	0.246
		0.25<0.5	0.651
		0.5<1.0	0.294
		1.0<1.5	0.527
		1.5<2.0	0.767
		2.0<2.5	0.895
		2.5<3.0	0.492
		3.0<3.5	0.087
		3.5<4.0	0.02
		4.0<4.5	0.026
		>4.5	0.627
Black oat	Day 58	0<0.25	0.718
		0.25<0.5	0.887
		0.5<1.0	0.907
		1.0<1.5	0.991
		1.5<2.0	0.607
		2.0<2.5	0.907
		2.5<3.0	0.381
		3.0<3.5	0.401
		3.5<4.0	0.362
		4.0<4.5	0.403
		>4.5	0.421
Tillage radish	Day 20	0<0.25	0.926
		0.25<0.5	0.636
		0.5<1.0	0.835
		1.0<1.5	0.986
		1.5<2.0	0.751
		2.0<2.5	0.788
		2.5<3.0	0.787
		3.0<3.5	0.488
		3.5<4.0	0.724
		4.0<4.5	0.862
		>4.5	0.279
Tillage radish	Day 58	0<0.25	0.614
		0.25<0.5	0.486
		0.5<1.0	0.952
		1.0<1.5	0.969
		1.5<2.0	0.94
		2.0<2.5	0.824

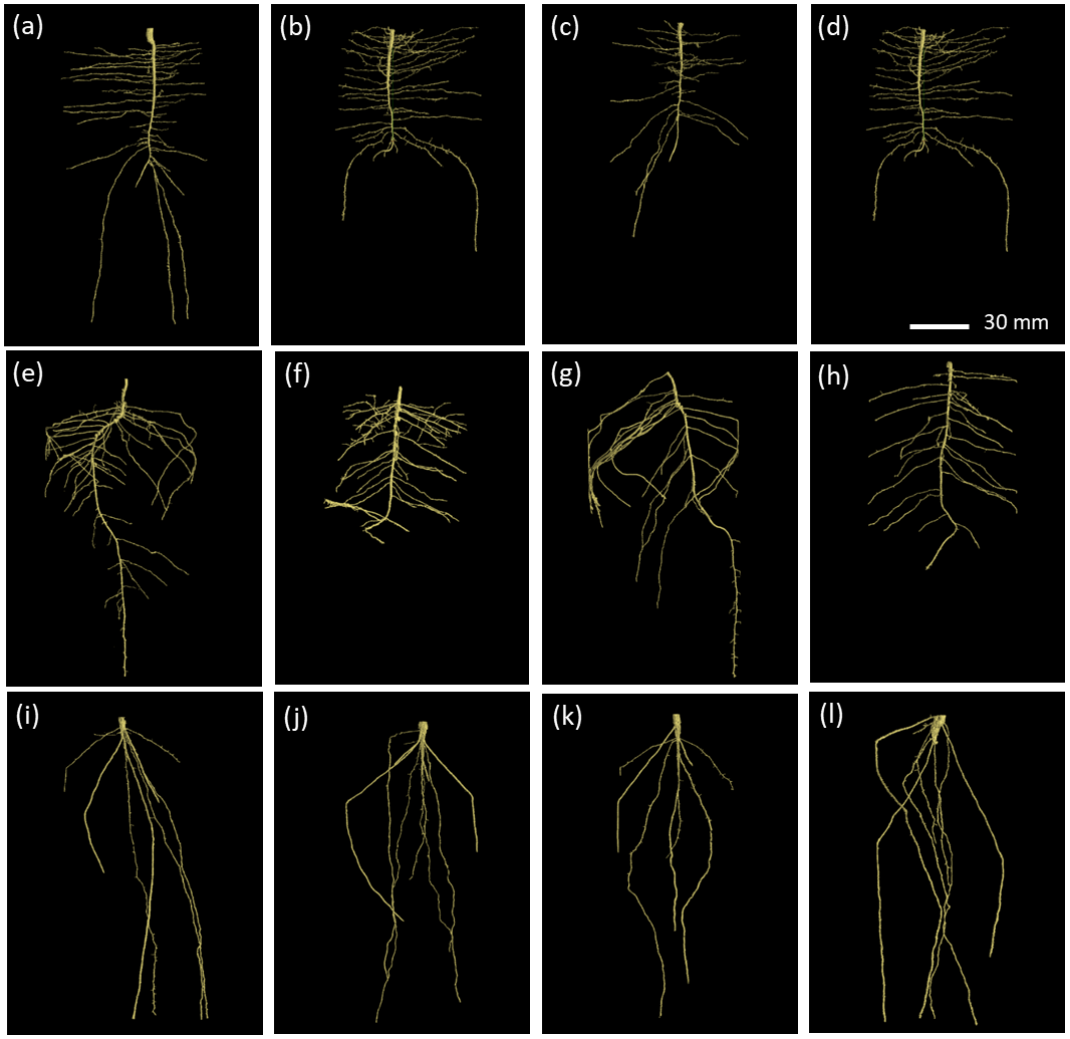
		2.5<3.0	0.826
		3.0<3.5	0.972
		3.5<4.0	0.92
		4.0<4.5	0.494
		>4.5	0.451
Vetch	Day 20	0<0.25	0.114
		0.25<0.5	0.264
		0.5<1.0	0.116
		1.0<1.5	0.035
		1.5<2.0	0.005
		2.0<2.5	0.037
		2.5<3.0	0.646
		3.0<3.5	0.763
		3.5<4.0	0.374
		4.0<4.5	0.374
		>4.5	0.301
Vetch	Day 58	0<0.25	0.263
		0.25<0.5	0.939
		0.5<1.0	0.117
		1.0<1.5	0.111
		1.5<2.0	0.63
		2.0<2.5	0.36
		2.5<3.0	0.694
		3.0<3.5	0.774
		3.5<4.0	0.63
		4.0<4.5	0.788
		>4.5	0.536



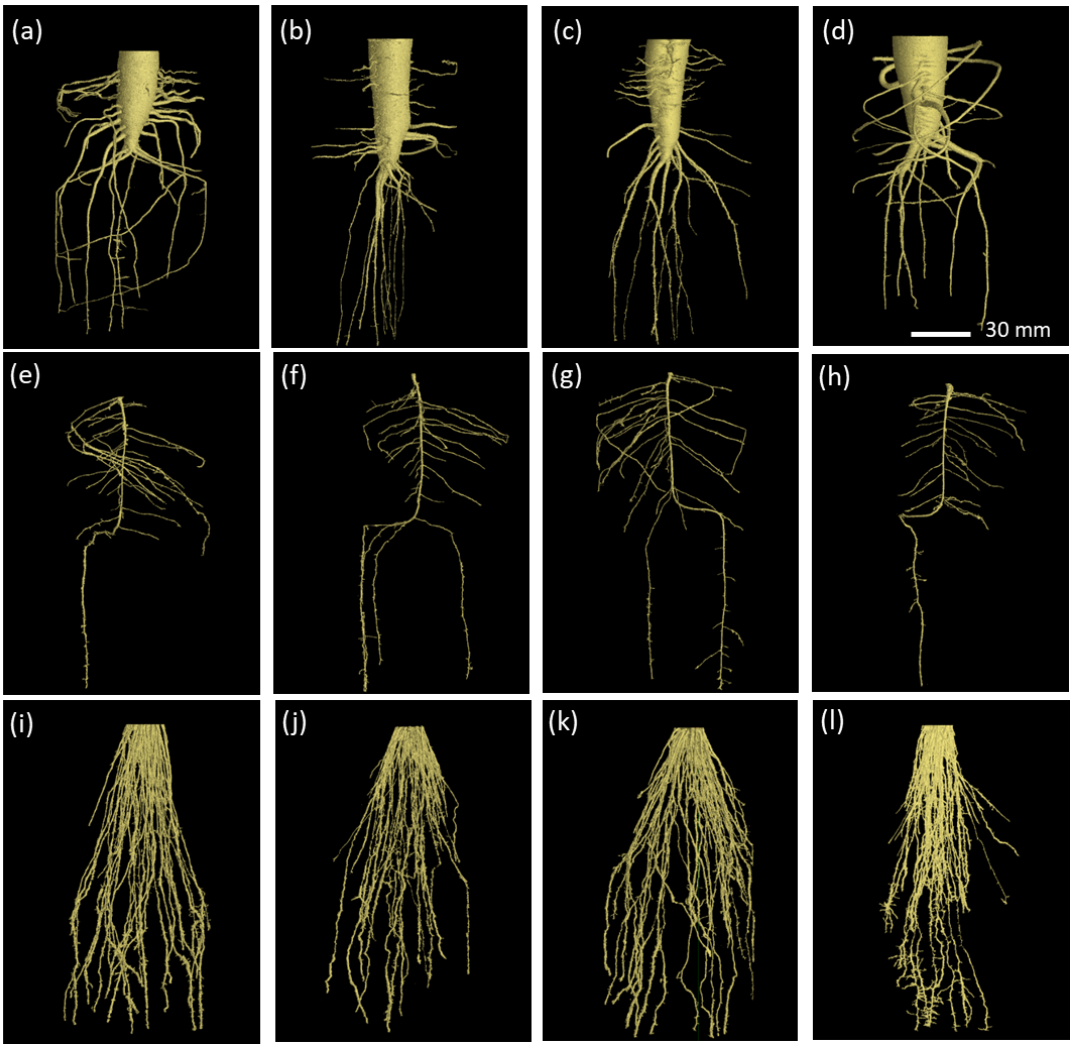
A.3.1: 2D images of cover crop plants grown for 20 days scanned using WinRHIZO. (a-d) tillage radish, (e-h) vetch, (i-l) black oat.



A.3.2: 2D images of cover crop plants grown for 58 days scanned using WinRHIZO. (a-d) tillage radish, (e-h) vetch, (i-l) black oat.



A.3.3: X-ray CT visualisations of cover crop plants grown for 20 days scanned at 60 µm. (a-d) tillage radish, (e-h) vetch, (i-l) black oat.



A.3.4: X-ray CT visualisations of cover crop plants grown for 58 days scanned at 60 µm. (a-d) tillage radish, (e-h) vetch, (i-l) black oat.

T.3.2: Supplimentary data for published manuscript, indicates representative soil porosity of low and high phases within soil columns across the study period.

All core	Species	Phase	Time	Rep	Porosity %
1	Control	Low	0	1	2.49
1	Control	High	0	1	2.96
2	Control	Low	0	2	8.65
2	Control	High	0	2	4.10
3	Control	Low	0	3	7.37
3	Control	High	0	3	8.00
4	Control	Low	0	4	8.23
4	Control	High	0	4	3.71
5	Tillage radish	Low	20	1	8.25
5	Tillage radish	High	20	1	6.14
6	Tillage radish	Low	20	2	6.72
6	Tillage radish	High	20	2	6.58
7	Tillage radish	Low	20	3	14.12
7	Tillage radish	High	20	3	5.38
8	Tillage radish	Low	20	4	13.42
8	Tillage radish	High	20	4	6.18
9	Vetch	Low	20	1	3.82
9	Vetch	High	20	1	5.82
10	Vetch	Low	20	2	5.09
10	Vetch	High	20	2	5.53
11	Vetch	Low	20	3	7.59
11	Vetch	High	20	3	4.65
12	Vetch	Low	20	4	7.18
12	Vetch	High	20	4	6.13
13	Black oat	Low	20	1	12.80
13	Black oat	High	20	1	5.98
14	Black oat	Low	20	2	3.29
14	Black oat	High	20	2	4.12
15	Black oat	Low	20	3	6.83
15	Black oat	High	20	3	2.29
16	Black oat	Low	20	4	7.92
16	Black oat	High	20	4	6.83
17	Tillage radish	Low	58	1	9.71
17	Tillage radish	High	58	1	3.97
18	Tillage radish	Low	58	2	5.34
18	Tillage radish	High	58	2	10.08

19	Tillage radish	Low	58	3	5.47
19	Tillage radish	High	58	3	4.44
20	Tillage radish	Low	58	4	6.30
20	Tillage radish	High	58	4	3.90
21	Vetch	Low	58	1	14.38
21	Vetch	High	58	1	9.52
22	Vetch	Low	58	2	10.80
22	Vetch	High	58	2	4.51
23	Vetch	Low	58	3	3.77
23	Vetch	High	58	3	3.05
24	Vetch	Low	58	4	8.58
24	Vetch	High	58	4	5.41
25	Black oat	Low	58	1	14.00
25	Black oat	High	58	1	6.44
26	Black oat	Low	58	2	7.15
26	Black oat	High	58	2	8.70
27	Black oat	Low	58	3	7.24
27	Black oat	High	58	3	4.67
28	Black oat	Low	58	4	9.47
28	Black oat	High	58	4	4.68

T.3.3: Supplimentary data for published manuscript, indicates representative whole root system characteristics within a column.

Species	Time	Rep	Surface area (cm2)	Root volume as (%) of column	Convex hull (cm^3)	Solidity
Tillage Radish	20	1	23.97	0.04	304.06	0.000852
Tillage Radish	20	2	15.05	0.02	150.20	0.00104
Tillage Radish	20	3	18.04	0.03	205.03	0.000893
Tillage Radish	20	4	13.57	0.02	111.99	0.001239
Vetch	20	1	39.01	0.07	320.61	0.001574
Vetch	20	2	33.15	0.06	211.24	0.002046
Vetch	20	3	38.07	0.07	404.02	0.001279
Vetch	20	4	26.87	0.05	240.80	0.001363
Oat	20	1	23.11	0.05	263.76	0.001237
Oat	20	2	22.14	0.05	311.64	0.001099
Oat	20	3	19.42	0.05	231.05	0.001373
Oat	20	4	33.64	0.09	299.76	0.002018
Tillage Radish	58	1	117.51	1.98	497.09	0.027791
Tillage Radish	58	2	104.90	2.35	415.84	0.040014
Tillage Radish	58	3	94.96	1.83	425.70	0.030077
Tillage Radish	58	4	150.36	3.46	478.27	0.049653
Vetch	58	1	32.17	0.06	314.52	0.001283
Vetch	58	2	37.73	0.07	346.58	0.001115
Vetch	58	3	26.11	0.05	426.42	0.001111
Vetch	58	4	32.10	0.05	280.93	0.001243
Oat	58	1	190.74	1.17	488.51	0.006038
Oat	58	2	202.46	1.32	405.93	0.004767
Oat	58	3	170.07	0.99	501.41	0.006835
Oat	58	4	187.78	1.20	340.81	0.007418

T.3.4: Supplimentary data for published manuscript, indicates representative root system characteristics confined to different bulk density layers within a column.

Species	Time	Phase	Rep	Lateral frequency	Lateral angle (degrees)	Surface area (cm2)	Root volume (%) of soil layer
Tillage radish	20	Low	1	1	87.2	15.08	0.02
Tillage radish	20	Low	2	2	87.1	7.70	0.01
Tillage radish	20	Low	3	2	84.3	11.92	0.01
Tillage radish	20	Low	4	1	80.3	7.52	0.01
Tillage radish	20	High	1	3	70.9	8.91	0.02
Tillage radish	20	High	2	1	57.1	7.34	0.01
Tillage radish	20	High	3	1	62.4	6.13	0.01
Tillage radish	20	High	4	1	62.6	7.52	0.01
Tillage radish	58	Low	1	9	76.4	80.14	5.03
Tillage radish	58	Low	2	1	77.8	66.46	5.64
Tillage radish	58	Low	3	6	68.8	61.77	4.57
Tillage radish	58	Low	4	8	58.2	102.04	8.79
Tillage radish	58	High	1	9	37.1	37.48	0.15
Tillage radish	58	High	2	8	36.4	36.16	0.15
Tillage radish	58	High	3	9	26.6	34.35	0.16
Tillage radish	58	High	4	6	45.4	49.90	0.41
Vetch	20	Low	1	15	70.7	29.07	0.15
Vetch	20	Low	2	13	66.2	22.42	0.12
Vetch	20	Low	3	13	67.4	24.57	0.14
Vetch	20	Low	4	8	72.1	13.59	0.07
Vetch	20	High	1	3	65.9	10.03	0.03
Vetch	20	High	2	1	68.6	10.74	0.03
Vetch	20	High	3	1	62.6	13.60	0.04
Vetch	20	High	4	1	61.9	13.33	0.03
Vetch	58	Low	1	11	75.7	23.22	0.11
Vetch	58	Low	2	9	72.4	26.16	0.13
Vetch	58	Low	3	13	75.9	16.32	0.09
Vetch	58	Low	4	8	74.1	21.90	0.10
Vetch	58	High	1	3	67.6	8.98	0.03
Vetch	58	High	2	4	68.6	11.61	0.03
Vetch	58	High	3	2	65.8	9.80	0.03
Vetch	58	High	4	1	67.6	10.10	0.03
Black oat	20	Low	1	-	-	10.61	0.07
Black oat	20	Low	2	-	-	13.19	0.09

Black oat	20	Low	3	-	-	10.95	0.08
Black oat	20	Low	4	-	-	16.58	0.13
Black oat	20	High	1	-	-	12.52	0.04
Black oat	20	High	2	-	-	8.98	0.03
Black oat	20	High	3	-	-	8.48	0.03
Black oat	20	High	4	-	-	17.09	0.06
Black oat	58	Low	1	-	-	87.06	0.32
Black oat	58	Low	2	-	-	108.99	0.48
Black oat	58	Low	3	-	-	96.64	0.39
Black oat	58	Low	4	-	-	97.57	0.38
Black oat	58	High	1	-	-	103.84	0.22
Black oat	58	High	2	-	-	93.66	0.19
Black oat	58	High	3	-	-	73.60	0.12
Black oat	58	High	4	-	-	90.23	0.15



A.3.5: Tillage radish plants, *(Raphanus sativus)* grown in soil columns with dimensions of 85 cm depth, 17 cm width, packed to a bulk density of 1.5 g cm-3 with a soil mixture of Broughton clay loam soil 70%, Tunstall silver sand 30%, for 65 days.

Appendix Chapter 4

A.4.1 Ecoflora liaison emails

On 25 Nov 2015, at 14:13, Jasmine Burr-Hersey <stxjeb@nottingham.ac.uk> wrote:

Dear Henry,

Thanks so much for getting back to me so swiftly.

If it would be possible to obtain the root classification data en mass that would be brilliant. So far I have been manually going through selecting traits to try and cross compare species which have more than one trait present but it is proving to be a little time consuming. The characteristics im after would include; Root depth type 1, Root depth type 2 (Cm), Root hair length (mm), Root Hairs, Root persistence and Root system type. However is most convenient for you to select and relay this data would be great.

When you say the data has been taken from literature, are you referring to published papers or from text books/ guides etc? Do you have a list of the literature consulted? If so would it be possible to view this?

Thank you for passing on her contact address, I will indeed email Helen to see what additional information I can find out about the root catergorisation process.

Of course as my project progresses I would be more than happy to share with you any data I come across or collect personally. That is extremely interesting that you were developing a program so closely linked to my topic of research! I am hoping to use X-Ray CT to develop 3D visualisations of my plant roots but not entirely sure about the programs used to do so, but I will let you know how I get on.

Thanks again for getting back to me so quickly, greatly appreciated,

Jasmine

On 25 Nov 2015, at 16:32, Henry Ford < mailto:hen3ryford@googlemail.com> wrote:

OK will do,
root data en mass on its way, together with the sources - it varies, some are simply the floras, some are specific papers, but every data item has a source, even if it is only Stace interpreted by HF. I will check with Alastair to see if he has any more up to data data - in which case i will remonstrate with him for not telling me :-)

at a guess the data will be in this form

table one : species name, UID (my internal plant number so if you get more data I can upload id easily :0) ,trait number, trait name, trait value source number.
then in a separate tale source number, source details

As regards the programs : the x-ray ct scans are good way to visualise, but to understand the processes I think simulation would be a good idea. very zen. you have to become the root. I am afraid I use the granddaddy of simulation languages which is no longer generally available, but get hold of any object oriented language with good random number sequences (do borrow a statistician here as different random number sequences apply to different processes) and make sure tha death is a part of the process. This ensures that you are simulating the growth process, not just drawing the system as some applications of L-systems do.

I look forward to seeing your pictures.

I am in the middle of a data update at the moment. Give me a day or so. If the update goes well it will be done by the time I take the dog for a walk. If not I will be working tonight :-)

OK should be done by the end of the week.

H

From: Henry Ford [mailto:hen3ryford@googlemail.com]
Sent: 27 November 2015 12:08
To: Jasmine Burr-Hersey
Subject: Re: ecoflora data base enquiry- PhD student University of Nottingham

Jasmine,

here are the data in three tables
the species table: names , plant_no(the uid - the unique identifier), authority, family, genus and vernacular name
the data: plant_no(referring to the above); char_no, char_value, source_no (referring to below),char qual (generally an alternative value to char_value), subspecies (generally a qualifier or comment for char_value) and uk data (missing value assumes that it is uk data)

the source: source_no (uid, see above) authors, journal, year, volume, page_no, title1,2,3

I have given these in a csv format. so you can spreadsheet them or sql them. There are disappointingly little data in the system - I look forward to a healthy contribution from your PhD, which will of course be well acknowledged as a source :-) and if you find any sources at all, that you are not using do pass them my way. Again your contribution will be noted.

I hope I have done this correctly but anything else, just ask.

hope this helps, and enjoy your phd.

I look forward to hearing about it

Take care,
Henry

A.4.2 Weed experts liaison emails

From: Jasmine Burr-Hersey [stxjeb@nottingham.ac.uk]
Sent: 26 January 2016 10:18
To: r.j.froud-williams@reading.ac.uk
Subject: Scientific enquiry, PhD student at the University of Nottingham.

Dear Mr Froud-Williams

I am a first year PhD student at the University of Nottingham. I am researching root: soil interactions in non-crop species in relation to soil structural conditioning. So far my research has lead me to start investigating the potential utilisation of a number of weed species with relation to soil remediation (specifically looking at plants which have an ability to grow on heavily compacted soils). I am particularly interested in identifying tap-rooted species.

I have come across your work with weeds at the University of Reading and would firstly like to ask if you had come across any species which have a notable taproot or which grow in highly compacted soils. And secondly if you could advise on where I might be able to obtain a number of species seeds, specifically; Creeping Thistle (Cirsium arvense), (I have searched online and the Kew database but am particularly struggling to find this thistle species for sale).

Any help in this matter would be greatly appreciated,

Thanks,

Jasmine Burr-Hersey

From: Bob Froud-Williams [r.j.froud-williams@reading.ac.uk]
Sent: 28 January 2016 08:53
To: Jasmine Burr-Hersey
Subject: RE: Scientific enquiry, PhD student at the University of Nottingham.

Dear Jasmine,

thank you for your enquiry. I am now retired from the university, but for the moment retain my e-mail address.

Regarding weed seed suppliers I would recommend Herbiseed who are based at New Farm, Mire Lane, West End, Twyford, Berks, RG10 0NJ or may be contacted by telephone on 0189 349464. The proprietors are Vera and Martin Parham. Alternatively, you can go to www.herbiseed.com A word of caution concerning *Cirsium arvense* seed is that this species often produces a large quantity of non-viable seed, but I think that Herbiseed have an effective seed screening system. However, you may be better advised to work with vegetatively propagated root fragments. From experience lateral spread may amount to several metres within one year. Of course *Cirsium arvense* doesn't have a tap-root, but a series of horizontally and vertically creeping roots.

Regarding other weed species, those arable weeds with strong tap roots include *Aethusa cynapium* (fools parsley) *Chenopodium album* (fat-hen) *Matricaria* spp. (mayweeds) *Polygonum aviculare* (knotweed) and *Sonchus* spp(sowthistles).

Other less notable arable weeds with tap roots include *Arctium lappa* (burdock) *Dipsacus fullonum* (Teasel) *Lactuca serriola* (prickly lettuce) and *Rumex* spp (docks), but I suspect that you wouldn't be forgiven for propagating docks as there seeds are particularly persistent in the soil seedbank. An alternative grassland species is *Cichorum intybus* (Chicory), but you may consider this more of a crop species.

If you really want species of heavily consolidated soil such as farm gateways you could consider *Matricaria discoidea* (pineapple weed) or *Plantago* spp. (plantains).

I hope that this is of some value to you. Good luck with your studies. Who is supervising your project?

Bob Froud-Williams

From: Jasmine Burr-Hersey [stxjeb@nottingham.ac.uk]
Sent: 29 January 2016 11:02
To: r.j.froud-williams@reading.ac.uk
Subject: RE: Scientific enquiry, PhD student at the University of Nottingham.

Dear Bob,

Thank you for taking the time to reply to me, your expertise are invaluable in this sort of research.

Thank you for your advice about the propagation of Creeping thistle no doubt this may save me a considerable amount of time if the seeds I obtain do not germinate in the first instance.

A number of the species you have suggested I have in my 'short list' of desirable species including; *Matricaria discoidea* (pineapple weed), *Rumex* spp (docks) and *Cichorum intybus* (Chicory). The others which you have suggested I intend to do some further research into, and will hopefuly include some of this in my initial screen of species, thank you again for suggesting them to me in this instance.

My primary supervisor is Prof Karl Ritz at the University of Nottingham.

Once again I am grateful for your help,

Best wishes,

Jasmine

A.4.3: Herbiseed liaison emails

From: Jasmine Burr-Hersey [mailto:stxjeb@nottingham.ac.uk]
Sent: 16 May 2016 09:48
To: technical@herbiseed.com
Subject: Technical enquiry- PhD student University of Nottingham

To whom it may concern,

I am a first year PhD student at the University of Nottingham, studying novel plant species and their potential to remediate sites of heavily compacted land.

I am interested in purchasing a number of your weed species for experimental trials. Outlined below are the species I am hoping to order, I was hoping it would be possible for you to provide me with some additional information. Ideally I need at least 100 seeds of each species, on your website it suggests that the expected that around 60% of the seeds will be viable. As the orders are placed in grams of seed I was hoping you could suggest an approximate average number of grams of seed to order per species? Additionally I was wondering if any of the trials you conduct yourself feature testing species in compacted soils? If so, which species are you investigating? Finally if any of the below species have a particularly low germination rate or specific germination requirements please could you provide me with this information.

Species list:

-Creeping Thistle Cirsium arvense
-Curled Dock Rumex crispus
-Broad Leaf Dock Rumex obtusifolius
-Perineal Sow Thistle Sonchus arvensis
-Ribwort Plantain Plantago lanceolate
-Quak Grass Elymus repens
-Pineapple weed Matricaria discoidea
-Burdock Arctium lappa
-Common Lamsquartes Chenopodium albam

Thank you for your help,

Jasmine Burr-Hersey
University of Nottingham

From: Steve Morton [technical@herbiseed.com]
Sent: 16 May 2016 15:54
To: Jasmine Burr-Hersey
Subject: Technical enquiry- PhD student University of Nottingham

Hi Jasmine

I think we can help here – if you simply send your delivery address I will send you samples of all these species with germination details without charge. You can expect in excess of 80% emergence in all these species as research samples.

Apologies for stating the obvious from here on ....

Emergence in compact soils is not a problem, subsequent establishment and development are clearly the issues. Compact soils particularly from the surface present the biggest challenge to establishment, not only for root penetration but moisture retention. In these conditions the seed is effectively surface sown and prone to the highest fluctuations in available moisture. Once emerged root penetration in compact soil will stunt the plant development and often results in premature flowering and thus shortened life. This is the key factor as it restricts the substantial root development required for soil improvement.

I look forward to seeing how you get on !.

Please send you delivery address and we will have seed with you in a few days

Regards

Steve

T.4.1: Ecoflora output database generated from online database resource.

Latin name	Deep roots	Roots >100	Taproot	Adventitious root	Contractile root	Native	Mycohrrizal	Total
Cirsium arvense	1	1	1	1		1	1	6
Campanula rotundifolia	1		1	1		1	1	5
Chamaenerion angustifoliu	1		1	1		1	1	5
Epilobium angustifolium	1		1	1		1	1	5
Equisetum sylvaticum	1	1		1		1	1	5
Equisetum telmateia	1	1		1		1	1	5
Equisetum variegatum	1	1		1		1	1	5
Galium verum	1	1	1			1	1	5
Helianthemum canum	1	1	1			1	1	5
Lathyrus japonicus	1	1	1			1	1	5
Lotus corniculatus	1	1	1			1	1	5
Ononis repens	1	1	1			1	1	5
Plantago lanceolata	1		1	1		1	1	5
Potentilla anserina	1		1	1		1	1	5
Pulsatilla vulgaris	1		1	1		1	1	5
Rumex crispus	1	1	1			1	1	5
Rumex obtusifolius	1	1	1			1	1	5
Sonchus arvensis	1	1	1			1	1	5
Cynoglossum officinale	1	1	1			1		4
Equisetum arvense	1	1		1			1	4
Equisetum fluviatile	1	1		1		1		4
Equisetum hyemale	1	1		1		1		4
Equisetum palustre	1	1		1			1	4
Equisetum pratense	1	1		1		1		4
Equisetum ramosissimum	1	1		1		1		4
Hypochaeris maculata	1		1		1	1		4
Melilotus albus	1		1	1			1	4
Onobrychis viciifolia	1	1	1				1	4
Ulex gallii	1		1	1		1		4
Campanula giesekiana	1		1	1				3
Elymus repens	1	1		1				3
Endymion non-scriptus	1			1	1			3
Lathyrus maritimus	1	1	1					3
Lepidium draba	1	1	1					3
Melilotus alba	1		1	1				3
Thymus drucei	1	1		1				3
Thymus polytrichus	1	1		1				3
Thymus praecox	1	1		1				3

T.4.2: Plant germination database detailing germination conditions and success rate (part 1)

Species			Growth conditions								Germination result	
Common name	Scientific name	Provider	Medium		Temp	Moisture	Location	Light	Days	Other	Germinated	%
Tillage radish	Raphanus sativus	Frontier Agriculture	Petri dish	Seed	18	Moist	Desk draw	Dark	2	-	9	90
Tillage radish	Raphanus sativus	Frontier Agriculture	Petri dish	Seed	22	Moist	Soil prep room	Dark	2	-	8	80
Tillage radish	Raphanus sativus	Frontier Agriculture	Petri dish	Seed	26	Moist	Furnace	Dark	2	-	6	60
Horsetail	Equisetum	Self obtained	Soil column	Rhizome	20	16%	Hounsfield glasshouse	Day/ night re	14	-	0	0
Couch grass	Elymus repens	Self obtained	Soil column	Rhizome	20	16%	Hounsfield glasshouse	Day/ night re	14	-	2	24
Couch grass	Elymus repens	Herbiseed	Petri dish	Seed	19	Moist	Soil prep room	Dark	4	-	0	0
Couch grass	Elymus repens	Herbiseed	Petri dish	Seed	19	Moist	Soil prep room	Dark	4	Vernalised	0	0
Couch grass	Elymus repens	Herbiseed	Petri dish	Seed	25	Moist	Growth room	Dark	5	-	0	0
Couch grass	Elymus repens	Herbiseed	Petri dish	Seed	25	Moist	Growth room	Dark	5	Vernalised	0	0
Couch grass	Elymus repens	Herbiseed	Petri dish	Seed	27	Moist	Furnace	Dark	10	-	0	0
Couch grass	Elymus repens	Herbiseed	Petri dish	Seed	27	Moist	Furnace	Dark	10	Vernalised	0	0
Dandelion (D1)	-	Self obtained	Petri dish	Seed	19	Moist	Soil prep room	Dark	4	-	0	0
Dandelion (D1)	-	Self obtained	Petri dish	Seed	19	Moist	Soil prep room	Dark	4	Vernalised	0	0
Dandelion (D1)	-	Self obtained	Petri dish	Seed	20	Moist	Hounsfield glasshouse	Day/ night re	4	-	0	0
Dandelion (D1)	-	Self obtained	Soil column	Seed	20	Moist	Hounsfield glasshouse	Day/ night re	28	-	1	10
Dandelion (D1)	-	Self obtained	Petri dish	Seed	27	Moist	Muffle Furnace	Dark	4	-	0	0
Dandelion (D1)	-	Self obtained	Petri dish	Seed	27	Moist	Muffle Furnace	Dark	4	Vernalised	0	0
Dandelion (D2)		Yellow Flag Wild Flowers	Petri dish	Seed	19	Moist	Soil prep room	Dark	4	-	0	0
Dandelion (D2)	-	Yellow Flag Wild Flowers	Petri dish	Seed	19	Moist	Soil prep room	Dark	4	Vernalised	0	0
Dandelion (D2)	-	Yellow Flag Wild Flowers	Soil column	Seed	20	Moist	Hounsfield glasshouse	Day/ night re	28	-	0	0
Dandelion (D2)	-	Yellow Flag Wild Flowers	Soil column	Seed	20	Moist	Hounsfield glasshouse	Day/ night re	4	Vernalised	0	0
Dandelion (D2)	-	Yellow Flag Wild Flowers	Petri dish	Seed	27	Moist	Muffle Furnace	Dark	4	-	0	0
Dandelion (D2)	-	Yellow Flag Wild Flowers	Petri dish	Seed	27	Moist	Muffle Furnace	Dark	4	Vernalised	0	0
Dandelion (D2)	-	Yellow Flag Wild Flowers	Petri dish	Seed	27	Moist	Muffle Furnace	Dark	10	Scarified	0	0
Dandelion (D2)	-	Yellow Flag Wild Flowers	Petri dish	Seed	27	Moist	Muffle Furnace	Dark	10	Vernalised/ Scarified	0	0
Dandelion (D3)	-	Self obtained	Petri dish	Seed	19	Moist	Soil prep room	Dark	4	-	6	60
Dandelion (D3)	-	Self obtained	Petri dish	Seed	20	Moist	Hounsfield glasshouse	Day/ night re	4	-	0	0
Dandelion (D3)	-	Self obtained	Soil column	Seed	20	Moist	Hounsfield glasshouse	Day/ night re	28	-	2	20
Dandelion (D3)	-	Self obtained	Petri dish	Seed	27	Moist	Muffle Furnace	Dark	4	-	0	0
Dandelion (D3)	-	Self obtained	Petri dish	Seed	27	Moist	Muffle Furnace	Dark	10	-	0	0
Dandelion (D4)	-	Self obtained	Petri dish	Seed	19	Moist	Soil prep room	Dark	4	-	3	30
Dandelion (D4)	-	Self obtained	Petri dish	Seed	20	Moist	Hounsfield glasshouse	Day/ night re	4	-	0	0
Dandelion (D4)	-	Self obtained	Soil column	Seed	20	Moist	Hounsfield glasshouse	Day/ night re	28	-	0	0
Dandelion (D4)	-	Self obtained	Petri dish	Seed	27	Moist	Muffle Furnace	Dark	4	-	0	0
Dandelion (D4)	-	Self obtained	Petri dish	Seed	27	Moist	Muffle Furnace	Dark	10	-	0	0
Thistle (T1)	-	Self obtained	Petri dish	Seed	19	Moist	Soil prep room	Dark	4	-	6	60
Thistle (T1)	-	Self obtained	Petri dish	Seed	20	Moist	Hounsfield glasshouse	Day/ night re	4	-	0	0
Thistle (T1)	-	Self obtained	Soil column	Seed	20	Moist	Hounsfield glasshouse	Day/ night re	28	-	7	70
Thistle (T1)	-	Self obtained	Petri dish	Seed	27	Moist	Muffle Furnace	Dark	4	-	0	0
Thistle (T2)	-	Self obtained	Petri dish	Seed	19	Moist	Soil prep room	Dark	4	-	0	0
Thistle (T2)	-	Self obtained	Petri dish	Seed	19	Moist	Soil prep room	Dark	4	Vernalised	0	0
Thistle (T2)	-	Self obtained	Petri dish	Seed	20	Moist	Hounsfield glasshouse	Day/ night re	4	-	0	0
Thistle (T2)	-	Self obtained	Petri dish	Seed	20	Moist	Hounsfield glasshouse	Day/ night re	28	Vernalised	0	0
Thistle (T2)	-	Self obtained	Soil column	Seed	20	Moist	Hounsfield glasshouse	Day/ night re	28	-	0	0
Thistle (T2)	-	Self obtained	Soil column	Seed	20	Moist	Hounsfield glasshouse	Day/ night re	4	Vernalised	0	0
Thistle (T2)	-	Self obtained	Petri dish	Seed	27	Moist	Muffle Furnace	Dark	4	-	0	0
Thistle (T2)	-	Self obtained	Petri dish	Seed	27	Moist	Muffle Furnace	Dark	4	Vernalised	0	0
Thistle (T2)	-	Self obtained	Petri dish	Seed	27	Moist	Muffle Furnace	Dark	10	Scarified	0	0
Thistle (T2)	-	Self obtained	Petri dish	Seed	27	Moist	Muffle Furnace	Dark	10	Vernalised/ Scarified	0	0
Creeping thistle	Cirsium arvense	Herbiseed	Petri dish	Seed	19	Moist	Soil prep room	Dark	4	-	0	0
Creeping thistle	Cirsium arvense	Herbiseed	Petri dish	Seed	19	Moist	Soil prep room	Dark	4	Vernalised	0	0
Creeping thistle	Cirsium arvense	Herbiseed	Petri dish	Seed	20	Moist	Hounsfield glasshouse	Day/ night re	4	-	0	0
Creeping thistle	Cirsium arvense	Herbiseed	Petri dish	Seed	20	Moist	Hounsfield glasshouse	Day/ night re	28	Vernalised	0	0
Creeping thistle	Cirsium arvense	Herbiseed	Soil column	Seed	20	Moist	Hounsfield glasshouse	Day/ night re	28	-	0	0
Creeping thistle	Cirsium arvense	Herbiseed	Soil column	Seed	20	Moist	Hounsfield glasshouse	Day/ night re	4	Vernalised	0	0
Creeping thistle	Cirsium arvense	Herbiseed	Petri dish	Seed	27	Moist	Muffle Furnace	Dark	4	-	0	0
Creeping thistle	Cirsium arvense	Herbiseed	Petri dish	Seed	27	Moist	Muffle Furnace	Dark	4	Vernalised	0	0
Creeping thistle	Cirsium arvense	Herbiseed	Petri dish	Seed	27	Moist	Muffle Furnace	Dark	10	Scarified	0	0
Creeping thistle	Cirsium arvense	Herbiseed	Petri dish	Seed	27	Moist	Muffle Furnace	Dark	10	Vernalised/ Scarified	0	0
Pineapple weed	Matricaria discoidea	Herbiseed	Petri dish	Seed	19	Moist	Soil prep room	Dark	4	-	0	0
Pineapple weed	Matricaria discoidea	Herbiseed	Petri dish	Seed	19	Moist	Soil prep room	Dark	4	Vernalised	0	0
Pineapple weed	Matricaria discoidea	Herbiseed	Petri dish	Seed	20	Moist	Hounsfield glasshouse	Day/ night re	4	-	0	0
Pineapple weed	Matricaria discoidea	Herbiseed	Petri dish	Seed	20	Moist	Hounsfield glasshouse	Day/ night re	4	Vernalised	0	0
Pineapple weed	Matricaria discoidea	Herbiseed	Soil column	Seed	20	Moist	Hounsfield glasshouse	Day/ night re	28	-	1	10
Pineapple weed	Matricaria discoidea	Herbiseed	Soil column	Seed	20	Moist	Hounsfield glasshouse	Day/ night re	28	Vernalised	0	0
Pineapple weed	Matricaria discoidea	Herbiseed	Petri dish	Seed	25	Moist	Growth room	Dark	4	-	0	0
Pineapple weed	Matricaria discoidea	Herbiseed	Petri dish	Seed	25	Moist	Growth room	Dark	4	Vernalised	0	0
Pineapple weed	Matricaria discoidea	Herbiseed	Petri dish	Seed	27	Moist	Muffle Furnace	Dark	4	-	0	0
Pineapple weed	Matricaria discoidea	Herbiseed	Petri dish	Seed	27	Moist	Muffle Furnace	Dark	4	Vernalised	0	0
Pineapple weed	Matricaria discoidea	Herbiseed	Petri dish	Seed	27	Moist	Muffle Furnace	Dark	10	Scarified	0	0
Pineapple weed	Matricaria discoidea	Herbiseed	Petri dish	Seed	27	Moist	Muffle Furnace	Dark	10	Vernalised/ Scarified	0	0
Ribwort plantain	Plantago lanceloata	Herbiseed	Petri dish	Seed	19	Moist	Soil prep room	Dark	4	-	7	70
Ribwort plantain	Plantago lanceloata	Herbiseed	Petri dish	Seed	19	Moist	Soil prep room	Dark	4	Vernalised	5	50
Ribwort plantain	Plantago lanceloata	Herbiseed	Petri dish	Seed	20	Moist	Hounsfield glasshouse	Day/ night re	4	-	0	0
Ribwort plantain	Plantago lanceloata	Herbiseed	Petri dish	Seed	20	Moist	Hounsfield glasshouse	Day/ night re	4	Vernalised	0	0
Ribwort plantain	Plantago lanceloata	Herbiseed	Soil column	Seed	20	Moist	Hounsfield glasshouse	Day/ night re	28	-	6	60
Ribwort plantain	Plantago lanceloata	Herbiseed	Soil column	Seed	20	Moist	Hounsfield glasshouse	Day/ night re	28	Vernalised	4	40
Ribwort plantain	Plantago lanceloata	Herbiseed	Petri dish	Seed	25	Moist	Growth room	Dark	4	-	0	0
Ribwort plantain	Plantago lanceloata	Herbiseed	Petri dish	Seed	25	Moist	Growth room	Dark	4	Vernalised	0	0
Ribwort plantain	Plantago lanceloata	Herbiseed	Petri dish	Seed	27	Moist	Muffle Furnace	Dark	4	-	0	0
Ribwort plantain	Plantago lanceloata	Herbiseed	Petri dish	Seed	27	Moist	Muffle Furnace	Dark	4	Vernalised	0	0
Ribwort plantain	Plantago lanceloata	Herbiseed	Petri dish	Seed	27	Moist	Muffle Furnace	Dark	10	Scarified	0	0
Ribwort plantain	Plantago lanceloata	Herbiseed	Petri dish	Seed	27	Moist	Muffle Furnace	Dark	10	Vernalised/ Scarified	0	0

T.4.2: Plant germination database detailing germination conditions and success rate (part 2).

Species			Growth conditions								Germination result	
Common name	Scientific name	Provider	Medium		Temp	Moisture	Location	Light	Days	Other	Germinated	%
Plantain	-	Self obtained	Petri dish	Seed	19	Moist	Soil prep room	Dark	4	-	0	0
Plantain	-	Self obtained	Petri dish	Seed	19	Moist	Soil prep room	Dark	4	Vernalised	0	0
Plantain	-	Self obtained	Petri dish	Seed	20	Moist	Hounsfield glasshouse	Day/ night re	4	-	0	0
Plantain	-	Self obtained	Petri dish	Seed	20	Moist	Hounsfield glasshouse	Day/ night re	28	Vernalised	0	0
Plantain	-	Self obtained	Soil column	Seed	20	Moist	Hounsfield glasshouse	Day/ night re	28	-	0	0
Plantain	-	Self obtained	Soil column	Seed	20	Moist	Hounsfield glasshouse	Day/ night re	4	Vernalised	0	0
Plantain	-	Self obtained	Petri dish	Seed	27	Moist	Muffle Furnace	Dark	4	-	0	0
Plantain	-	Self obtained	Petri dish	Seed	27	Moist	Muffle Furnace	Dark	4	Vernalised	0	0
Plantain	-	Self obtained	Petri dish	Seed	27	Moist	Muffle Furnace	Dark	10	Scarified	0	0
Plantain	-	Self obtained	Petri dish	Seed	27	Moist	Muffle Furnace	Dark	10	Vernalised/ Scarified	0	0
Greater burdock	Arctium lappa	Herbiseed	Petri dish	Seed	19	Moist	Soil prep room	Dark	4	-	0	0
Greater burdock	Arctium lappa	Herbiseed	Petri dish	Seed	19	Moist	Soil prep room	Dark	4	Vernalised	0	0
Greater burdock	Arctium lappa	Herbiseed	Petri dish	Seed	20	Moist	Hounsfield glasshouse	Day/ night re	4	-	0	0
Greater burdock	Arctium lappa	Herbiseed	Petri dish	Seed	20	Moist	Hounsfield glasshouse	Day/ night re	4	Vernalised	0	0
Greater burdock	Arctium lappa	Herbiseed	Soil column	Seed	20	Moist	Hounsfield glasshouse	Day/ night re	28	-	0	0
Greater burdock	Arctium lappa	Herbiseed	Soil column	Seed	20	Moist	Hounsfield glasshouse	Day/ night re	28	Vernalised	0	0
Greater burdock	Arctium lappa	Herbiseed	Petri dish	Seed	25	Moist	Growth room	Dark	4	-	0	0
Greater burdock	Arctium lappa	Herbiseed	Petri dish	Seed	25	Moist	Growth room	Dark	4	Vernalised	0	0
Greater burdock	Arctium lappa	Herbiseed	Petri dish	Seed	27	Moist	Muffle Furnace	Dark	4	-	0	0
Greater burdock	Arctium lappa	Herbiseed	Petri dish	Seed	27	Moist	Muffle Furnace	Dark	4	Vernalised	0	0
Greater burdock	Arctium lappa	Herbiseed	Petri dish	Seed	27	Moist	Muffle Furnace	Dark	10	Scarified	0	0
Greater burdock	Arctium lappa	Herbiseed	Petri dish	Seed	27	Moist	Muffle Furnace	Dark	10	Vernalised/ Scarified	0	0
Sow thistle	Sonchus oleraceus	Herbiseed	Petri dish	Seed	19	Moist	Soil prep room	Dark	4	-	7	70
Sow thistle	Sonchus oleraceus	Herbiseed	Petri dish	Seed	19	Moist	Soil prep room	Dark	4	Vernalised	0	0
Sow thistle	Sonchus oleraceus	Herbiseed	Petri dish	Seed	20	Moist	Hounsfield glasshouse	Day/ night re	4	-	0	0
Sow thistle	Sonchus oleraceus	Herbiseed	Petri dish	Seed	20	Moist	Hounsfield glasshouse	Day/ night re	4	Vernalised	0	0
Sow thistle	Sonchus oleraceus	Herbiseed	Soil column	Seed	20	Moist	Hounsfield glasshouse	Day/ night re	28	-	0	0
Sow thistle	Sonchus oleraceus	Herbiseed	Soil column	Seed	20	Moist	Hounsfield glasshouse	Day/ night re	28	Vernalised	0	0
Sow thistle	Sonchus oleraceus	Herbiseed	Petri dish	Seed	25	Moist	Growth room	Dark	4	-	0	0
Sow thistle	Sonchus oleraceus	Herbiseed	Petri dish	Seed	25	Moist	Growth room	Dark	4	Vernalised	0	0
Sow thistle	Sonchus oleraceus	Herbiseed	Petri dish	Seed	27	Moist	Muffle Furnace	Dark	4	-	0	0
Sow thistle	Sonchus oleraceus	Herbiseed	Petri dish	Seed	27	Moist	Muffle Furnace	Dark	4	Vernalised	0	0
Sow thistle	Sonchus oleraceus	Herbiseed	Petri dish	Seed	27	Moist	Muffle Furnace	Dark	10	Scarified	0	0
Sow thistle	Sonchus oleraceus	Herbiseed	Petri dish	Seed	27	Moist	Muffle Furnace	Dark	10	Vernalised/ Scarified	0	0
Broad leaf dock	Rumex onstusifolius	Herbiseed	Petri dish	Seed	19	Moist	Soil prep room	Dark	4	-	0	0
Broad leaf dock	Rumex onstusifolius	Herbiseed	Petri dish	Seed	19	Moist	Soil prep room	Dark	4	Vernalised	0	0
Broad leaf dock	Rumex onstusifolius	Herbiseed	Petri dish	Seed	20	Moist	Hounsfield glasshouse	Day/ night re	4	-	0	0
Broad leaf dock	Rumex onstusifolius	Herbiseed	Petri dish	Seed	20	Moist	Hounsfield glasshouse	Day/ night re	4	Vernalised	0	0
Broad leaf dock	Rumex onstusifolius	Herbiseed	Soil column	Seed	20	Moist	Hounsfield glasshouse	Day/ night re	28	-	0	0
Broad leaf dock	Rumex onstusifolius	Herbiseed	Soil column	Seed	20	Moist	Hounsfield glasshouse	Day/ night re	28	Vernalised	0	0
Broad leaf dock	Rumex onstusifolius	Herbiseed	Petri dish	Seed	25	Moist	Growth room	Dark	4	-	0	0
Broad leaf dock	Rumex onstusifolius	Herbiseed	Petri dish	Seed	25	Moist	Growth room	Dark	4	Vernalised	0	0
Broad leaf dock	Rumex onstusifolius	Herbiseed	Petri dish	Seed	27	Moist	Muffle Furnace	Dark	4	-	0	0
Broad leaf dock	Rumex onstusifolius	Herbiseed	Petri dish	Seed	27	Moist	Muffle Furnace	Dark	4	Vernalised	0	0
Broad leaf dock	Rumex onstusifolius	Herbiseed	Petri dish	Seed	27	Moist	Muffle Furnace	Dark	10	Scarified	0	0
Broad leaf dock	Rumex onstusifolius	Herbiseed	Petri dish	Seed	27	Moist	Muffle Furnace	Dark	10	Vernalised/ Scarified	0	0
Curly dock	Rumex crispus	Herbiseed	Petri dish	Seed	19	Moist	Soil prep room	Dark	4	-	0	0
Curly dock	Rumex crispus	Herbiseed	Petri dish	Seed	19	Moist	Soil prep room	Dark	4	Vernalised	0	0
Curly dock	Rumex crispus	Herbiseed	Petri dish	Seed	20	Moist	Hounsfield glasshouse	Day/ night re	4	-	0	0
Curly dock	Rumex crispus	Herbiseed	Petri dish	Seed	20	Moist	Hounsfield glasshouse	Day/ night re	4	Vernalised	0	0
Curly dock	Rumex crispus	Herbiseed	Soil column	Seed	20	Moist	Hounsfield glasshouse	Day/ night re	28	-	0	0
Curly dock	Rumex crispus	Herbiseed	Soil column	Seed	20	Moist	Hounsfield glasshouse	Day/ night re	28	Vernalised	0	0
Curly dock	Rumex crispus	Herbiseed	Petri dish	Seed	25	Moist	Growth room	Dark	4	-	0	0
Curly dock	Rumex crispus	Herbiseed	Petri dish	Seed	25	Moist	Growth room	Dark	4	Vernalised	0	0
Curly dock	Rumex crispus	Herbiseed	Petri dish	Seed	27	Moist	Muffle Furnace	Dark	4	-	0	0
Curly dock	Rumex crispus	Herbiseed	Petri dish	Seed	27	Moist	Muffle Furnace	Dark	4	Vernalised	0	0
Curly dock	Rumex crispus	Herbiseed	Petri dish	Seed	27	Moist	Muffle Furnace	Dark	10	Scarified	0	0
Curly dock	Rumex crispus	Herbiseed	Petri dish	Seed	27	Moist	Muffle Furnace	Dark	10	Vernalised/ Scarified	0	0
Dock leave	-	Self obtained	Petri dish	Seed	19	Moist	Soil prep room	Dark	4	-	0	0
Dock leave	-	Self obtained	Petri dish	Seed	19	Moist	Soil prep room	Dark	4	Vernalised	0	0
Dock leave	-	Self obtained	Petri dish	Seed	20	Moist	Hounsfield glasshouse	Day/ night re	4	-	0	0
Dock leave	-	Self obtained	Petri dish	Seed	20	Moist	Hounsfield glasshouse	Day/ night re	4	Vernalised	0	0
Dock leave	-	Self obtained	Soil column	Seed	20	Moist	Hounsfield glasshouse	Day/ night re	28	-	0	0
Dock leave	-	Self obtained	Soil column	Seed	20	Moist	Hounsfield glasshouse	Day/ night re	28	Vernalised	0	0
Dock leave	-	Self obtained	Petri dish	Seed	25	Moist	Growth room	Dark	4	-	0	0
Dock leave	-	Self obtained	Petri dish	Seed	25	Moist	Growth room	Dark	4	Vernalised	0	0
Dock leave	-	Self obtained	Petri dish	Seed	27	Moist	Muffle Furnace	Dark	4	-	0	0
Dock leave	-	Self obtained	Petri dish	Seed	27	Moist	Muffle Furnace	Dark	4	Vernalised	0	0
Dock leave	-	Self obtained	Petri dish	Seed	27	Moist	Muffle Furnace	Dark	10	Scarified	0	0
Dock leave	-	Self obtained	Petri dish	Seed	27	Moist	Muffle Furnace	Dark	10	Vernalised/ Scarified	0	0

A.4.4 VG Studio root segmentation method

Open VG Studio and select a project to open. Once the file has loaded select the volume to work on from the Scene tree tab. Next scroll through the image stack and find an area you know to be plant root. Use the region grower tool to select an area of root, adjust the tolerance search values to an appropriate range, ensure the tool is set to dynamic mode and is ignoring other visible ROI's. Click on the area of root and add it to a new region of interest. Name the region 'Root' in the Scene tree tab. Continue to click on areas of root and add them to the same region. To visualise the root system in 3D turn the transparency to 100.

A.4.5 RooTrak root segmentation method

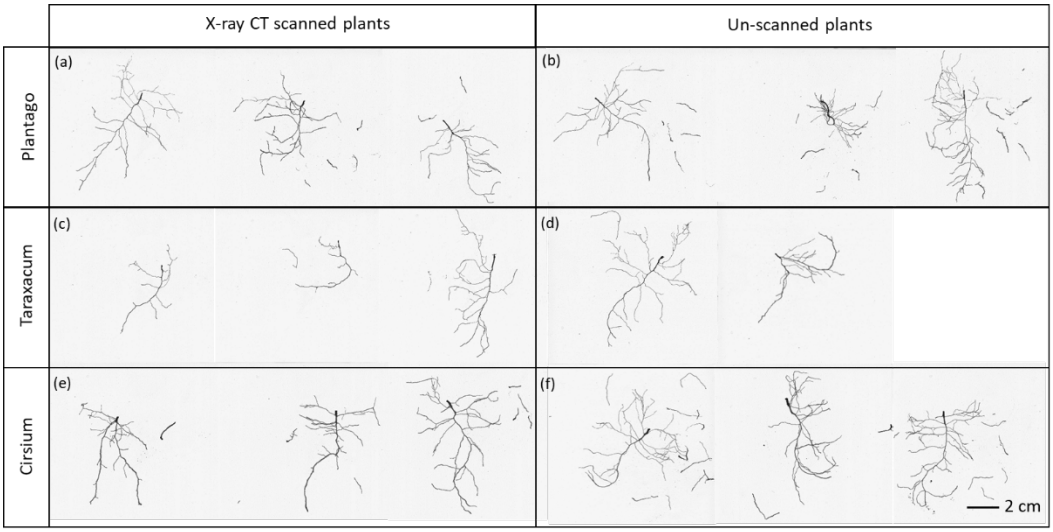
Ensure the image stack you want to work on is saved as a .raw for input into RooTrak. To load the file select tools, tracker, load .vgl raw file. Next select the output save directory file folder. Select a seed point to start the segmentation. Skip through the top section of the image stack and find the first slice that contains root (usually the taproot). Select this root as the start seed point. Next set the tolerance values smoothness and similarity. The smoothness parameter has the greatest effect on small objects and works as a noise control mechanism. The similarity parameter takes into account the greyscale values of the three surround pixels and determines how similar they are to the original and whether to class them as root. Once the parameters

are set, start the tracking algorthim. This will work its way down through the image stack determining if pixels hold the same grey value as the ones determined as root from the previous slice. Once the program reaches the bottom of the stack, save the output file. This can then be viewed in the RooTrak dashboard to visualise the root system and obtain quantitative parameters about the system, such as volume (cm^3), surface area (cm^2) total root depth (cm), total root width (cm) and convex hull (cm^3).

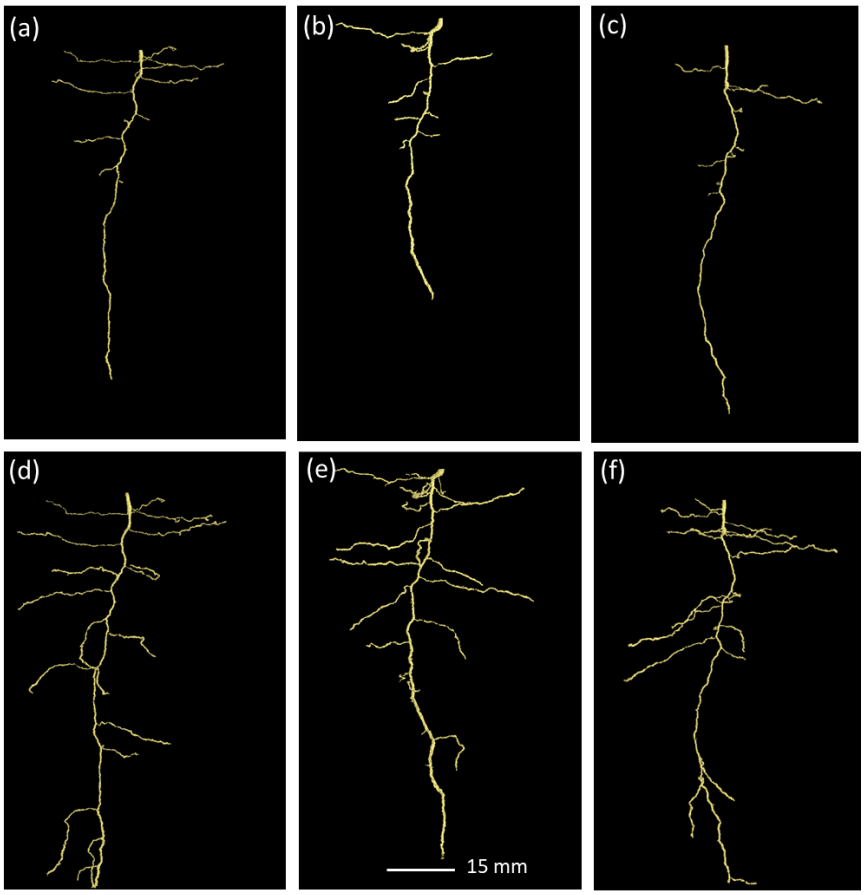
A.4.6 Rooth image analysis method

Using the control panel select the.bmp file to import into the program using file> open. Once the file is loaded select 'Analyse'. The program will have now identified the root skeleton (Figure 4.6b) and the root order must now be checked. Root number 1 will be allocated to the primary root (in this case the taproot) (Figure 4.6c). To check the root pathway use the mouse wheel to scroll down the root and use the arrow keys to change path if necessary. At this stage the root colouration key as is follows; Green is the confirmed selected section of root, Red is the unselected section which suggests the root pathway (Figure 4.6d&e). If you do not agree with the selected root pathway you have the option to reassign it. Here Blue is the unselected alternate navigation path and Yellow is the selected navigation option (Figure 4.6f). Use the arrow keys to choose between the Blue and Yellow paths and press enter when you have selected the correct root pathway. Once you have confirmed the primary taproot root pathway you can then allocate each of the lateral

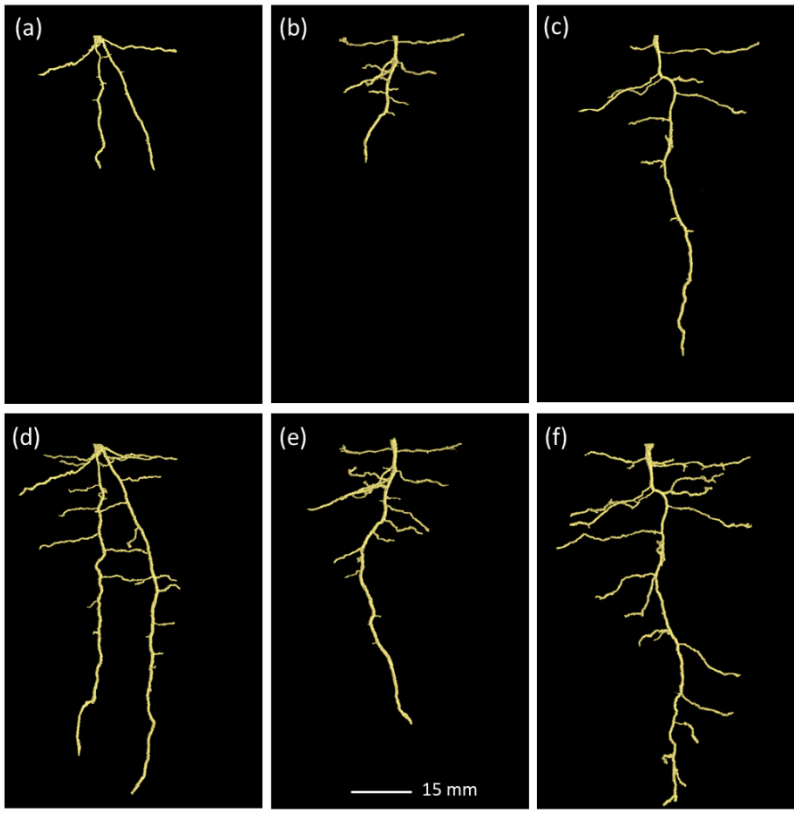
roots a root number using the same process. Once the root system is correctly connected the program is able to generate root specific data. To do this select the 'Snakes' tab. Select 'Tools' and 'Combine Side Sweeps' (Figure 4.6g&h). This combines control points from different sweep orientations which feed into the active contour model. An example of the fitted contour model can be seen in Figure 4.6i. Once the contours are fitted to the root skeleton can exported in *.RSML file format for further analysis including extraction of local root trait data.



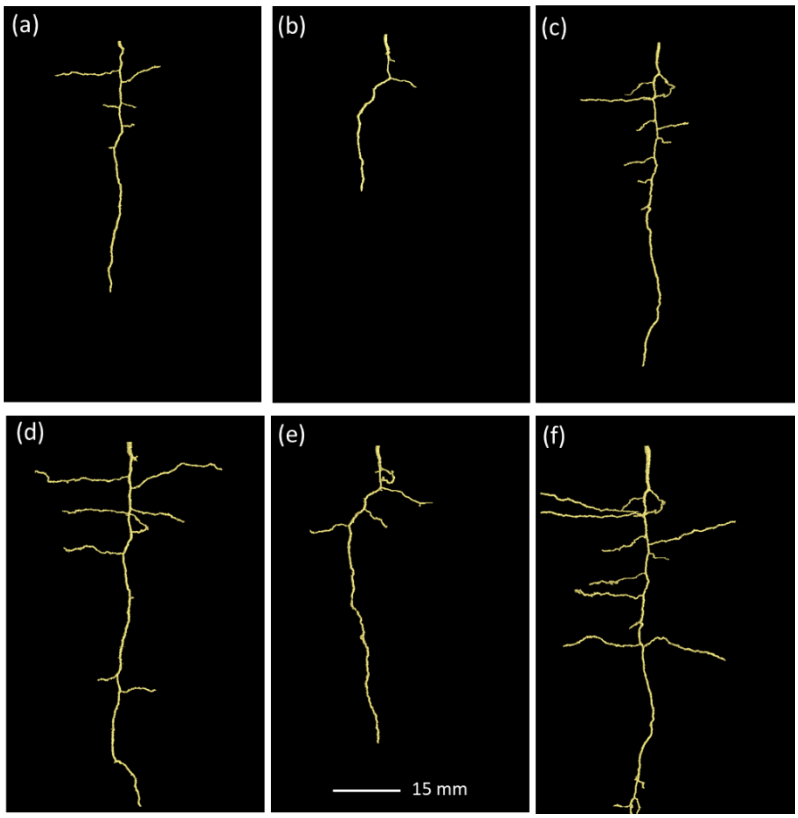
A 4.7: 2D images of novel species grown for 28 days scanned using WinRHIZO. (a) Plantago, (c) Taraxacum, (e) Cirsium plants all subject to x-ray CT. (b) Plantago, (d) Taraxacum, (f) Cirsium plants not subject to x-ray CT.



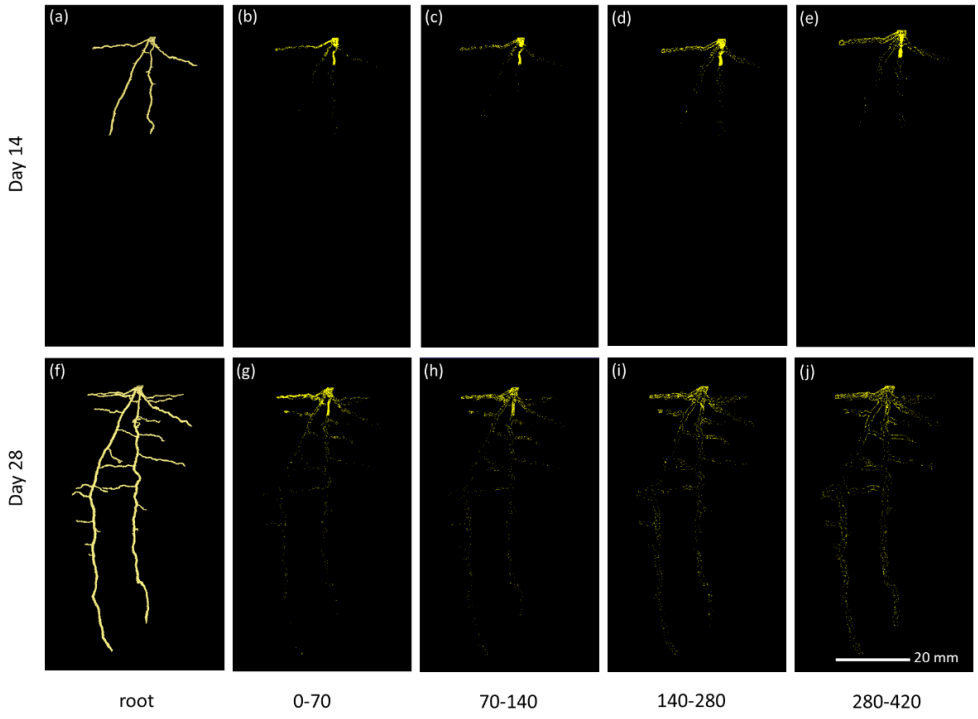
A.4.8: X-ray CT visualisations of Plantago plants (a-c) grown for 14 days, (d-f) grown for 28 days. Visualised using VG Studio Max V.2.2.



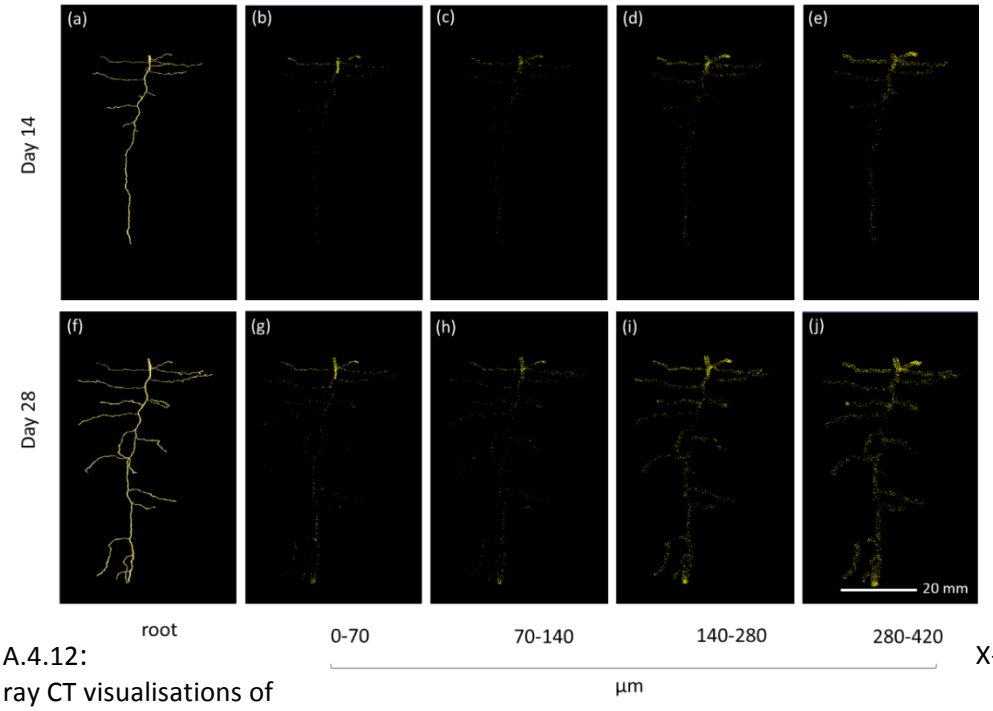
A 4.9: X-ray CT visualisations of Cirsium plants (a-c) grown for 14 days, (d-f) grown for 28 days. Visualised using VG Studio Max V.2.2.



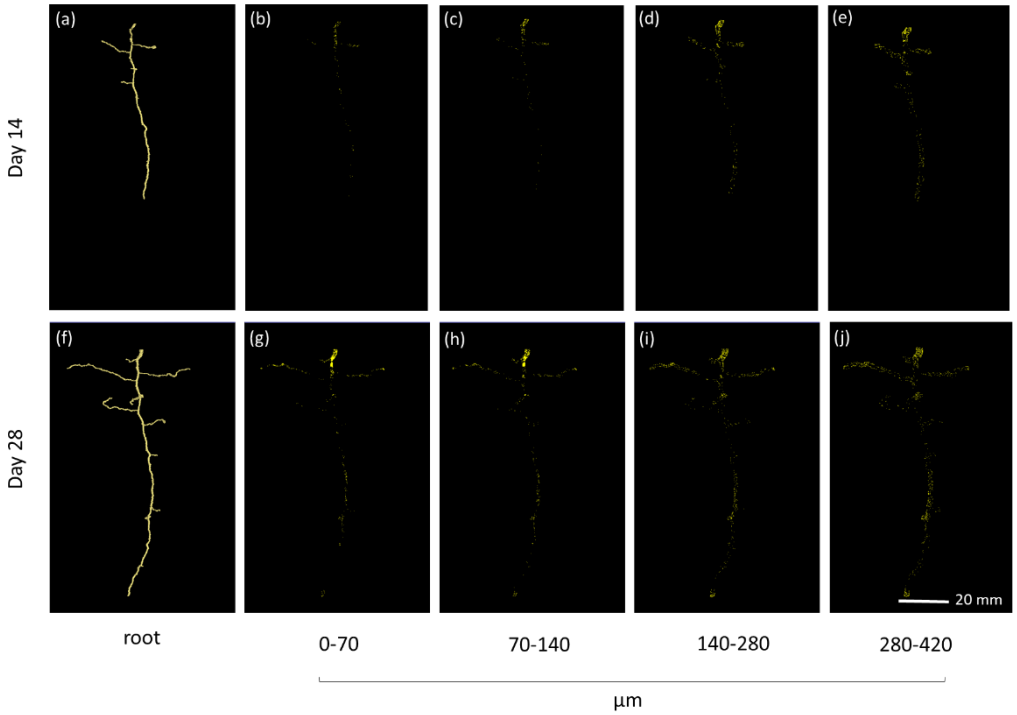
A 4.10: X-ray CT visualisations of Taraxacum plants (a-c) grown for 14 days, (d-f) grown for 28 days. Visualised using VG Studio Max V.2.2.



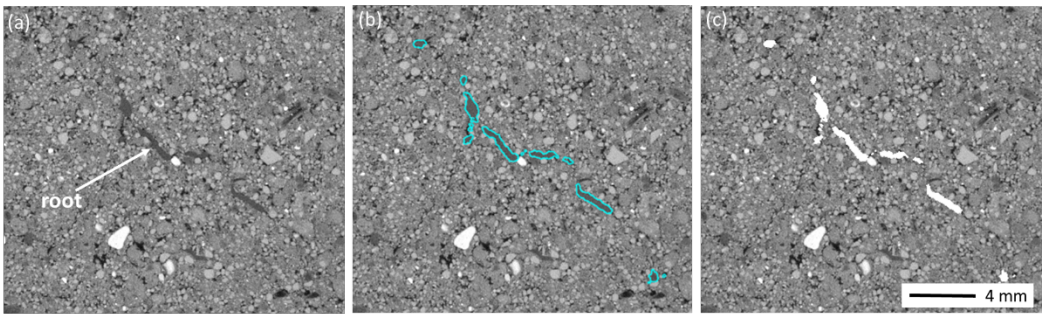
A.4.11: X-ray CT visualisations of Cirsium plants (a) grown for 14 days, (f) grown for 28 days. (b-e) and (g-j) visualisation of soil pore space with distance from the root surface at 0-70, 70-140, 140-280 and 280-420 µm. Visualised using VG Studio Max V.2.2.



A.4.12: X-ray CT visualisations of Plantago plants (a) grown for 14 days, (f) grown for 28 days. (b-e) and (g-j) visualisation of soil pore space with distance from the root surface at 0-70, 70-140, 140-280 and 280-420 µm. Visualised using VG Studio Max V.2.2.

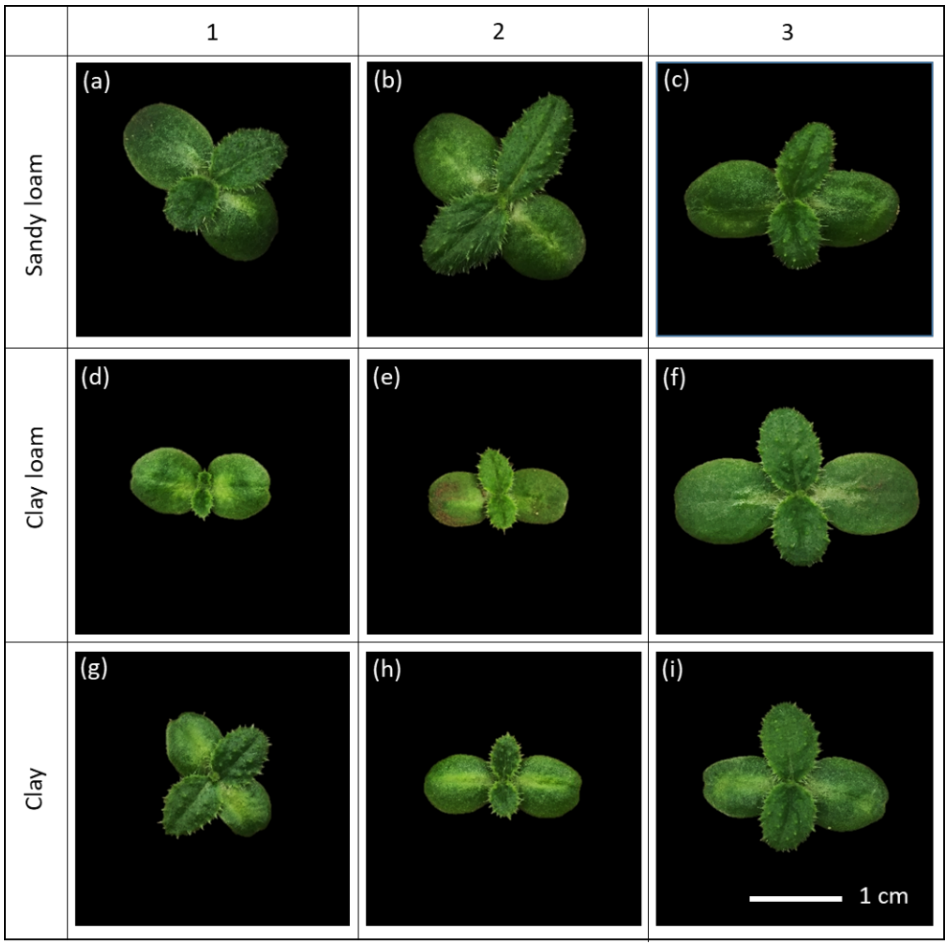


A.4.13: X-ray CT visualisations of Taraxacum plants (a) grown for 14 days, (f) grown for 28 days. (b-e) and (g-j) visualisation of soil pore space with distance from the root surface at 0-70, 70-140, 140-280 and 280-420 µm. Visualised using VG Studio Max V.2.2.

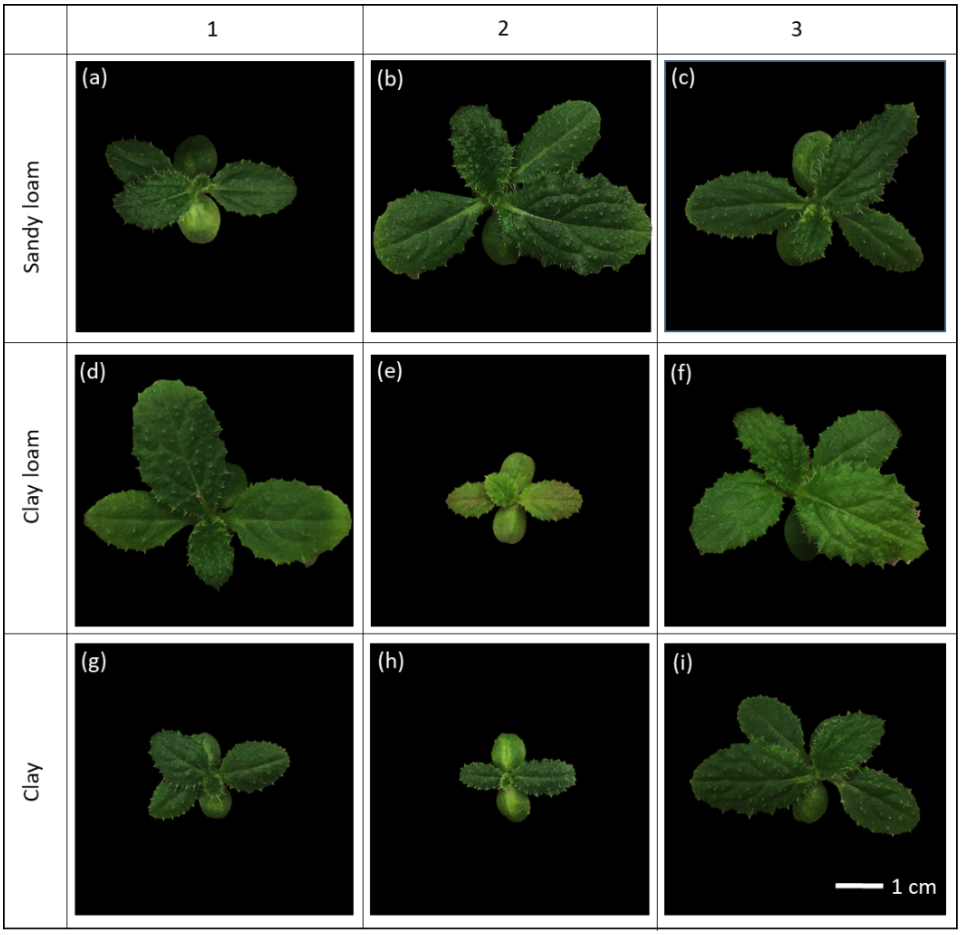


A.4.14: Example or Root Mask for *Cirsium* at Day 14 overlaying greyscale soil imagery for soil porosity calculation. (a) Original grey scale image, (b) Segmented root system highlighted by blue outline, (c) White root mask overlaying original greyscale image. Images generated using Visual Graphics StudioMAX V2.2.3

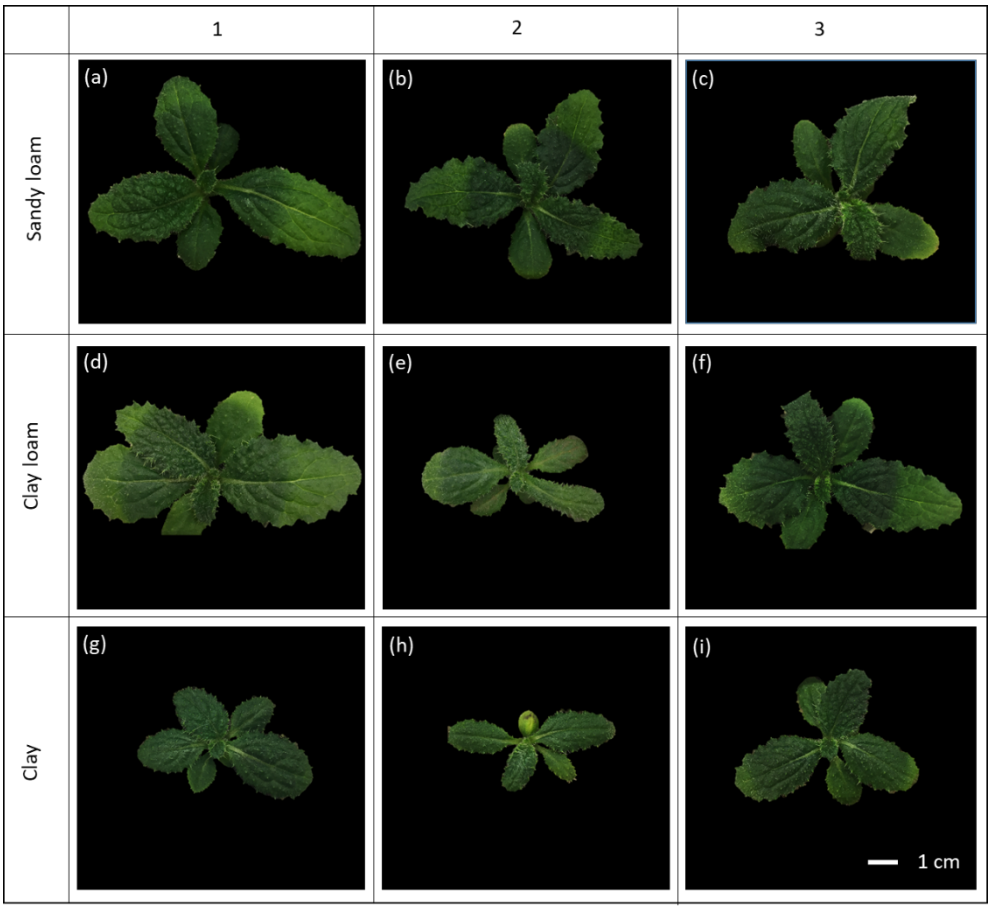
Appendix Chapter 5



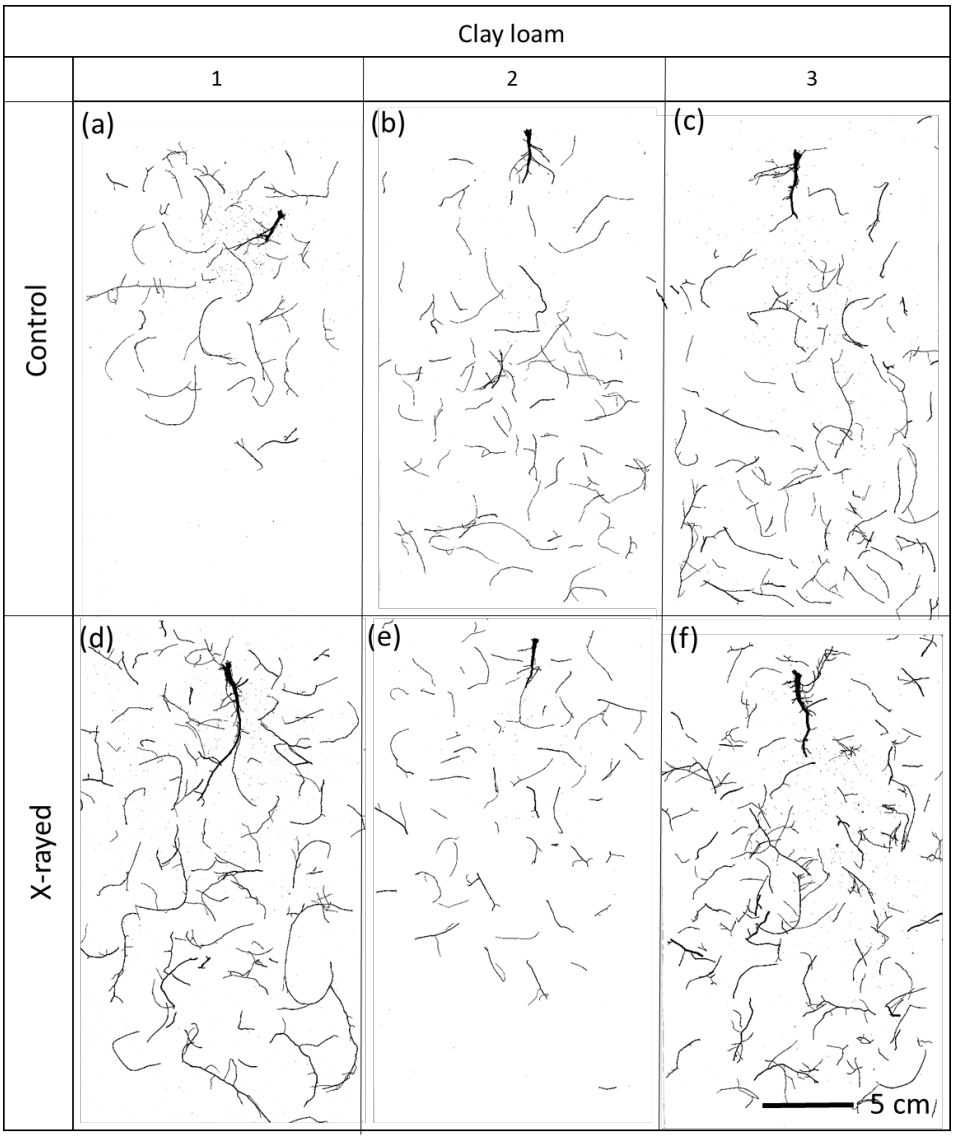
A.5.1: *Cirisum* plant shoots, (a-c) grown in sandy loam soil, (d-f) grown in clay loam soil, (g-i) grown in clay soil for 14 days. Photos were taken using an iPhone 6 and manipulated using ImageJ.



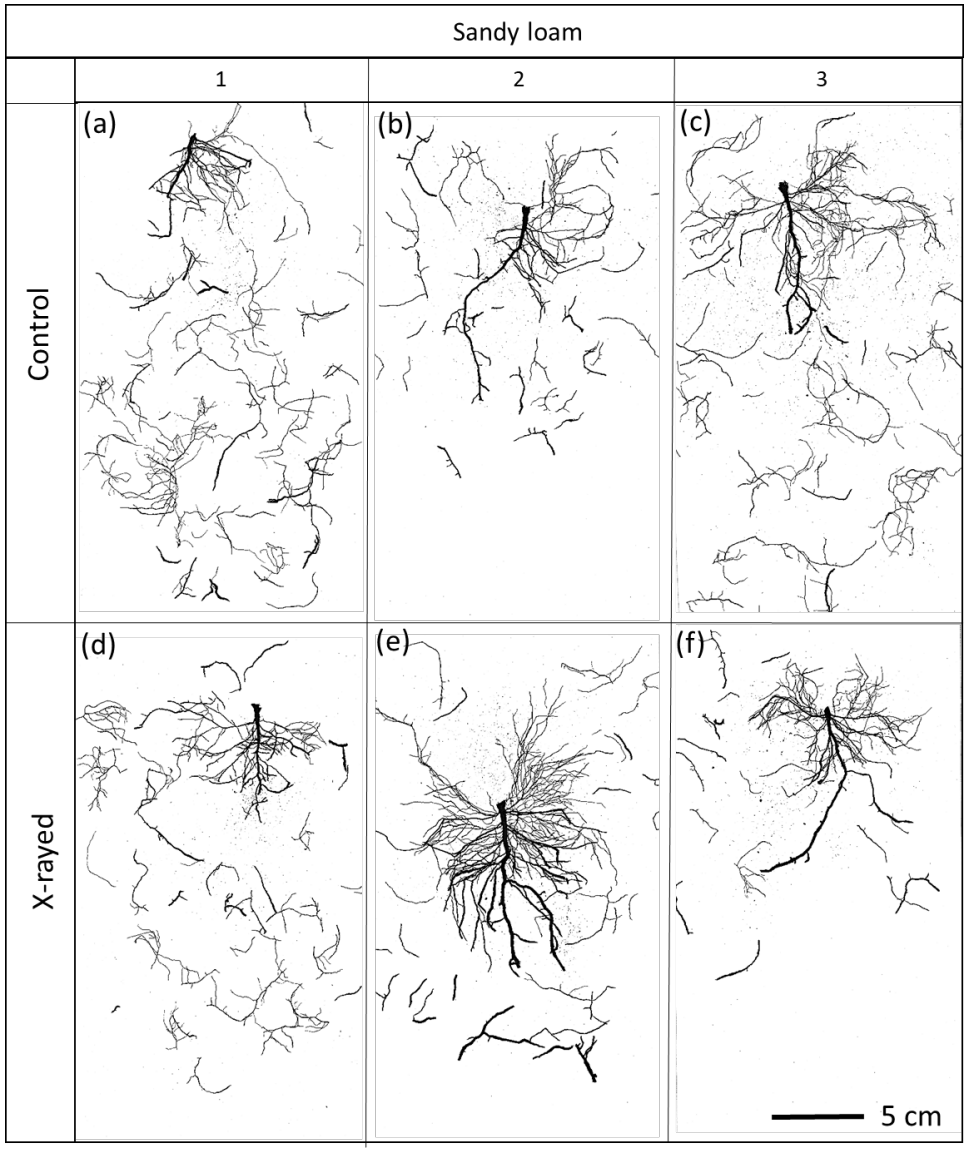
A.5.2: *Cirisum* plant shoots, (a-c) grown in sandy loam soil, (d-f) grown in clay loam soil, (g-i) grown in clay soil for 28 days. Photos were taken using an iPhone 6 and manipulated using ImageJ.



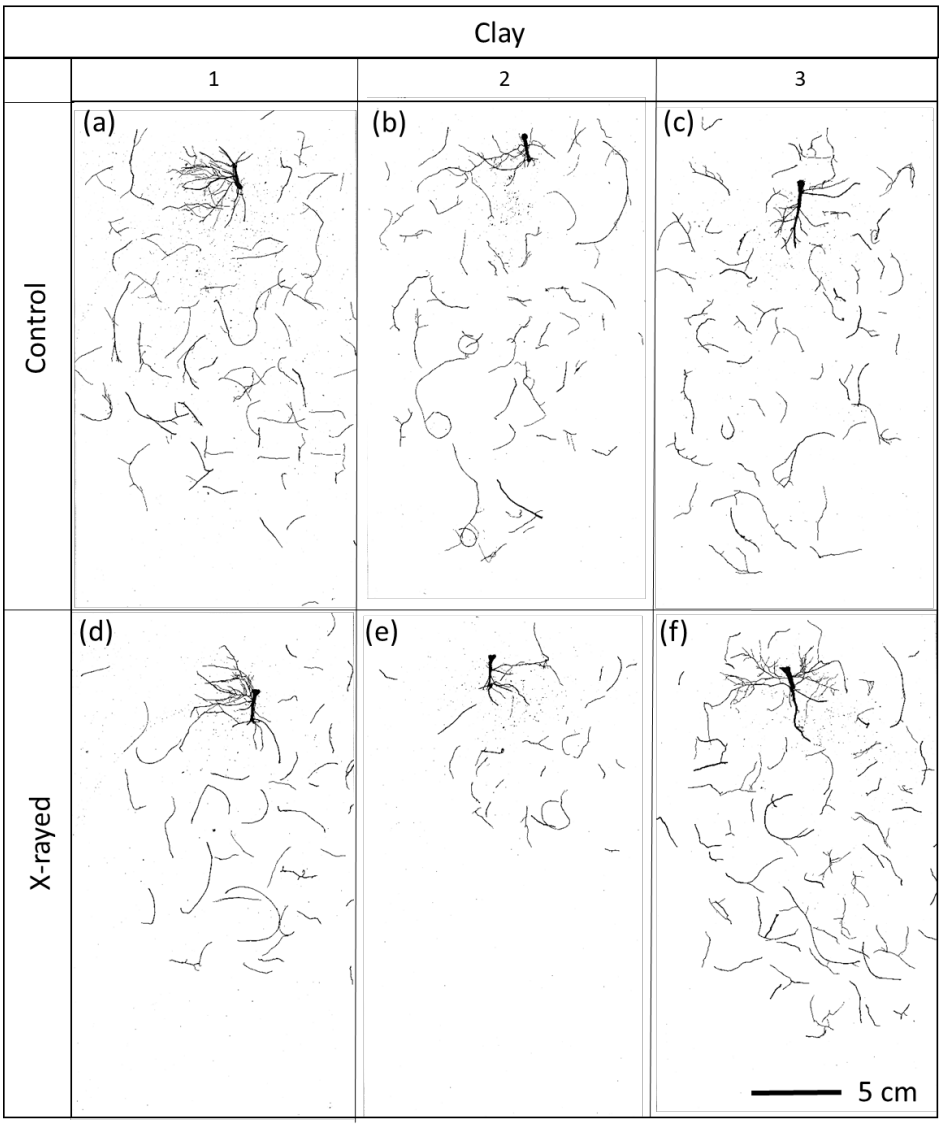
A.5.3: *Cirisum* plant shoots, (a-c) grown in sandy loam soil, (d-f) grown in clay loam soil, (g-i) grown in clay soil for 42 days. Photos were taken using an iPhone 6 and manipulated using ImageJ.



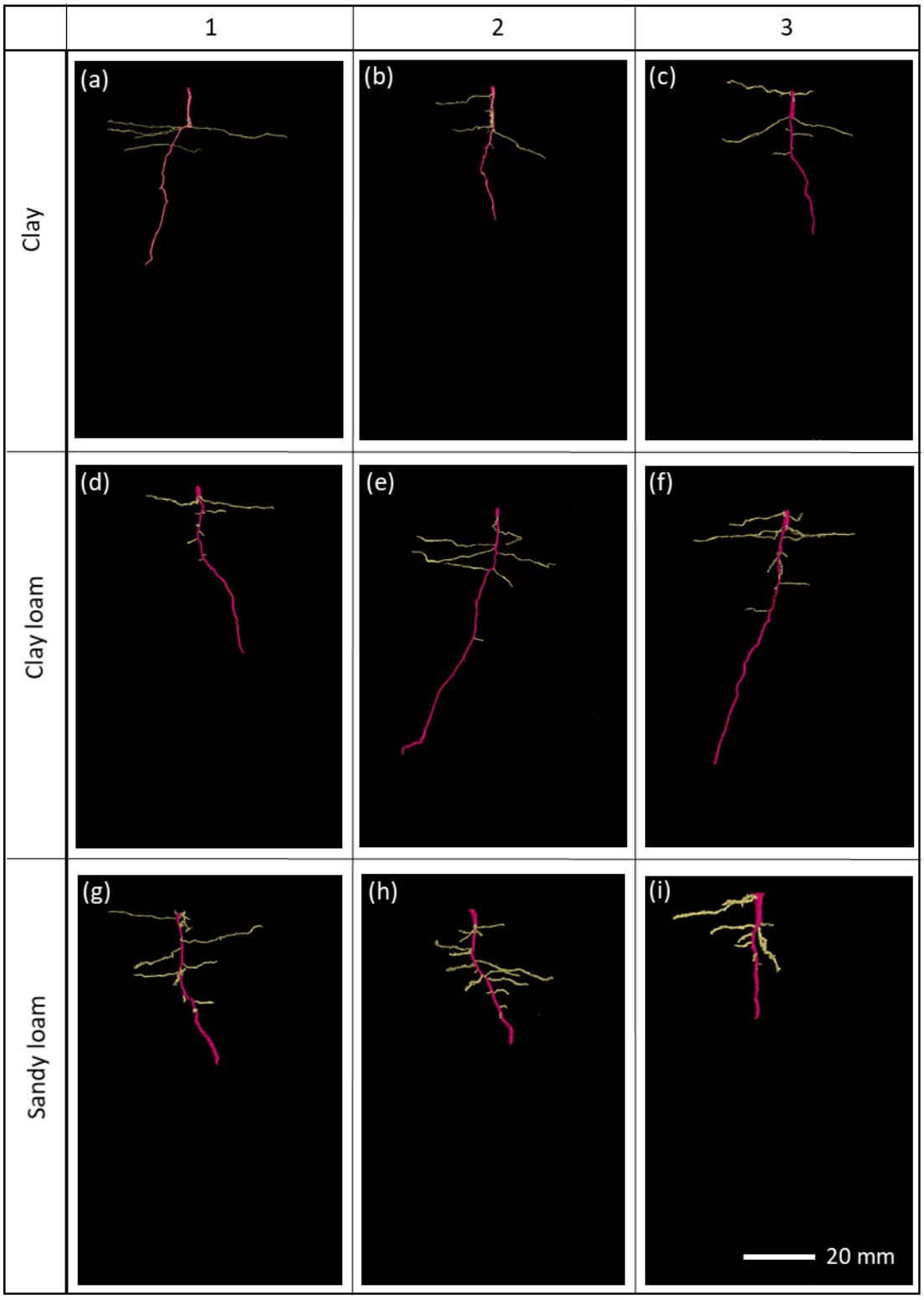
A.5.4: 2D WinRHIZO scans of *Cirsium* plant roots grown in clay loam soil for 42 days. (a-c) control plants not subject to x-ray exposure, (d-f) plants subject to x-ray exposure.



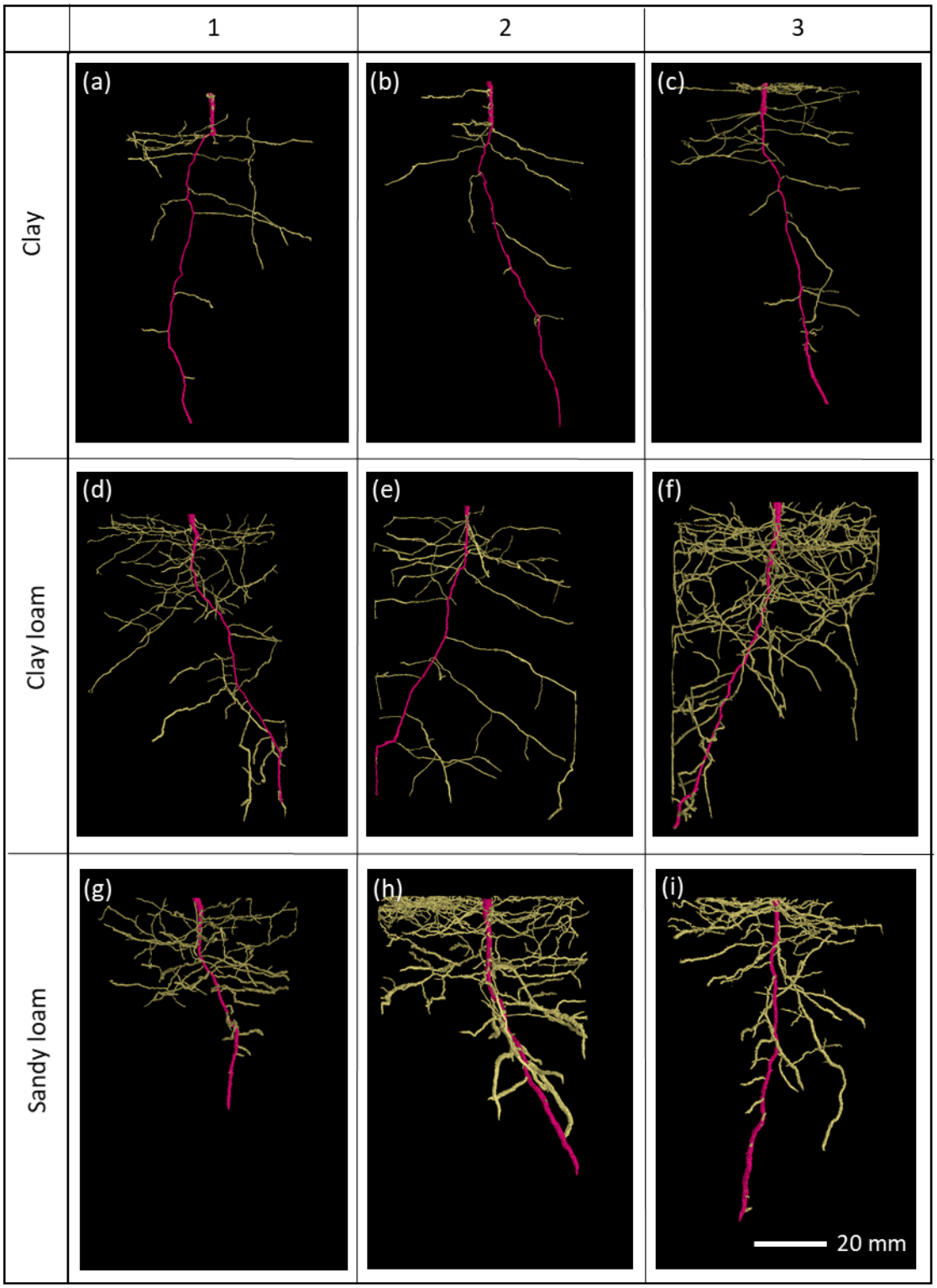
A.5.5: 2D WinRHIZO scans of *Cirsium* plant roots grown in sandy loam soil for 42 days. (a-c) control plants not subject to x-ray exposure, (d-f) plants subject to x-ray exposure.



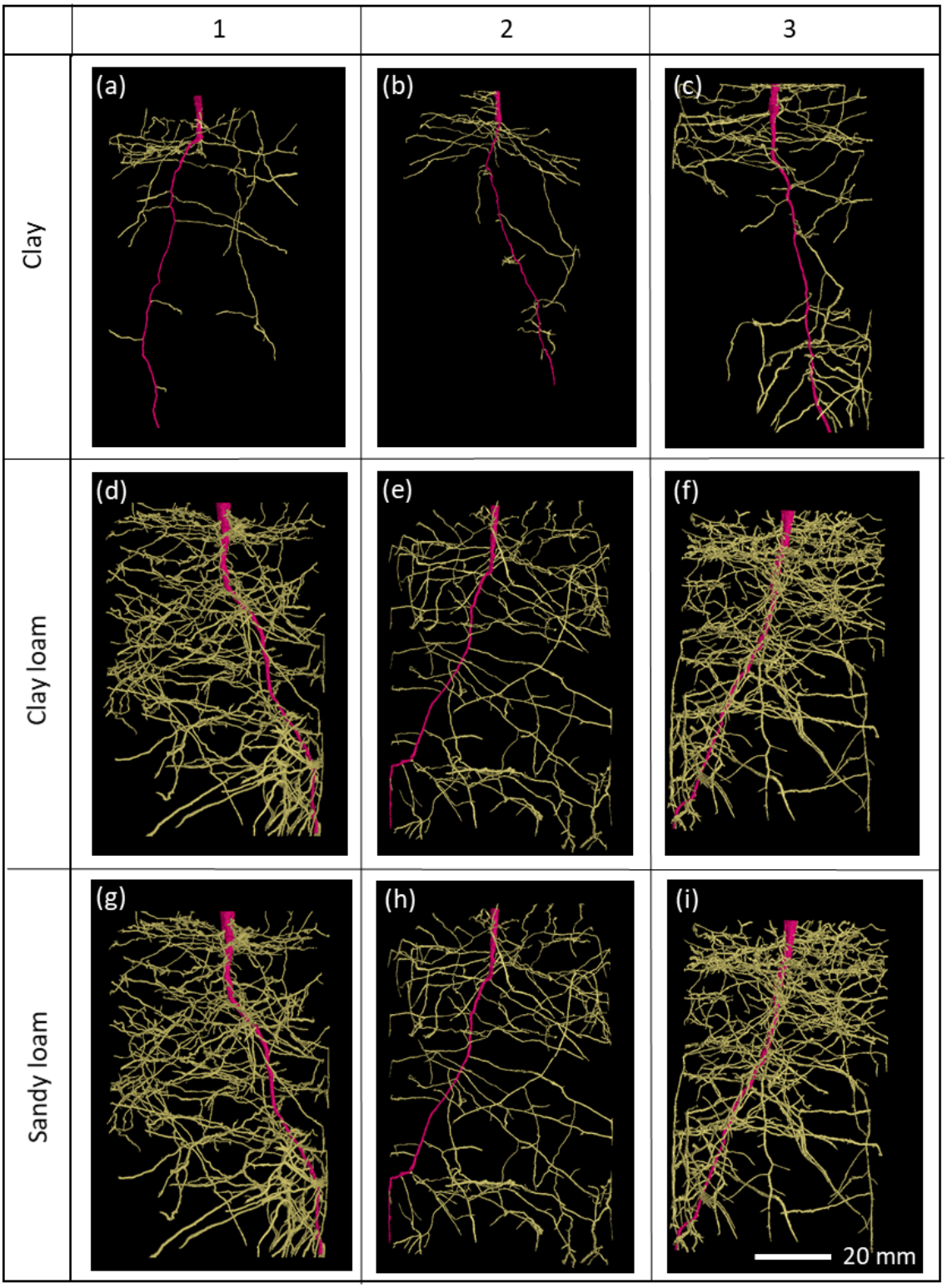
A.5.6: 2D WinRHIZO scans of *Cirsium* plant roots grown in clay soil for 42 days. (a-c) control plants not subject to x-ray exposure, (d-f) plants subject to x-ray exposure.



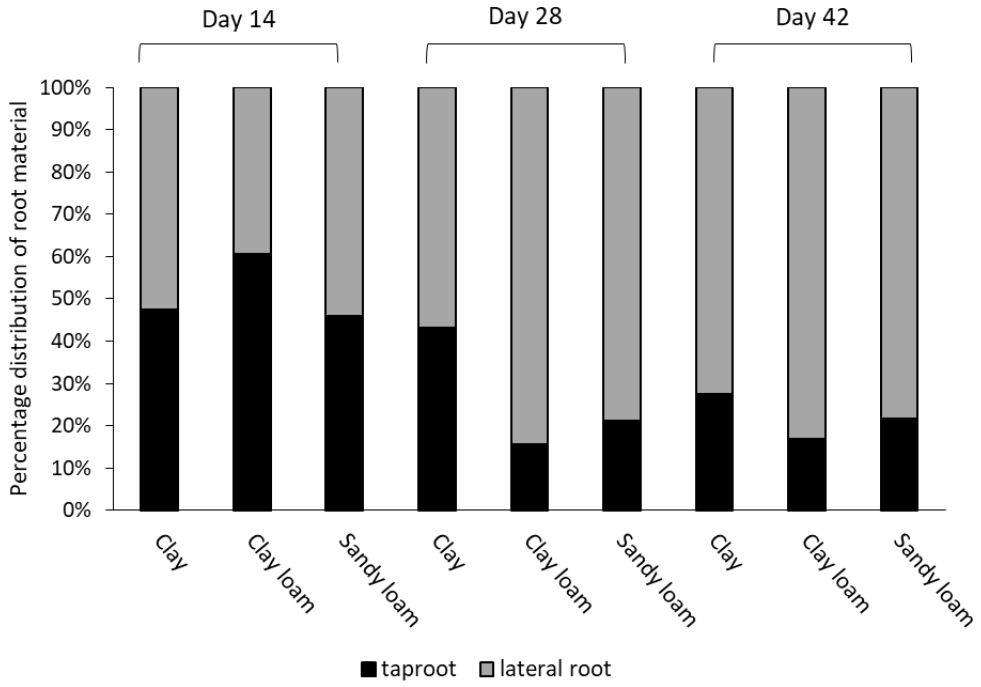
A.5.7: 3D visualisations of Cirsium plants grown for 14 days. Pink colouration indicates taproot, yellow indicates lateral roots. (a-c) 3 replicates grown in clay soil, (d-f) 3 replicates grown in clay loam soil, (g-i) 3 replicates grown in sandy loam soil. Plants were imaged at a resolution of 33 µm. Renderings generated using Root1 in ImageJ and were visualised using VG Studio Max V.2.2.



A.5.8: 3D visualisations of Cirsium plants grown for 28 days. Pink colouration indicates taproot, yellow indicates lateral roots. (a-c) 3 replicates grown in clay soil, (d-f) 3 replicates grown in clay loam soil, (g-i) 3 replicates grown in sandy loam soil. Plants were imaged at a resolution of 33 µm. Renderings generated using Root1 in ImageJ and were visualised using VG Studio Max V.2.2.



A.5.9: 3D visualisations of Cirsium plants grown for 42 days. Pink colouration indicates taproot, yellow indicates lateral roots. (a-c) 3 replicates grown in clay soil, (d-f) 3 replicates grown in clay loam soil, (g-i) 3 replicates grown in sandy loam soil. Plants were imaged at a resolution of 33 µm. Renderings generated using Root1 in ImageJ and were visualised using VG Studio Max V.2.2.



A.5.10: Percentage distribution of root mass between taproot and lateral roots of Cirsium plants grown for 14, 28 and 42 days in Clay, Clay loam and Sandy loam soil.

A.5.11: RooT1 macro

```
//RUN 1
//Opening image stack
run("Image Sequence...", "open=[F:/ROOT 1/input/1/image stack/image stack0000.tif] number=2988 starting=1 increment=1 scale=100 file=[] sort");
// run root1
run("Duplicate...", "title=[Edges] duplicate");
                    setSlice(nSlices);
                    run("Find Edges", "stack");
                    setAutoThreshold("Default dark"); //*************
                    run("Convert to Mask", " stack black");
                    run("Replace value", "pattern=0 replacement=1");
                    run("Replace value", "pattern=255 replacement=0");
                    selectWindow("image stack");
                    run("Duplicate...", "title=[ThBits] duplicate");
                    selectWindow("ThBits");
                    setThreshold(5000,6000);
                    run("Convert to Mask", " stack background=Dark black");
                    imageCalculator("Multiply create stack", "Edges","ThBits");
                    selectWindow("Edges");
                    close();
                    selectWindow("ThBits");
                    close();
                    selectWindow("Result of Edges");
                    run("Median (3D)");
                    rename("Root");
//Creating new folder
File.makeDirectory("F:/ROOT 1/output/1/image stack")
//Save image stack
//selectWindow("roots");
run("Image Sequence... ", "format=TIFF name=root start=0 digits=4 save=[F:/ROOT 1/output/1/image stack/image stack0000.tif]");
close();
// Closing image stack
selectWindow("Result of Edges");
close();
selectWindow("image stack");
close();
```

A.5.12 RooT1 Method

Load the image stack in VG and scroll through to determine the greyscale range of the root system. Note down these numbers for input into the Root1 macro code. Prepare a folder for each image stack to be analysed and label these in ascending order. Create the same number of output file folders and label these with the corresponding numbers to save the Root1 output into. Load the Root1 macro code into ImageJ. Change the highlighted parts of the macrocode to correspond to your sample, i.e.; folder number, number of images slices and threshold range. Once these have been modified click run. The macro code will run the segmentation over a few hours. Once complete load the saved output file into VG studio. Manipulate this and clean it using the stay in ROI tool to remove any disjointed segmented particles. Use the erase tool to remove any areas of the segmentation you know not to be root. Visualise the output in VG Studio by changing the transparency to 100.